# DEGENERATION OF THE NEUROMUSCULAR SYNAPTIC COMPARTMENT IN NORMAL AND WLD$^S$ MUTANT MICE

Thomas H Gillingwater

Submitted for the degree of PhD in Neuroscience
at the University of Edinburgh

2001

## Declaration

I hereby declare that the work described within, and composition of, this thesis is my own and has not been submitted for any other degree.

Thomas Henry Gillingwater

This thesis is dedicated to 'Joe' Blake

## Acknowledgements

I would like to extend my thanks to the many people who have helped me throughout the course of my doctoral studies. First, I would like to thank my supervisor, Dr. Richard Ribchester, for continually providing the guidance and enthusiasm which has been a constant, stabilising factor throughout the last three years. I would also like to thank Derek Thomson, not only for his expert technical assistance and allowing me to use his data in the current thesis for comparative purposes, but also for being a great friend; all other members of the 'Ribchester Lab' past and present (especially Drs. Jacki Barry, Ellen Costanzo and Rick Mattison) for helpful discussions, encouragement and life-long memories; the staff of the MFAA for excellent animal care; and all of the postgraduate and postdoctoral workers in the Department of Neuroscience. I would also like to thank my second supervisor, Dr. Cali Ingham, as well as all of the staff in the electron microscopy unit of the Department of Preclinical Veterinary Sciences, for expert advice and technical assistance.

I would like to thank all of my family, and especially my parents Roberta and David and sister Catherine, for their continued love, support and understanding throughout my studies, even though trips south remain few and far between. Last, but certainly not least, all my love and gratitude goes to 'family-to-be' Lel. Your love and support mean everything to me.

This work was supported by a PhD Studentship from the Medical Research Council.

## Abstract

Nerve section results in the rapid, Wallerian degeneration of distal axons and motor nerve terminals. This process is normally complete within 24-48 hours in wild-type rodents. By contrast, motor nerve terminals of the spontaneous mutant $Wld^s$ mouse persist, both functionally and morphologically, for up to two weeks following nerve injury. This thesis aims first, to extend knowledge and understanding of the fate of neuromuscular junctions (NMJ) in normal and $Wld^s$ mice following axotomy; second, to test the hypothesis that the $Wld^s$ phenotype is age-dependent; and third, to test the hypothesis that the $Wld^s$ phenotype is produced as a result of the expression of a Ube4b/Nmnat chimeric gene.

Immunocytochemical, confocal and vital staining experiments revealed marked differences between the mechanisms of nerve terminal removal in axotomised wild-type and $Wld^s$ preparations. Wild-type preparations endured a rapid, fragmentary type of degeneration (the characteristics of classical Wallerian degeneration), whereas $Wld^s$ nerve terminals appeared to be withdrawn from endplates in a piecemeal fashion. Ultrastructural analysis confirmed that axotomised wild-type NMJs exhibited all of the classical signs of Wallerian degeneration, including in-situ nerve terminal fragmentation, mitochondrial swelling and lysis and phagocytosis by the terminal Schwann cell. Electron micrographs of axotomised $Wld^s$ NMJs demonstrated a retention of nerve terminal architecture, including synaptic vesicles and mitochondria.

Together, these data suggest that when axonal degeneration is delayed, as in the Wld$^s$ mouse, a novel form of synaptic withdrawal is unmasked, and that aspects of this process resemble those which occur during the formation of mature innervation patterns in postnatal development.

The effect of age on the phenotypic expression of the Wld$^s$ mutation was studied in 2, 4, 7 and 12 month old Wld$^s$ mice using morphological and ultrastructural techniques. As the mice matured, the rate of nerve terminal loss progressively increased, with animals of 7 months and older exhibiting wild-type characteristics (most terminals being lost within 24-48 hours of axotomy). The nature of nerve terminal loss also changed from apparent piecemeal withdrawal to classical Wallerian degeneration with increasing age. In Wld$^s$ mice of 7 months and older, partial occupancy of an endplate was rarely observed, whereas the incidence of fragmented, degenerating nerve terminals increased. Ultrastructural analysis supported these findings: thus mainly degenerating nerve terminal profiles were observed in Wld$^s$ mice of 7 months or older. Interestingly the transition from withdrawal to degeneration appeared to be gradual with evidence of both mechanisms operating at individual NMJs in 4 month old Wld$^s$ mice. These studies suggest that the loss of nerve terminal withdrawal characteristics in older Wld$^s$ mice may be accounted for by an age-related decline in the levels of a 'synaptic maintenance factor' within a neuron. Such a factor may be responsible for initiating the withdrawal of nerve terminals under conditions such as axotomy or disuse.

Similar morphological and ultrastructural analyses were performed on nerve/muscle preparations from transgenic mice expressing the candidate $Wld^s$ gene (Ube4b/Nmnat) under a β-actin promoter. Transgenic mice strongly expressing the Ube4b/Nmnat chimeric gene also showed prolonged retention of axons and motor nerve terminals following axotomy, at similar levels to those found in $Wld^s$ mice. Evidence of partially occupied endplates suggested that piecemeal withdrawal of motor nerve terminals also occurred in transgenic mice, and ultrastructural analysis reported a retention of nerve terminal architecture. These findings support the hypothesis that the Ube4b/Nmnat chimeric gene is responsible for the $Wld^s$ phenotype, and suggests that synapse specific events unmasked when axonal Wallerian degeneration is delayed are not unique to the $Wld^s$ mouse.

My studies provide evidence for a compartmental model of neurodegeneration. Whereas it is widely acknowledged that the somatic and axonal portions of a neuron have separate, compartmentalised mechanisms of degeneration, data presented here suggest that degeneration of synaptic terminals is also controlled by at least one other, independent mechanism, that is distinct from those found in the cell body and axon.

## Abbreviations

| | |
|---|---|
| α-BTX | Alpha-bungarotoxin |
| Ach | Acetylcholine |
| AchR | Acetylcholine receptors |
| ATP | Adenosine Triphosphate |
| BSA | Bovine Serum Albumin |
| BTX | Bungarotoxin |
| CNS | Central Nervous System |
| CNTF | Ciliary Neurotrophic Factor |
| EM | Electron Microscopy |
| EPP | End-Plate Potential |
| FDB | Flexor Digitorum Brevis |
| FITC | Fluorescein Isothiocyanate |
| INOS | Inducible Nitric Oxide Synthase |
| LTX | Latrotoxin |
| MAG | Myelin-Associated Glycoprotein |
| MEPP | Minature End-Plate Potential |
| NAD | Nicotinamide Adenine Dinucleotide |
| N-CAM | Neural Cell Adhesion Molecule |
| NF | Neurofilament |
| NGF | Nerve Growth Factor |
| NMJ | Neuromuscular Junction |
| Nmnat | Nicotinamide Mononucleotide Adenylyltransferase |
| PBS | Phosphate Buffered Saline |
| PNS | Peripheral Nervous System |
| SD | Standard Deviation |
| SEM | Standard Error of the Mean |
| STX | Steatoda Toxin |
| SV | Synaptic Vesicles |
| TA | Transversus Abdominus |
| TEM | Transmission Electron Microscopy |
| TRITC | Tetramethylrhodamine Isothiocyanate |
| Ube4b | Human Ubiquitination Factor E4b |
| 4DL | Fourth Deep Lumbrical |

# Table of Contents

# General Introduction

## 1.1 General Introduction

The vertebrate nervous system is the most complex assembly of cells found in any living organism. It is a highly specialised unit, organised to continually receive, process and act upon information produced from within the animal as well as its surrounding environment. The central nervous system (CNS; comprising the brain and spinal cord) is the division responsible for the majority of 'higher' functions such as decision making, learning and multiple input integration. The peripheral nervous system (PNS; comprising all neural tissue outside the CNS) is responsible for providing the sensory input to and carrying the motor output from the CNS. Yet the connections within the nervous system are not immutable. Some of the most fascinating scientific discoveries of recent years have greatly enhanced our understanding of the role of plasticity within these systems. Thus, it has become increasingly apparent that the nervous system is not a 'hardwired', inflexible unit (as was originally thought by early neurobiologists; for review see Albright et al., 2000), but rather a very dynamic entity, capable of altering both its structure and function in response to a variety of circumstances. Whilst most current research focuses on plasticity in the CNS (for example, the role of plastic mechanisms in learning and memory; for review see Martin et al., 2000), there has been a steady accumulation of literature over the past few decades concerning plasticity in the PNS, not least with regard to the formation, development, stabilisation and repair of neuromuscular connections (for general review see Grinnell, 1995).

Neuronal degeneration has also been the subject of intensive study in recent years. Even though degenerative processes underlie many common disorders of the nervous system, including multiple sclerosis (Perry and Anthony, 1999), spinal cord injury (Zhang et al., 1996), stroke and peripheral neuropathy (Wang et al., 2001), little is known with regard to the underlying cellular and molecular control mechanisms. Recent advances have suggested however that cell body degeneration and axonal degeneration occur via separate and distinct pathways (Deckwerth and Johnson, 1994). However, most of these studies have overlooked the specific involvement of synapses, regarding the synaptic component of a neurone as a simple extension of the axon. As a result, evidence of synapse specific events occurring during neuronal degeneration has, in the majority of cases, gone unreported. It is only with the publication of recent studies, which have focused on synaptic rather than axonal events, that evidence for direct synaptic involvement in neuronal degeneration has emerged. For example, it has been shown that apoptotic biochemical cascades can be activated locally in synapses (Mattson et al., 1998a and 1998b).

Thus, a deeper understanding of the independent mechanisms involved in neuronal degeneration is essential for producing specific preventative and therapeutic strategies for those diseases where all, or only selective portions, of the neurone degenerate.

## 1.2 Purpose and Overview of the Present Study

This thesis addresses current issues concerning the morphological events and underlying mechanisms of synaptic plasticity and degeneration at axotomised peripheral synapses. The main techniques I have used are electron microscopy, confocal microscopy, conventional fluorescence microscopy and vital staining techniques. The studies have focused on the naturally occurring C57Bl/Wld$^s$ mutant mouse, in which axonal Wallerian degeneration is significantly delayed. Evidence has accumulated that a distinct form of synapse specific degeneration can be unmasked by axotomy in this mutant. The studies described in this thesis suggest that synaptic responses to axotomy are completely different and distinct from degeneration of the cell body and axon. On the other hand, there are some remarkable similarities in morphology and time-course to the processes of synapse elimination which occurs during development or following reinnervation.

The controversy over the age dependence of the Wld$^s$ phenotype is also addressed within this thesis. Experimental data I present unequivocally shows that at the synaptic level, the expression of the Wld$^s$ phenotype at NMJs is lost with age, and that the *mechanism* of motor nerve terminal loss is also fundamentally altered. Finally, a contribution to the hypothesis that the Wld$^s$ phenotype results from the expression of a novel gene is described. Experiments utilising transgenic mice suggest that the Ube4b/Nmnat chimeric gene is both necessary and sufficient to confer slow

degeneration of both axons and motor nerve terminals following nerve lesion. Finally, taking all the data together, a model is proposed, in which synapses have their own distinct and separate mechanisms of degeneration, independent of somatic and axonal degeneration.

The remainder of this chapter introduces the mammalian NMJ, Wallerian degeneration and the Wld$^s$ mutant mouse. The present view of neurodegenerative mechanisms and of synapse elimination at the NMJ are also described. Chapter 2 contains information on the materials and methods used throughout the current study. In chapter 3, experimental data is presented comparing the morphological characteristics of control and axotomised NMJs in wild-type and Wld$^s$ mutant mice. In chapter 4, data is presented to address the effect of age on the phenotypic expression of the Wld$^s$ mutation at NMJs. Chapter 5 contains results from experiments aimed at assessing the role of the Ube4b/Nmnat chimeric gene in producing the Wld$^s$ phenotype at axotomised NMJs. In the final chapter (chapter 6) I argue that the results of the previous chapters lead to the proposal of a compartmental model of the neurone with regard to neurodegeneration as well as differentiation, and specifically that the degeneration of synaptic terminals is regulated by at least one and possibly several distinct cellular mechanisms.

## 1.3 The Vertebrate Neuromuscular Junction

The neuromuscular junction (NMJ) is the best understood chemical synapse. It is formed where axons of spinal motor neurones terminate and become morphologically specialised to create synapses with their target skeletal muscle fibres. The vertebrate NMJ is arguably the best preparation for analysis of synaptic development (Sanes and Lichtman, 1999), refinement of synaptic connections and long-term morphological and functional synaptic plasticity (Grinnell, 1995).

### 1.3.1 Historical Perspective

Santiago Ramon Y Cajal (1928) was one of the major innovators of, and subscribers to, the 'neuronal doctrine'. This proposed that neurones are discreet, membrane bound cells, which are not linked via a continuation of neurofibrils from one cell to another, as had previously been argued by other neurobiologists including Camillo Golgi. Ramon Y Cajal's findings suggested that nerves only contact other cells at specific points of apposition: sites that were later named *synapses* by Charles Sherrington (Sherrington, 1897; 1906). Whilst NMJs were used experimentally as 'model synapses' throughout the earlier part of the 20$^{th}$ century, it was only following the advent of electron microscopy that they were unequivocally shown to be an apposition between a motor axon terminal and a skeletal muscle fibre, separated from each other by a 50nm synaptic cleft (Reger, 1954; Reger, 1955; Reger, 1958; Birks, Huxley and Katz, 1960).

Whilst the existence of both electrical and chemical synaptic transmission in both vertebrate and invertebrate nervous systems is now widely acknowledged (Bennett, 2000), it was the vertebrate NMJ which was the first synapse to be clearly shown to release the chemical neurotransmitter acetylcholine (Dale et al., 1936). A couple of decades later, the vertebrate NMJ was utilised in a classic series of experiments by Katz and colleagues to demonstrate the precise nature of chemical synaptic transmission. Fatt and Katz (Fatt and Katz, 1951; Fatt and Katz, 1952) showed that chemical synaptic transmission is produced as a result of a change in the permeability of neural membranes to ions, a situation summarised by the 'ionic hypothesis' (Hodgkin et al., 1952). In these studies Fatt and Katz showed that the membrane permeability of a muscle fibre is altered following the binding of acetylcholine. Subsequent work revealed that neurotransmitter release from motor nerve terminals occurs not by the release of single molecules, but rather by the release of multimolecular packets of around 5000 molecules known as 'quanta' (Fatt and Katz, 1952; del Castillo and Katz, 1954; Katz, 1969; Kuffler and Yoshikami, 1975). It was also demonstrated using these NMJ preparations that transmitter release occurs, not only by evoked means (producing end plate potentials), but also as random, spontaneous events: as evidenced by the occurrence of miniature end plate potentials (MEPPs; Fatt and Katz, 1952; Katz and Miledi, 1969). The spontaneous events were shown, largely through the statistical analysis of endplate recordings, to be equivalent to the unitary quanta underlying stimulation-evoked endplate potentials.

### 1.3.2 General Structure of the NMJ

Present understanding indicates that the vertebrate NMJ is constructed from highly specialised portions of three cells: motor neurone, skeletal muscle fibre and a specific class of Schwann cell known as the 'terminal', or 'perijunctional', Schwann cell (Grinnell, 1995; Son and Thompson, 1995a). The synaptic area of each of these cells is morphologically distinct from the rest of the cell due to higher or lower levels of organelles and molecules which are not found extrasynaptically (Figure 1.1). The detailed structure of the synaptic region in each of the cells is described below.

### 1.3.3 Structure of the Motor Nerve Terminal

The motor nerve terminal has a highly polarised ultrastructure. Clustered close to the presynaptic membrane are clear, 50nm synaptic vesicles (Palade and Palay, 1954; Robertson, 1956), each containing one 'quantum' (ca. 5000 molecules; see above) of the neurotransmitter acetylcholine (Whittaker et al., 1964). So far, a direct demonstration that exocytosis of synaptic vesicles is responsible for neurotransmitter secretion which produces postsynaptic activation has only been possible using mouse mast cells and adrenal chromaffin cells (Alvarez de Toledo et al., 1993; Chow et al., 1992). However, the indirect evidence that neurotransmitter is released by exocytosis at NMJs is none the less compelling (e.g. Betz and Angleson, 1998; Richards et al., 2000). Synaptic vesicles often aggregate around hot spots of exocytosis on the

presynaptic membrane, appearing as electron dense regions down the EM, known as 'active zones' (Hirokawa et al., 1989). There is considerable evidence that the population of vesicles within a nerve terminal is split into two functionally and spatially distinct populations: a ready-releasable pool and a larger reserve pool, which is available for release under more strenuous conditions such as during trains of stimuli (Betz and Bewick, 1992; Kelly, 1993; Kuromi and Kidokoro, 1998; Delgado et al., 2000; Richards et al., 2000). Sometimes 'omega' (Ω) figures can be detected on the presynaptic membrane. These are thought to form by vesicular membrane fusion with the presynaptic membrane (Heuser et al., 1979).

Within, or in close proximity to active zones is the molecular machinery responsible for regulating and driving the synaptic vesicle cycle (docking, fusion, endocytosis and subsequent recycling; Betz and Angleson, 1998). P-type calcium channels are distributed widely throughout the presynaptic membrane to allow $Ca^{2+}$ entry (Uchitel et al., 1992) which is essential for calcium-dependent vesicle exocytosis. To enhance the secretion of neurotransmitter, voltage-gated potassium and calcium channels are also heavily localised within active zones (Robitaille et al., 1993; Day et al., 1997). Syntaxins have been identified in the presynaptic membrane and are thought to play a major role in vesicle docking at the presynaptic membrane (Pevsner et al., 1994). Specific integrins are also present in active zones, one example being $\alpha 3\beta 1$ (Cohen et al., 2000). Integrins securely attach the nerve terminal to the basal lamina, thereby keeping neurotransmitter release sites firmly anchored opposite postsynaptic receptors.

**Fig. 1.1 Diagrammatical Representation of the Neuromuscular Junction.**

(A) The cellular organisation of a motor neurone, skeletal muscle fibre and Schwann cells.

(B) Distal to the last myelin sheath, the presynaptic axon diversifies into numerous varicosities called synaptic boutons.

(C) Each nerve terminal bouton is separated from the skeletal muscle fibre by a ~50nm synaptic cleft, in which the synaptic basal lamina lies. The postsynaptic area of a skeletal muscle fibre is convoluted into junctional folds, at the top of which can be found the AchRs .

Figure adapted from Kandel, E.R., Schwartz, J.H. & Jessell, T.M. (1991) *'Principles of Neural Science'* 3rd Edition. Elsevier Science Publishing, USA.

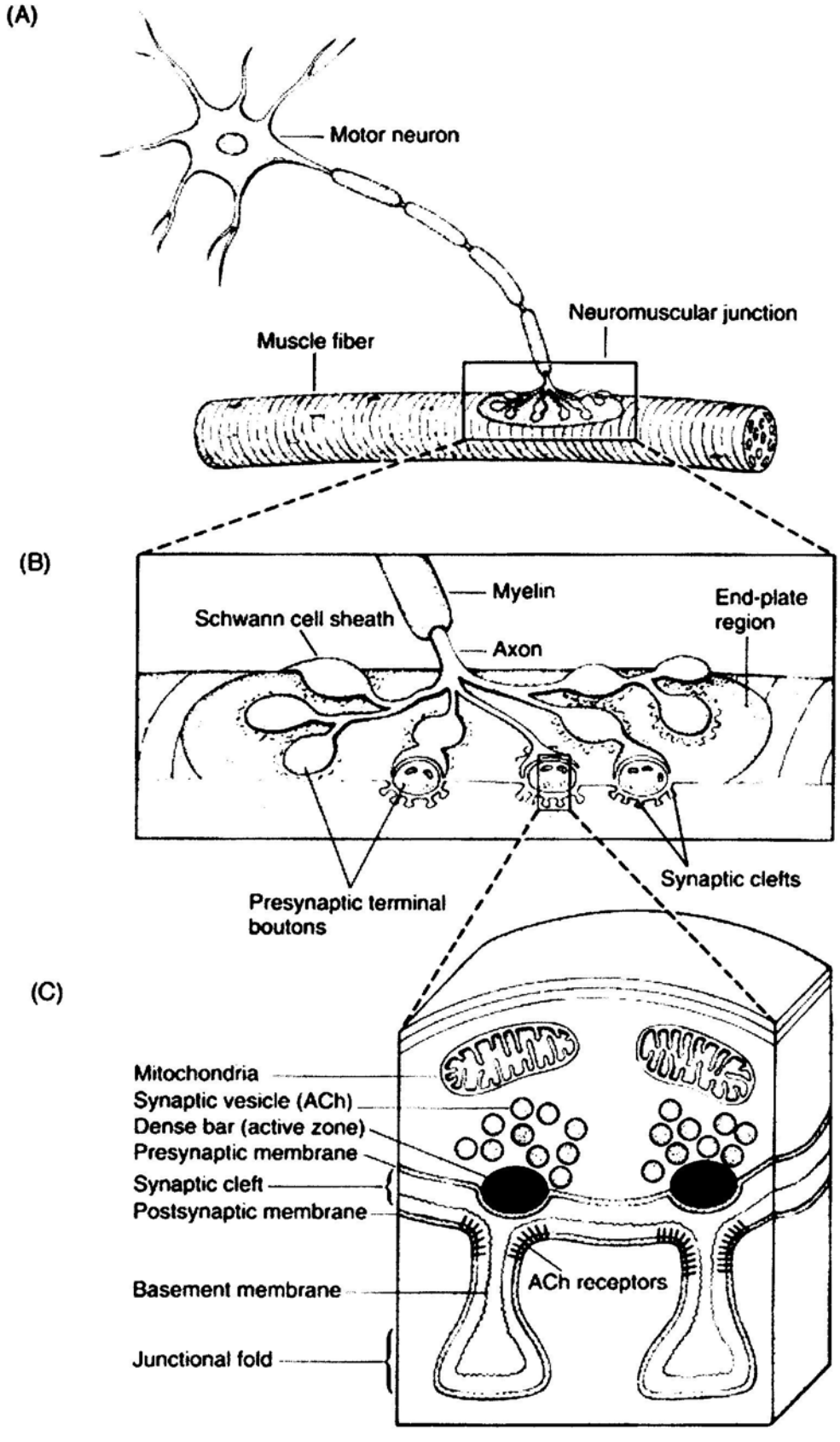
(A)
Motor neuron
Neuromuscular junction
Muscle fiber
(B)
Myelin
Schwann cell sheath
Axon
End-plate region
Presynaptic terminal boutons
Synaptic clefts
(C)
Mitochondria
Synaptic vesicle (ACh)
Dense bar (active zone)
Presynaptic membrane
Synaptic cleft
Postsynaptic membrane
Basement membrane
Junctional fold
ACh receptors

Integrins are also thought to assist in facilitating neurotransmitter release (Chen and Grinnell, 1995). The membranes of vesicles themselves contain many of the interactive molecules required for anchoring, docking, fusion, release and recycling. Some examples include synaptophysin and synaptobrevins (Elferink and Scheller, 1993), Synapsins I and II (Sudhof and Jahn, 1991) and the vesicular Ach transporter (Erickson et al., 1994).

Distal from the presynaptic membrane are numerous nerve terminal mitochondria, intermingled between which can be found a few sparse microtubules and neurofilaments. Whilst microtubules and neurofilaments exist in abundance pre-terminally, their incidence decreases markedly within the nerve terminal itself (Yee et al., 1988).

Each nerve terminal is split up into many individual boutons, each of which contain all of the ultrastructural features described above. Although the gross structure of a motor nerve terminal may be subdivided, it has been shown that all boutons function as a single unit. For example, when an action potential passes from a motor axon collateral into the nerve terminal, all boutons appear to be activated in a simultaneous, synchronous fashion. Evidence for this comes from studies where neuromuscular junctions have their synaptic vesicular membranes loaded with the styryl dye FM1-43. Upon the induction of nerve stimulation in these preparation, all boutons are depleted of

the dye at a similar rate (Betz et al., 1992; Betz and Bewick, 1992; Ribchester et al., 1994).

### 1.3.4 Structure of the Postsynaptic Specialisation

The motor endplate of a skeletal muscle fibre is easily recognised in the EM due to the folding of the postsynaptic membrane (junctional folds). These folds occur where regions of electron dense postsynaptic membrane become convoluted into peaks and troughs, extending down into the endplate for ~1$\mu$m. This arrangement is thought to increase the safety factor for neuromuscular transmission (Martin, 1979; Wood and Slater, 1997). The opening of a junctional fold is also positioned directly opposite an active zone on the opposing motor nerve terminal (Patton et al., 2001).

The postsynaptic membrane is densely populated with nicotinic AChRs (>10 000 / $\mu m^2$; Salpeter and Loring, 1985). The majority of these are located at the peaks, and a short way down the sides, of junctional folds. In the troughs of the junctional folds are voltage-gated sodium channels (Flucher and Daniels, 1989). These are responsible for responding to the local endplate potential (EPP) produced by activation of the AChRs, thereby triggering a muscle action potential.

The postsynaptic apparatus has a complex molecular network of cytoskeletal elements associated with it. These are thought to play a role in generating and maintaining the

postsynaptic folds as well as the different domains within them (Sanes and Lichtman, 1999). Cytoskeletal elements such as rapsyn (Wang et al., 1999), utrophin (Gramolini et al., 2000), and α-dystrobrevin-1, a member of the dystrophin family of proteins (Peters et al., 1998), are found to be associated with the AChRs at the top of junctional folds. In the depths of the folds other cytoskeletal proteins such as ankyrin (Zhou et al., 1998), β-spectrin (Wood and Slater, 1998) and α-dystrobrevin-2 (a COOH-terminal truncated version of α-dystrobrevin-1; Peters et al., 1998) are present.

Immediately beneath the foldings of the postsynaptic membrane are numerous postsynaptic mitochondria as well as clusters of synaptic nuclei (Couteaux, 1973). A recent study by Apel and colleagues (2000) has provided evidence for a novel protein which may be involved in the formation and maintenance of nuclear clusters at the NMJ: synaptic nuclear envelope-1 (Syne-1). Synaptic nuclei are larger and rounder than those found extrasynaptically (Brosamle and Kuffler, 1996) and have been shown to be transcriptionally specialised to exclusively express genes coding for synapse-specific proteins such as the AchR subunits δ and ε, utrophin and acetylcholinesterase (Schaeffer et al., 2001).

### 1.3.5 Terminal Schwann Cells

Most Schwann cells in the PNS form myelin sheathes around axons (Waxman, 1997). Myelin increases the conduction velocity of action potentials along the axon. Myelin-

forming Schwann cells are also thought to provide the axon with trophic sustenance (Oorschot and McLennan, 1998). The Schwann cells associated with the nerve terminal itself, however, are a different, non-myelinating population. The extended processes of these terminal Schwann cells cover the terminal arborisations, insulating them from the surrounding environment. Whilst both myelinating and terminal Schwann cells arise from the same progenitors, they express different genes during development; for example, terminal Schwann cells strongly express S-100 and N-CAM whilst myelinating Schwann cells have much higher expression levels of myelin basic protein, $P_0$ and myelin-associated glycoprotein (Mirsky and Jessen, 1996).

Terminal Schwann cells, though not necessary, have been shown to play an important role in the development, repair and maintenance of NMJs (Meier and Wallace, 1998). It has been demonstrated, for example, that synpatogenesis can be induced by the release of soluble glia-derived signals (Nagler et al., 2001). Furthermore, following denervation, terminal Schwann cells sprout processes (Reynolds and Woolf, 1992) which guide regenerating axons back to the original sites of innervation (Son and Thompson, 1995a). Following a partial denervation, similar sprouts are produced by terminal Schwann cells, but these are directed to nearby innervated endplates. These processes are capable of inducing intact nerve terminals to sprout along 'bridges' back to reinnervate the denervated sites (Son and Thompson, 1995b). Sprouting of a Schwann cell from a denervated site to a nearby innervated site also induces mitosis of the resident Schwann cells at the innervated, but not at the denervated, endplate (Love

and Thompson, 1998). These findings suggest that whilst terminal Schwann cells become mitotic during reinnervation, previous studies have been correct in concluding that denervation itself does not cause terminal Schwann cell mitosis (Connor et al., 1987). These 'reactive' Schwann cells (i.e. those responding to the loss of nerve terminal contact) are identifiable by an increase in the extent of cellular processes (Torigoe et al., 1999), and are also capable of producing structural alterations in the apposition of the pre- and post-synaptic apparatus (Trachtenberg and Thompson, 1997).

Under normal conditions terminal Schwann cells express muscarinic and purinergic receptors, which respond to the release of acetylcholine and ATP respectively, from the motor nerve terminal (Robitaille, 1995; Robitaille et al., 1997; Rochon et al., 2001). These studies suggest that terminal Schwann cells can detect activity levels at the NMJ, supported by findings that synaptic activity leads to an elevation of intracellular calcium (Jahromi et al., 1992). The end result of such an increase in intracellular calcium appears to be alterations in gene expression. For example, a blockade of activity stimulates the expression of the gene for glial fibrillary acidic protein, which has been shown to play a role in the formation of terminal Schwann cell sprouts (Love and Thompson, 1998; Georgiou et al., 1994). There is also increasing evidence that glial cells can actively modulate synaptic transmission, for example via the production of a glia-derived soluble acetylcholine-binding protein (AchBP) in response to presynaptic release of acetylcholine (Smit et al., 2001), or via the release of neurotransmitters (Bezzi et al., 1998; Araque et al., 2000). A recent study suggests that withdrawal of

terminal Schwann cells from innervated endplates induces abnormal nerve branching, accumulation of neurofilaments, and intermittent failure of synaptic transmission (Court, Brophy and Ribchester, 2001, in press).

### 1.3.6 Basal Lamina

A basal lamina ensheathes each individual skeletal muscle fibre. It passes through the synaptic cleft and extends into the postsynaptic folds. Whilst the major components of the muscle fibre's basal lamina are similar to the majority of other basal laminae found throughout the body (collagen IV, laminin, entactin and heparan sulfate proteoglycans), the synaptic portion differs in its isoform composition (Sanes and Lichtman, 1999). The synaptic basal lamina also contains molecules which are crucial for the establishment, maintenance and function of the NMJ, for example: acetylcholinesterase (Krejci et al., 1997) and agrin. Agrin is a signalling molecule which is present throughout the basal lamina of developing myotubes (Bowe and Fallon, 1995) as well as being synthesised by motor neurones, which transport it to and release it from motor nerve terminals before being incorporated into the synaptic basal lamina (McMahan, 1990; Reist et al., 1992; Cohen and Godfrey, 1992). The presence of certain isoforms of nerve-derived agrin in the synaptic basal lamina has been shown to be crucial for postsynaptic differentiation (McMahan, 1990; Gesemann et al., 1995; Gautam et al., 1996; Jones et al., 1997; Cohen et al., 1997) and may have a role in the maintenance of

the NMJ as it can still be found at synaptic sites (but not throughout the whole basal lamina) in adult muscle fibres (Sanes and Lichtman, 1999).

Another signalling molecule found incorporated into the synaptic basal lamina is neureglin, previously known as acetylcholine receptor-inducing activity (ARIA). This molecule is produced, much the same as agrin, in motor neurones before being released from the motor nerve terminals and incorporated into the basal lamina (Goodearl et al., 1995). It has been suggested that neureglin may have a role in inducing AchR clustering at differentiating postsynaptic sites (Sanes and Lichtman, 1999).

## 1.4 Wallerian Degeneration

A peripheral nerve is a relatively well protected structure, surrounded and cosseted by supporting glial cells, basal lamina and the perineurium. Minor pressure injuries applied to such a nerve rarely result in more than a rapidly reversible compression of its cytoskeletal elements. A major injury to the axonal process of a neurone, such as a prolonged crush or lesion, results in a rapid disintegration of the portion of axon distal to the lesion site however, including its motor nerve terminal. This occurs via a process known as Wallerian degeneration (Figure 1.2). Nerve fibres located proximal to the site of injury, which remain in contact with their soma, not only survive the insult but are also primed for regeneration.

As well as being the major degenerative machinery instigated in an axotomised distal nerve stump following lesion of a nerve, Wallerian degeneration is thought to play a role in axonal death ('dying back' neuropathies) in many diseases of the central and peripheral nervous systems; such as multiple sclerosis, amyotrophic lateral sclerosis, peripheral neuropathies, human transmissible spongiform encephalopathies and Guillain-Barre syndrome (Perry and Anthony, 1999; Narayanan et al., 1997; Dalcanto and Gurney, 1995; Fujimura et al., 1991; El Hachimi et al., 1998; Trojaborg, 1998). Whilst the morphological characteristics of Wallerian degeneration have been well documented, the underlying mechanisms remain unclear.

**Fig. 1.2 Schematic Representation of Wallerian Degeneration.**

A. The cellular organisation of a motor neurone, skeletal muscle fibre and Schwann cells.

B. Following an axonal lesion, the distal stump of the axon and its motor nerve terminal degenerate. The resident Schwann cells dedifferentiate and proliferate. The axonal, nerve terminal and myelin debris are removed by phagocytosing Schwann cells as well as invading macrophages. The cell body undergoes chromatolysis and the nucleus translocates.

C. After the removal of all debris and the formation of Bands of Büngner by Schwann cells, the proximal nerve stump regenerates back to the denervated muscle fibre.

Adapted from Nicholls, J.G., Martin, A.R. & Wallace, B.G. (1992) '*From neuron to brain*' 3rd Edition. Sinauer Associates Massachusetts, USA.

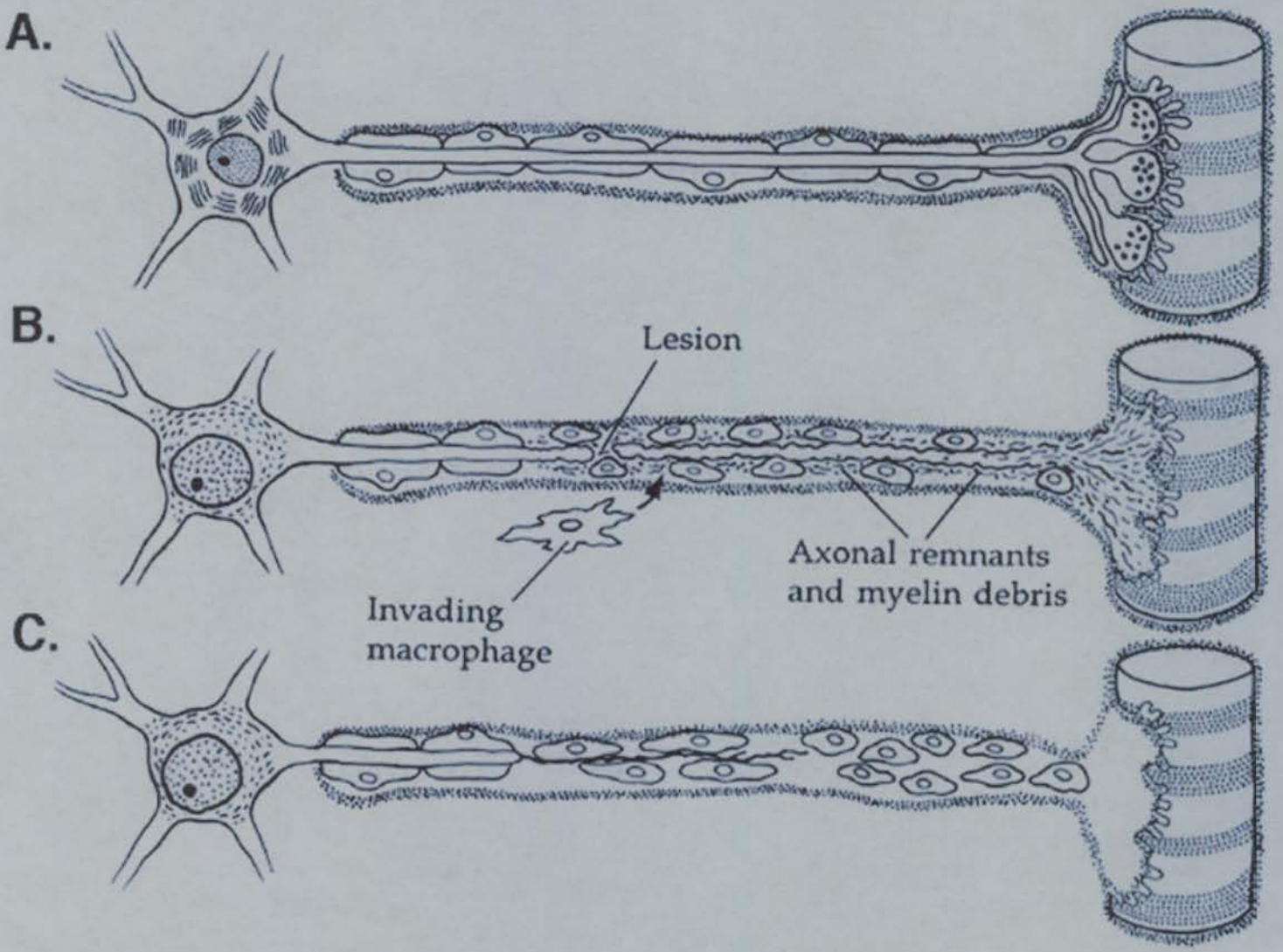
A.
B.
Lesion
Axonal remnants
and myelin debris
Invading
macrophage
C.

### 1.4.1 Historical Perspectives

Wallerian degeneration was first described by Augustus Waller in 1850. He examined the effects of lesioning the hypoglossal and glossopharyngeal nerves upon the innervation of the tongue in the frog. After 3 days, he found a loss of both muscular contraction and sensation in the muscle. Upon examination of the distal nerve stump, he described the axons as appearing discontinuous, fragmented and granulated. He suggested that these events were due to a degenerative process caused by the separation of an axon from its cell body, and hence due to a loss of trophic support.

Whilst Waller's findings were not universally accepted due to constraints imposed by the staining techniques available during that period, his conclusions were supported by subsequent findings from Ranvier in the late 19$^{th}$ century (1878) who gave a more detailed description of the process of Wallerian degeneration. He observed the fragmentation and granulation of the axon following nerve lesion as well as the formation of ovoid bodies following the contraction of myelin and the subsequent invasion of phagocytotic leucocytes. Ranvier's description of Schwann cell division during this process was supported by the findings of Büngner (1891), who observed the mitosis of Schwann cells following axotomy and their joining together to form longitudinal bands, subsequently named 'bands of Büngner'. These early studies finally gained acceptance following the corroborative findings produced by Ramon y Cajal

(1928) who utilised silver staining techniques to conclusively demonstrate that axotomy produces a specific degeneration of the distal nerve stump.

### 1.4.2 Wallerian Degeneration of the Axon

The primary event in Wallerian degeneration is axonal fragmentation and degradation, accompanied by a failure of the nerve to conduct action potentials (Vial., 1958; McDonald, 1972; Mastalgia et al., 1976; Allt, 1976; Hallpike, 1976; Nicholls et al., 1992). The length of lag period following axotomy before changes can be detected in the axon varies between species. In mice; for example, the sciatic nerve becomes incapable of conducting compound action potentials 1 to 2 days following axotomy. A similar time course prevails in the guinea pig, in contrast to axotomised frog sciatic nerve where compound action potentials can be recorded for up to 7 days post lesion (Levenson and Rosenbluth, 1990; Chaudry, Glass and Griffin, 1992). In the giant squid, crayfish and fish however, isolated axons are preserved for months rather than days (Sheller and Bittner, 1992; Tanner et al., 1995; Raabe et al., 1996). Electron microscopy has demonstrated that major early axonal changes include fragmentation of endoplasmic reticulum and disintegration of neurofilaments and microtubules within 24-72 hours following nerve transection (Vial, 1958; Honjin et al., 1959; Ballin and Thomas, 1969; Donat and Wisniewski, 1973; Schlaepfer and Hasler, 1979a). Soon after the onset of these events it is also possible to detect a more distinctive degenerative marker, the swelling and lysis of axonal mitochondria. These changes are thought to be

mediated by a rise in the intracellular calcium concentration: when a threshold concentration of 0.2mM is reached, neurofilament degradation occurs (Glass et al., 1994). Possible mechanisms for this intracellular rise include; i) the reverse operation of the $Na^{+}$-$Ca^{2+}$ exchanger (LoPachin and Lehning, 1997), ii) release from intracellular calcium stores, and iii) entry of extracellular calcium through $Ca^{2+}$ channels (George et al., 1995). Further evidence to support the hypothesis that a rise in intracellular calcium levels initiates axonal degeneration comes from experiments which show that neurofilaments do not degenerate when in a calcium-free environment (Schlaepfer and Hasler, 1979b). The ability of calcium to produce axonal degeneration is thought to be mediated by calcium dependent proteases known as calpains (for review see; Croall and DeMartino, 1991; Chan and Mattson, 1999).

Following axonal fragmentation and degradation, the subsequent breakdown and removal of the myelin sheath occurs by phagocytosis involving the invasion of myelomonocytic cells (Beuche and Friede, 1984). Once the lesioned axon has begun to fragment, the myelin sheath retracts from the nodes of Ranvier creating enlarged nodal spaces. These then segregate the nerve into 'digestive chambers' or 'ellipsoids' (Allt, 1976). Within each of these compartments, the axon fragments proceed to a state of complete degradation.

As degradation of the distal stump continues, 'ellipsoids' are removed by phagocytosing Schwann cells and invading macrophages. At the same time, Schwann cells proliferate:

in rabbit sciatic nerve, 25 days post-lesion, there are up to 13 times the number present before injury (Abercrombie and Johnson, 1946). The Schwann cells join together, tip to tip, forming the longitudinal 'bands of Büngner'. These bands play a major role in inducing and guiding the regenerating proximal nerve stump axons back to denervated sites, aided by the secretion of many different growth and adhesive factors such as NGF (Heumann et al., 1987), N-CAM (Nieke and Schachner, 1985) and cytokines (including members of the interleukin (IL-x) family (Rutkowski et al., 1999; for review see Fu and Gordon, 1997)) from the Schwann cells.

The rate at which Wallerian degeneration proceeds is dependent upon temperature, the age of the animal and the calibre and myelination of the nerve. Cold temperatures have been shown to slow the rate of progression of Wallerian degeneration in mammalian, lower vertebrate and invertebrate axons (Usherwood et al., 1968; Wang, 1985; Bittner, 1988; Sea et al., 1995; Tsao et al., 1999). The optic nerve of cats has also been shown to degenerate slower in older animals than in their younger counterparts (Cook et al., 1974). Unmyelinated axons degenerate first, followed by the smallest myelinated fibres with the largest myelinated fibres degenerating last (Weddel and Glees, 1941; Friede and Martinez, 1970; Lubinska, 1977). Recent experiments indicate that levels of inducible nitric oxide synthase (iNOS) may also control the rate of Wallerian degeneration, evidenced by findings that mice which lack iNOS have slowed Wallerian degeneration in myelinated axons (Levy et al., 2001).

In adults the proximal portion of an axotomised motor neurone does not normally degenerate alongside the distal stump following axotomy, at least in the short term (Romanes, 1941; Johnson and Duberley, 1998). However, marked changes occur to both the cell body and its nucleus (Nicholls et al., 1992). The cell body swells, the nucleus translocates, and the Nissl substance (endoplasmic reticulum) becomes dispersed.

In contrast, survival of neonatal motoneurones is strongly dependent upon their maintaining synaptic contact with their target muscles. Thus neonatal motoneurones normally die by apoptosis within a few days of nerve section. In this case, motoneurone death is mitigated by neurotrophic factors originating in the target muscles signalling through transmembrane receptors to the Bax/Bcl-2/Bcl-X system, activating calcium-dependent proteases (Arce et al., 1998; Knudson et al., 1995; Martinou et al., 1994; Villa et al., 1998; reviewed by Pettmann and Henderson, 1998).

Immediate early genes (IEGs; see Morgan and Curran, 1991), which control the cell body response following axotomy of adult motoneurones, are activated by transcription factors including c-Jun and JunD, which are selectively expressed in axotomised peripheral and central neurones within 10-15 hours of nerve lesion (for review see Herdegen and Leah, 1998). By contrast, c-Fos, FosB, JunB and Fras expression do not occur at all (Leah et al., 1991; Jenkins and Hunt, 1991; Herdegen and Zimmermann, 1994). Induction of c-Jun precedes the activation of several regeneration associated

genes such as GAP-43, tubulins and other cytoskeletal proteins required for axon regeneration (Herdegen and Zimmermann, 1994; Mikucki and Oblinger, 1991; Tetzlaff et al., 1991).

### 1.4.3 Wallerian Degeneration of the Motor Nerve Terminal

The progress of Wallerian degeneration at the mammalian NMJ has been well documented by - amongst others - Reger (1959), Birks, Katz and Miledi (1960), Miledi and Slater (1968 and 1970), Manolov (1974) and Winlow and Usherwood (1975). Axotomy induces degeneration of nerve terminals before the degeneration of their motor axons. The abrupt failure of neuromuscular transmission is one of the first detectable events following nerve damage (Birks, Katz and Miledi, 1960; Miledi and Slater, 1970): occurring within 24-26 hours after axotomy in rodents. Initial degenerative changes in the nerve terminal include (after a lag period of 3-8 hours; Manolov, 1974; Miledi and Slater, 1970): i) the swelling, partial disruption of cristae and destruction of mitochondrial membranes; ii) reduction in the number of, and clustering of the remaining, 50nm clear synaptic vesicles; and iii) the active invasion of terminal Schwann cell processes into the synaptic cleft. More advanced degenerative changes include: i) intensification of intra-terminal disintegration; ii) gross fragmentation of nerve terminal membranes; and iii) phagocytosis of the engulfed nerve terminal by the terminal Schwann cell. After phagocytosis of the nerve terminal is

complete, terminal Schwann cells sometimes remain apposed to the post-synaptic folds for up to 3 weeks (see above).

Mitochondria are often used as a definitive marker of nerve terminal degeneration. Miledi and Slater (1970) quantified the changes in mitochondria at axotomised NMJs, showing that degenerating mitochondria acquire an enlarged, spherical profile, swelling from a diameter of 0.1-0.2$\mu$m in control preparations up to as much as 0.7$\mu$m. The cristae in these mitochondria often appeared 'disorganized and broken up into small vesicular fragments' (Miledi and Slater, 1970). The same was described by Manolov (1974), who also reported the occasional occurrence of 'dense bodies' substituted for mitochondria. Manolov's (1974) investigations also identified the sporadic occurrence of membrane whorl structures, often associated with degenerating mitochondria or vesicular aggregations (see below).

Reger (1959), Manolov (1974) and Winlow and Usherwood (1975) have described changes in the numbers and localisation of the synaptic vesicle population in degenerating motor nerve terminals. The numbers of synaptic vesicles dramatically decrease with increasing time following axotomy. For example, in the experiments of Manolov and Winlow and Usherwood, nerve terminal profiles from 3 hours post-axotomy onwards showed a small reduction in vesicle numbers. This is in marked contrast to the many nerve terminal profiles (from >6 hours post-axotomy) which contained no vesicles. Reger (1959) found that there was no incidence of degeneration

at neuromuscular synapses until more than 24 hours post-axotomy, and as a result he quantified synaptic vesicle densities in degenerating nerve terminals for up to 120 hours following nerve lesion. By 48 hours, there had been a 79.2% decrease in the number of synaptic vesicles, falling from 28-114 SVs/$\mu m^2$ in control preparations to 0-24 SVs/$\mu m^2$. Interestingly, Manolov (1974) found that in many nerve terminals which survive for more than 20 hours post-axotomy, the reduction in synaptic vesicle number and the occurrence of degenerating mitochondria occurred in conjunction with a large increase in the levels of intra-terminal neurofilaments.

## 1.5 The Wld$^s$ Mutant Mouse

During their investigations into the role of recruited myelomonocytic cells in Wallerian degeneration of mouse peripheral nerve, M.C.Brown, V.H.Perry and their colleagues in Oxford discovered, quite serendipitously, a spontaneous mutation in the C57Bl/6 line of mice supplied originally from Olac laboratories (Lunn et al., 1989). Superficially, these mice showed no readily discernible phenotype and were easy to breed. What distinguished these mice was the findings that Wallerian degeneration is significantly delayed and protracted after axotomy. Thus, the distal portion of cut axons and their motor nerve terminals remain morphologically intact for as long as 2 weeks. A similar breeding colony, from the same original source, was found to be established in Edinburgh. In both colonies, the remarkable finding was made that isolated distal axons were still capable of conducting action potentials, and neuromuscular synapses continued to release neurotransmitter and recycle synaptic vesicles, despite being disconnected from their cell bodies (Tsao et al., 1994; Ribchester et al., 1995). Both sensory and motor axons are delayed in their degeneration in these "Ola" mice, and the mutation also delays Wallerian degeneration in the central nervous system, for example following section of the optic nerve (Perry et al., 1990a; Ludwin and Bisby, 1992).

### 1.5.1 Molecular Genetics of the Wld$^s$ Mouse

Genomic analysis of the mutant subsequently led to it's redesignation as Wld$^s$ (Lyon et al., 1993). The nature of the Wld$^s$ mutation has now also been almost unequivocally demonstrated (Figure 1.3).

Perry et al (1990b) produced genetic outcrosses and backcrosses with the Wld$^s$ mouse and as a result showed that the mutation is controlled by a single autosomal dominant gene. Further studies mapped the Wld locus to the distal end of chromosome 4, the region homologous with the human chromosomal region 1p34-1p36 (Lyon et al., 1993). The Wld locus was subsequently identified to be an 85-kb tandem triplication within the candidate region, although in some mice there is a duplication allele indicating that there may be some instability in the repeat copy number (Coleman et al., 1998).

Recent studies have identified exons of three genes located within the 85-kb repeat sequence which could account for the Wld$^s$ phenotype (Conforti et al., 2000). Two genes, ubiquitin fusion degradation protein 2 (Ufd2) and a novel gene, D4Cole1e, were reported to span the proximal and distal boundaries of the repeat unit, forming a chimeric gene with an open reading frame coding for a 43kDa fusion protein. The Wld$^s$ gene and its protein product are strongly expressed in the nervous system of Wld$^s$ mice.

**Fig 1.3** **Genetics of the Wld$^s$ Mouse.**

(A) Location of exons within the 85-Kb triplication repeat unit in the Wld$^s$ mutant mouse, showing the formation of the Ube4b/Nmnat chimeric gene and the triplication of the complete Rbp7 gene. (Based on Conforti et al. (2000)).

## C57Bl/6J

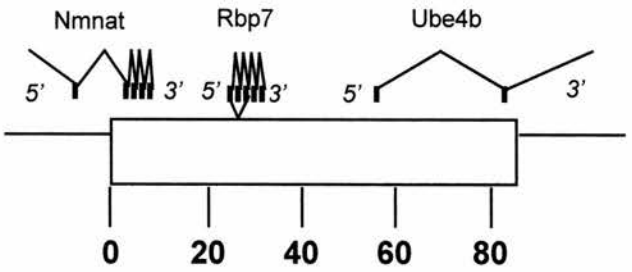


## C57Bl/Wld$^{S}$

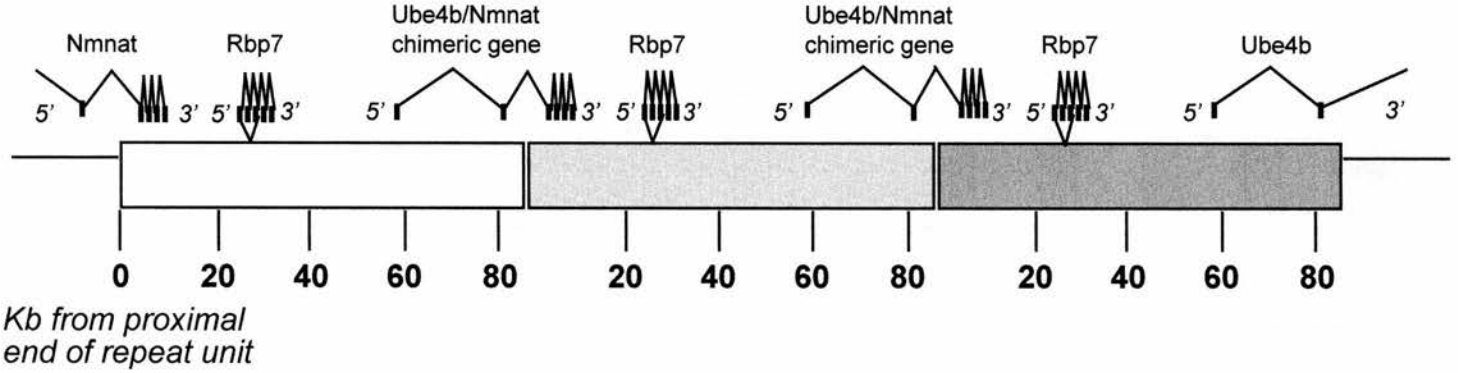

It has since been shown that the novel sequence D4Cole1e incorporates the complete sequence encoding Nicotinamide mononucleotide adenylyl transferase (Nmnat), the enzyme responsible for synthesising NAD (Emanuelli et al., 2001), but incorporating an N-terminal sequence of 18 amino acids that is not normally translated in Nmnat. Similarly, ubiquitin fusion degradation protein 2 (Ufd2) has been shown to be homologous to the human ubiquitination factor E4b (Ube4b; Mack et al., 2001 submitted).

### 1.5.2 Evidence that Slow Wallerian Degeneration in the Wld$^s$ Mouse is an Intrinsic Property of the Nerve

Despite the recent demonstration of the genetic characteristics of the Wld$^s$ mutant, the exact function of the gene and the mechanisms by which it confers protection from the effects of axonal injury are not known. In their initial paper describing the Wld$^s$ mouse, Lunn et al (1989) postulated that the reason for the slow progression of Wallerian degeneration was a problem with the recruitment of myelomonocytic cells to the distal portion of the axon. However, they subsequently refuted this hypothesis, by showing in transplant experiments that the phenotype was not due to a defect in the circulating monocyte population (Perry et al., 1990c). They concluded that the mutation therefore alters intrinsic properties of axons. These findings were supported by Glass et al (1993) who showed that Wld$^s$ axons still degenerate slowly within grafted peripheral nerve sheaths containing wild-type Schwann cells, while axotomised wild-type axons

degenerate normally within an environment containing Wld$^s$ Schwann cells. Likewise, axotomy of Wld$^s$ axons demyelinated by intraneural injection of lysophosphatidyl choline resulted in slow degeneration of the distal stump (Hall, 1993).

Axotomised Wld$^s$ neurites also persist in tissue culture. For example, Deckwerth and Johnson (1994) studied Wld$^s$ sympathetic neurones from the superior cervical ganglion. In wild type neurones the cell body and axons degenerate concurrently following the removal of NGF (Edwards and Tolkovsky, 1994). However, in cultures of Wld$^s$ neurones where NGF was absent, the axons survived whilst cell bodies underwent apoptosis. Distal neurites also persist following physical axotomy in culture (Glass et al., 1993), although the survival of axons depends on how long the neurones are cultured before cutting their axons (Buckmaster et al., 1995).

### 1.5.3 Effect of the Wld$^s$ Mutation on Axotomised Neuromuscular Junctions

As well as axons, axotomised motor nerve terminals are preserved as a result of the Wld$^s$ mutation. As mentioned above, Ribchester et al (1995) showed that Wld$^s$ NMJs are retained alongside their axons and sustain their ability to release neurotransmitter and recycle synaptic vesicle membrane for at least 3 days, and in some cases as long as 2 weeks, following nerve lesion. This study also provided some preliminary data concerning the ultrastructure of persistent motor nerve terminals in axotomised Wld$^s$

mice. The authors showed that the general architecture of a nerve terminal is preserved 5 days after axotomy with no signs of degeneration.

Furthermore, preliminary evidence of a piecemeal withdrawal process at axotomised $Wld^s$ nerve terminals has since been presented based on studies using vital dye labelling, immunocytochemistry, electrophysiology and nerve / muscle cultures (Mattison et al., 1996; Parson et al., 1998). These studies suggest that nerve terminals may retract from the endplate, bouton by bouton, until they form a characteristic bulbous swelling at the distal end of the axon and become detached from the endplate (R. Mattison, PhD Thesis, University of Edinburgh). Physiological changes at these synapses include a reduced quantal content and the occasional appearance of 'giant' MEPPs. Taken together, these findings suggest that the events taking place at axotomised $Wld^s$ NMJs are distinct from the synchronous degeneration of terminals observed at wild-type denervated NMJs. No systematic study of the morphology of axotomised synaptic boutons at an ultrastructural level had been carried out prior to those described in the present thesis.

### 1.5.4 Secondary Characteristics of the $Wld^s$ Mutation

Although the $Wld^s$ mouse appears indistinguishable in appearance and behaviour from the C57Bl/6J mouse, both operated and unoperated $Wld^s$ mice show some subtle, as yet

unexplained, phenotypic features, suggesting that slow nerve degeneration is not the only effect of the $Wld^s$ mutation.

Brown et al (1991) found that normal, unoperated $Wld^s$ soleus muscles express greater intrinsic tension, fewer macrophages per muscle fibre and lower basal levels of acetylcholine sensitivity than their wild type counterparts. Using high resolution $^1H$ magnetic resonance spectroscopy (MRS), Tsao et al (1999a) detected altered cerebral metabolism (indicated by decreased levels of glutamate and phosphocholine relative to total N-acetyl aspartate content) in $Wld^s$ mice compared to wild type controls.

Other studies describe specific axotomy-related secondary characteristics associated with the $Wld^s$ phenotype. For example, axotomy-induced motoneurone death in neonates (Lapper et al., 1994) and retrograde degeneration of cell bodies in axotomised adult retinal ganglion cells (Perry et al., 1990a) are also significantly delayed. In denervated $Wld^s$ muscles, the initiation of muscle atrophy and development of acetylcholine sensitivity have a slower onset, and the rise in serum creatine kinase levels is also delayed (Brown et al., 1991). Interestingly, the degenerative axonal response following exposure to the neurotoxin vincristine is delayed in the $Wld^s$ mouse, suggesting common pathophysiological mechanisms between Wallerian degeneration and toxic neuropathy (Wang et al., 2001).

Axon-glia signalling plays an important role in the maintenance and control of both cell types *in vivo*. Sprouting responses of non-myelinating terminal Schwann cells are delayed by several days (both *in vivo* and *in vitro*) following denervation in the $Wld^s$ (Barry et al., 1997; Parson et al., 1998a). The resident Schwann cells in peripheral nerve produce potential maintenance factors which are taken up by the axon: for example, ciliary neurotrophic factor (CNTF). Following axotomy in the $Wld^s$ mouse, both mRNA and protein levels of CNTF remain normal for up to 4 days, whereas in wild type animals they both decline rapidly and synchronously (Subang et al., 1997). However, by ten days after axotomy, CNTF mRNA levels in the $Wld^s$ mice have decreased to wild type levels, but levels of CNTF protein remain unchanged. This suggests that the CNTF protein is relatively stable in axotomised $Wld^s$ axons. Its retention could contribute some protection against degeneration.

The failure of macrophage recruitment after axotomy (see above) may be due to a failure of the nerve to produce a chemotactic signal, or there may be some form of blockade which prevents the myelomonocytic cells entering the nerve (Perry et al., 1990c). Some candidates for this chemotactic signal are the monocyte chemoattractant protein-1 (JE) which fails to be induced in $Wld^s$ mice following axotomy (Carroll and Frohnert, 1998) and granulocyte macrophage colony stimulating factor (GM-CSF) whose levels are also deficient following axotomy in $Wld^s$ Mice. It is also possible that persisting distal axons produce a factor that inhibits macrophage recruitment, whereas production of this normally ceases in axotomised wild-type axons (Ludwin and Bisby,

1992). Whether any or all of these features are related to Ube4b/Nmnat over expression in Wld$^s$ mice remains to be tested.

### 1.5.5 Effects of the Wld$^s$ Mutation on Nerve Regeneration

Following axotomy in the PNS, immediate-early gene expression is initiated within a few hours, and after an initial "dying back", the proximal axon stump is primed for regeneration, which begins 5-48hrs after the lesion (Ramon y Cajal 1928; Brecknell and Fawcett, 1996). In mice, this process gains momentum and proceeds over a number of days before achieving a reinnervation of skeletal muscle after about 2-3 weeks.

Previously Wallerian degeneration was thought to play a functional role in generating an environment conducive to nerve regeneration (Ramon y Cajal., 1928). It was therefore hypothesised that in the Wld$^s$ mouse, intact distal nerve stumps would be equivalent in their obstructive effect to intact nerves. Brown et al (1991a) showed that severed axons would not grow into a completely undegenerated portion of nerve. Remarkably however, regeneration of motor axons after a nerve crush injury in the Wld$^s$ is not prevented by the presence of axons in the remaining distal nerve stump (Lunn et al., 1989). This suggests that even though Wld$^s$ axons persist after axotomy and remain capable of functioning normally, they may undergo some conformational changes that allow regenerating nerves to progress along the distal stump.

Other studies suggest that whilst motor axons appear able to regenerate almost as well as in wild type mice, sensory nerve regeneration in $Wld^s$ mice is significantly impaired (Bisby and Chen, 1990; Brown et al., 1992). Sommer and Schafers (1998) showed that the delay in sensory nerve regeneration leads to prolonged mechanical allodynia (a condition in which ordinarily non-painful stimuli evoke pain). One possible explanation for the disparity between the regeneration of motor and sensory nerves is that axotomised sensory nerve axons degenerate and regenerate more slowly because they are responsive to NGF levels (Bisby and Chen, 1990) and NGF levels do not increase as rapidly after nerve section in $Wld^s$ mice compared to wild-type (Brown et al., 1991). Motor axons do not respond to NGF. They also appear to be more opportunistic, using myelinating and non-myelinating Schwann cells to guide regeneration (Brown et al., 1992; Brown et al., 1993). Tenascin-C is upregulated selectively in Schwann cells of axotomised muscle nerves of $Wld^s$ mice, and axons regenerate more rapidly in these nerves than in cutaneous nerves where there is delayed expression of Tenascin-C (Fruttiger et al., 1995). Conversely, Myelin-associated glycoprotein (MAG) normally inhibits axon regeneration, but the rate of axon regeneration in $Wld^s$ mice was partially restored when these mice were cross-bred with MAG knockout mice (Schafer et al., 1996).

Shi and Stanfield (1996) also reported differences in sprouting and regeneration patterns in the CNS of the $Wld^s$ mouse. In wild type mice, sprouting responses are detected in the septohippocampal and hippocampal commissural projections within 3 days of a

lesion to the perforant path to the dentate gyrus. However, in Wld$^s$ mice septohippocampal axonal sprouting was only observed 5-7 days after a perforant pathway lesion and changes in the distribution of commissural axons in the dentate gyrus were not observed before 12 days. It would clearly be of interest to establish the fate of axotomised synapses, and their associations with astrocytic neuroglia following axonal lesions in the brains of Wld$^s$ mice.

Alterations in the rate and extent of both motor and sensory reinnervation occurring as a result of the Wld$^s$ mutation are not due to problems with the cell body reaction to axotomy. The time-course of expression of transcription factors such as c-Jun is very similar in Wld$^s$ mice to those in BALB/c controls (Brown et al., 1993).

## 1.6 Mechanisms of Neurodegeneration

The distinctive nature of neuronal cell death by apoptosis (for reviews see Nijhawan et al., 2000; Yuan and Yanker, 2000), and the Wallerian degeneration of distal axons suggests that more than one mechanism is embedded in neurones for executing neurodegenerative processes.

### 1.6.1 Neuronal Apoptosis

The term 'apoptosis' was coined by Kerr et al (1972), to describe a process involved in the normal turnover of hepatocytes: intrinsic cell suicide. It was subsequently shown to be a widespread mechanism found in almost all tissues of the body. There are three main regulators of apoptosis in neurones: the Bcl-2 family of proteins, an adaptor protein known as apoptotic protease-activating factor 1 (Apaf-1) and the cysteine protease caspase family (Yuan and Yanker, 2000). Recent evidence has complicated the matter however, by showing that the "involvement of specific caspases and the occurrence of caspase-independent programmed cell death may be dependent on brain region, cell type, age, and species" (Oppenheim et al., 2001). In the majority of instances, neuronal apoptosis is also inhibited by growth factors and by over-expression of genes such as Bcl-2. By contrast, Wallerian degeneration appears to be independent of the same growth factors from the cell bodies, and is unaffected by the overexpression of Bcl-2 (Dubois-Dauphon et al., 1994; Sagot et al., 1995; Burne et al., 1996).

### 1.6.2 'Cytoplastic' Apoptosis of Axons

Whilst some of the cellular processes which occur during Wallerian degeneration (for example; ellipsoid body formation) are remarkably similar to those seen during apoptosis, Wallerian degeneration obviously cannot involve all apoptotic cellular processes (eg. DNA degradation) because axotomised distal stumps do not include motoneurone cell bodies. However, it has previously been shown that apoptosis can occur in the absence of RNA or protein synthesis (Martin, 1993) and in cells lacking nuclei (Ellerby et al., 1997; Jacobson et al., 1994). Thus, a number of authors have suggested that axonal degeneration might be viewed as a form of 'cytoplastic apoptosis' (Ribchester et al., 1995; Buckmaster et al., 1995; Alvarez et al., 2000). Studies in which the role of Bcl-2 in axonal degeneration was examined also concluded that the molecular mechanisms involved are distinct from those activated during apoptosis of neuronal cell bodies. Burne et al (1996) showed that over-expression of the human Bcl-2 protein in retinal ganglion cells protects the cell body as expected. However, the axons were not protected from Wallerian degeneration. Similar findings were reported in a study by Sagot et al (1995) who examined the fate of cell bodies and axons in a mouse model of motor neurone disease with Bcl-2 over-expression. The increased level of Bcl-2 rescued facial motoneurones and restored their soma size and choline acetyltransferase expression. However, there was no effect on the rate of axonal degeneration in facial and phrenic motoneurones. Thus it seems unlikely that Bcl-2 itself plays a significant role in axon degeneration.

Finn et al (2000) recently examined whether the molecular machinery of Wallerian degeneration depends upon the caspase family of cysteine proteases. They found that caspase-3 (which is thought to be important for apoptosis in neurones) was not activated in the axon during Wallerian degeneration. Thus, they argued that Wallerian degeneration is molecularly distinct from the classical caspase-dependent apoptotic process implicated in axonal degeneration.

### 1.6.3 'Synaptic Apoptosis'

Evidence in support of the hypothesis that the degeneration of synapses is regulated independently from that of cell bodies or axons is currently lacking in comparison to the data available concerning somatic and axonal degeneration. Some data has been obtained in recent studies of CNS neurones however. For example, Ivins et al (1998) have shown that exposure to an apoptotic stimulus (amyloid β-peptide) plays a crucial role in inducing the activation of caspases and hence apoptosis in cultured hippocampal neurones. Using the same cell-death stimulus, Mattson et al (1998b) found no caspase activation in axons, but instead reported that caspases were activated in cortical synaptosomes. Their data also provide evidence that apoptotic biochemical cascades (such as caspase activation) are selectively triggered at synaptic sites following exposure to staurosporine and $Fe^{2+}$. The term 'synaptic apoptosis' was proposed (Mattson et al., 1998a; Mattson et al., 1998b; Mattson, 2000; Guo and Mattson, 2000).

## 1.7 Synapse Elimination

The withdrawal of nerve terminals during synapse elimination is currently the best understood incidence of synapse specific rearrangement and plasticity in the mammalian nervous system. As it has been suggested that the withdrawal of axotomised synaptic terminals in $Wld^s$ mice may resemble certain aspects of synapse elimination (Mattison et al., 1996; Parson et al., 1998; R. Mattison, PhD Thesis, University of Edinburgh), it would hardly be surprising if common mechanisms were involved.

Early studies by Tello (1917) and Boeke (1921) described how neonatal mammalian skeletal muscle fibres are innervated at a single site by multiple motor nerve terminals arising from several motoneurones ('polyneuronal innervation'; Redfern, 1970; Brown et al., 1976). A similar innervation pattern is re-established following nerve injury and subsequent regeneration in adult muscle (McArdle, 1975; Ribchester, 1988; Costanzo et al., 1999; Costanzo et al., 2000). A refinement of these synaptic connections occurs with time via a process known as synapse elimination, resulting in the vast majority of endplates being innervated by a single motor axon (see Ribchester, 2001 for recent review).

Whilst the majority of research into synapse elimination has been undertaken using NMJ preparations, there are numerous other studies which describe developmental

synapse elimination occurring in regions of the CNS: in the visual system (Hubel et al., 1977), in autonomic ganglia (Lichtman, 1977) and in the cerebellum (Lohof et al., 1996). These can involve multiple inputs being withdrawn, leading to single innervation, as at climbing fibre/Purkinje cell synapses in the cerebellum, or can involve a 'rearrangement' of many inputs whilst maintaining multiple innervation such as occurs during the development of thalamocortical / cortical layer 4 synapses in the visual system. As this study concentrates on plastic mechanisms at the NMJ, the following introduction will refer to the transition from multiple to single innervation.

### 1.7.1 The Nature of Synapse Elimination at the NMJ

Neuromuscular synaptogenesis begins shortly after myoblast fusion occurs during development (Bennett and Pettigrew, 1974). It appears to occur in a random manner, with each motor neurone establishing synapses on many different muscle fibres (Jennings, 1994). The end result of this synaptogenic period is that each skeletal muscle fibre receives convergent inputs from more than one motor axon. In rodents it is not until the first few postnatal weeks however that synapse elimination refines these connections (Redfern, 1970; Brown et al., 1976; Betz et al., 1979). Other studies extended these findings to show that synapse elimination occurs in the nervous systems of other species such as kittens (Bagust et al., 1973) and humans (Huttenlocher et al., 1982; Ijkema-Paassen and Gramsbergen, 1998).

Brown and colleagues showed, in their now-classic (1976) study on innervation of the neonatal soleus muscle, that the elimination of polyneuronal innervation does not occur by axonal death or degeneration (Brown et al., 1976). Evidence for this was provided by demonstrating that during the transition from poly- to mono-innervation there was no reduction in the number of motor neurones innervating the muscle. They therefore concluded that the removal of supernumerary inputs reflects a reduction in the number of synaptic connections made by each individual motor neurone. Furthermore, these authors demonstrated that the process of synapse elimination occurs without transient denervation of endplates. Moreover, such a retention of synaptic interactions has subsequently been shown to be crucial for the normal postnatal development of other extra-synaptic portions of the neurone, such as the soma and dendrites (Dekkers and Navarrete, 1998).

When the ultrastructure of nerve terminals on neonatal muscle fibres was examined using the electron microscope, convincing evidence was provided that synapses are indeed retracted from endplates during synapse elimination rather than undergoing a degenerative process similar to Wallerian degeneration. Both Korneliussen and Jansen (1976) and Bixby (1981) found no signs of degenerative processes occurring in any nerve terminal profiles during the period of synapse elimination in rats and rabbits respectively. These findings were extended in studies by Riley who observed axonal retraction during synapse elimination using both the light and electron microscope (Riley, 1977; Riley, 1981). He described how axons and their nerve terminals which

are withdrawing from an endplate forming 'retraction bulbs', characterised by a terminal oval enlargement. Ultrastructural observation of such bulbs showed them to be laden with vesicles, strongly suggesting that they are the morphological manifestations of a packaged up nerve terminal.

There has been one study however which proposes that supernumerary terminals are removed by degenerative mechanisms. Rosenthal and Taraskevich (1977) described ultrastructural profiles of neonatal endplates showing signs of "abnormal structure" during the period of synapse elimination. Some of the terminals they examined showed a clustering of synaptic vesicles as well as terminal Schwann cell encroachment into the synaptic cleft. They also described the presence of large areas of postsynaptic membrane with only a Schwann cell present. All of these are characteristics associated with Wallerian degeneration of motor nerve terminals. Despite this study, for which an adequate explanation has yet to be provided, the vast majority of evidence supports the hypothesis that supernumerary inputs are removed by a process of withdrawal rather than degeneration.

### 1.7.2 Mechanisms Underlying Synapse Elimination at the NMJ

Although the current study is not specifically directed towards the study of synapse elimination, an understanding of the mechanisms which underlie this phenomenon,

whilst demonstrating the fine cellular control present at synaptic connections in general, may also provide insights into the machinery which is responsible for regulating the synaptic events occurring at axotomised $Wld^s$ NMJs.

The occurrence of synapse elimination is neither spontaneous nor random (Costanzo et al., 2000). It is usually considered to be a competitive process whereby neurones and their synapses compete within spatial and / or consumptive constraints (Betz et al., 1980; Ribchester and Barry, 1994). However, other studies (Thompson and Jansen, 1977; Fladby and Jansen, 1987) have shown that nerve terminals can be withdrawn from the endplate, even in the absence of competitors, thereby suggesting that such terminals are capable of responding to an intrinsic programme of the motor neurone to reduce its number of synapses. Smallheiser and Crain (1984) proposed a similar intrinsic mechanism of nerve terminal loss, whereby the process of synapse elimination is driven by 'sibling neurite bias'. Whilst the reasons underlying the conflicting results from these studies have yet to adequately addressed, it remains possible that both mechanisms may occur during synapse elimination, acting either in conjunction with one another or independently.

One hypothesis which explains synapse elimination as a competitive phenomenon utilises the 'neurotrophic theory'. It proposes that neurones depend upon their target organs (in the case of the NMJ, skeletal muscle fibres) for trophic sustenance (Purves, 1988). This leads to a situation whereby neurones compete for a limited amount of a

trophic substance (neurotrophic factor) provided by the muscle fibre (Grinnell et al., 1979; Purves and Lichtman, 1985; Ribchester and Barry, 1994). Those terminals best capable of securing and utilising such a factor may therefore gain a competitive advantage over neighbouring terminals competing for the same resource.

It is also thought that orthograde patterns of activity in a neurone may have a role in controlling the level of production, availability and / or accessibility of trophic factors from the target organ (Ribchester and Barry, 1994). For example: upon the initial, polyneuronal, innervation of a muscle fibre, general activity levels are relatively low, leading to large amounts of neurotrophic factor release. As receptors on the motor nerve terminals are therefore binding high levels of such a factor, they gradually increase their ability to release neurotransmitter (Ribchester et al., 1998) thereby upregulating their level of activity. An increased level of motor neurone activity then suppresses the production of neurotrophic factors by the muscle fibres. If one of the competing inputs manages to take up more of the trophic substance than others, it gains a major competitive advantage as it can strengthen it's own connection whilst reducing the levels of trophic factor being produced. With a lower level of trophic factor present, other competing inputs can no longer gain enough to sustain themselves nor strengthen their connections. This situation could quite feasibly lead to a domination by a single input, and a subsequent withdrawal of all others.

The neurotrophic theory of synapse elimination is probably an oversimplification however. A more intricate mechanism for synapse elimination has since been proposed in an elegant series of experiments by Balice-Gordon and Lichtman (1994). These authors focally applied α-bungarotoxin to a small region of a NMJ. This block in neurotransmission led to long-lasting synapse elimination at that portion of the endplate. In contrast they showed that an application of α-bungarotoxin to the whole of a NMJ did not lead to any synapse elimination. From these experiments they concluded that active synapses produce both an elimination and a protective signal, whilst inactive synapses produce neither. This, they argued, can lead to the elimination of an inactive synapse and the retention of it's active 'competitor'. Whilst it is unlikely that any of the converging inputs at an endplate would be completely inactive, this model can easily be applied to a more subtle situation, where slightly stronger inputs (possibly due to the effect of a simple 'neurotrophic' style competition) are able to both protect themselves better, at the same time as producing a stronger elimination signal, than weaker inputs.

Many studies have shown that the pattern of neural activity is a major driving force behind synapse elimination (Hubel at el, 1977; LeVay et al., 1980; Wiesel, 1982; Jennings, 1994; Lohof et al., 1996; Sanes and Lichtman, 1999). Experiments utilising the NMJ have addressed the hypothesis that an asynchronous activation of postsynaptic receptors is responsible for the initiation of synapse elimination (Balice-Gordon and Lichtman, 1994). Over the course of several days following the application of a saturising dose of bungarotoxin, receptors were lost from the post synaptic apparatus.

Following this, nerve terminals which were previously overlying the now vacated receptor sites were seen to retract from the endplate. These events reflect both the time course and pattern of events witnessed during naturally occurring synapse elimination (Lichtman and Colman, 2000). In a recent study by Bussetto and colleagues (Bussetto et al., 2000), these findings were further extended by showing that synchronous axonal activation indeed prevents synapse elimination. The conclusions to be drawn from these studies imply that it is not activity per se, but rather the relative size, strengths and firing patterns of different portions of the NMJ which are responsible for determining the likelihood of withdrawal of small, inactive inputs. Furthermore, recent evidence suggests that these processes may be mediated by the differing roles played by presynaptic calcium channel types at separate inputs converging on a polyneuronally innervated NMJ (Santafe et al., 2001).

Whilst it is almost universally accepted that activity is influential on synapse elimination, the hypothesis which states that the level and synchronisation of activity is the main underlying force responsible for driving synapse elimination is slowly being refuted. Studies have shown that if a portion of axons supplying a muscle are blocked during development, the inactive axon collaterals are less susceptible to synapse elimination than their active counterparts (Callaway et al., 1987). Studies of NMJs in control and reinnervated muscle preparations have provided evidence for the persistence of polyneuronal innervation in a few junctions, many months after the synapse elimination period is completed (Werle and Herrera, 1987; Jordan et al., 1988; Werle

and Herrera, 1991; Barry and Ribchester, 1995). The only possible way in which these results can support the activity hypothesis is if the activity patterns of converging inputs at these persistent junctions are synchronous. Whilst this is not impossible, it has to be considered highly unlikely.

Further evidence has recently been provided to show that activity, whilst being influential, is neither sufficient nor necessary for synapse elimination (Costanzo et al., 1999 and 2000), which appears to refute the activity hypothesis of Balice-Gordon and Lichtman (1994). These studies demonstrated that activation (either evoked or spontaneous) of postsynaptic receptor sites is not required for the competitive elimination of an existing terminals by a regenerating axon, and that the remodelling of synapses in general can continue in the absence of activity.

## 1.8 Aims of the Present Study

This thesis has three main aims;

1) To extend knowledge and understanding of the fate of NMJs in normal and $Wld^s$ mice following axotomy. Qualitative and quantitative vital staining, immunocytochemical and ultrastructural experiments were carried out on control and axotomised $Wld^s$ nerve/muscle preparations. One purpose of these experiments was to seek evidence in support of previous studies which have shown that axotomised $Wld^s$ motor nerve terminals are lost by a process of piecemeal withdrawal. The main purpose however, was to extend these findings to include a systematic study of the morphology of axotomised synaptic boutons at an ultrastructural level. The latter was aimed at providing unequivocal evidence that the loss of axotomised nerve terminals from young (<2 month old) $Wld^s$ mice occurs via a process separate and distinct from that of Wallerian degeneration. In order to achieve this, both qualitative and quantitative data from control NMJ profiles were compared to those from axotomised $Wld^s$ NMJ profiles at 3, 4, 5 and 7 days post axotomy.

2) To address the controversy in the literature over a possible age-dependent expression of the $Wld^s$ phenotype. This was achieved by a qualitative and quantitative comparison of the morphological and ultrastructural events occurring at axotomised NMJs from $Wld^s$ of 2, 4 and 7 months of age. These experiments were designed not

only to assess variations in the rate, but also the mechanisms, of nerve terminal loss in Wld$^s$ of different ages. By comparing these findings to those produced from wild-type preparations as well as previous descriptions of the morphological events underlying Wallerian degeneration, it was possible to assess the incidence of the latter at axotomised nerve terminals from all Wld$^s$ age groups. An examination of cross sections from the tibial nerve, from both above and below the site of nerve lesion, allowed for a comparison of alterations in the rate of axonal and nerve terminal degeneration from young and old Wld$^s$ mice.

3) To test the hypothesis that the Wld$^s$ phenotype is produced as a result of the expression of a Ube4b/Nmnat chimeric gene. This hypothesis was tested by examining the effect of axotomy on NMJs from transgenic mice engineered to strongly express the Ube4b/Nmnat chimeric gene and its protein under a β-actin promoter. Morphological and ultrastructural analysis of these preparations, alongside comparisons made against the findings from Wld$^s$ and wild-type studies described above, allowed an assessment of the level of expression of the Wld$^s$ phenotype in Ube4b/Nmnat transgenic mice.

# General Methods

## 2.1 General

The protocols detailed in this section are common to all chapters. Procedures specific to an individual chapter are detailed in subsequent sections.

### 2.1.1 Animals and Animal Care

Male and Female C57Bl/Wld$^{s}$ mice, female C57Bl/6J, C3H and Swiss mice were used for experiments. Animals were housed in cages of 5 or less with free access to food and water. Environmental conditions were those of a standard animal house.

### 2.1.2 Aseptic Procedures

All surgical procedures were undertaken in aseptic conditions and were fully licensed by the UK Home Office. All instruments, cloths and gowns used were sterilised on site. Other equipment such as gloves and suture threads were sterilised by the manufacturer before delivery. The operative areas of the animal were shaved and swabbed with antiseptic (Betadine; Seton Healthcare Group, Plc.) before incisions were made.

### 2.1.3 Operative Procedures

*Anaesthesia*

Anaesthesia was induced via inhalation, by placing the animal in a sealed perspex chamber into which Halothane (Rhone-Poulenc Rorer, Ltd.) at 5% in $N_2O$ / $O_2$ (1:1) was delivered, using a Fluovac System (International Market Supply). Upon the induction of anaesthesia, the animal was transferred to the operating table where anaesthetic was continued to be delivered via a face mask. Following a toe-pinch reflex test to assess the level of anaesthesia, the level of halothane was reduced to 1% in $N_2O$ / $O_2$ (1:1). The animal was monitored throughout the procedures to maintain the correct level of anaesthesia.

*Nerve Cut*

Once a suitable depth of anaesthesia had been achieved, the skin and fascia covering either the sciatic nerve in the thigh, or the tibial nerve in the calf, were opened and reflected. When the nerve was sufficiently exposed a 1-2mm section was cut out using sharp dissection scissors. The wound site was closed and the skin was sutured using 7/0 silk suture (Ethicon).

### 2.1.4 Animal Sacrifice

All animals were killed either by cervical dislocation or by exposure to ever increasing levels of $CO_2$, in accordance with schedule 1 of the licensing regulations provided by the UK Home Office.

### 2.1.5 Nerve-Muscle Preparations

***Flexor Digitorum Brevis (FDB)***

Immediately following sacrifice, hind limbs were removed and FDB muscles were dissected, with or without their intact nerve supply, in mammalian physiological saline (mM concentrations: NaCl 120; KCl 5; $CaCl_2$ 2; $MgCl_2$ 1; $NaHCO_3$ 23.8; D-glucose 5.6), bubbled with $O_2$ / $CO_2$ (95% / 5%). Dissected FDB preparations were pinned out in Sylgard (Dow Corning) coated petri dishes, containing the oxygenated physiological saline, using 0.2mm diameter minutien pins (Interfocus Ltd).

***Transversus Abdominus (TA)***

Immediately following sacrifice, the rib cage and its attached inferior musculature were removed. The gross dissections were pinned out in Sylgard coated petri dishes, containing oxygenated physiological saline, using 0.2mm diameter minutien pins. The TA muscle, and it's nerve supply if required, were then exposed by dissecting away overlying fascia.

*Lumbrical Muscles*

Immediately following sacrifice, hind limbs were removed and 1DLs and/or 4DLs were dissected, with or without their intact (dual in the case of 4DL) nerve supply, in oxygenated mammalian physiological saline. Dissected preparations were pinned out in Sylgard coated petri dishes, containing the oxygenated physiological saline, using 0.2mm diameter minutien pins.

## 2.2 Fluorescent Labelling of the Postsynaptic Apparatus

Muscle preparations pinned out in a Sylgard-lined dish were fixed in a 4% paraformaldehyde (Sigma) solution for 45mins before incubation in a 5$\mu$g/ml TRITC-$\alpha$-BTX solution to label AchRs. The solution was kept in permanent motion by placing the dish on a rotating platform for 30mins. The $\alpha$-BTX solution was discarded and the preparation washed in 0.1M PB. See end of chapter for detailed protocol.

## 2.3 Labelling of Axons and Motor Nerve Terminals using Immunocytochemistry

Following labelling of postsynaptic sites with $\alpha$-BTX, muscles were permeabilised and tagged with 1° monoclonal antibodies (Developmental Studies Hybridoma Bank)

directed against synaptic vesicle (SV) proteins (SV2) and 165kDa neurofilament (NF) proteins (2H3). The 1° antibodies were then labelled with FITC-conjugated sheep anti-mouse 2° antibodies (Diagnostics Scotland, Law Hospital, Carluke, Lanarkshire, UK). See end of chapter for detailed protocol.

### 2.4.1 Visualisation of Fluorescent 2° Antibodies / Dyes (Standard Fluorescence Microscope)

Immunocytochemically labelled nerve/muscle preparations were viewed in a fluorescence microscope (CF Fluorescent, Nikon) using a Zeiss 40x water immersion objective and a mercury lamp (Nikon HBO-100W/2). An FITC excitation/emission filter block (450-490nm excitation filter, 510nm dichroic mirror and 510-520 emission filter; Nikon) was used for visualising FITC labelled antibodies, a TRITC excitation/emission filter block (510-560nm excitation filter, 580nm dichroic mirror and 590 emission filter; Nikon) was used for visualising TRITC labelled αBTX, and a triple band pass filter (with excitation and emission filters containing selective filters for both FITC and TRITC and the dichroic mirror containing complementary reflection and transmission bands specific to the excitation and emission filters; Chroma) was used for visualising both FITC and TRITC simultaneously.

The fluorescence microscope was mounted on a stage support (Microinstruments M2B) attached to an anti-vibration table (Newport). Images were captured using a colour

chilled 3CCD camera (Hamamatsu C5810) connected to an Apple G4 computer running Openlab (Improvision) and Adobe Photoshop software. Images were enhanced and analysed using Adobe Photoshop before being printed on an Epson Stylus Colour 900 printer.

### 2.4.2 Quantification of Immunocytochemically Labelled Neuromuscular Junctions

All NMJs on every slide were counted and assessed. Each NMJ was scored with regard to the proportion of the endplate which was contacted by an overlying nerve terminal, and placed into one of the following categories: 100% occupied, 99-75% occupied, 74-50% occupied, 49-25% occupied, 24-1% occupied or vacant. All data were inserted into a Microsoft Excel 2001 spreadsheet for further analysis, and graphs were produced in SigmaPlot (SPSS Science).

### 2.4.3 Visualisation of Fluorescent 2° Antibodies / Dyes (Confocal Microscope)

Some immunocytochemically labelled nerve/muscle preparations were viewed in a Radiance 2000 confocal microscope (Biorad) attached to a Nikon Eclipse E600 microscope equipped with a 40x water immersion objective (Nikon). Images were captured using Lasersharp 2000 software running on a Dell Poweredge 1400 computer.

TIFF files were exported into Adobe Photoshop before being printed on an Epson Stylus Colour 900 printer.

Some confocal images were created as stereo pairs. These images were produced using the Lasersharp 2000 software which can rotate confocal views. An original confocal image was rotated by +6 degrees and –6 degrees, thereby producing two separate rotated images. When these images are placed adjacent to one another, and the two profiles fused by the eyes of the viewer, a three-dimensional image is produced.

## 2.5 Visualisation of NMJ Ultrastructure using Transmission Electron Microscopy

Preparations were pinned out on dental wax before being immersed in a 4% paraformaldehyde / 2.5% glutaraldehyde (Sigma) solution for 4-6 hours at 4 °C. The fixed preparation was then washed and post-fixed in a 1% osmium tetroxide (Sigma) solution before dehydrating through a series of alcohols (incorporating a uranyl acetate stain; Sigma) and embedding in Durcupan resin (Sigma). 70-90nm sections were cut using a Diatome Ultra 45 diamond knife on a Reichert 'Ultracut' ultramicrotome (Reichert). Sections were picked up on 2x1mm Formvar slot grids (Agar Scientific) and stained with Reynold's lead citrate before viewing in a Philips CM12 transmission electron microscope. See end of chapter for detailed protocol.

## 2.6 Ultrastructural Quantification of Withdrawing / Degenerating Motor Nerve Terminals

To prevent counting any one nerve terminal more than once, thin sections were cut at 50$\mu$m intervals. Stained grids (see above) were examined in the electron microscope and all nerve terminal profiles were scored as either normal, partially occupied with no signs of degeneration, partially occupied with signs of degeneration, degenerating or vacant (with or without terminal Schwann cell remaining opposed to the postsynaptic folds). Markers of degeneration included: more than 20% of mitochondria with swelling and disruption of membranes (up to 19% is observed in control preparations and is thought to represent the normal turnover of terminal mitochondria; Winlow and Usherwood, 1975), nerve terminal membrane fragmentation and terminal Schwann cell phagocytosis. Synaptic vesicle levels were also analysed (see below). All data was entered into a Microsoft Excel 2001 spreadsheet for further analysis.

## 2.7 Ultrastructural Quantification of Sub-Cellular Organelles at the NMJ

A new series of thin sections were cut as described above. The reason that the initial set of electron micrographs, used for the analysis of partial occupancy, could not be used for quantitative analysis was that they were taken over a large range of magnifications (2500x up to 120000x). This is not suitable for accurate quantification, therefore TEM

negatives of nerve terminal profiles from the new series of sections, all taken at 13000x magnification, were scanned at 600dpi using a Linoscan 1200 transparency scanner (Heidelberg) connected to an Apple iMac equipped with Linocolour Elite 6.0 software (Heidelberg). TIFF files were created and exported into Adobe Photoshop for contrast enhancement and printing on an Epson Stylus Colour 900 printer. These images were then subjected to two forms of quantitative analysis.

### 2.7.1 Quantification of Organelles at the NMJ

A dot grid (25 x 27 dots at 4mm spacing) acetate sheet was superimposed on individual electron micrographs (adapted from the method described by Hirji et al., 2000). The area of an individual nerve terminal was calculated (using units of dots/terminal$^{-1}$) by counting the total number of dots landing within or contacting the outer membranes of the terminal. The number of dots landing within or contacting the membranes of synaptic vesicles, neurofilaments and mitochondria within the terminal were also recorded.

### 2.7.2 Quantification of Overall Synaptic Vesicle Density at the NMJ

Synaptic vesicles to be counted were identified using a slight modification of the criterion established by Winlow and Usherwood (1975). To be included in the count,

vesicles had to display: a) a clear lumen, b) an unbroken membrane, and c) a diameter of no more than approximately 120nm. Coated vesicles, dense core vesicles and cisternae were included in the count, although they were only occasionally observed.

Synaptic vesicle density within a nerve terminal profile was calculated using the following formula (where 121 represents the number of dots on the counting grid equivalent to $1\mu m^2$):

$$\text{SV density (SV}/\mu m^2) = \text{Number of SV profiles} \div \frac{\text{Total Terminal Area}}{121}$$

### 2.7.3 Quantification of Synaptic Vesicle Packing Density at the NMJ

The proportion of the terminal filled by neurofilaments and mitochondria was calculated and then subtracted from the total area of the terminal, thereby leaving the area in which it is theoretically possible for synaptic vesicles to occur (this method is adapted from that used in previous studies by Usherwood and Rees (1973) and Winlow and Usherwood (1975)):

Total Terminal Area - (NF Area + Mitochondria Area) = Area Available For SV

The percentage of the area available for synaptic vesicles which was actually occupied by vesicles (synaptic vesicle packing density) could then be calculated:

$$\% \text{ of Available Terminal Occupied by SV} = \frac{\text{SV Area}}{\text{(NF Area + Mitochondria Area)}} \times 100$$

All raw data were entered into a Microsoft Excel 2001 spreadsheet where standard statistics were calculated.

### 2.7.4 Localisation of the Synaptic Vesicle Population at the NMJ

Whilst the quantitative analysis described above provides accurate data with regard to the numbers of synaptic vesicles, it gives no indication as to their localisation within a nerve terminal. To establish the numbers of vesicles located at, or near, active zones on the presynaptic membrane (representing 'docked' vesicles from the functionally and morphologically distinct 'ready releasable pool'; Sudhof, 2000; Schikorski and Stevens,2001), a 4.5mm radius circle marked on an acetate sheet was superimposed onto individual electron micrographs (producing a 125nm radius circle on the scale of the electron micrograph). The centre of the measuring circle was placed directly on top

of an active zone on the presynaptic membrane. Active zones were identified as the area of presynaptic membrane (sometimes appearing more electron dense than the membranous regions either side of the zone) directly opposing the opening of a postsynaptic junctional fold. The number of vesicle profiles either within the circle or contacting the boundaries of the circle were counted. The criteria used for the identification of synaptic vesicles was the same as described previously. This procedure was repeated at up to 4 active zones on each terminal. This method is similar to that recently published by Schikorski and Stevens (2001).

The raw data were entered into a Microsoft Excel 2001 spreadsheet where standard statistics were calculated.

## 2.8 Statistical Analysis

Unless otherwise stated, the following statistical tests were performed using Instat (Graphpad Software) running on an Apple iMac computer:

i) Unpaired, nonparametric tests (e.g. Mann Whitney).

ii) Unpaired t tests (eg. Student t test or Welch's test).

## 2.9 Neurofilament, Synaptic Vesicle and AchR Immunocytochemistry Protocol

1. Preparations were fixed in 4% Paraformaldehyde for 40mins:

   4g Paraformaldehyde
   100ml 1 x Phosphate Buffered Saline (PBS; Sigma)
   Heat to 60-70°C whilst stirring continuously
   Add 4-5 drops of 0.1M NaOH
   Wait until solution clears
   Chill to 4°C in fridge

2. Wash 3 times for 10mins in fresh 1 x PBS

*All steps now undertaken on a platform rotator at room temperature and in a sealed, dark box to keep light out.*

3. Incubate in a 0.1M glycine solution for 1hour

4. Incubate in a fresh 5$\mu$g/ml TRITC-$\alpha$-BTX solution for 30mins

5. Wash 3 times for 10mins (or 6x5mins) in blocking soln;

   In 1xPBS
   4% BSA
   0.5% Triton X-100
   0.1M Lysine

6. Incubate in 1° antibody solution overnight:
   4ml Blocking soln
   20$\mu$l NF antibody
   20$\mu$l SV2 antibody

7. Incubate for 1 hour in fresh primary soln.

8. Wash 3 times for 10mins in blocker

9. Incubate in 2° antibody solution for 4 hours:
   4ml 1x PBS
   20$\mu$l FITC sheep-anti-mouse antibody

10. Wash 3 times for 30mins in 1xPBS

11. Mount preparation in Vectashield (Vector Laboratories Inc.) on a slide and coverslip.

12. Store in dark box at 4°C

## 2.10 Transmission Electron Microscopy Protocol

1. Preparations were fixed in a fresh 4% Paraformaldehyde / 2.5% Glutaraldehyde solution for 4-6 hours at 4 °C:

   4g Paraformaldehyde
   35ml $ddH_2O$
   Heat to 60-70°C whilst stirring continuously
   Add 4-5 drops of 0.1M NaOH
   Wait until solution clears
   Filter solution

   Add 10ml of 25% Glutaraldehyde stock solution
   Add 50ml 0.2M PB
   Make up to 100mls with $ddH_2O$
   Chill to 4°C in fridge

2. Wash 3 times for 10mins in fresh 0.1M PB at 4 °C

3. Post-fix preparations in 1% Osmium tetroxide for 45mins on rotator:

   5ml 4% Osmium Stock Solution
   5ml $ddH_2O$
   10ml 0.2M PB

4. Wash 2 times for 10mins in fresh 0.1M PB at 4 °C

5. Wash 2 times for 10mins in $ddH^2O$

6. Dehydrate through a descending series of alcohols;

   50% for 10mins
   70% (including 1% Uranyl Acetate (Sigma)) for 45mins
   90% for 15mins
   100% for 15mins
   100% (with dry filters) for 15mins

7. Immerse in propylene oxide for 2 x 15mins

8. Leave specimens in Durcupan resin overnight at room temperature

9. Block out specimens in resin and leave in oven (65°C) for 48 hours

10. Blocks were trimmed to a $1mm^2$ cutting face using a razor blade before thick sections were taken using a glass knife. Light microscopic analysis of thick sections identified when a suitable area of the muscle had been reached.

11. Thin (70-90nm) sections were cut on a Diatome Ultra Diamond knife and collected on the surface of double distilled, boiled water contained within the attached 'boat'.

12. Sections were exposed to chloroform to remove any excess folding before being collected on Formvar slot grids and left to dry naturally.

13. Grids were stained with uranyl acetate and lead citrate in a LKB 'Ultrostainer' (LKB) before viewing under a Philips CM12 TEM.

# Results Chapter 3

# 3. Responses of Normal and Wld$^s$ Motor Nerve Terminals to Axotomy

## 3.1 Background

Lesion of a vertebrate nerve normally results in the rapid degeneration and subsequent phagocytosis of distal axon stumps and motor nerve terminals, via the process of Wallerian degeneration. The specific characteristics of Wallerian degeneration at motor nerve terminals have been well documented (see chapter 1; Reger, 1959; Miledi and Slater, 1968; Miledi and Slater, 1970; Manolov, 1974; Winlow and Usherwood, 1975). In the naturally occurring Wld$^s$ mutant mouse, degeneration of the axon and motor nerve terminals is significantly delayed following axotomy (Lunn et al., 1989; Tsao et al., 1994; Ribchester et al., 1995). Furthermore, previous studies have suggested that axotomised motor nerve terminals in these mice may undergo a separate kind of degenerative process, morphologically and functionally distinct from that of Wallerian degeneration. There is immunocytochemical evidence for an intermediate stage of partial occupancy of endplates, whereby areas of postsynaptic receptors are present but not contacted by an overlying terminal. This suggests that Wld$^s$ nerve terminals may be retracted in a piecemeal fashion from the endplate following axotomy (Ribchester et al., 1995; Mattison et al., 1996; Parson et al., 1998; Ribchester et al., 1999). Ribchester et al. (1995) also provided a limited account of the ultrastructural preservation of Wld$^s$ motor nerve terminals, showing that terminal architecture is

retained for up to 5 days post axotomy. Electrophysiological investigation of axotomised Wld$^s$ NMJs suggested that nerve terminal withdrawal is accompanied by a progressive weakening of synaptic transmission, as indicated by an increased variance in EPP amplitude and a reduced quantal content (Ribchester et al., 1999; Derek Thomson, personal communication).

This chapter confirms and extends the above findings, and includes evidence which supports the hypothesis that axotomised Wld$^s$ nerve terminals are lost by a mechanism that is distinct from the mechanism of degeneration at wild-type NMJs.

First, I present experimental data regarding the morphological and ultrastructural characteristics of unoperated, axotomised and toxin-treated wild-type mouse NMJs using immunocytochemistry, vital-dye staining, confocal microscopy and electron microscopy. Although the events which occur at axotomised wild-type NMJs have been well documented (see chapter 1), and a few comparisons within this thesis are made using previously published findings, this 'control' data was generated for several reasons. Firstly, it provided an accurate representation of wild-type characteristics using the tissue processing techniques specific to this study. Other authors have used experimental protocols which differ from those described in this thesis to assess the role of axotomy at the NMJ. Some examples of these differences include: Miledi and Slater (1970) and Manolov (1974), who both used rats rather than mice; Miledi and Slater (1970), Manolov (1974) and Winlow and Usherwood (1975), who all used diaphragm

muscle preparations rather than FDB muscle preparations; Manolov (1974), who relied on a single osmium fixation step rather than inserting a paraformaldehyde / glutaraldehyde fixation step before post-fixation in osmium; and Winlow and Usherwood (1975), who used Araldite resin to embed their tissue rather than Durcupan resin. Whilst these methods may only deviate slightly from my own, and variability of results should theoretically be minimal between these different studies, by producing wild-type data using the same techniques as those used for $Wld^S$ preparations described later in this study, comparisons between different experimental groups should be more accurate. Secondly, control preparations were treated with α-latrotoxin and *Steatoda* toxin in order to assess the sensitivity of the ultrastructural quantification techniques used in this study. Application of purified α-latrotoxin (2nM) produces very high, sustained MEPP frequencies (several hundred $sec^{-1}$; Ribchester et al., 1998) within five minutes of application. Similarly, application of gland extract from the theridiid spider, *Steatoda paykulliana* (often mistaken for the black widow spider; Cavalieri et al., 1987) increases the MEPP rate from less than one $sec^{-1}$ to several hundred $sec^{-1}$ (Gillingwater et al., 1999). Both of these toxins produce rises in intracellular calcium via the insertion of $Ca^{2+}$ channels in membranes (Usmanov et al., 1985), and as a result a mass exocytosis of synaptic vesicles. Following application of either toxin for more than 20 minutes, MEPP frequency declines until no further signs of spontaneous transmitter release can be detected. Ultrastructural analysis confirmed a resultant depletion of synaptic vesicles, yet a retention of the overall architecture at all nerve terminal profiles (Gillingwater et al., 1999). By analysing nerve terminal profiles which have undergone

a confirmed qualitative ultrastructural alteration, it is possible to compare quantitative data from control preparations with these data from the toxin treated preparations, the result of which provides a good indicator as to the sensitivity of the synaptic vesicle quantification methods used in the current study (see chapter 2).

The second part of this chapter provides a qualitative and quantitative immunocytochemical and ultrastructural analysis of axotomised $Wld^s$ mouse NMJs. By analysing immunocytochemically labelled NMJs from young $Wld^s$ mice at 3, 4, 5 and 7 days post axotomy, it has been possible to produce a more complete appraisal of the temporal and morphological aspects of nerve terminal degeneration in the $Wld^s$ mouse. This part of the study was carried out in parallel with a series of electrophysiological and molecular experiments, performed by others: the contralateral FDB muscle to the one prepared for immunocytochemistry was used for intracellular recording by Mr D. Thomson in our laboratory, and several organs from the same mouse (including the brain, spleen and portion of muscle) were frozen in liquid nitrogen and shipped to Dr M.P. Coleman's lab in Cologne for molecular analysis (see discussion). My ultrastructural analysis of nerve terminal profiles from $Wld^s$ mice at 3, 4, 5 and 7 days post axotomy has also provided novel data on the nature of axotomy-induced degeneration of motor nerve terminals.

## 3.2 Methods

The majority of experiments contained within this chapter were carried out using methods described in chapter 2. The following section describes methods which are specific to this chapter.

### 3.2.1 Styryl Dye Staining of Motor Nerve Terminals

Recycling synaptic vesicles at motor nerve terminals on FDB and TA muscle preparations from unoperated $Wld^s$, Swiss, C57Bl/6 and C3H mice were stained using the vital aminostyryl dye FM1-43 (Molecular Probes; for mechanism of action see Betz et al., 1992). 1mg/ml stock (in $dH_2O$) FM1-43, stored in a -20°C freezer, was diluted with oxygenated physiological saline to produce a final working concentration of 5$\mu$M. Nerve/muscle preparations were bathed in the FM1-43 solution for 5mins prior to loading, whilst the nerve was taken up into a suction electrode connected to a pulse stimulator (Harvard). Pulses were delivered to the nerve at 20Hz, 10V, 0.1ms bandwidth for 10mins. Following nerve stimulation, the preparation was left in the FM1-43/Ringers solution for a further 5 minutes before washing for 30-60mins in oxygenated saline. After washing, postsynaptic receptor sites were labelled by incubation in a 5$\mu$g/ml solution of TRITC-$\alpha$-BTX (Molecular Probes) in oxygenated saline for 10mins. Preparations were washed for a further 20mins in oxygenated saline before viewing and subsequent quantification in a in a fluorescence microscope (CF

Fluorescent, Nikon) using a Zeiss 40x water immersion objective and a mercury lamp (Nikon HBO-100W/2). A customised filter block (435nm excitation filter, 455nm dichroic mirror and 515 IF emission filter; Nikon) was used for visualising FM1-43 fluorescence and a standard TRITC excitation/emission filter block (510-560nm excitation filter, 580nm dichroic mirror and 590 emission filter; Nikon) was used for visualising TRITC labelled αBTX. Individual NMJs were analysed as to their level of occupancy using the same method applied to immunocytochemically stained preparations.

### 3.2.2 Depletion of Synaptic Vesicles by Toxin Application

FDB and TA muscle preparations were dissected from C57Bl/6 mice and bathed in normal physiological saline (with 2mM $Ca^{2+}$) containing either 2nM purified α-latrotoxin (kindly supplied by Dr Y. Ushkaryov) or 5μM partially-purified Steatoda toxin (kindly supplied by Dr D. Kalikulov) for 20 minutes. Muscle preparations were then immediately immersed in a 4% paraformaldehyde / 2.5% glutaraldehyde (Sigma) solution for 4-6 hours at 4 °C. The fixed preparation was washed and post-fixed in a 1% osmium tetroxide (Sigma) solution before being processed for standard electron microscopy (see chapter 2). Ultrastructural quantification was carried out using the methods described in Chapter 2.

## 3.3 Results

### 3.3.1 Morphology and Ultrastructure of the Mouse Neuromuscular Junction

#### 3.3.1.1 Morphological Correlation of the Pre- and Post-Synaptic Apparatus

NMJs from unoperated $Wld^s$ (n=274, N=2), Swiss (n=724, N=2) and C3H (n=736, N=2) mice FDB muscles were labelled immunocytochemically for NF, SV2 and α-BTX. Each NMJ was individually assessed as to its level of occupancy, with the majority of those studied showing exact matching of the pre and post-synaptic apparatus (Figure 3.1). Evidence of partial occupancy (the occurrence of areas of AchRs with no overlying nerve terminal) at a small number of control NMJs from unoperated $Wld^s$ (N=3), C57Bl/6 (N=2) and Swiss (N=2) mice FDB and TA muscles labelled with FM1-43 and α-BTX, is provided in Figure 3.2. In the majority of these cases, only one or two nerve terminal boutons were missing from the endplate. Evidence for partial occupancy was detected in all immunocytochemically labelled control preparations: 3.07% ±0.24 (SEM) of wild-type unoperated endplates had areas of unoccupied AChRs (Figure 3.3).

### 3.3.1.2 Ultrastructural Correlation of the Pre- and Post-Synaptic Apparatus

Electron microscopic analysis of NMJ profiles from unoperated Wld$^s$ mice FDB muscles (n=34, N=4) confirmed the exact coordination of the pre- and post-synaptic apparatus at the majority of endplates (Figure 3.4). A polarised distribution of 50nm clear synaptic vesicles and nerve terminal mitochondria is easily detected in these preparations. Quantitative analysis of SV density within control nerve terminals revealed levels ranging from 35.18 SV/$\mu m^2$ up to 184 SV/$\mu m^2$ (n=34, N=4). The density of packing of these vesicles ranged from 6.82% (of the total area available for SVs; see chapter 2) up to 52.08% (n=34, N=4). The number of synaptic vesicles within a 125nm radius of the active zone varied from 2 to 11 (n=75, N=4). The percentage of terminal occupied by mitochondria and neurofilaments ranged from 0% to 44.09% and from 0% to 7.09% respectively. Occasionally, a terminal Schwann cell process was identified in the synaptic cleft. This invasion of the cleft did not appear to be phagocytotic in nature, however.

As in the immunocytochemically labelled preparations described above, there was evidence for partial occupancy at some ultrastructurally examined control NMJs from unoperated Wld$^s$ FDB muscles. Out of 120 NMJ profiles located (N=4 muscles), three were partially occupied, with areas of secondary postsynaptic folds not contacted by overlying nerve terminal, and one was vacant. The overall degree of remodelling

detected by ultrastructural analysis (3.33%) resembles the levels observed in immunocytochemical experiments (3.07%).

### 3.3.2 Ultrastructural Analysis and Quantification of Synaptic Vesicle Depletion in Wild-Type NMJs Following Toxin Treatment

Following 20 minutes of either α-latrotoxin or steatoda toxin treatment, nerve terminal profiles from C57Bl/6 mice FDB and TA muscles (n=6, N=2) showed retained pre- and post-synaptic architecture, except for a conspicuous decrease in the numbers of synaptic vesicles (Figure 3.5). Some nerve terminal mitochondria had swollen profiles with disrupted membranes and cristae. Qualitative analysis suggested that in the two nerve terminal profiles with the least synaptic vesicles, the postsynaptic folds appeared flattened and compressed into the endplate (Figure 3.5 panel B). Quantitative comparisons between the SV densities in control and toxin treated terminals revealed a significant decrease in the latter ($P<0.001$ for both α-latrotoxin and steatoda toxin; Figure 3.6a). Whereas control terminals had a mean SV density of 78.31 SV/$\mu m^2$ (±6.04 SEM), α-latrotoxin and steatoda toxin treated terminals had densities of 16.53 SV/$\mu m^2$ (±2.78) and 4.11 SV/$\mu m^2$ (±0.88) respectively. The number of synaptic vesicles located proximal to the presynaptic membrane (within a 125nm radius) also declined significantly in toxin treated preparations ($P<0.001$ for both α-latrotoxin and steatoda toxin; Figure 3.6b). α-latrotoxin treated terminals had a mean of 0.67 (±0.28

SEM) SVs within a 125nm radius whilst Steatoda treated terminals had a mean of 0.60 (±0.24). This contrasts with control preparations which had a mean of 5.04 (±0.18) SVs within a 125nm radius. Unsurprisingly, the packing density of synaptic vesicles in the toxin treated terminals was also significantly reduced compared to controls ($P<0.001$ for both α-latrotoxin and steatoda toxin).

### 3.3.3 Morphology and Ultrastructure of Axotomised Wild-Type Mouse NMJs

#### 3.3.3.1 Morphological Correlates of Wallerian Degeneration at Axotomised Wild-Type NMJs

NMJs from 1 day (n=1137, N=2) and 2 day (n=842, N=2) axotomised C57Bl/6J mice FDB muscles were labelled immunocytochemically for NF, SV2 and α-BTX. Each NMJ was individually assessed as to its state and level of occupancy. At both time points following axotomy, the majority of NMJs were vacant, with most remaining terminals being fully occupied (out of the 25 occupied terminals visualised, only 1 was partially occupied) yet with punctuated and fragmented nerve terminal staining (Figures 3.7 and 3.8a). Intramuscular nerves also appeared very fragmented in these preparations (Figure 3.8a). Figure 3.8b illustrates the levels of occupancy recorded at 1

and 2 days post axotomy. Within 24 hours of axotomy, the level of occupied terminals in wild-type FDB muscles was reduced to <1% of those found in control muscles.

### 3.3.3.2 Ultrastructural Correlates of Wallerian Degeneration at Axotomised Wild-Type NMJs

Out of the 28 NMJ profiles from 1-day axotomised C57Bl/6 mouse FDB muscles (N=3) located in the electron microscope, only one was occupied (Figure 3.9a). This profile displayed a fragmented nerve terminal being phagocytosed in-situ by a terminal Schwann cell. A few SVs and dense bodies (remnants of mitochondria; Manolov, 1974) were still identifiable within the engulfed terminal. All of the remaining 27 NMJ profiles which were examined were vacant, with Schwann cell processes located close to the vacated postsynaptic folds (Figure 3.9b).

## 3.3.4 Morphological and Ultrastructural Preservation of Motor Nerve Terminals at Axotomised Wld$^s$ NMJs

Immunocytochemically labelled NMJs (NF, SV2 and α-BTX) from 3 day (n=1795, N=6), 5 day (n=1398, N=7) and 7 day (n=1136, N=6) axotomised 2 month old Wld$^s$ mice FDB muscles were individually assessed as to their level of occupancy. At 3 days post axotomy, in stark contrast to wild-types, the majority of Wld$^s$ endplates (95.31%

±1.39 SEM) were still occupied. This prevalence decreased to 74.05% ±2.51 at 5 days and 52.29% ±4.26 at 7 days (Figure 3.10). None of the nerve terminals observed had the fragmented staining patterns associated with most axotomised wild-type NMJs. Qualitative ultrastructural analysis of nerve terminal profiles from 3, 5 and 7 day axotomised Wld$^s$ NMJs confirmed that nerve terminals were preserved without any degenerative changes (Figure 3.11).

### 3.3.5 Partial Occupancy at Endplates of Axotomised Wld$^s$ NMJs

#### 3.3.5.1 Immunocytochemistry of Partial Occupancy at Axotomised Wld$^s$ NMJs

A significant proportion of immunocytochemically labelled NMJs from 2 month Wld$^s$ mice showed evidence of partial occupancy, at all time points following axotomy (3, 5 and 7 days). Examples of endplates across the whole spectrum of occupancy (1-100%) were identified in all muscles that were analysed (Figure 3.12). As expected, the boutons which were initially lost at partially occupied endplates were located at the extremities of each branch of the motor nerve terminal, but not necessarily at the extremities of the endplate (see Figure 3.12). Nerve terminals enduring at partially occupied endplates appeared healthy, with no signs of fragmentation of terminal

boutons or motor axon collaterals. The last boutons remaining at partially occupied endplates took the form of 'retraction bulbs' (Figure 3.13). These are classified as swellings at the distal end of a motor axon branch, often located over a small patch of postsynaptic receptors, but occasionally appearing isolated from any endplate.

Data from the morphological quantification of the incidence of partial occupancy at axotomised $Wld^s$ NMJs are summarised in Figure 3.14. Whilst there is a small incidence of partial occupancy in control (unoperated) preparations (3.07% ±0.24 SEM), this figure increased to 25.10% ±4.98 in 3 day axotomised preparations, peaking at 54.58% ±3.22 in 5 day preparations before falling to 47.24% ±4.58 7 days after axotomy. The occurrence of differing states of occupancy between neighbouring endplates (for example, a fully occupied endplate can often be found next to a partially occupied endplate, with both neighbouring a vacant endplate) suggests that the piecemeal removal of motor nerve terminals occurs in a asynchronous fashion, whereby individual nerve terminals withdraw from their endplate at different times to terminals at adjacent endplates (Figures 3.15 and 3.16).

Following axotomy, motor axon branches supplying NMJs in 2 month old $Wld^s$ mice also have a distinctive morphology. Immunocytochemically labelled $Wld^s$ FDB muscle preparations (NF, SV2 and α-BTX) from 3, 5 and 7 days post axotomy have axon branches which appear very thin and wispy, occasionally interrupted by brightly stained, large accumulations of neurofilament (Figure 3.17). This pattern of bright NF

staining also occurs in Wld$^s$ nerve terminals, suggesting that NF accumulation may also occur in nerve terminal boutons (see below).

### 3.3.5.2 Ultrastructural Features of Partial Occupancy at Axotomised Wld$^s$ NMJs

Electron microscopical examination of NMJs from axotomised 2 month old Wld$^s$ mice FDB muscle preparations provided ultrastructural evidence of partial occupancy. An endplate was classified as partially occupied when there was an expanse of postsynaptic foldings with no overlying nerve terminal, as well as an area of occupied postsynaptic folds, on the same muscle fibre (Figure 3.18). Ultrastructural quantification of the levels of occupancy and partial occupancy (Figure 3.19) provided similar data to that gained from immunocytochemical experiments shown previously. In 3 day axotomised FDB preparations (n=105, N=3) 89.84% ±3.64 (SEM) of endplates were occupied (1-100%) and 32.76% ±3.16 of endplates were partially occupied (1-99%). Analysis of 4 day axotomised preparations (n=96, N=3) showed that 86.83% ±2.87 of endplates and 43.33% ±5.71 of endplates were fully and partially occupied respectively, whilst at 7 days after axotomy (n=95, N=3), those levels had dropped to 53.18% ±12.58 and 31.18% ±1.81 respectively.

Accumulation of neurofilaments was conspicuous in many of the nerve terminal profiles examined at all time points post axotomy. This build-up of neurofilament proteins

appeared to have displaced organelles from the centre of nerve terminal boutons, but did not appear to disrupt the overall polarised distribution of SVs and mitochondria (Figure 3.20). Quantification of neurofilament levels within nerve terminal profiles revealed that there was a increase at terminal profiles from 3 days post axotomy (n=26, N=4), where 5.37% ±1.58 of the terminal was filled with NF, compared to controls where 1.42% ±0.33 of the terminal was filled with NF, although this did not reach statistical significance (P=0.4273). Significantly higher levels of NF were found in nerve terminals at 4, 5 and 7 days post axotomy however (P=<0.0001 for all time points compared to controls). At 4 days post axotomy (n=7, N=2), 19.28% ±5.33 of the terminal was occupied by neurofilaments, with similar values of 17.32% ±2.63 and 20.53% at 5 (n=26, N=4) and 7 (n=1, N=1) days respectively (Figure 3.21). Furthermore, it is possible to estimate the rate of axonal neurofilament transport from the current data. Assuming that the tibial nerve stump is between ten and fifteen millimetres long, that bi-directional transport of neurofilament occurs equally in both directions (whereby only 50% of the axonal NF is transported distally), and that NF accumulation saturation point is reached by 4 days post axotomy (as evidenced by the graph in Figure 3.21), the rate of 1.25-1.88mm/day can be calculated.

Despite the evidence for partial occupancy and accumulation of neurofilaments, the incidence of degenerative markers within nerve terminal profiles from 3,4,5 and 7 day axotomised 2 month old $Wld^s$ mice was minimal. Out of the 294 motor nerve terminals examined (N=9) for their levels of occupancy (at all time points following axotomy),

only 7 (3.1%) were classified as having signs of degeneration. In all of these cases, the only reason that the terminal was classified as degenerating was because more than 20% of mitochondria had disrupted profiles. No evidence for nerve terminal membrane fragmentation and/or terminal Schwann cell phagocytosis of the nerve terminal was found.

Qualitative analysis of the synaptic vesicle population within axotomised $Wld^s$ nerve terminals suggested that there was no reduction in either their numbers or distribution, although 'giant' vesicles of more than 50nm diameter (in some instances as large as 150nm), rarely observed in control preparations, were occasionally identified (Figure 3.22). Quantification of the synaptic vesicle density within axotomised 2 month old $Wld^s$ nerve terminals confirmed these findings. There was no significant reduction in the density of synaptic vesicles at any time point following axotomy (Figure 3.23a). Levels of 78.31 SV/$\mu m^2$ ±6.04 in controls (n=34, N=4) were maintained at 3 (83.76 SV/$\mu m^2$ ±5.70 SEM; n=26, N=4), 4 (79.03 SV/$\mu m^2$ ±11.33; n=7, N=2), 5 (78.75 SV/$\mu m^2$ ±5.72, n=26, N=4) and 7 (80.44 SV/$\mu m^2$; n=1, N=1) days post axotomy. Subsequent analysis showed that there was no significant difference in the SV density between fully and partially occupied nerve terminals (Figure 3.23b). The density of packing of SVs within axotomised $Wld^s$ nerve terminals was significantly higher ($P=<0.0001$ at all time points following axotomy) than in control preparations (Figure 3.24a). Whilst control preparations (n=34, N=4) had 28.25% ±1.95 of the area available to SVs actually occupied by SVs, 3 day axotomised $Wld^s$ terminals (n=26, N=4) had

40.64% ±1.71, 4 day axotomised Wld$^s$ terminals (n=7, N=2) 54.91% ±3.96, 5 day axotomised Wld$^s$ terminals (n=26, N=4) 41.40% ±2.18 and 7 day axotomised Wld$^s$ terminals (n=1, N=1) 48.55% occupied by SVs. There was a significantly higher density of packing in partially occupied terminals compared to fully occupied terminals at 3 days (P=0.0275) and 5 days (P=0.0303) post axotomy, but no significant difference at 4 days (Figure 3.24b). There was no significant reduction (P=>0.12 in all analyses) in the numbers of vesicles within a 125nm radius of an active zone at any time-point following axotomy in Wld$^s$ nerve terminals compared to controls (Figure 3.25). Levels of 5.04 ±0.18 vesicles in controls (n=75, N=4) were maintained at terminals from 3 (5.41 ±0.16; n=75, N=4), 4 (5.07 ±0.47; n=15, N=2), 5 (5.25 ±0.17; n=55, N=4) and 7 (4.67; 0.33; n=3, N=1) days post axotomy.

**Fig. 3.1 Morphology of control (unoperated) NMJs.**

(A) Confocal image of four NMJs from a $Wld^s$ mouse FDB (NF, SV2 and α-BTX). Note the alignment of pre- and post-synaptic structures. Scale bar = 20μm.

(B & C) Standard fluorescence microscope image of a NMJ from a C57Bl/6 mouse FDB. Panel B shows the axonal and motor nerve terminal component stained for NF and SV2 (green). The triple band pass image (panel C) demonstrates the almost perfect alignment of presynaptic structures with the postsynaptic AchRs (labelled with α-BTX; red). Scale bar = 20μm.

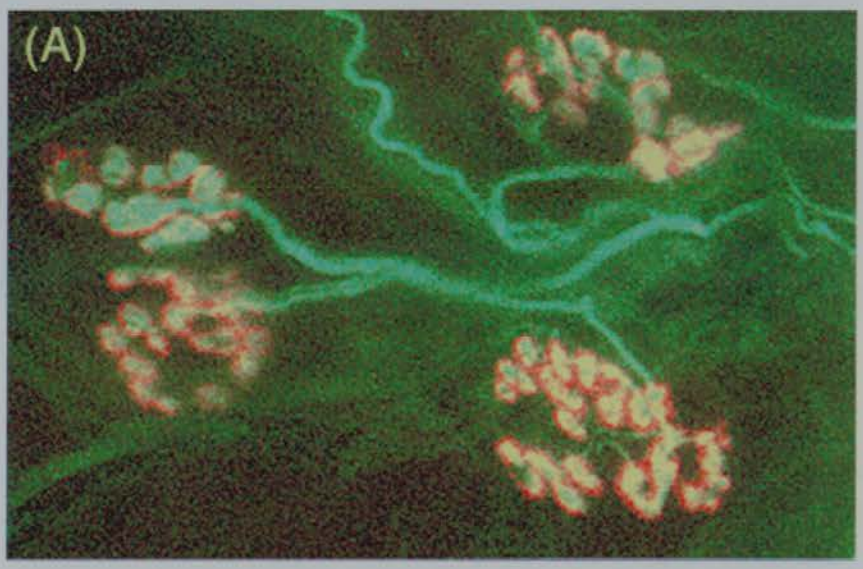
(A)

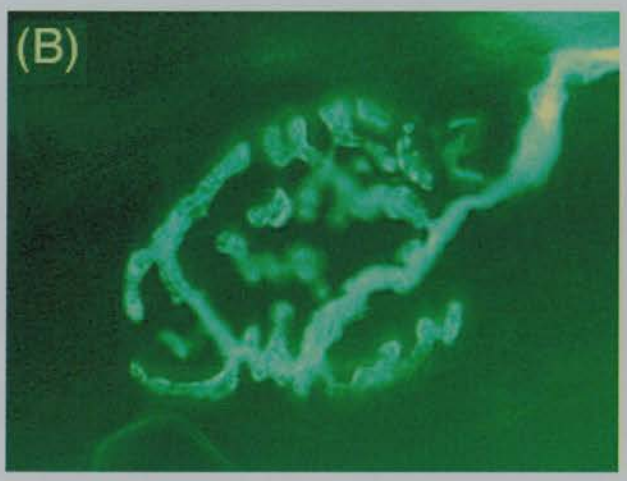
(B)


(C)

**Fig. 3.2 Evidence for Remodelling of Neuromuscular Synapses Under Normal Conditions (FM1-43)**

(A) & (B) Two examples of FM1-43 labelled nerve terminals and α-BTX labelled AchRs from an unoperated $Wld^s$ FDB muscle. Areas of unoccupied receptors with no overlying terminal are indicated by arrows. Scale bars = 20μm.

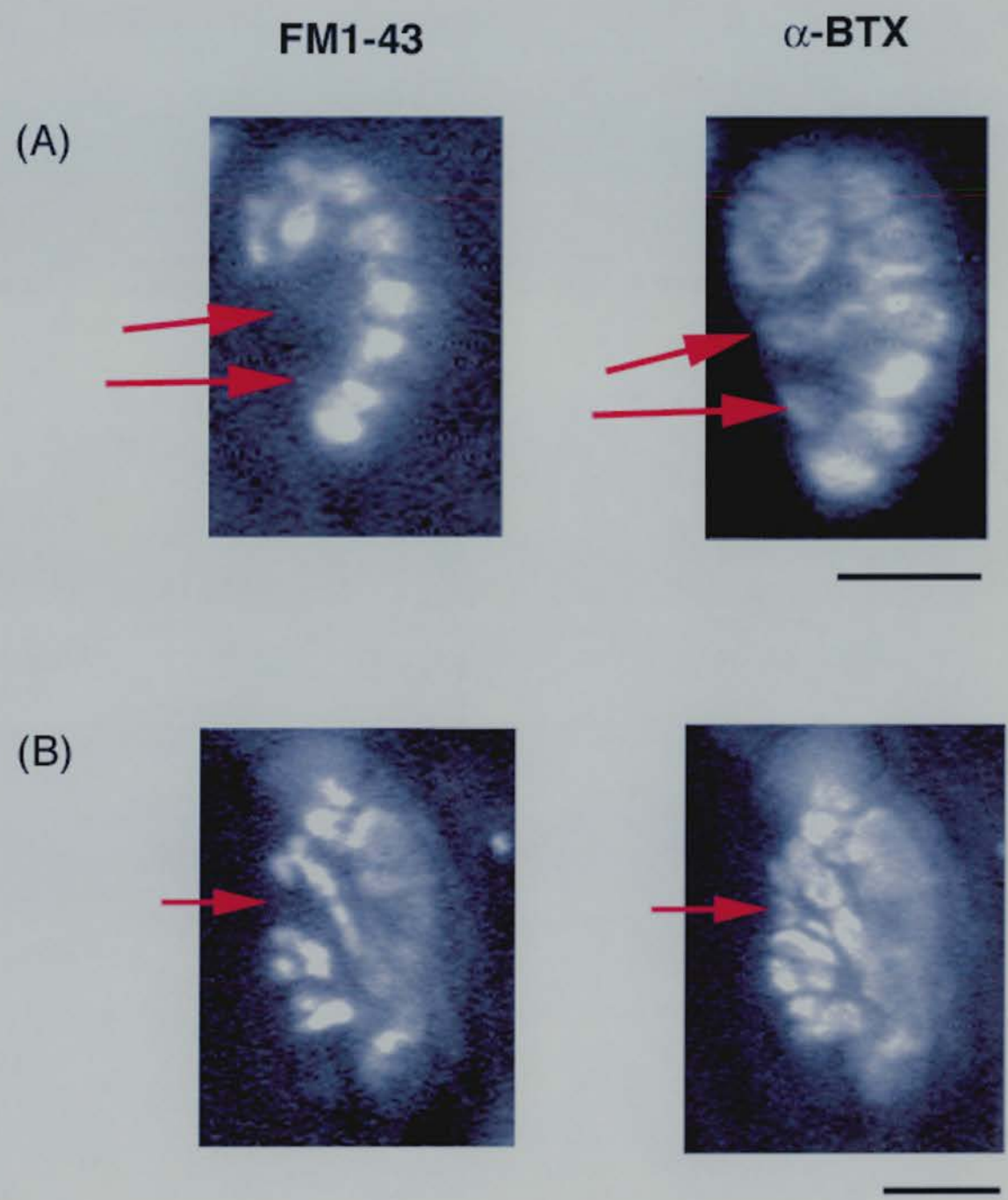
FM1-43
α-BTX
(A)
(B)

**Fig. 3.3 Evidence for Remodelling of Neuromuscular Synapses Under Normal Conditions (Immunocytochemistry)**

(A, B & C) Immunocytochemically stained nerve terminals and AchRs (A = NF, SV2 and α-BTX; B = NF and SV2; C = only α-BTX channel shown from image A) from an unoperated Swiss mouse FDB. Areas of vacant receptors with no overlying terminal are indicated by arrows. Note how the brightness of α-BTX staining is reduced at unoccupied compared to occupied boutons. Scale bar = 20μm.

(D) Table summarising immunocytochemical data on the occurrence of fractional occupancy at NMJs in control $Wld^s$, Swiss and C3H mice FDB muscles.

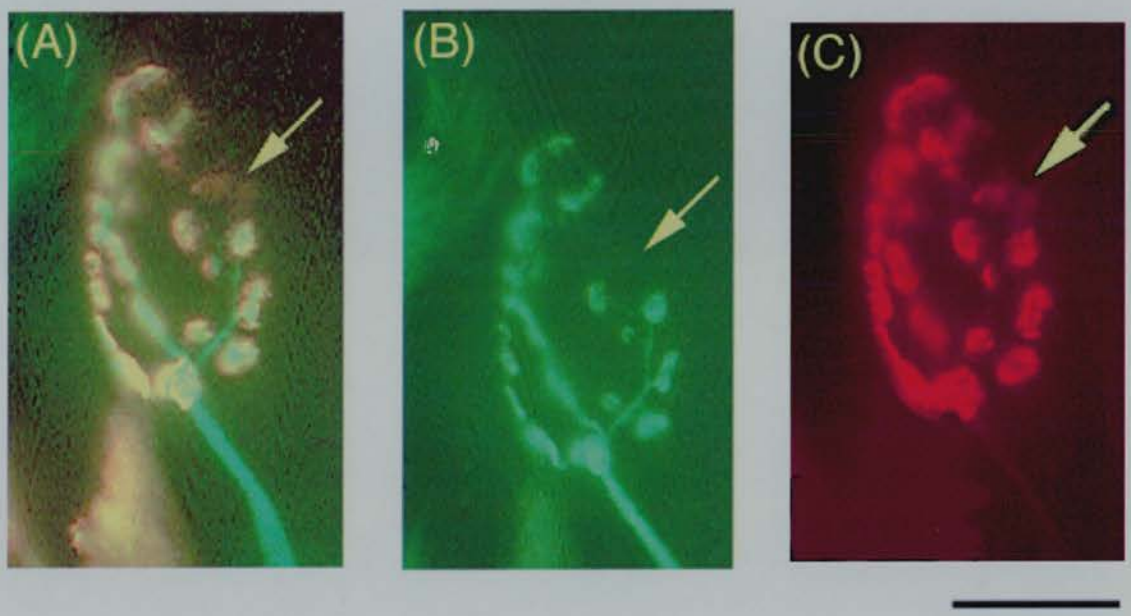


(D)

| Mouse Strain | % of Partially Occupied Endplates Muscle 1 | % of Partially Occupied Endplates Muscle 2 |
|---|---|---|
| Wlds | 4 | 2.68 |
| Swiss | 3.27 | 2.23 |
| C3H | 3.24 | 3.02 |

**Fig. 3.4 Ultrastructure of Control NMJs.**

(A) Ultrastructural profile of a nerve terminal bouton from a control $Wld^s$ mouse FDB muscle. The nerve terminal contains numerous mitochondria distal to the presynaptic membrane (red arrows) and numerous clear ~50nm synaptic vesicles proximal to the presynaptic membrane (red arrowhead). The nerve terminal is capped by a terminal Schwann cell (blue arrow) and directly opposes the secondary postsynaptic folds on the skeletal muscle fibre (blue arrowheads). Scale bar = 0.5$\mu$m.

(B) Summary table of the levels and distribution of sub-cellular organelles within a control nerve terminal, as calculated using the ultrastructural quantification methods described in chapter 2. All data is presented as mean±SEM.

(A)

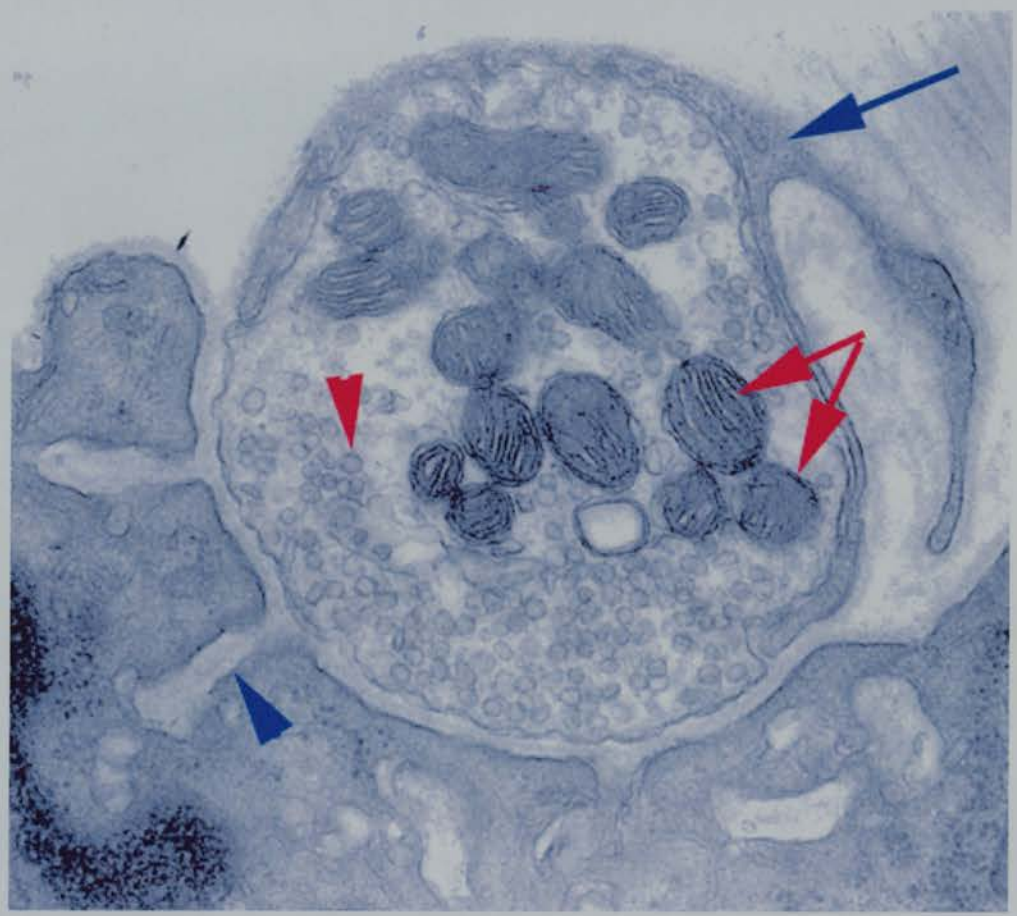

(B)

| | % of Terminal Occupied by Mitochondria | % of Terminal Occupied by NF | SV Density (SV / μm2) | SV Packing Density (% of Area Available for SVs) | No. of SVs Within 125nm Radius of Active Zone |
|---|---|---|---|---|---|
| Control Wlds (n=34, N=4) | 23.36±1.67 | 1.42±0.33 | 78.31±6.04 | 28.25±1.95 | 5.04±0.18 |

**Fig. 3.5 Ultrastructure of α-latrotoxin and Steatoda Toxin Treated NMJs.**

(A) Ultrastructural profile of a nerve terminal bouton from a C57Bl/6 mouse exposed to 2nM purified α-latrotoxin for 20mins before immediate fixation. Note the paucity of synaptic vesicles within the terminal. Scale bar = 0.5μm

(B) Ultrastructural profile of a nerve terminal bouton from a C57Bl/6 mouse exposed to 5μM partially-purified Steatoda toxin for 20mins before immediate fixation. Synaptic vesicles were even more scarce than in the α-latrotoxin terminal shown above, but the rest of the nerve terminal architecture was preserved. In this example, the postsynaptic foldings appear to be compressed and compacted into the endplate. Scale bar = 0.5μm

(A)

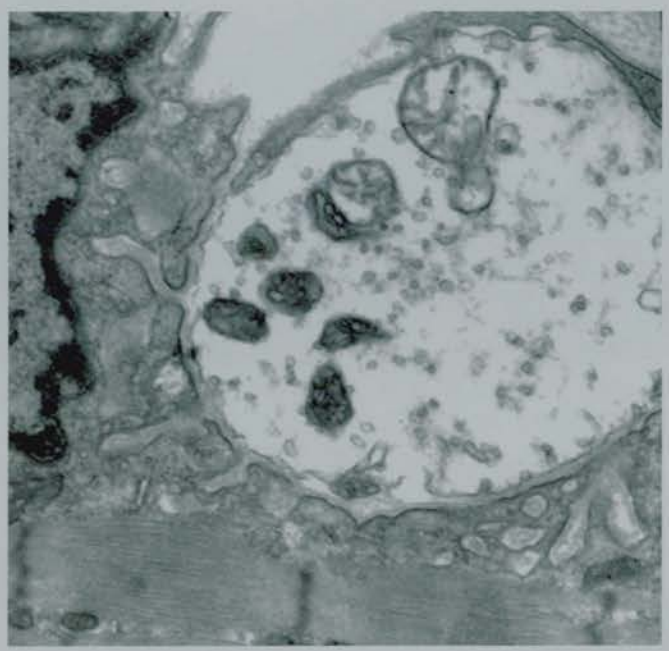

(B)

**Fig. 3.6 Quantification of Synaptic Vesicle Density and Localisation in Nerve Terminals from α-latrotoxin and Steatoda Toxin Treated NMJs.**

(A) Bar chart comparing synaptic vesicle densities at control (n=34, N=4), α-latrotoxin (n=4, N=1) and Steatoda Toxin (n=2, N=1) treated NMJs. Both LTX ($p<0.001$) and STX ($p<0.001$) treated preparations had significantly reduced densities of synaptic vesicles compared to control preparations (unpaired t-test). Error bars represent ±SEM.

(B) Bar chart showing comparative synaptic vesicle localisation towards active zones at control (n=75, N=4), α-latrotoxin (n=12, N=1) and Steatoda Toxin (n=5, N=1) treated NMJs. Both LTX ($p<0.001$) and STX ($p<0.001$) treated preparations had significantly reduced numbers of synaptic vesicles clustered by active zones compared to control preparations (unpaired t-test ). Error bars represent ±SEM.

(A)

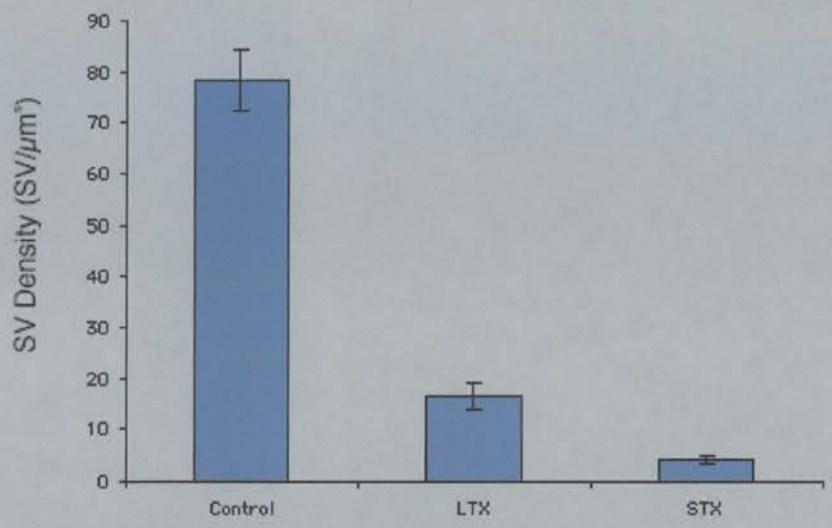
SV Density (SV/μm³)
90
80
70
60
50
40
30
20
10
0
Control
LTX
STX

(B)

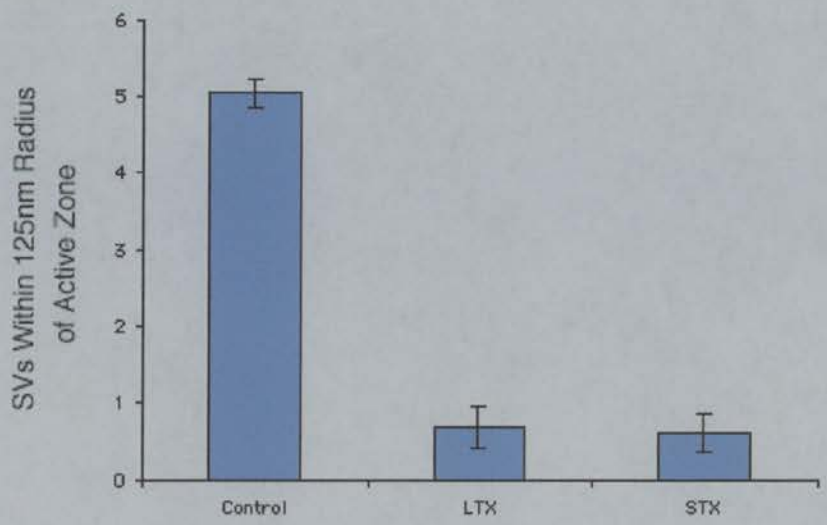
SVs Within 125nm Radius of Active Zone
6
5
4
3
2
1
0
Control
LTX
STX

**Fig. 3.7 Morphology of Axotomised Wild-Type NMJs**

(A & B) Standard fluorescence microscope image of two immunocytochemically labelled (A = NF, SV2 and α-BTX; B = NF and SV2 only) NMJs from a 1 day axotomised wild-type C57Bl/6 FDB muscle. These are both examples of fully occupied endplates with exact alignment of pre- and postsynaptic structures and no signs of fragmentation or degeneration. Scale bar = 20$\mu$m

(C & D) Immunocytochemically labelled (A = NF, SV2 and α-BTX; B = NF and SV2 only) NMJ from a 1 day post-axotomy wild-type C57Bl/6 FDB muscle. Note the grossly fragmented and degenerating nerve terminal and how the process appears to be synchronous, with no single portion of terminal undergoing degeneration before another. Scale bar = 20$\mu$m

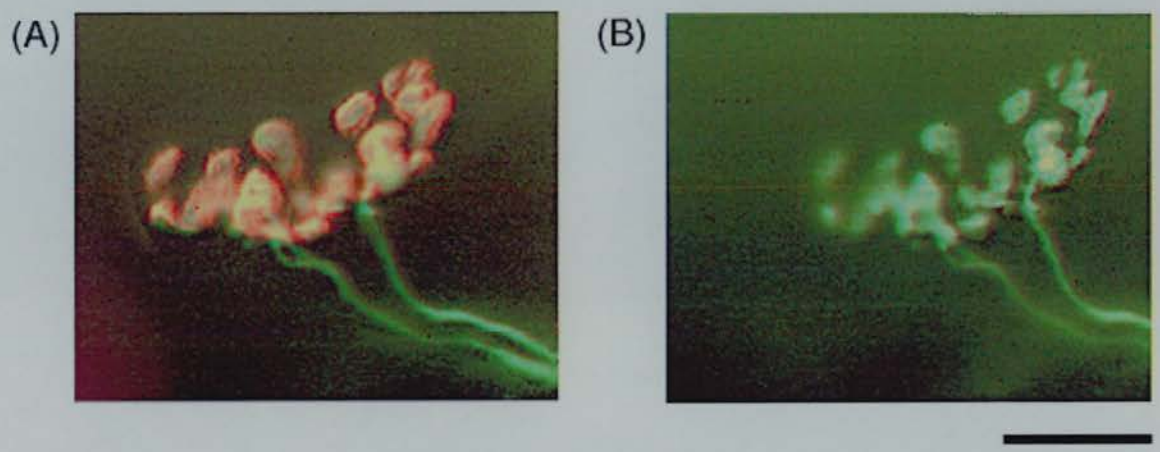
(A)
(B)

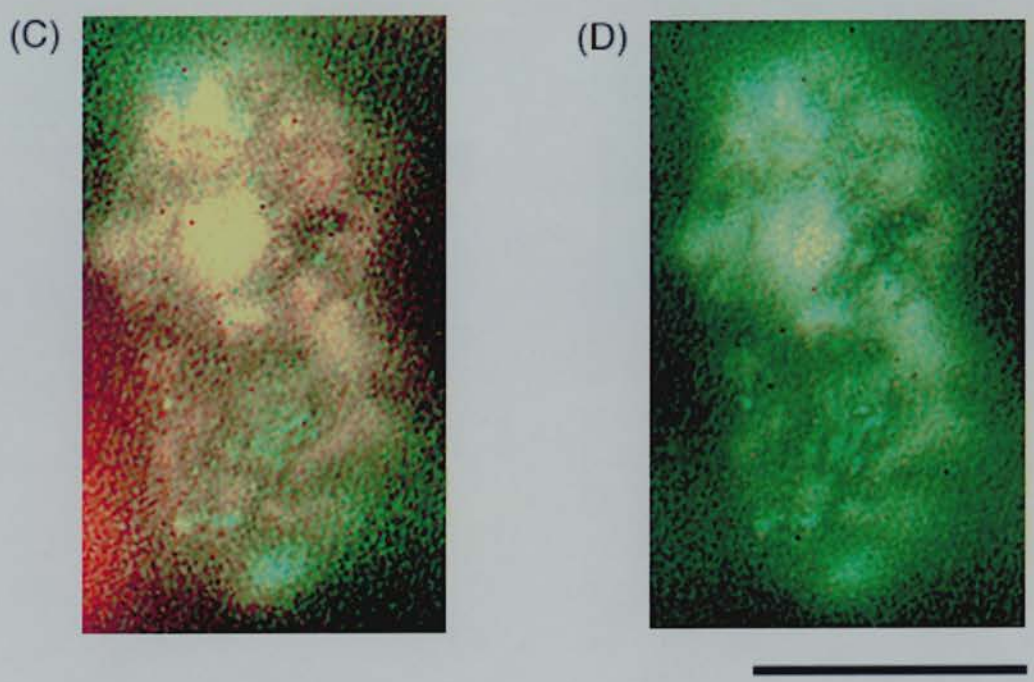
(C)
(D)

**Fig. 3.8 Morphology and Quantification of Axotomised Wild-Type NMJs**

(A) Immunocytochemically labelled (NF, SV2 and α-BTX) NMJs from a 1 day axotomised C57Bl/6 FDB muscle. This example includes two vacant endplates and a nearby degenerating intramuscular nerve. Scale bar = 20μm

(B) Graph showing the rapid decline of endplate occupation at wild-type (C57Bl/6) FDB NMJs following tibial nerve section. Red triangles represent the mean value from two muscles at each time point.

(A)

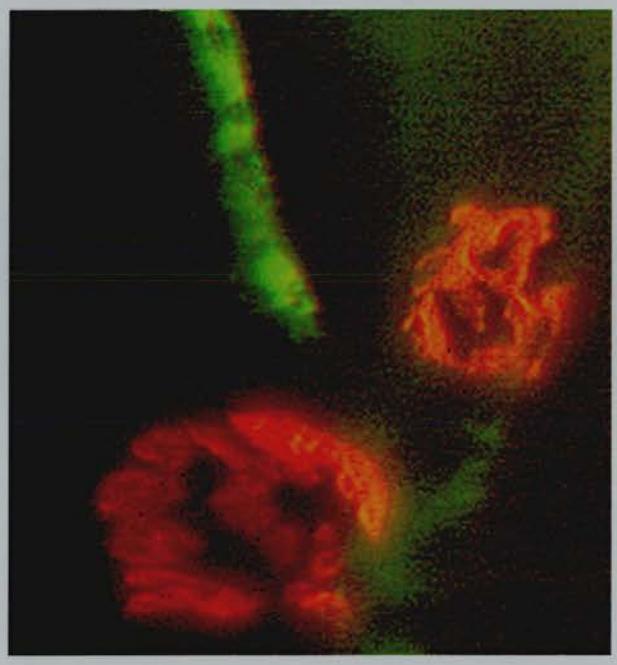

(B)

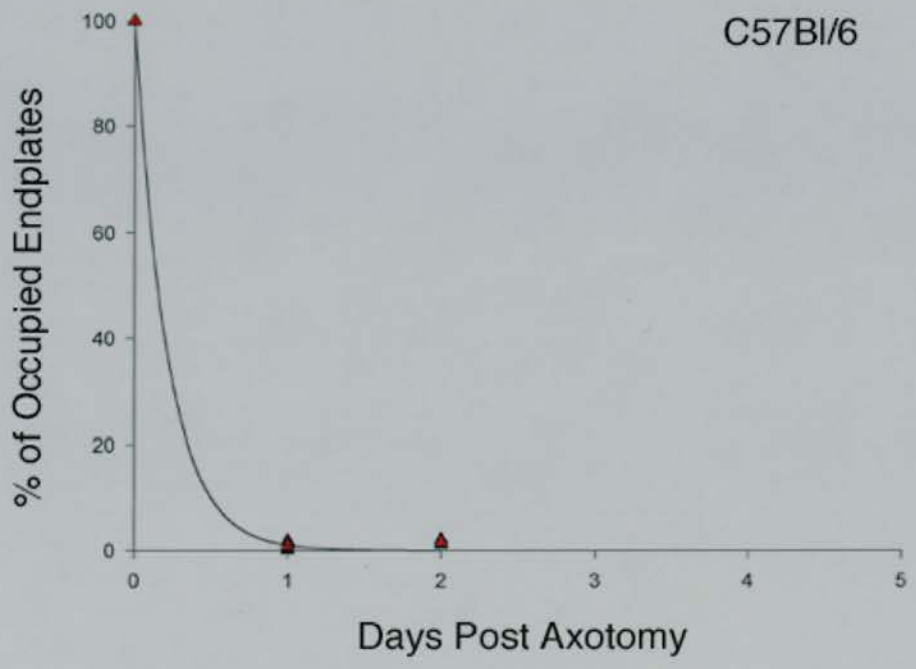
C57Bl/6
% of Occupied Endplates
100
80
60
40
20
0
0
1
2
3
4
5
Days Post Axotomy

**Fig. 3.9 Ultrastructure of Axotomised Wild-Type NMJs**

(A) Electron micrograph of a 1 day post axotomy C57Bl/6 mouse NMJ. The grossly fragmented nerve terminal (red star) is being phagocytosed in-situ by a another cell, presumably the terminal Schwann cell (blue star). Scale bar = 1$\mu$m

(B) Electron micrograph of a 1 day post axotomy C57Bl/6 mouse NMJ. All nerve terminal debris has been removed and a terminal Schwann cell profile is left opposing the postsynaptic folds. Scale bar = 1$\mu$m

(A)

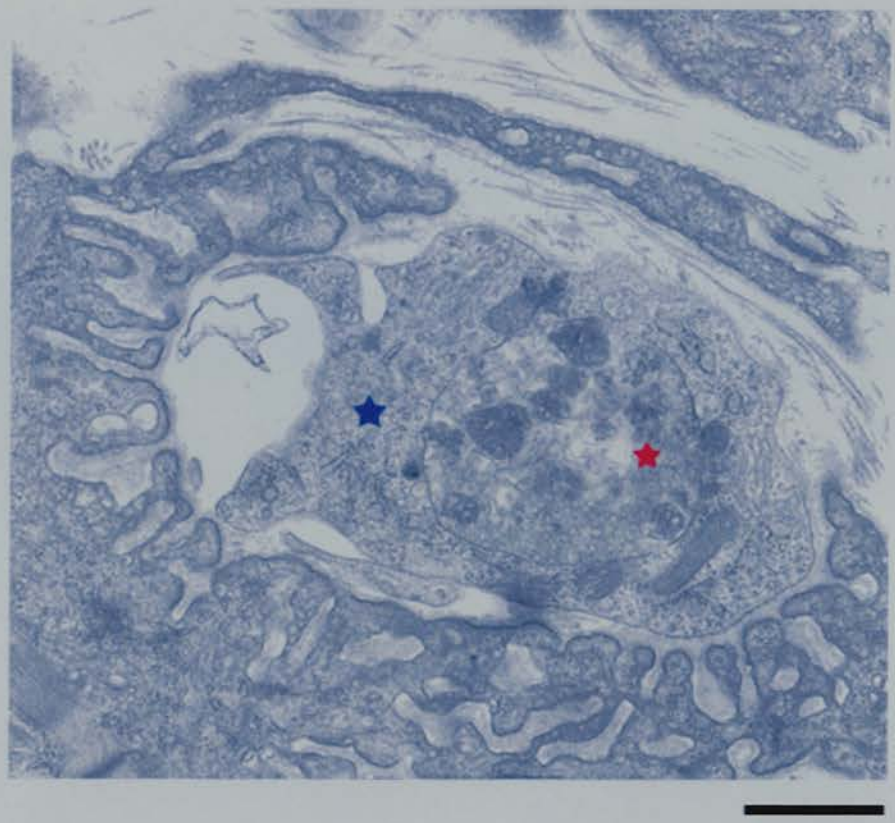

(B)

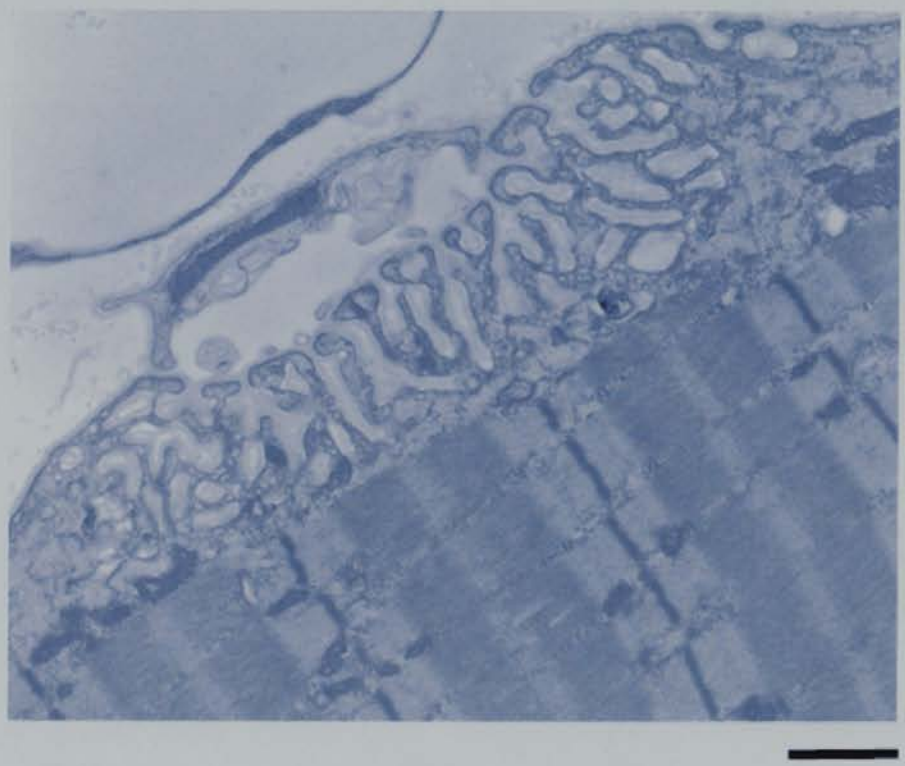

**Fig. 3.10 Preservation of Motor Nerve Terminals at Axotomised Wld$^s$ NMJs**

(A & B) Confocal micrographs from a 3 day axotomised Wld$^s$ FDB (NF, SV2 and α-BTX). An example of a fully occupied endplate with no signs of nerve terminal degeneration is shown in panel A. Two examples of partially occupied endplates (see below) with no degenerative markers are shown in panel B. Scale bars = 20$\mu$m

(C) Graph of the percentage of occupied endplates against days post axotomy in 2 month old Wld$^s$ mice. Black triangles represent data from individual muscles and red triangles represent mean values.

(A)

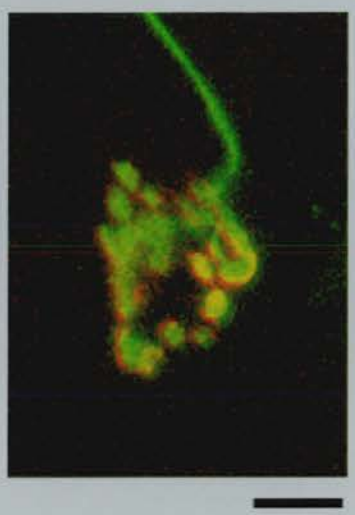

(B)

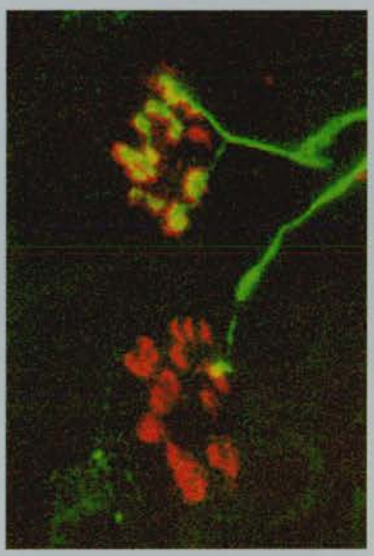

(C)

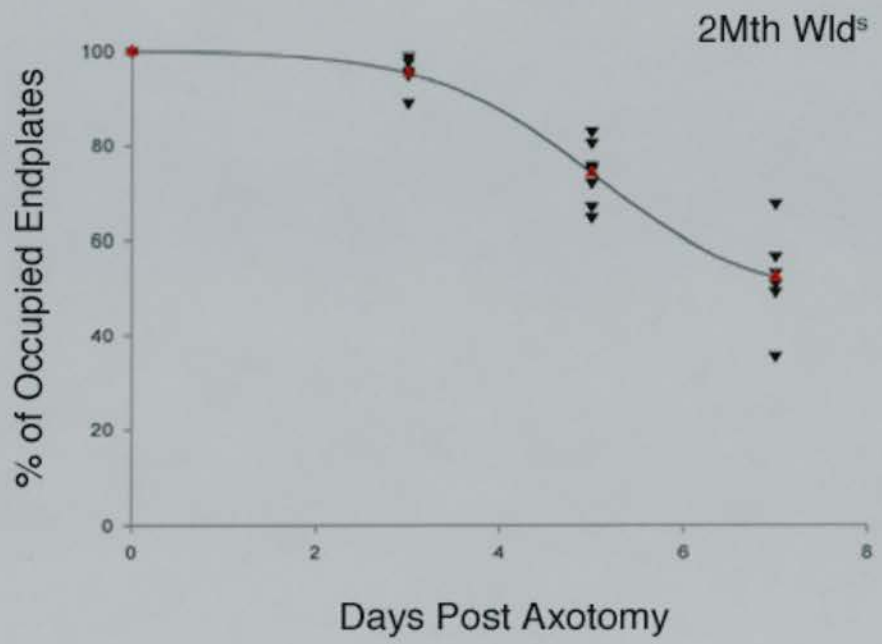
2Mth Wld$^s$
% of Occupied Endplates
100
80
60
40
20
0
0
2
4
6
8
Days Post Axotomy

**Fig. 3.11 Ultrastructural Preservation of Motor Nerve Terminals at Axotomised Wld$^s$ NMJs**

(A) Electron micrograph from a 3 day axotomised FDB muscle from a 2 month old Wld$^s$ mouse. The ultrastructure of the nerve terminal is wholly intact, with a uniform distribution of mitochondria and synaptic vesicles. Scale bar = 1$\mu$m

(A)

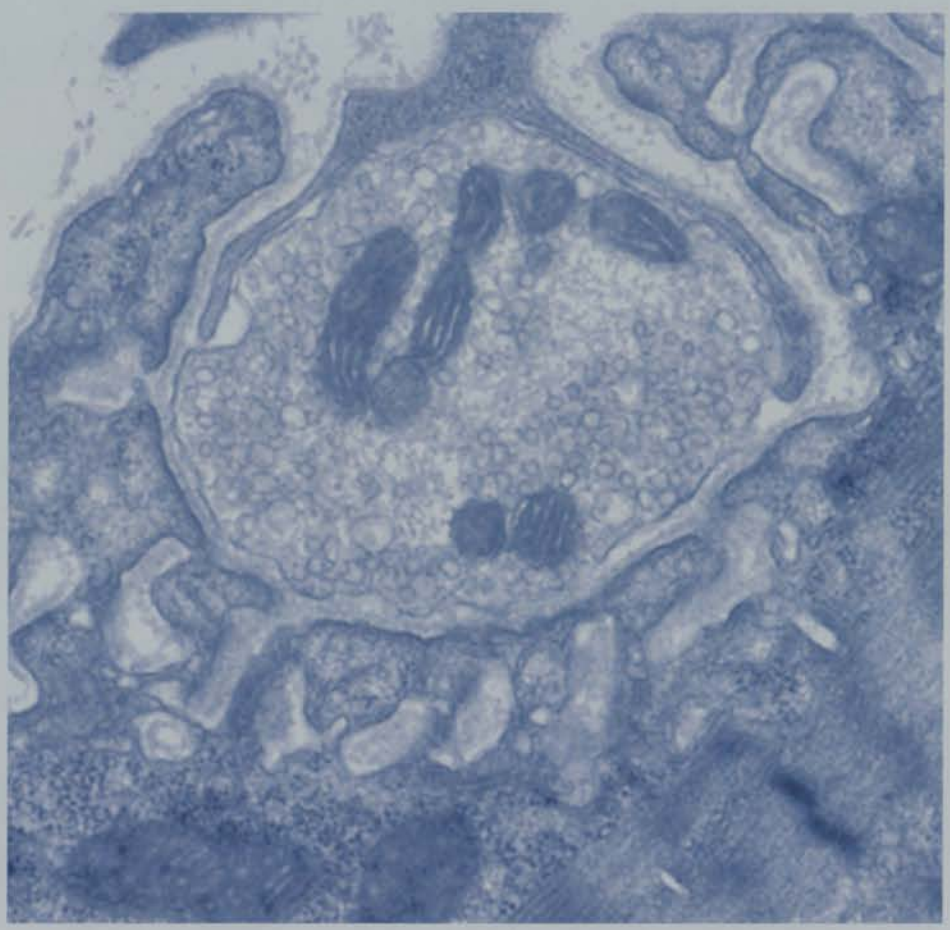

**Fig. 3.12 Immunocytochemical Evidence of Partial Occupancy at Endplates of Axotomised Wld$^s$ NMJs**

(A & B) Fluorescence micrographs from a 2 month Wld$^s$ mouse, 3 days post axotomy (A = NF, SV2 and α-BTX. B = NF and SV2 only). A partially occupied endplate with approximately 10-15% of AchRs not contacted by overlying nerve terminal is shown. Scale bar = 20μm

(C & D) Fluorescence micrographs from a 2 month Wld$^s$ mouse, 7 days post axotomy (A = NF, SV2 and α-BTX. B = NF and SV2 only). A partially occupied endplate with approximately 40-50% of AchRs not contacted by overlying nerve terminal is shown. Scale bar = 20μm

(E) Confocal micrograph from a 2 month Wld$^s$ mouse, 3 days post axotomy (NF, SV2 and α-BTX). A partially occupied endplate with approximately 50-60% of AchRs not contacted by overlying nerve terminal is shown. Scale bar = 20μm

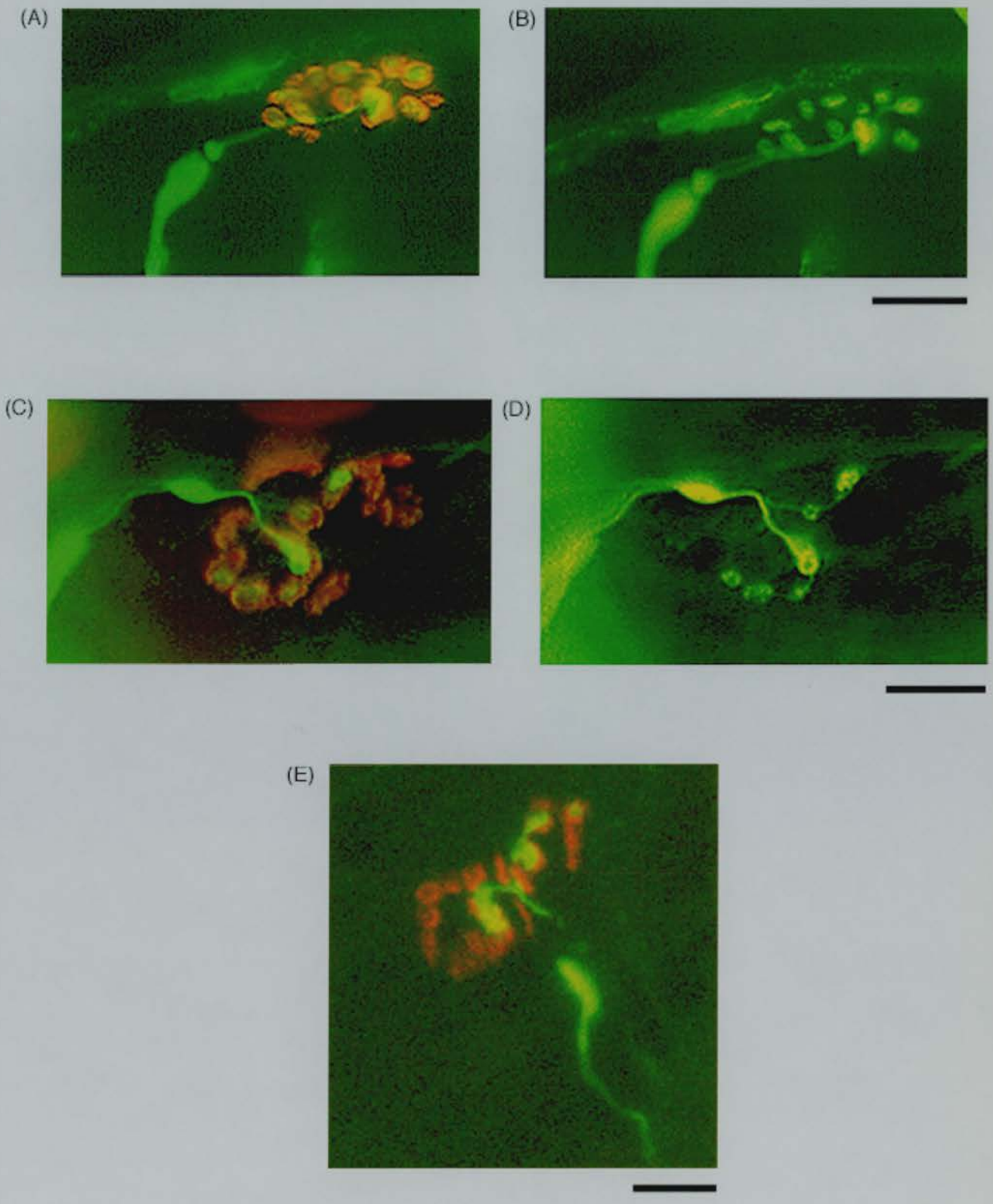
(A)
(B)
(C)
(D)
(E)

**Fig. 3.13 Immunocytochemical Evidence of Retraction Bulb Formation at Axotomised Wld$^s$ NMJs**

(A & B) Fluorescence micrographs from two, 2 month Wld$^s$ mice, 3 days post axotomy (NF, SV2 and α-BTX). Retraction bulbs, indicated by the bulbous swelling at the termination of the axon, have formed at both endplates. Panel B is a higher power image of one NMJ shown previously in Figure 3.10b. Scale bars = 20μm.

(A)

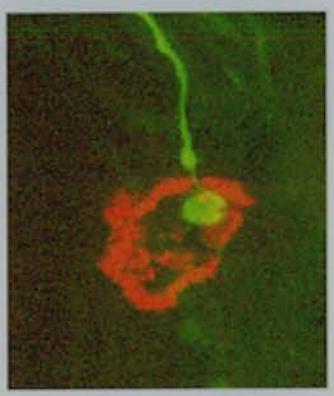

(B)

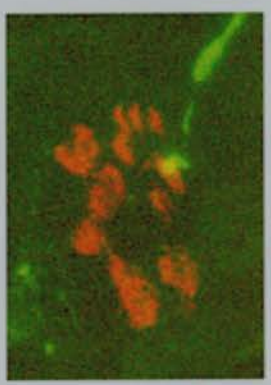

**Fig. 3.14 Incidence of Partial Occupancy at Axotomised Wld$^s$ NMJs (Immunocytochemical Analysis) in 2 month Wld$^s$ mice FDB muscles**

(A) Graph of the percentage of partially occupied (ranging from 1 to 99% occupied) endplates against days post axotomy. Note that the data plotted for 0 days post axotomy represents the level of remodelling seen in unoperated control preparations (see Fig 3.3). Black triangles represent data from individual muscles and red triangles represent the mean value at each time point.

(A)

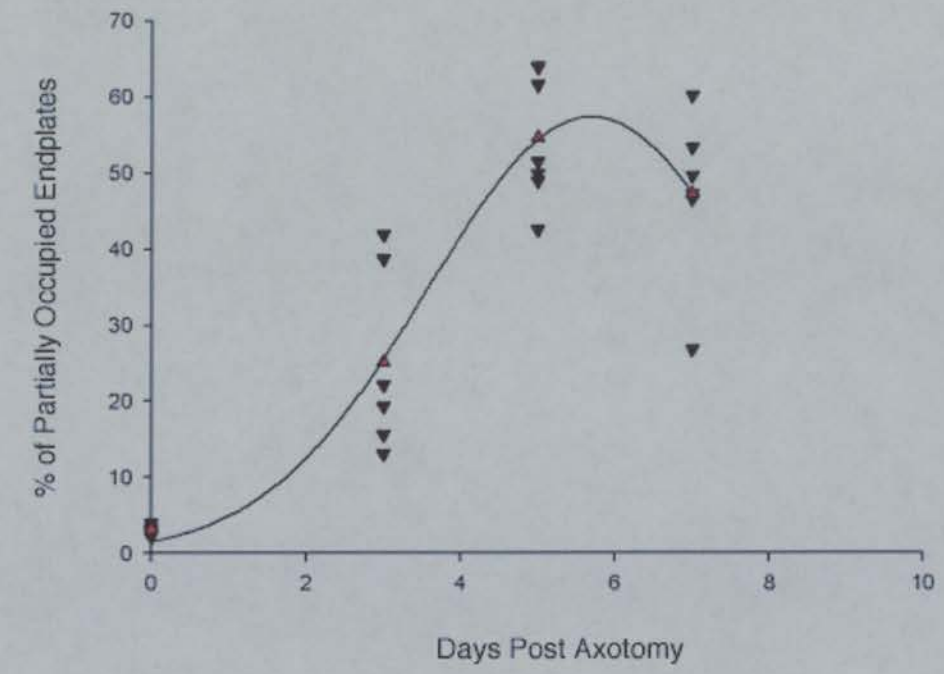
% of Partially Occupied Endplates
70
60
50
40
30
20
10
0
0
2
4
6
8
10
Days Post Axotomy

**Fig. 3.15 Asynchronous Withdrawal of Axotomised Nerve Terminals in Wld$^s$ Mice**

(A) Confocal micrograph from a 2 month Wld$^s$ mouse FDB, 3 days post axotomy (NF, SV2 and α-BTX). 3 neighbouring endplates are shown in varying states of occupancy. The endplate on the left is fully occupied, the middle endplate is partially occupied and the endplate on the right is vacant. Scale bar = 20μm

(B) Confocal micrograph from a 2 month Wld$^s$ mouse FDB, 3 days post axotomy (NF, SV2 and α-BTX). 4 neighbouring endplates are shown in varying states of occupancy. The endplate on the top right is fully occupied, the top left and bottom right endplates are partially occupied (arrows indicate vacant portions of AChRs) and the endplate on the bottom left is almost vacant, with only a small area of receptors contacted by a retraction bulb. This panel contains two of the endplates previously shown in Figure 3.10b. Scale bar = 20μm

(A)

(B)

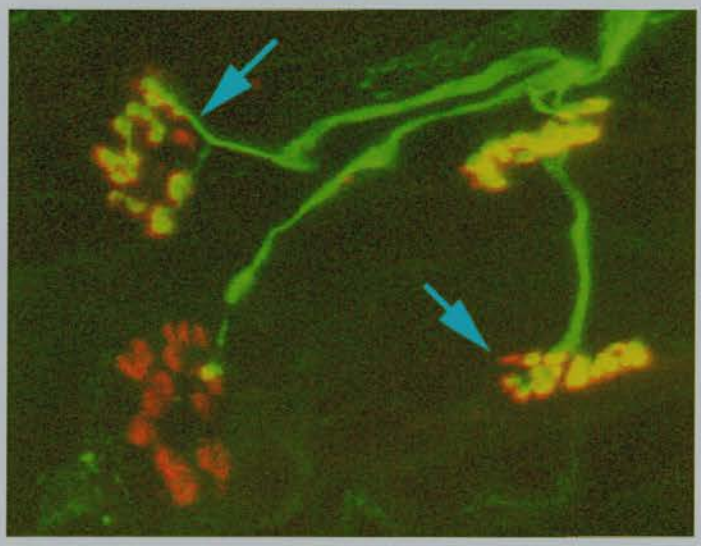

**Fig. 3.16 Asynchronous Withdrawal of Axotomised Nerve Terminals in Wld$^s$ Mice (Confocal Stereo Pair)**

(A) Stereo pair of confocal micrographs from a 2 month Wld$^s$ mouse FDB, 3 days post axotomy (NF, SV2 and α-BTX). 6 neighbouring endplates (and an incoming axon bundle) are shown in varying states of occupancy. The endplates present are either fully or partially occupied. To create a three-dimensional image, fuse the two images by eye to produce a third, central view. Visual accommodation and focussing on the central panel should yield a 3D image. Scale bar = 20μm

A)

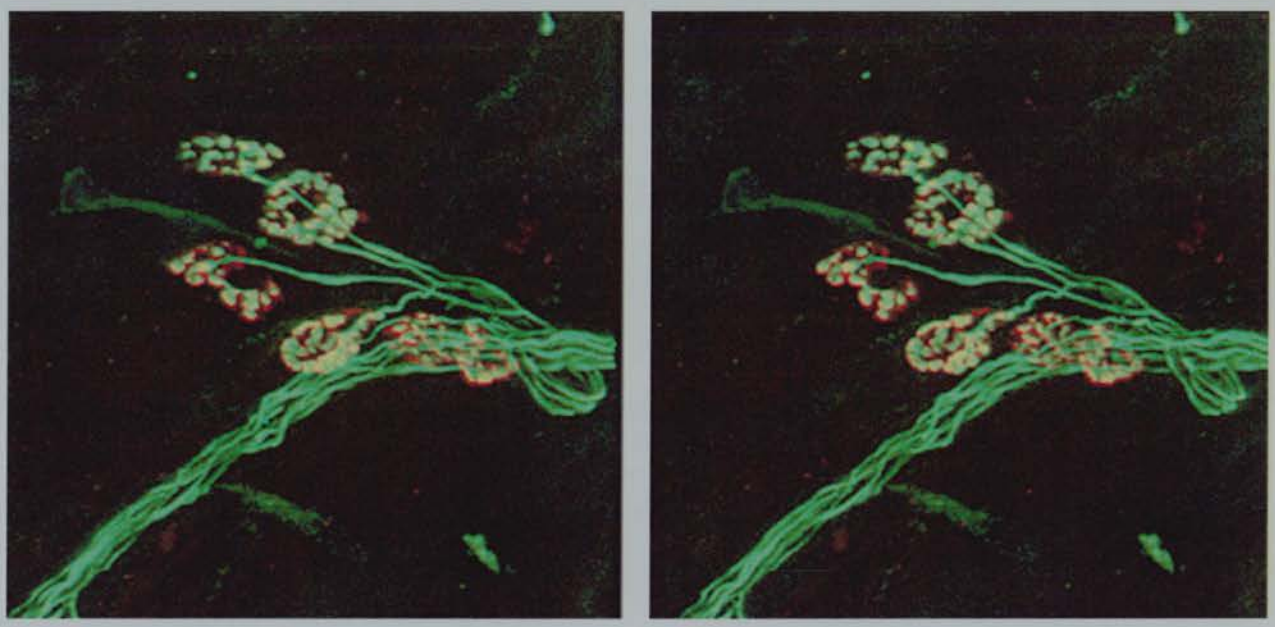

**Fig. 3.17 Distinct Morphology of Motor Axon Branches in Wld$^s$ Mice Following Axotomy**

(A) Confocal micrograph from a 2 month Wld$^s$ mouse FDB, 3 days post axotomy (NF, SV2 and α-BTX). Two neighbouring endplates are shown, both with an incoming motor axon branch showing characteristics observed in the majority of axotomised Wld$^s$ preparations: axon branches are thin, with occasional swellings showing accumulations of neurofilament (arrows). Scale bar = 20μm

(B & C) Fluorescence micrographs from a 2 month Wld$^s$ mouse FDB, 7 days post axotomy (B = NF, SV2 and α-BTX; C = NF and SV2 only). Another example of the neurofilament accumulations (arrows) and thin axonal profiles often observed in axotomised Wld$^s$ preparations is shown. Scale bar = 20μm

(A)

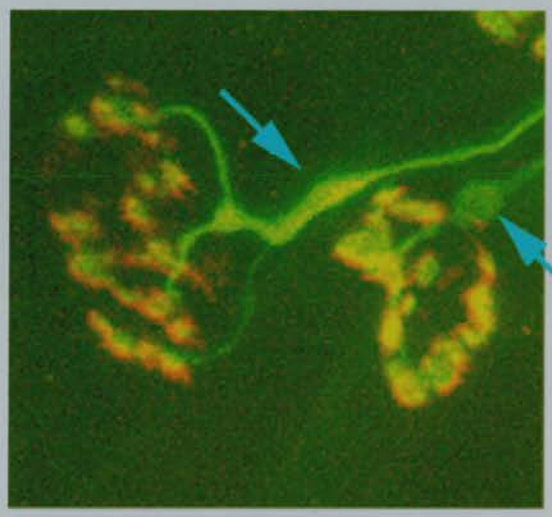

(B)

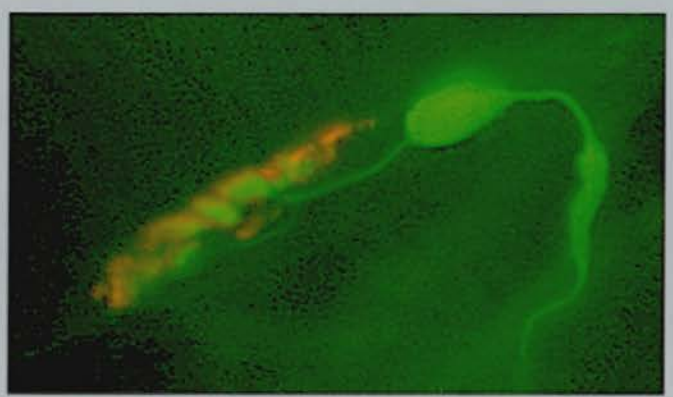

(C)

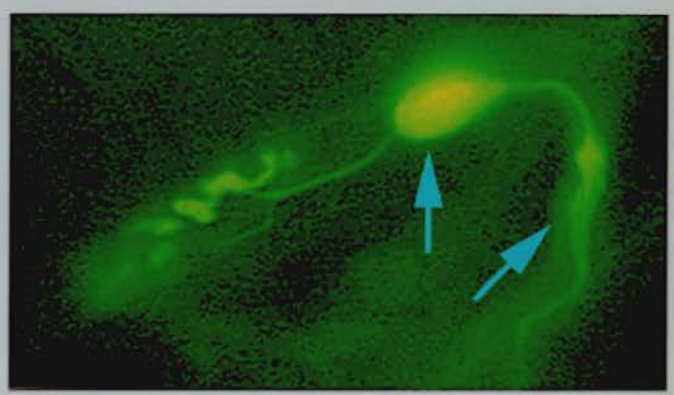

**Fig. 3.18 Electron Microscopic Evidence for Partial Occupancy at Axotomised Wld$^s$ NMJs.**

(A) Electron micrograph from a 2 month Wld$^s$ mouse FDB, 3 days post axotomy. This portion of an NMJ has postsynaptic receptor sites with no overlying nerve terminal present. Schwann cell occupation at some of the vacated synaptic sites is indicated (arrows). Scale bar = 2$\mu$m

(B) Electron micrograph from a 2 month Wld$^s$ mouse FDB, 3 days post axotomy. This nerve terminal bouton is from the same NMJ as (A), thereby permitting classification as a partially occupied endplate. The terminal architecture appears intact, with a uniform distribution and normal numbers of SVs and mitochondria. Scale bar = 1$\mu$m

(A)

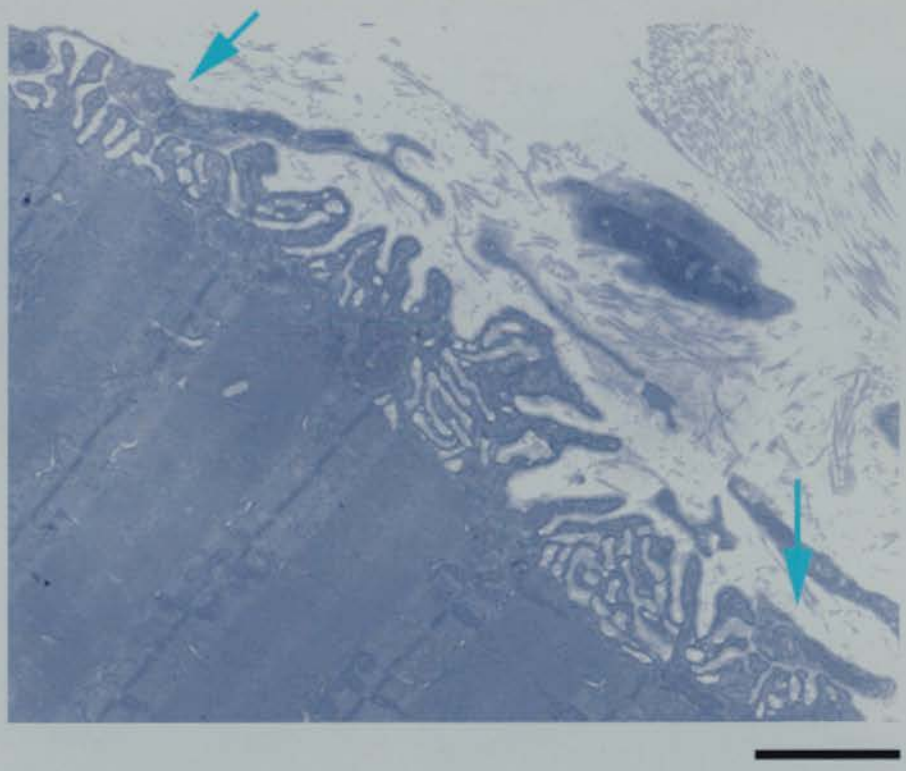

(B)

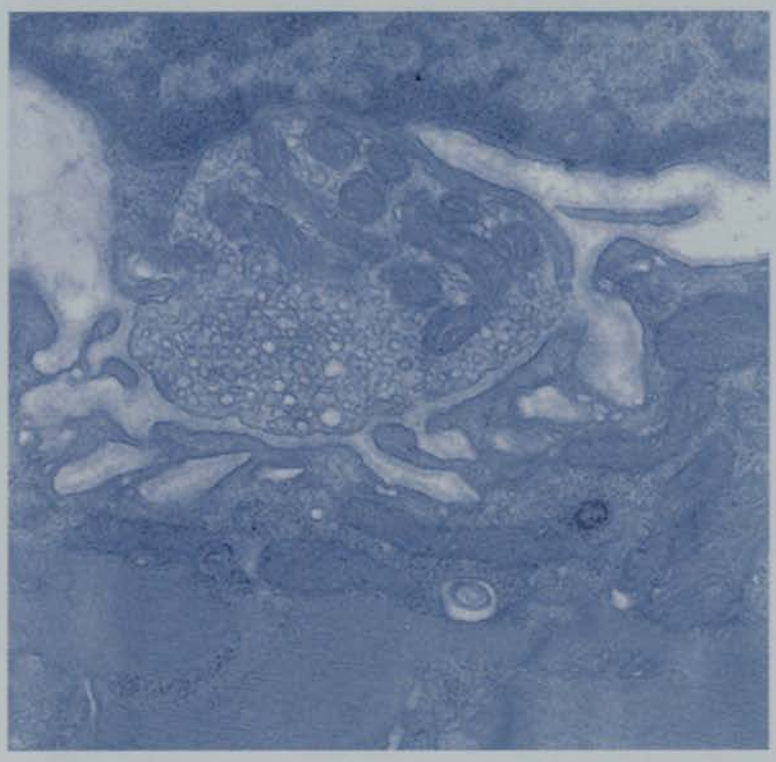

**Fig. 3.19 Levels of Occupancy and Partial Occupancy at Axotomised Wld$^s$ NMJs (Electron Microscopical Analysis)**

(A) Graph of the percentage of occupied endplates (all from 1 to 100% occupied are included) against time after axotomy in 2 month Wld$^s$ FDB muscle. Note that the data plotted for 0 days post axotomy represents the level of remodelling observed in unoperated control preparations. Black triangles represent data from individual muscles and red triangles represent the mean value at each time point.

(B) Graph of the percentage of partially occupied endplates (all from 1 to 99% occupied are included) against time after axotomy in 2 month Wld$^s$ FDB muscle. Note that the data plotted for 0 days post axotomy represents the level of remodelling observed in unoperated control preparations. Black triangles represent data from individual muscles and red triangles represent the mean value at each time point.

(A)

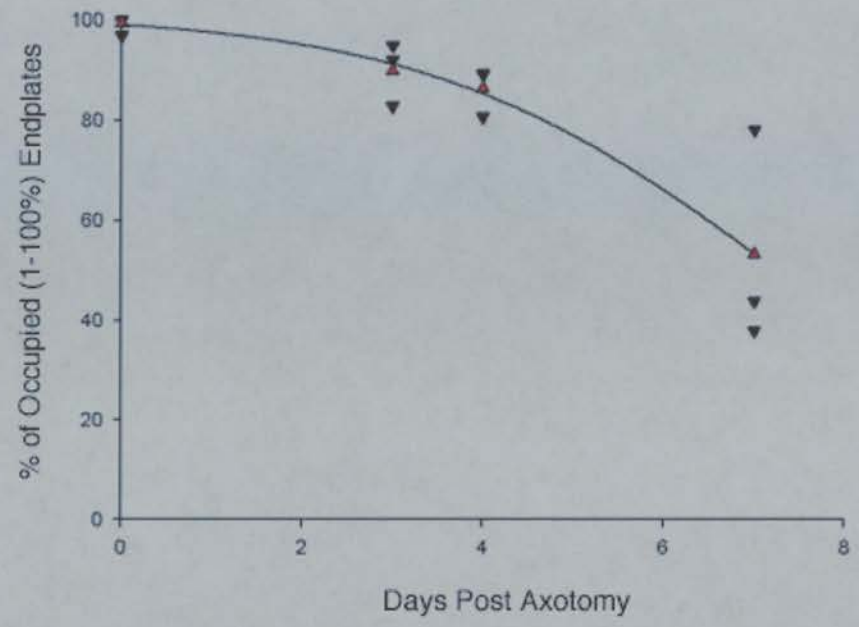
% of Occupied (1-100%) Endplates
100
80
60
40
20
0
0
2
4
6
8
Days Post Axotomy

(B)

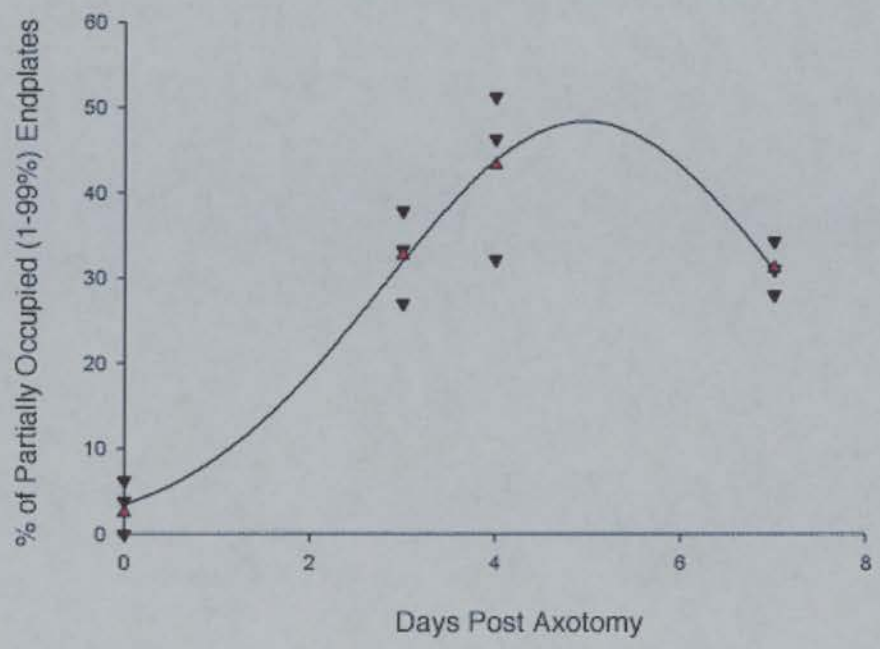
% of Partially Occupied (1-99%) Endplates
60
50
40
30
20
10
0
0
2
4
6
8
Days Post Axotomy

**Fig. 3.20 Neurofilament Accumulation in Axotomised Wld$^s$ Motor Nerve Terminals**

(A) Electron micrograph from a 2 month Wld$^s$ mouse, 3 days post axotomy. Note the conspicuous neurofilament accumulation in the centre of the nerve terminal (arrows). Scale bar = 0.5$\mu$m

(B) Electron micrograph from a 2 month Wld$^s$ mouse, 3 days post axotomy. Neurofilament accumulation in the centre of the nerve terminal is again present (arrows). Scale bar = 0.5$\mu$m

(A)

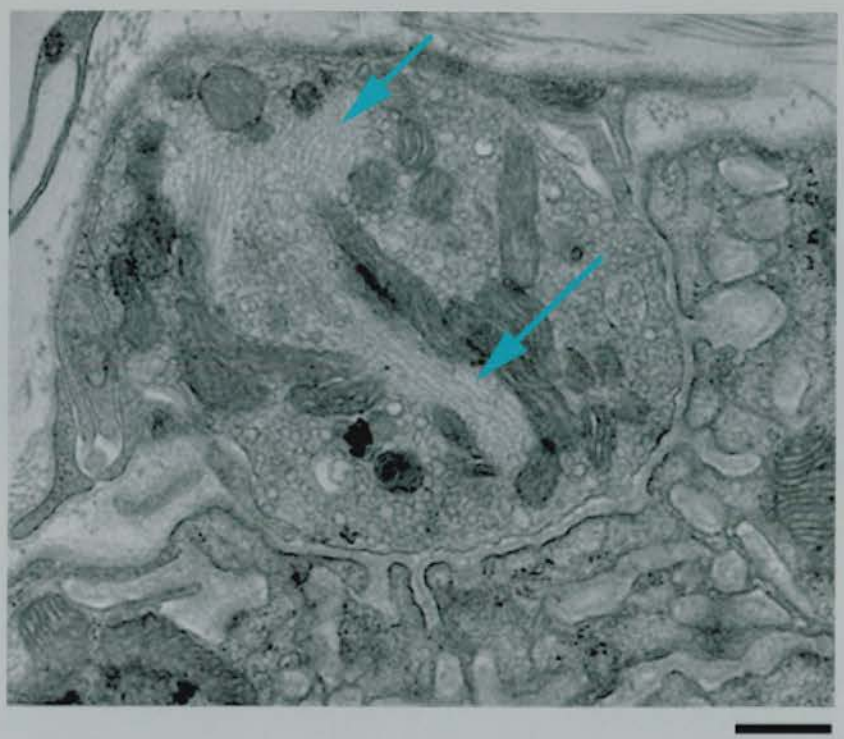

(B)

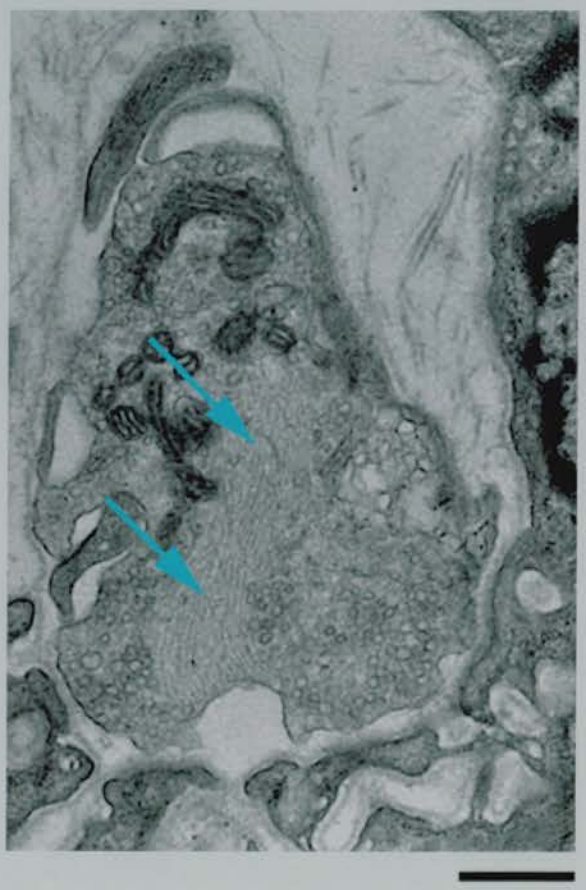

**Fig. 3.21 Quantification of Neurofilament Accumulation in Axotomised Wld$^s$ Motor Nerve Terminals**

(A) Graph of the percentage of nerve terminal occupied by neurofilaments against time after axotomy in 2 month Wld$^s$ mice FDB muscles. There is no significant difference between the levels of neurofilament in control (0 day) and 3 day post axotomy nerve terminals ($P = 0.4273$), but there is a significant accumulation in 4, 5 and 7 day axotomised terminals (all are $P = <0.0001$). Error bars = SEM (no error bar for 7 day data as was only one data point). All statistical tests = Mann Whitney.

(A)

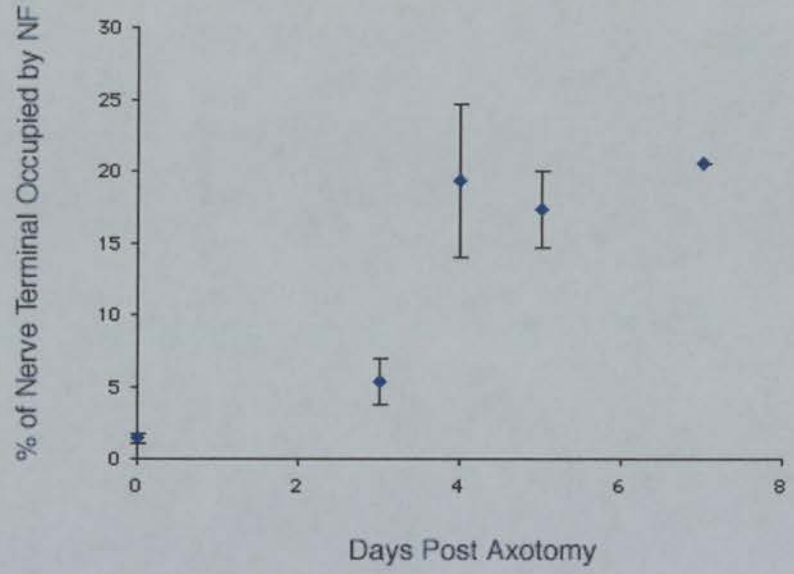
% of Nerve Terminal Occupied by NF
30
25
20
15
10
5
0
0
2
4
6
8
Days Post Axotomy

**Fig. 3.22 Synaptic Vesicle Preservation in Axotomised Wld$^s$ Motor Nerve Terminals**

(A) Electron micrograph of a NMJ from a 2 month Wld$^s$ mouse, 5 days post axotomy. Despite the accumulation of NF, qualitatively the synaptic vesicles appear normal in both number and distribution, located as they are proximal the presynaptic membrane. Scale bar = 0.5$\mu$m

(A) Electron micrograph from a 2 month Wld$^s$ mouse, 5 days post axotomy. This nerve terminal profile contains an example of a 'giant' vesicle (arrow). Scale bar = 0.5$\mu$m

(A)

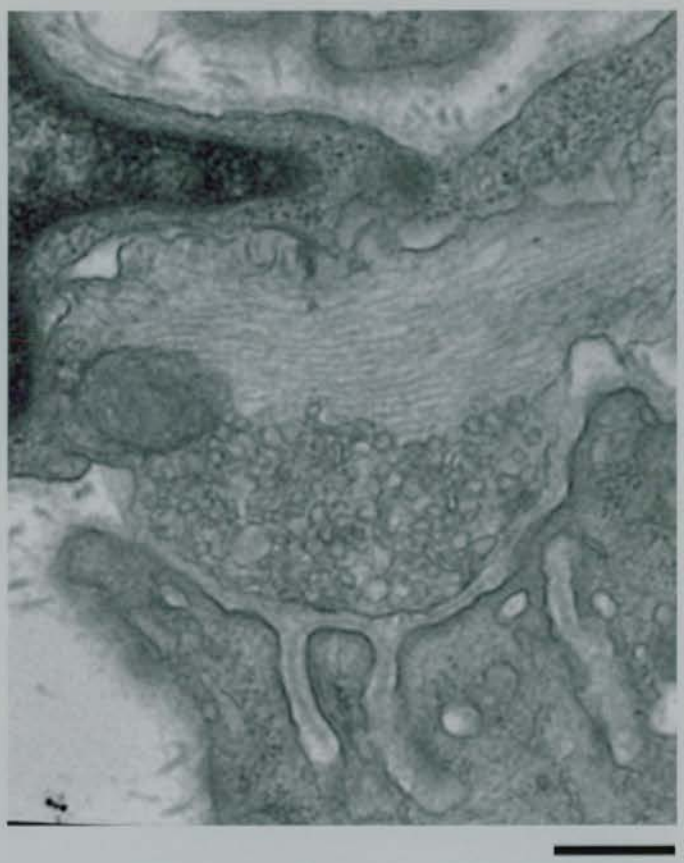

(B)

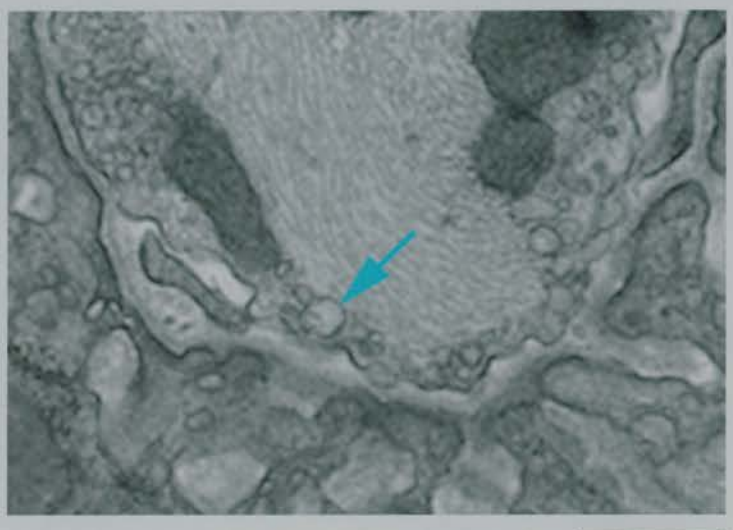

**Fig. 3.23 Quantification of Overall Synaptic Vesicle Density Within Axotomised Wld$^s$ Motor Nerve Terminals**

(A) Graph of the number of SVs per $\mu m^2$ against time after axotomy in 2 month Wld$^s$ mice. There was no significant difference between the SV density in nerve terminals from 3, 4, 5 or 7 days post axotomy compared to controls. Error bars = SEM. Statistical tests = Unpaired t test.

(B) Bar chart of the number of SVs per $\mu m^2$ against time after axotomy (in fully versus partially occupied profiles) in 2 month Wld$^s$ mice. At all time points post axotomy, there was no significant difference between partially and fully occupied terminals. Error bars = SEM. Statistical tests = Unpaired t test.

(A)

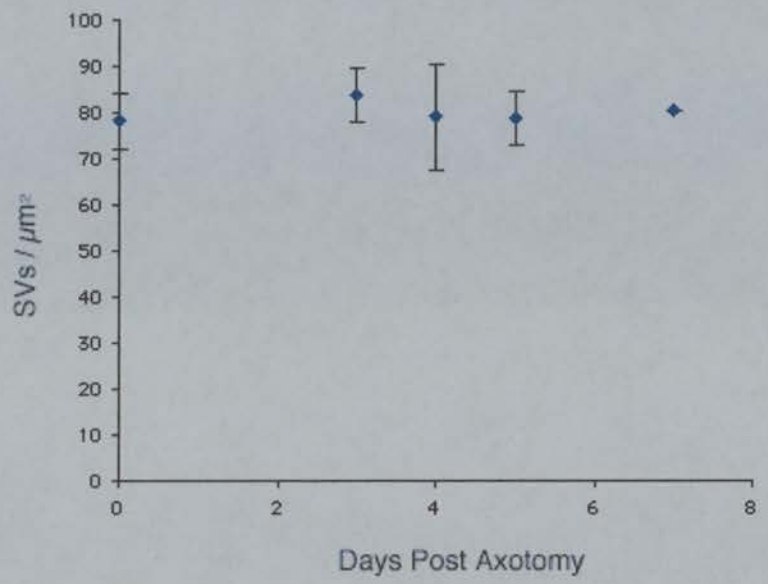
100
90
80
70
60
50
40
30
20
10
0
SVs / µm²
0
2
4
6
8
Days Post Axotomy

(B)

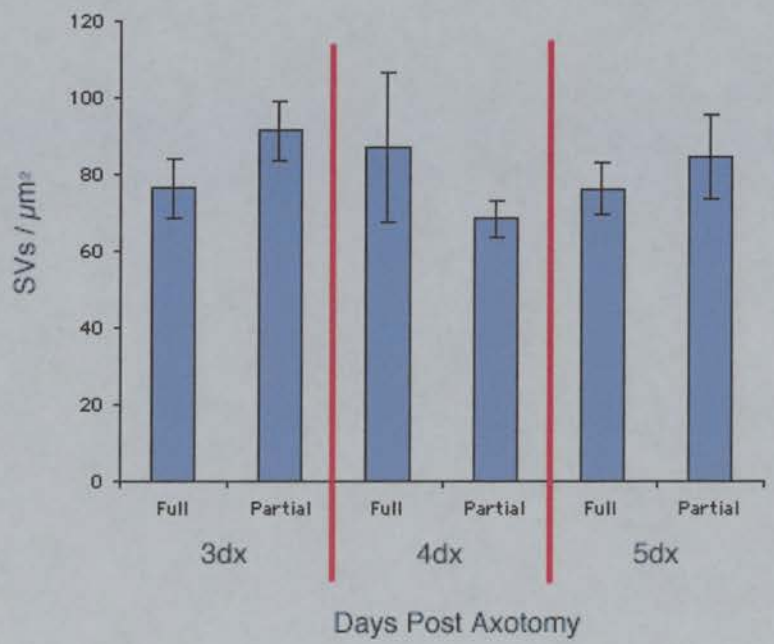
120
100
80
60
40
20
0
SVs / µm²
Full
Partial
Full
Partial
Full
Partial
3dx
4dx
5dx
Days Post Axotomy

**Fig. 3.24 Quantification of Synaptic Vesicle Packing Density Within Axotomised Wld$^s$ Motor Nerve Terminals**

(A) Graph of the percentage of terminal area available for synaptic vesicles (total terminal area minus area occupied by mitochondria and NF; see chapter 2 for details) occupied by synaptic vesicles against days post axotomy in 2 month Wld$^s$ mice. At all time points following axotomy, the density of SV packing was significantly higher ($P = <0.0001$) than in controls. Error bars = SEM. Statistical tests = Mann Whitney.

(B) Bar chart of the percentage of terminal area available for SVs occupied by synaptic vesicles against days post axotomy (in fully versus partially occupied profiles) in 2 month Wld$^s$ mice. In mice 3 days post-axotomy, there was a higher density of SVs in partially occupied terminals compared to fully occupied terminals ($P = 0.0275$). In 4 day axotomised preparations there was no significant difference between fully and partially occupied terminals ($P = 0.4$) whilst, as in the 3 day axotomised terminals, 5 day axotomised partially occupied terminals had a higher SV density than fully occupied terminals ($P = 0.0303$). Error bars = SEM. Statistical tests = Mann Whitney.

(A)

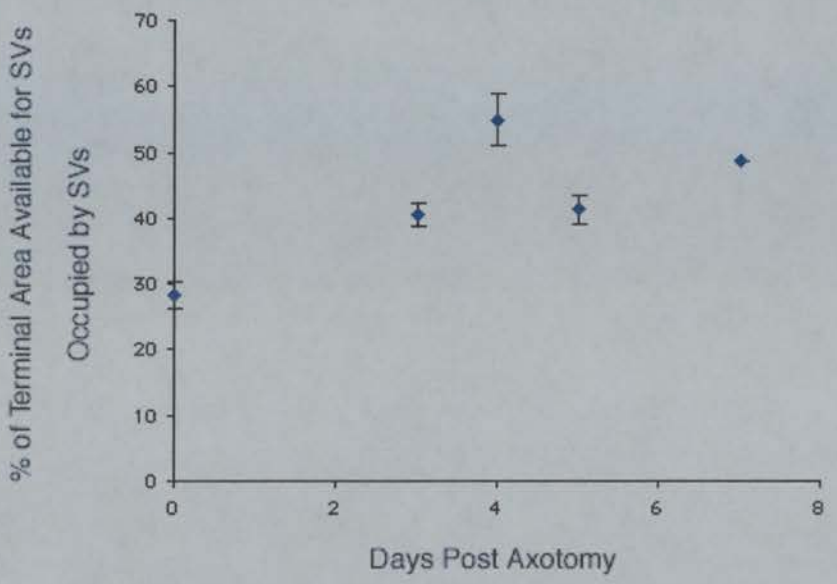
% of Terminal Area Available for SVs Occupied by SVs
70
60
50
40
30
20
10
0
0
2
4
6
8
Days Post Axotomy

(B)

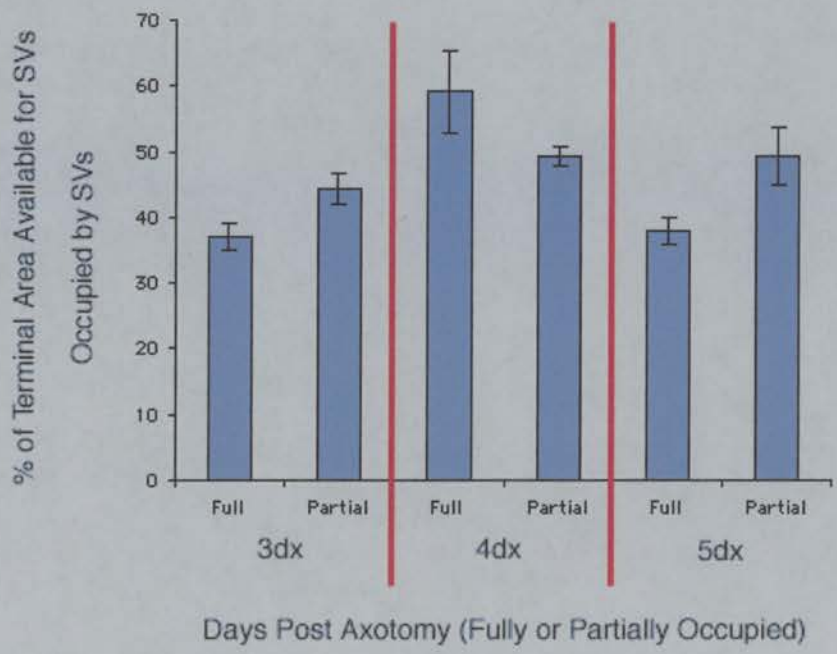
% of Terminal Area Available for SVs Occupied by SVs
70
60
50
40
30
20
10
0
Full
Partial
Full
Partial
Full
Partial
3dx
4dx
5dx
Days Post Axotomy (Fully or Partially Occupied)

**Fig. 3.25 Quantification of Synaptic Vesicle Population Localisation Within Axotomised Wld$^s$ Motor Nerve Terminals**

(A) Graph of the number of synaptic vesicles within a 125nm radius of an active zone ('docked' vesicles) against time after axotomy in 2 month Wld$^s$ mice. At all time points post-axotomy, there was no significant reduction (in all cases P = >0.12) in the numbers of SVs clustered toward active zones on the presynaptic membrane Error bars = SEM. Statistical tests = Unpaired t test.

(A)

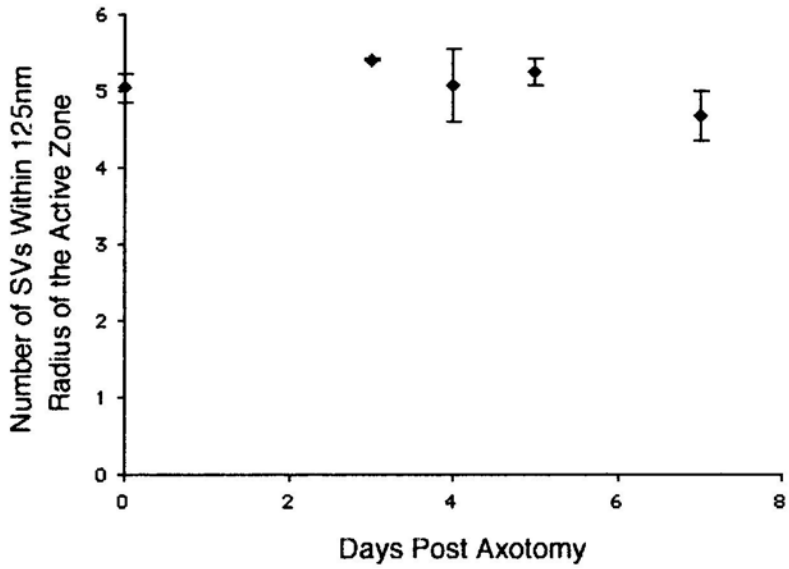
Number of SVs Within 125nm
Radius of the Active Zone
0
1
2
3
4
5
6
0
2
4
6
8
Days Post Axotomy

## 3.4 Discussion

In this chapter I compared the effects of axotomy on Wld$^s$ mouse neuromuscular junctions with wild-type mouse NMJs. The morphological and ultrastructural techniques I used strongly suggest that the mechanisms of nerve terminal loss occurring at axotomised Wld$^s$ NMJs are fundamentally different from those which occur during wild-type degeneration. The interpretations of my observations alongside potential sources of error are considered in this discussion, and the emerging hypothesis, that presynaptic nerve terminal degeneration is regulated by mechanisms distinct from axon degeneration, is pursued in following chapters.

### 3.4.1 Accuracy of the Quantification Methods Used in the Present Study

The immunocytochemical and electron microscopical data reported in this study have been generated using techniques adapted from previous studies alongside novel methods of analysis. Comparison of data from this study with those provided in the literature suggests that the techniques used have produced accurate and reliable results. For example, the ultrastructural preservation of healthy looking mitochondria in control preparations, as was achieved with the current tissue processing protocol (Figure 3.4), is a key factor if subsequent use of degenerating mitochondrial profiles as a marker of degeneration is to be used. The majority of mitochondrial profiles from control

micrographs had a well preserved ultrastructure (fulfilling the same criteria as those defined by Miledi and Slater (1970), Manolov (1974) and Winlow and Usherwood (1975)), and those that did not were very similar in appearance to mitochondria identified by Winlow and Usherwood (1975) to be undergoing a process of natural turnover. Similarly, when calculating the density of synaptic vesicles within motor nerve terminals using the current method, a range of values from 35 SV/$\mu m^2$ to 184 SV/$\mu m^2$ was generated. These figures resemble the control levels as reported by Reger (28-114 SV/$\mu m^2$; 1959) and Winlow and Usherwood (36-209 SV/$\mu m^2$; 1975). The slight variation between the three sets of data most probably represents differences in the calculation methods used as well as a small diversification in nerve terminal morphology between individual muscles and animals.

Closer scrutiny of the methods used for the quantification of SV density and localisation within nerve terminals, by comparing control with toxin treated preparations, confirmed that they are sensitive enough to detect changes in all parameters of the SV population (Figures 3.5 and 3.6). Interestingly, some of the NMJ profiles from toxin-treated muscles appeared to indicate a compression and flattening of the secondary postsynaptic folds. One plausible hypothesis to explain this phenomenon is that a compression occurs as a result of a significant increase in the total membrane area of the nerve terminal due to the large amount of SV exocytosis that is caused by toxin application. A mass exocytosis of synaptic vesicles has previously been shown to cause a large

expansion in the size of the nerve terminal, and hence a compression of the postsynaptic apparatus (O'Hanlon et al., 2001).

### 3.4.2 Remodelling of Neuromuscular Connections

The immunocytochemical and ultrastructural evidence for partial occupancy in control preparations (Figures 3.2 and 3.3) suggests that *in vivo* remodelling at synaptic connections of NMJs on FDB and TA muscles in adult mice is relatively common. One possible criticism of the FM1-43 experimental data however, is that even though some terminal boutons are not labelled with FM1-43, it does not mean that they are not present. This explanation is plausible if the unstained boutons are present but 'silent', thereby not recycling any synaptic vesicles and as a result blocking the uptake of FM1-43. This proposal seems unlikely however, as it has been shown that all boutons of a motor nerve terminal operate as a single functional unit (Betz et al., 1992; Ribchester et al., 1994). Immunocytochemical and ultrastructural experiments, which do not require boutons to be active to allow identification, support the FM1-43 findings however, thereby unequivocally demonstrating the occurrence of partial occupancy at control NMJs from a number of different strains of mice ($Wld^s$, Swiss, C3H and C57Bl/6).

Remodelling of neuromuscular synapses has been previously reported in a variety of other muscle preparations, including: mouse sternomastoid (Lichtman et al., 1987), frog sartorius (Herrera et al., 1990), mouse soleus (Wigston, 1989), rat soleus (Cardasis and

Padykula, 1981) and mouse pectineus (Hill et al., 1991). The level of remodelling apparent in these muscles appears to differ however. For example, this study of mouse FDB muscle suggests that approximately 3% of NMJs are undergoing remodelling at any one time, whereas Lichtman and colleagues report a level of <1% in mouse sternomastoid muscle (Lichtman et al., 1987). One possible reason for this difference may be the staining techniques used. Lichtman and colleagues (1987) used 4-Di-2-ASP to label motor nerve terminals, a technique which sometimes produces an incomplete stain (Wigston, 1989). This could feasibly lead to slight differences in the counting criteria used in the different studies. A more plausible hypothesis is that differences in the composition and activity levels of the muscles studied require higher or lower levels of remodelling to maintain suitable synaptic connections. For example, fast-twitch muscle NMJs are known to have a more complex morphology than those found on slow-twitch muscle fibres (Lømo and Waerhaug, 1985), therefore any slight change in the properties of the muscle fibre (as has been shown to occur in rat soleus; Kugelberg, 1976) would require a more rigorous remodelling process of the motor nerve terminals than would be required on stable muscle fibres. Alternatively, differences in the patterns or amounts of neural activity occurring at different muscle groups may produce different rates of remodelling (Wigston, 1989).

The ultrastructural evidence for partial occupancy at control nerve terminal profiles presented in this chapter closely resembles the findings of Cardasis and Padykula (1981), who described the ultrastructural characteristics of remodelling NMJs in rat

soleus muscle preparations. These authors described the occurrence of vacant junctional folds, not associated with nerve terminals, residing next to regions of intact synaptic associations. They also noted the occasional intervention of terminal Schwann cell processes into the synaptic cleft. Both of these situations were observed at a minority of control nerve terminal profiles assessed in the current study. Indeed, it raises the possibility that a Schwann cell invasion of an otherwise 'normal' appearing NMJ synaptic cleft may represent the initiation of remodelling processes at the specific bouton(s) involved.

### 3.4.3 Retention and Withdrawal of Motor Nerve Terminals Following Axotomy in the Wld$^s$ Mouse

The data presented in this chapter confirm previous findings that motor nerve terminals are preserved, alongside their axons, for several days following axotomy in Wld$^s$ mice of 2 months or younger (Ribchester et al., 1995; Mattison et al., 1996; Parson et al., 1998). Immunocytochemical data report that at 7 days post axotomy, 52.29% of endplates were occupied in Wld$^s$ FDB muscle preparations (Figure 3.10). This level of retention is significantly higher than the levels observed using FM1-43 staining in axotomised Wld$^s$ TA muscle (approximately 19%; Mattison, R.J. 1999, PhD Thesis, University of Edinburgh). This difference could derive from many sources; firstly, that the length of the distal axonal stump was shorter in axotomised TA preparations; secondly, that FM1-43 staining was reduced as a result of a loss of function at

remaining nerve terminals; and thirdly, that nerve terminals on TA muscle fibres are more susceptible to axotomy in the $Wld^s$ mouse than terminals on FDB muscle fibres. With regard to the nerve stump dependence hypothesis, it has been shown that the length of the distal axonal stump alters the rate of degeneration at both wild-type (Luco and Eyzaguirre, 1955; Birks, Katz and Miledi, 1960; Miledi and Slater, 1970) and $Wld^s$ (Ribchester et al., 1995) nerve terminals. In $Wld^s$ mice, an increase of 1cm in the length of the distal stump delayed degeneration by ~1-2 days (Ribchester et al., 1995). Therefore, if the distal nerve stumps in the TA preparations used in Mattison's TA experiments were 1cm shorter than those left in my FDB preparations, a comparable level of occupancy nearing 50% would be expected (5 day data from Mattison, R.J. 1999, PhD Thesis, University of Edinburgh), the same level observed at 7 days in the present study. The distal stump in my FDB muscle preparations was ~10-15mm in length, similar to the nerve stump length left in TA preparations (Dr R Ribchester, personal communication). Because there was no specific data on the length of distal nerve stumps given in Mattison's experiments, it is not possible to accurately assess whether or not a difference in stump length underlies the differences between the two studies. It remains possible therefore, that differences in staining patterns between FM1-43 and NF/SV2 labelled preparations may be the cause of the discrepancy. As it has been suggested that axotomised $Wld^s$ nerve terminals undergo a progressive weakening of synaptic transmission (Ribchester et al., 1999; D.Thomson, personal communication), it is possible to speculate that some persistent terminals may not be recycling synaptic vesicles. Such terminals would be detected using NF/SV2 staining,

but not FM1-43, possibly explaining the higher levels of occupancy in my immunocytochemical experiments. Finally, it is plausible that the properties of individual motor units, and differences in the muscle fibre type(s) they innervate, may provide the overriding factor in controlling the susceptibility to axotomy of nerve terminals. This hypothesis could be addressed by utilising a muscle preparation in which all nerve terminals from a single motor unit are identified (see Lichtman and Wilkinson, 1987). If the loss of a nerve terminal *is* controlled by the properties of its motor unit, it would be expected that all other nerve terminals from the same unit should be lost synchronously and at the same rate.

As the immunocytochemical analysis of nerve terminal loss at axotomised $Wld^s$ FDB muscle preparations was carried out in conjunction with electrophysiological studies (contralateral axotomised FDB muscles were used for intracellular recording by Mr D. Thomson), a comparison of the findings has proved important (Figure 3.26). The percentage of occupied fibres as calculated from the electrophysiological data (an occupied endplate being identified if an individual muscle fibre showed evoked responses following nerve stimulation) was significantly lower ($P=0.0426$; Mann Whitney test) than those detected using the morphological data, with levels of 31.00% ±5.86 (SEM) and 52.29% ±4.26 respectively at 7 days post axotomy.

**Fig. 3.26 Comparison of Morphological and Electrophysiological Analyses of Nerve Terminal Loss at Axotomised Wld$^s$ FDB Muscle Preparations.**

(A) Graph of number of occupied endplates versus days post axotomy from 2 month old Wld$^s$ mouse FDB muscle preparations analysed using immunocytochemical techniques (NF, SV2 and α-BTX). Black triangles represent data from individual muscles and red triangles represent the mean value (reproduced from Figure 3.10).

(B) Graph of number of occupied endplates versus days post axotomy from 2 month old Wld$^s$ mouse FDB muscle preparations analysed using electrophysiological techniques. Black triangles represent data from individual muscles and red triangles represent the mean value. Unpublished data courtesy of Mr D. Thomson and Dr R. Ribchester.

(A)

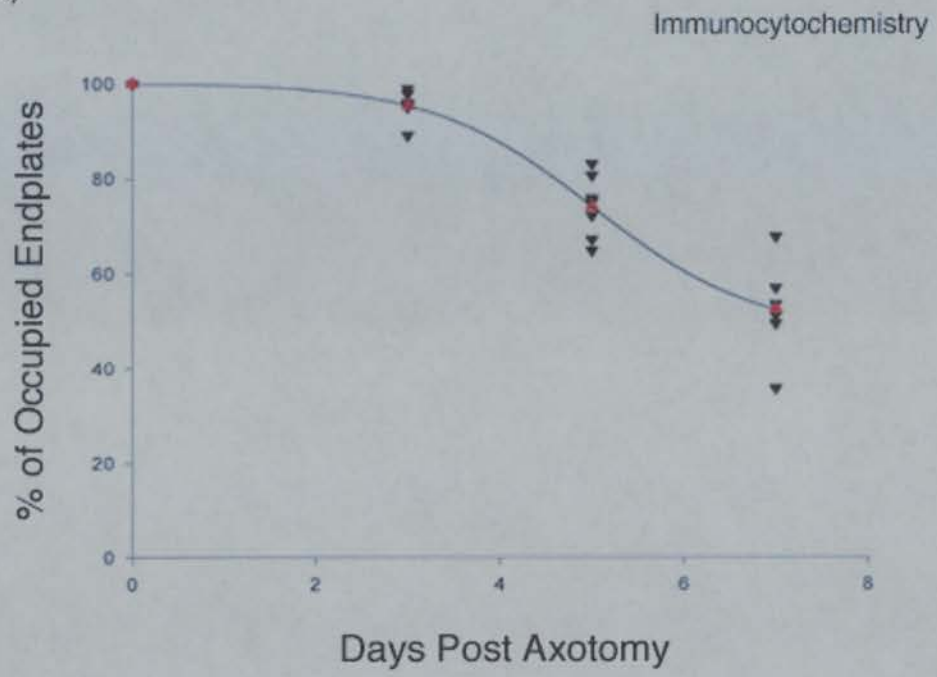
Immunocytochemistry
% of Occupied Endplates
100
80
60
40
20
0
0
2
4
6
8
Days Post Axotomy

(B)

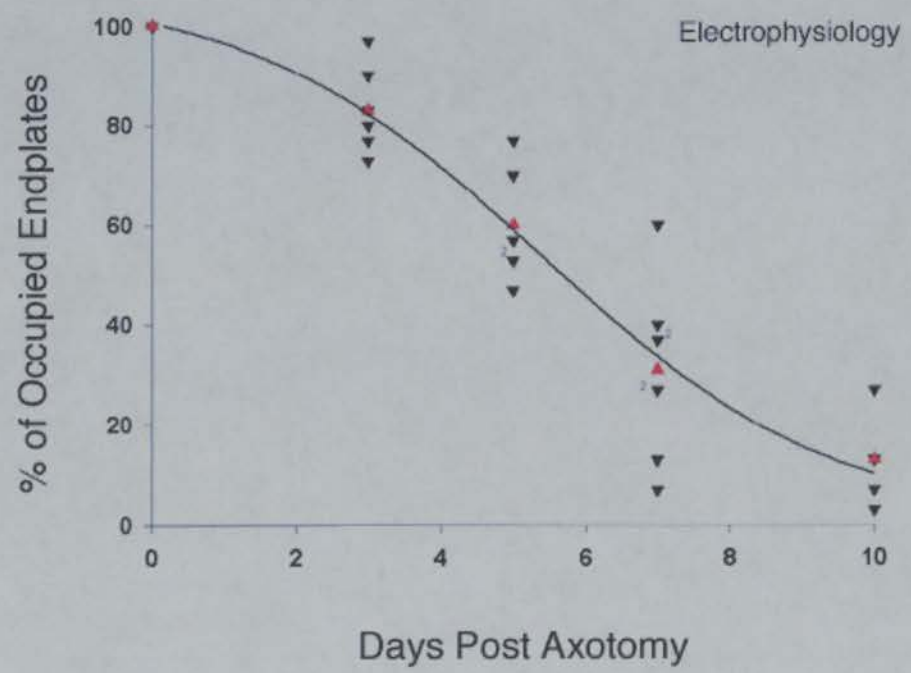
Electrophysiology
% of Occupied Endplates
100
80
60
40
20
0
0
2
4
6
8
10
Days Post Axotomy

Similar differences were observed when comparing the 3 day and 5 day post axotomy data. The most likely explanation for the discrepancy between these two sets of data is that the electrophysiological data was gained from the analysis of endplates showing evoked responses only, rather than evoked and spontaneous responses. This raises the possibility that any terminals which were present but did not have either enough surface area to produce a postsynaptic endplate potential upon evoked release, or had severely impaired evoked release mechanisms, were not detected using the electrophysiological method of analysis. Further scope for discrepancy is introduced when the fact that the functional data was gathered using a very small sample size (only 30 fibres were impaled per muscle) compared to the whole muscle analysis undertaken using morphological techniques. When comparing the current morphological data with previously published intracellular recording measurements from axotomised $Wld^s$ soleus muscles however, similar levels of approximately 50% occupancy were detected at 7 days post axotomy using either method (Ribchester et al., 1995).

Ultrastructural analysis of the preservation of motor nerve terminals in $Wld^s$ mice following axotomy lends further support to the immunocytochemical findings (Figures 3.11 and 3.19). Quantification of electron micrographs from 7 day axotomised $Wld^s$ mouse FDB muscles showed that 53.18% ±12.58(SEM) of endplates were occupied in comparison to 52.29% ±4.26 of endplates from the morphological analysis. A qualitative comparison between electron micrographs at 5 days post axotomy from the current study and those shown in Ribchester and colleagues (1995) study shows a

similar retention of terminal architecture, although the degree of mitochondrial damage depicted in the previous study's unquantified micrographs are never observed in my preparations. The most obvious explanation for these findings is that different tissue processing techniques were used, whereby the current study's protocol was much more suitable for fast and strong fixation than that used previously. The use of a strong paraformaldehyde / glutaraldehyde fixation solution followed by an immediate osmium post-fixation step was employed after initial experiments using fixation protocols, such as that used by Ribchester et al. (1995), proved to be unreliable (unpublished observations).

In $Wld^s$ mice NMJs at 4 days post axotomy and beyond, ultrastructural profiles from many of the remaining terminals showed signs of neurofilament accumulation within the centre of synaptic boutons (Figure 3.20 and 3.21). This phenomenon has been observed in a previous study of axotomised $Wld^s$ NMJs (Ribchester et al., 1995) as well as in the last few remaining nerve terminals undergoing Wallerian degeneration in wild-type preparations (Manolov, 1974). The most likely explanation for these events is provided from a study by Watson et al. (1993) who showed that within a few days of axotomy, there was a marked accumulation of alpha- and beta-tubulin, actin, and nonphosphorylated neurofilament epitopes at the proximal and distal ends of transected axons, suggesting that bi-directional transport continues in the distal nerve stump. Furthermore, these authors showed that there was a loss of these proteins from the centre of the isolated nerve segment. This study was limited in its resolution by the use

of biochemical techniques however. The results from the current study, which provided a high enough resolution to study axonal events at the distal extremities of the nerve, suggest that the accumulation of NF is not continuous. Thus, axonal branches supplying motor nerve terminals often appeared thin and wispy, only occasionally interrupted by large accumulations of neurofilament proteins (Figure 3.17). One possible explanation for this is that the axons observed in the current study are still undergoing the translocation of NFs from the middle of the axon to the extremes of the axon segment (hence the thin axonal appearance), and that the neurofilament accumulations may represent an aggregation of NFs which are in the process being transported the final few microns to the extremities of the axon segment. To address this hypothesis, real-time visualisation of these neurofilament bundles is required, to assess whether or not they are still being transported towards the nerve terminals. Alternatively, it is possible that the retraction of nerve terminals into the axon reverses this process, resulting in the compression and subsequent movement of NF accumulations back towards the centre of the nerve. As a further point of interest, the current study estimates that the rate of slow axonal transport (by which neurofilaments are transported bi-directionally in the axon; Vallee and Bloom, 1991; Glass and Griffin, 1991) is ~1.25-1.88mm/day in $Wld^s$ mouse tibial nerve. This value falls well within the accepted range of rates for slow axonal transport as reported by Glass and Griffin (0.1-4mm/day; 1994).

If these axonal aggregations of NF observed at axotomised Wld$^s$ motor axon collaterals are not simply 'in transit', a different explanation may be required. Pathological aggregations of NF proteins in axons have been described as a hallmark of amyotrophic lateral sclerosis (ALS; Hirano et al., 1984; de Aguilar et al., 1999), a condition in which motoneurone degeneration has been observed (Lim et al., 2000). Furthermore, in a pathological study of superoxide dismutase (SOD-1) transgenic mice which develop strong ALS symptomatology and pathology, Morrison and colleagues (2000) have described sporadic accumulations of NF within sciatic nerve axons which qualitatively resemble those seen in axotomised Wld$^s$ motor axon collaterals. These authors proposed that deficits in axon transport may underlie their observed pathology, a mechanism which has previously been ruled out in the Wld$^s$ mouse however (Glass and Griffin, 1991; Glass and Griffin, 1994). Nevertheless, any developments from studies on the SOD-1 transgenic mouse with regard to NF accumulations may be applicable to the Wld$^s$ phenotype. Indeed it may be of interest to ALS researchers to learn that the Wld$^s$ mouse, whilst containing similar NF aggregations, shows no readily discernable ALS-like symptomology. As a further point of interest, the similar time-course of NF accumulation in Wld$^s$ and wild-type NMJs provides further evidence that neither the rate of axonal transport of NFs, nor NF stability, is affected by the Wld$^s$ mutation (Glass and Griffin, 1991; Tsao et al., 1994; Glass and Griffin, 1994).

Previous reports suggesting that nerve terminals withdraw from their endplates in young Wld$^s$ mice following axotomy are supported by findings from the present study.

Lesioned axons from Wld$^s$ mice, whilst being preserved for several weeks, do eventually degenerate (Lunn et al., 1989; Tsao et al., 1994). Whether this process occurs via the same mechanisms as classical Wallerian degeneration or not has yet to be definitively addressed however (Brown et al., 1992). This would suggest that motor nerve terminals should undergo a similar, delayed but eventual, process of Wallerian or Wallerian-like degeneration. In contrast, evidence that nerve terminals appear to be lost via a gradual piecemeal retraction from the endplate has been presented, using vital dye staining as well as NF/SV2 immunocytochemical staining (Parson et al., 1998; Ribchester et al., 1999; Mattison, R.J. 1999, PhD Thesis, University of Edinburgh). Morphological evidence of endplates at all states of partial occupancy (1-99% occupied) is presented in the current study from 2 month old Wld$^s$ mice at 3, 5 and 7 days post axotomy (Figures 3.12, 3.13 and 3.14). Immunocytochemically labelled partially occupied NMJs visualised in the present study have the same type of appearance as those described in previous studies which have used FM1-43 labelling alongside immunocytochemistry (Parson et al., 1998; Ribchester et al., 1999; Mattison, R.J. 1999, PhD Thesis, University of Edinburgh). Areas of vacated AchRs appear as brightly labelled as neighbouring occupied regions, whilst nerve terminals at these endplates have healthy appearing boutons connected by thin, wispy axon strands. The identification of endplates at all levels of partial occupancy, from a single bouton unoccupied through to the formation of 'retraction bulbs' suggests that the process of withdrawal gradually proceeds, bouton by bouton, until all nerve terminal boutons have been retracted back into the parent axon. The observation that terminal boutons at the

extremities of nerve terminal branches (but not necessarily at the extremes of the endplate) are lost first, rather than in a non-sequential manner, provides further evidence that boutons are 'retracted' back into their parent axon (Figure 3.12). This temporal hypothesis can not be wholly accepted however until real-time visualisation of axotomised $Wld^s$ nerve terminals has been accomplished. Real-time techniques have been used to visualise the withdrawal of nerve terminals from polyneuronally innervated NMJs during development (for example; Balice-Gordon and Lichtman, 1993) and their application to observing synaptic events at axotomised NMJs of $Wld^s$ mice either in vitro or in vivo will hopefully be achieved in the near future (S.H.Parson and R.R.Ribchester, personal communication).

Whilst similar immunocytochemical experiments to those described in this chapter have previously been undertaken, no study to date has analysed the process of nerve terminal withdrawal in conjunction with providing data on in vivo synaptic remodelling. Data concerning the level of synaptic remodelling (see above) that occurs naturally at mammalian NMJs suggests that previous analyses of partial occupancy at axotomised $Wld^s$ NMJs may be slightly inaccurate. If 3% or more of nerve terminals are undergoing remodelling at any one point in time, as the data presented in this study suggest, then a simple identification of a partially occupied endplate in a $Wld^s$ muscle preparation may not be enough to assume that it is undergoing axotomy induced withdrawal. The current study takes background levels of remodelling into account

(see Figures 3.3, 3.14 and 3.19) by plotting accurate control data on those graphs which assess the trends of partial occupancy levels at various time points following axotomy.

Similarly, no other study to date has provided combined morphological and electrophysiological data from the same animals (Figure 3.26). Whilst the current findings suggest that isolated electrophysiological experiments may underestimate the true level of occupancy at axotomised Wld$^s$ FDB muscle preparations, the coordination of morphological and functional experiments has produced many interesting findings. Firstly, the increasing incidence of partially occupied endplates and NMJs exhibiting weak synaptic transmission, with progressive days following axotomy, matched each other closely (D.Thomson, personal communication). Thus, it is possible to conclude that a decline in the occupancy of the endplate may occur concurrently with a decline in synaptic function. This hypothesis is supported by a few intracellular recordings made from identified junctions by Ribchester et al. (1999), who showed that as the occupancy of an endplate declined, the incidence of failures increased. To adequately address the hypothesis however, many more of these identified recordings need to be made. Secondly, the occurrence of both an increased MEPP rate and increased incidence of 'giant' MEPPs (>1mV) in intracellular recordings from axotomised 2 month Wld$^s$ FDB muscle preparations could be explained by morphological and ultrastructural characteristics. At many of the immunocytochemically labelled partially occupied NMJ preparations from Wld$^s$ FDB muscles following axotomy, the intensity of FITC labelling over the endplate appeared more intense than in control preparations (Figure

3.12). This suggested either an accumulation of NF or SV2 proteins within the terminal, both of which were eventually identified at ultrastructural nerve terminal profiles (Figures 3.20, 3.21 and 3.24; for evaluation of increased NF levels see below). The increased packing density of SVs in regions close to the presynaptic membrane at many axotomised $Wld^s$ nerve terminal profiles provides a plausible reason for an increased MEPP rate. When there are more vesicles clustered towards the presynaptic membrane, the probability of spontaneous release will almost certainly be higher. Interestingly however, there was no increase in the number of 'docked' vesicles between control and axotomised $Wld^s$ nerve terminals (Figure 3.25) as may be expected if more vesicles are packed towards the presynaptic membrane. This finding suggests that maximal levels of docked vesicles may already be reached in control preparations. Finally, the increasing occurrence of 'giant' MEPPS in electrophysiological recordings from axotomised $Wld^s$ FDB muscles correlates with the increased incidence of giant vesicles, some of which were almost three times the diameter of normal vesicles, from ultrastructural profiles of axotomised $Wld^s$ nerve terminals, and which were rarely seen in control profiles (Figure 3.22). It seems quite plausible that the fusion of a 'giant' vesicle with the presynaptic membrane would release much more neurotransmitter than a regular vesicle, hence the increase in MEPP amplitude. The presence of giant vesicles suggests that there may be some impairment in the fine control of the synaptic vesicle recycling pathway, or subsequent fusion of pre-existing vesicles, within axotomised $Wld^s$ nerve terminals.

As has previously been noted (Ribchester et al., 1999; Mattison, R.J. 1999, PhD Thesis, University of Edinburgh), the asynchronous nature of nerve terminal loss and partial occupancy at axotomised Wld$^s$ NMJs (Figures 3.15 and 3.16) bear comparison with similar features of NMJs undergoing developmental synapse elimination. The current study supports these findings and suggests that the withdrawal of Wld$^s$ nerve terminals may represent a recapitulation of this process. On a basic level, both involve an apparent piecemeal withdrawal from the endplate alongside a lack of degenerative markers (O'Brien et al., 1978; see below). More specifically however, some of the most compelling evidence for this statement comes from observing the incidence and appearance of retraction bulbs at axotomised Wld$^s$ endplates (Figure 3.13). The distinguishing features of these terminal axon swellings closely resemble the retraction bulbs which have been observed during synapse elimination (Riley, 1977; Riley, 1981; Balice-Gordon et al., 1993). A more detailed discussion with regards to the implications of these associations can be found in the final discussion (Chapter 6). Some aspects of nerve terminal withdrawal at axotomised Wld$^s$ NMJs do not have parallels in synapse elimination, however. For example, whilst NF accumulation is a prominent feature in axotomised Wld$^s$ NMJs, Roden et al. (1991) have shown that loss of NF proteins from nerve terminals is a common feature during synapse elimination.

Whilst morphological evidence of partial occupancy has been reported previously, the presence of electron microscopical data in the current study provides the first ultrastructural description of this phenomenon at axotomised Wld$^s$ NMJs (Figures 3.18

and 3.10). It should be noted, however, that ultrastructural identification of partially occupied NMJs is not a particularly accurate measure (for example, compare figures 3.14 and 3.19b). The main reason for this is that: when observing a 70-90nm thick section through a NMJ down the electron microscope, it is only possible to visualise those synaptic boutons which are contained within that plane of section. Whilst this can provide enough information for an acceptable analysis of an NMJs level of occupancy in a number of cases (e.g. when there are areas of occupied and unoccupied postsynaptic folds in the same plane of section, thereby allowing identification as being partially occupied), when all boutons are occupied/unoccupied, it is not possible to say with conviction that the whole terminal is occupied or unoccupied as there may be boutons out of the plane of section which are in an opposing state. On some occasions it has been possible to look at sequential sections from the same NMJ, to include more boutons in the analysis of occupancy, but even this is not 100% accurate unless a NMJ is serially sectioned and *every* bouton is included. I considered doing this, but decided that it would have been largely confirmatory and ultimately too time-consuming for the likely added value in the context of the present research project.

Even though ultrastructural analyses appear to slightly underestimate the overall levels of partial occupancy occurring at axotomised $Wld^s$ NMJs, the current data strongly supports the morphological findings that boutons are removed in a piecemeal fashion from the endplate. Whilst, as in the immunocytochemical experiments, it has not been possible to isolate remodelling processes from withdrawing processes using

ultrastructural analyses, base levels of synaptic remodelling have been taken into account (Figure 3.19b). Interestingly, the ultrastructural correlates of partially occupied terminals from axotomised Wld$^s$ NMJs closely resemble the appearance of partially occupied terminals undergoing remodelling (see above; Cardasis and Padykula, 1981). The areas of unoccupied endplate appear normal under both conditions, with no disruption of the postsynaptic architecture or basal lamina, and are often clear of all cellular material except for the presence of terminal Schwann cell processes at a few profiles. This raises the possibility that the two processes may share some common mechanisms.

### 3.4.4 Wallerian Degeneration is Absent At Axotomised Nerve Terminals in the Wld$^s$ Mouse

Many previous functional and morphological studies of the piecemeal withdrawal of nerve terminals from axotomised Wld$^s$ endplates have hypothesised that Wallerian degeneration is not occurring at these synapses (Parson et al., 1998; Ribchester et al., 1999; Mattison, R.J. 1999, PhD Thesis, University of Edinburgh). The morphological data from the current study supports this hypothesis by demonstrating the lack of morphological markers of degeneration (a fragmented and vacuolated appearance; Figure 3.7; Kawabuchi et al., 1991) at all axotomised Wld$^s$ nerve terminals. The fact that partial occupancy occurs at all is also major evidence to support the hypothesis that Wld$^s$ nerve terminals are lost by a process distinct from that of Wallerian degeneration.

The classical description of Wallerian degeneration, corroborated by immunocytochemical and ultrastructural evidence from the present study (Figures 3.7, 3.8 and 3.9), involves a fragmentation and destruction of the endplate in situ (Reger, 1959; Miledi and Slater, 1970; Manolov, 1974; Winlow and Usherwood, 1975). Therefore, if the withdrawal of nerve terminals at $Wld^s$ NMJs is simply a protracted version of Wallerian degeneration, it would not be expected to observe partial occupancy, except at the small number of terminals undergoing remodelling.

Most knowledge of the cellular processes and identification of Wallerian degeneration at the NMJ has been derived from ultrastructural studies, and yet, to date there has not been a systematic morphological study of the ultrastructure of axotomised $Wld^s$ synaptic boutons. In the present study however, nerve terminals from axotomised 2 month old $Wld^s$ mice at 3, 4, 5 and 7 days post axotomy, at all states of occupancy, have been subjected to qualitative and quantitative examination. The results of these experiments unequivocally demonstrate that the process of nerve terminal withdrawal from axotomised $Wld^s$ endplates occurs by a mechanism separate and distinct to that of Wallerian degeneration.

Out of the 296 motor nerve terminals from two month old $Wld^s$ muscles analysed, only 7 (3.1%) were identified as showing possible signs of degeneration, a similar level to that which has been shown to occur during synapse elimination (Reier and Hughes, 1972). These data were derived from nerve terminal profiles at all levels of occupancy,

and at 3, 4, 5 and 7 days following axotomy. There is a strong likelihood however, that in this instance, levels of 3.1% may turn out to be an overestimate. The only reason that each of these terminals was categorised as degenerating was because they contained more than 20% of mitochondrial profiles showing signs of swelling and cristae fragmentation. Whilst disrupted mitochondrial profiles were rarely seen in my control preparations, the figure of 20% was used as a threshold level because of the findings of Winlow and Usherwood (1975) who showed that up to 19% of mitochondria in normal axon terminals were damaged, representing a natural turnover. As a result, it is possible to suggest that the slightly higher levels of disrupted mitochondrial profiles identified in my preparations represent an increased level of turnover rather than the onset of Wallerian degeneration. Further evidence to support the hypothesis that these terminals have been misidentified comes from the lack of other degenerative markers present. None of the 'degenerating' terminals had any signs of terminal membrane disruption, SV depletion and clustering or terminal Schwann cell phagocytosis. It remains a strong possibility therefore, that the identification of degenerating mitochondrial profiles is not occurring as a result of Wallerian degeneration at these nerve terminals.

Even if it transpires that the 3.1% of 'questionable' terminals are undergoing Wallerian degeneration, the reality remains that 96.9% of axotomised $Wld^s$ nerve terminals are removed from the endplate by a process which shows *no* signs of classical degeneration whatsoever (Figures 3.11 and 3.18-3.25. The data demonstrate that the overwhelming majority of nerve terminal loss at axotomised $Wld^s$ NMJs occurs without any reduction

in synaptic vesicle number, with no terminal membrane fragmentation and with no phagocytosis by a terminal Schwann cell. Thus, it appears that nerve terminal ultrastructure is retained throughout the withdrawal process. Indeed, it would be interesting to discover what the eventual fate of the retained subcellular organelles is following their retraction back into the parent axon.

Finally, the hypothesis that the withdrawal of nerve terminals following axotomy in young $Wld^s$ mice and during synapse elimination share some common mechanisms is further supported by the present ultrastructural findings. The retention of nerve terminal ultrastructure throughout the withdrawal process in young $Wld^s$ mice is unequivocally demonstrated in the present study. Similar demonstrations of the lack of degenerative processes occurring during synapse elimination have been provided from studies by Korneliussen and Jansen (1976), Riley (1981) and Bixby (1981; but see Rosenthal and Taraskevich, 1977). One major technical hurdle concerning the ultrastructural analysis of nerve terminal loss during synapse elimination, which has yet to be overcome, is the problem of identifying which synaptic bouton comes from which axonal branch at a polyinnervated endplate. This has limited previous studies to just being able to look for signs of degeneration across the whole nerve terminal rather than being able to look for subtle differences between competing synaptic boutons, one of which will end up being withdrawn. During the course of the present study, I made sustained and numerous attempts to use axotomised $Wld^s$ NMJs in order to overcome this problem, with the aim of allowing a more accurate comparison of the processes of nerve terminal withdrawal

occurring at axotomised Wld$^s$ NMJs and during synapse elimination. Unfortunately, standard and modified protocols of FM1-43 photoconversion (whereby identified fluorescently labelled frog motor nerve terminals illuminated under the standard fluorescence microscope are exposed to a diaminobenzidine solution, thereby converting fluorescence into an electron dense reaction product contained solely within FM1-43 loaded SVs, which is visible down the EM; see Henkel et al., 1996) could not be made to work in my preparations of lumbrical muscle, TA muscle or even levator auris longus muscle. It has subsequently been found that the concentration of FM1-43 contained within SVs is of paramount importance for producing photoconversion reaction product (Schikorski and Stevens, 2001). Thus, it appears that the concentrations of FM1-43 used in my unsuccessful experiments (5$\mu$M), which work adequately in the frog (Henkel et al., 1996; Richards et al., 2000; Prof. W.J. Betz, personal communication), may have been too dilute to produce photoconversion reaction product. If FM1-43 photoconversion could be made to work in the future, it should become possible to load nerve terminals supplied by one nerve whilst leaving others supplied by another nerve unstained (for example see; Costanzo et al., 1999; Costanzo et al., 2000). As a result, ultrastructural profiles of competing nerve terminals could be identified at polyinnervated NMJs undergoing synapse elimination.

### 3.4.5 Summary

The data presented in Chapter 3 of the current study unequivocally demonstrate that young $Wld^s$ motor nerve terminals are lost from the endplate, following axotomy, via a process separate and distinct from that of Wallerian degeneration. Furthermore, additional evidence is provided to support the hypothesis that this terminal loss occurs by a process of piecemeal withdrawal, whereby boutons are retracted, one at a time, back into the parent axon. The similarities between this withdrawal process and the retraction of supernumerary terminals during developmental synapse elimination are also apparent. Taken together, these findings support the hypothesis that independent mechanisms may underlie degenerative processes in separate compartments of the neurone, whereby synaptic degeneration is separate and distinct from that of somatic and axonal degeneration (see Chapter 6). Many unanswered questions remain however. For example, there is a long running debate as to what effect age has on the $Wld^s$ phenotype. Similarly, it is still unclear as to what in the $Wld^s$ genotype is responsible for producing the distinctive axotomy-induced phenotype described above. It is these two questions which are addressed in the subsequent chapters.

# Results Chapter 4

# 4. Effect of Age on the Phenotypic Expression of the Wld$^s$ Mutation

## 4.1 Background

Whilst the preservation of distal axons and motor nerve terminals following axotomy has been unequivocally demonstrated in Wld$^s$ mice of 2 months and under (Chapter 3; Lunn et al., 1989; Ribchester et al., 1995), there remains controversy over whether the effectiveness of this 'protection' declines with age. Perry and colleagues (1992) showed that the rate of axonal loss in axotomised sciatic nerve (as measured by the size of the compound action potential) increased with age in Wld$^s$ mice. For example, in 1 month old Wld$^s$ sciatic nerve, compound action potentials declined to ~70-80% of their normal amplitude at 5 days post-axotomy. In contrast, no compound action potentials could be excited from 1 year old Wld$^s$ preparations. The age-related decline in axonal preservation appeared to occur gradually however: intermediate levels of retention were detected in 3 to 6 month old mice preparations, whereby compound action potentials of ~20-30% of those seen in control preparations were recorded. A subsequent molecular study from the same lab supported these findings by showing that neurofilament levels in Wld$^s$ sciatic nerve following axotomy, as well as compound action potentials, declined faster with increasing age (Tsao et al., 1994).

Further evidence to support the hypothesis that increasing age reduces the effectiveness of the Wld$^s$ phenotype was provided in a study of motor nerve terminal loss following axotomy in Wld$^s$ mice by Ribchester and colleagues (1995). These authors demonstrated that the level of preservation of functional motor nerve terminals also declines with age. Thus, in FDB muscles from 4 month old Wld$^s$ mice, 2-3 days after axotomy, <1% of muscle fibres responded to nerve stimulation. This is in contrast to data from 1 month old Wld$^s$ mice at the same time post-axotomy, where ~90-100% of muscle fibres responded to nerve stimulation.

Despite the strong evidence for a decline in the effectiveness of the Wld$^s$ gene with age provided by Perry et al. (1992), Tsao et al. (1994) and Ribchester et al. (1995), a morphological study by Crawford et al. (1995) and a very recent biochemical study by M.P. Coleman (personal communication) appear to repudiate these findings. In the latter, it has been demonstrated that age has no effect on the retention of NF levels following axotomy in Wld$^s$ mice from the colony maintained in Cologne. In the earlier study, Crawford et al. showed that, in their Wld$^s$ breeding colony in Baltimore, the period of both axonal and motor nerve terminal survival after nerve lesion was the same in mice ranging from 1 to 16 months old. Thus, at 5 days after axotomy, ~80% of endplates were still innervated in both 1 and 7 month old Wld$^s$ mice (Figure 4.1). They tried to explain the differences in their findings by suggesting that the use of electrophysiological methods by previous investigators (Perry et al., 1992, Tsao et al., 1994) may have yielded false conclusions, owing to the possibility that old Wld$^s$ axons

**Fig. 4.1 Data from the Study by Crawford et al. (1995) on the Innervation of NMJs following Axotomy in Wld$^s$ mice of Different Ages.**

(A) Comparison of innervated NMJs at 0 and 5 days post axotomy in 1 month old and 7 month old Wld$^s$ mice (mean ± SD). There is a small loss of innervation after 5 days, but there is no significant difference between 1 month old and 7 month old animals.

Figure and legend adapted from Figure 7 in: Crawford, T.O., Hsieh, S-T., Schryer, B.L. & Glass, J.D. (1995) Prolonged axonal survival in transected nerves of C57Bl/Ola mice is independent of age. *Journal of Neurocytology* **24:** 333-340

(A)

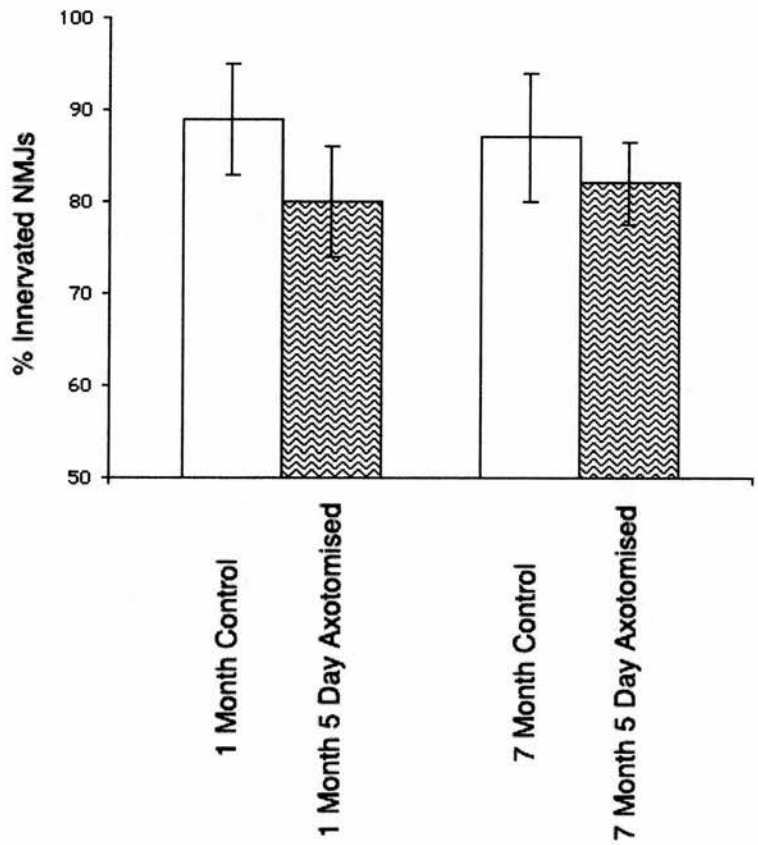
100
90
80
70
60
50
% Innervated NMJs
1 Month Control
1 Month 5 Day Axotomised
7 Month Control
7 Month 5 Day Axotomised

might survive axotomy, but age may have an effect on their conduction properties. This does not explain the findings of Tsao et al. (1994) however, that NF levels following axotomy also decline faster with age. Crawford and colleagues (1995) also left open an alternative possibility, that the disparity involving their findings and those described above may be due to differences between the separate breeding colonies used.

This chapter provides morphological data on axon numbers in lesioned distal nerve stumps and immunocytochemical and ultrastructural data on axotomised NMJs from $Wld^s$ mice of different ages, the latter of which was undertaken in parallel with a concurrent electrophysiological study (by Mr D. Thomson in our laboratory). Data from experiments regarding axon preservation following nerve lesion were not conclusive, neither supporting nor dismissing the age-related phenotypic loss hypothesis. However, unequivocal evidence is provided in support of the hypothesis that the effectiveness of the $Wld^s$ phenotype declines with age at axotomised motor nerve terminals. Thus, in our colony at least, mice older than 4 months do not express the $Wld^s$ phenotype at NMJs, at levels anywhere near those found in young (2 month old) mice. Furthermore, the data presented in this chapter provide evidence that it is not only the *rate* of nerve terminal loss that is modified with age. Immunocytochemical and electron microscopic findings suggest that the *nature* of nerve terminal loss too, appears to undergo a conversion with age in $Wld^s$ mice.

## 4.2 Methods

The majority of experiments contained within this chapter were carried out using methods described in chapter 2. The following section describes methods which are specific to this chapter.

### 4.2.1 Morphological Quantification of Axonal Preservation

Tibial nerve cuts were performed in 2 and 7 month old $Wld^s$ mice (see chapter 2). Four days later, the animal was killed and proximal and distal nerve stumps were dissected out and fixed in 4% paraformaldehyde / 2.5% glutaraldehyde for 4 hours. The first 2mm of the proximal and distal nerve stumps were discarded. The remaining stumps were prepared for electron microscopy using the same protocol as for muscle preparations (see chapter 2). Cross-sections (1$\mu$m) taken using a glass knife on a Reichert 'Ultracut' ultramicrotome were collected on glass slides before staining with toludine blue (1% in $dH_2O$; Sigma). Sections were examined using a Zeiss 40x water immersion objective attached to a standard light microscope. Images were captured and enhanced using the protocol described in Chapter 2.

The total number of myelinated axon profiles (non-myelinated axons were not readily detectable using the current protocol; cf. Crawford et al., 1995) were counted in cross-sections from both proximal and distal nerve stumps. To be included in the count,

axons had to exhibit normal myelin sheaths and a uniform axoplasm. Each cross-section was analysed on three separate occasions, to allow for human error in counting. Data were recorded on an Excel spreadsheet where standard statistical analysis was performed.

## 4.3 Results

### 4.3.1 Qualitative and Quantitative Morphological Comparison of the Preservation of Distal Axons in 2 and 7 Month $Wld^s$ Mice Tibial Nerve Following Axotomy

Semi-thin (1$\mu$m) sections of tibial nerve, taken from regions both proximal and distal to the site of a 4 days previous nerve lesion are shown in Figure 4.2. There were no qualitative differences apparent between the proximal and distal portions of the 2 month $Wld^s$ tibial nerve, with numerous myelinated axon profiles present in both (Figure 4.2a and 4.2b). The proximal portion of the 7 month $Wld^s$ tibial nerve appeared very similar to those obtained from 2 month old animals (Figure 4.2c), although there was a slight reduction in the number of myelinated axon profiles in the distal nerve stump (Figure 4.2d).

Quantitative analysis of axon counts from 2 month old $Wld^s$ tibial nerve indicated that there was no significant difference (P=0.0696, Unpaired t test) between the number of axon profiles proximal (597.33 ±1.15 SD; n=3, N=1) and distal (611.33 ±6.66; n=3, N=1) to the lesion (Figure 4.3). This was in contrast to the 7 month old data which showed that there were significantly fewer axon profiles (P=<0.001; unpaired t test) in

sections of tibial nerve distal to the lesion site (537.67 ±2.52; n=3, N=1) compared to regions of the nerve proximal to the lesion (578.67 ±2.08; n=3, N=1). The loss of 7% of axons in the distal stump of 7 month old $Wld^s$ mouse 4 days after axotomy, whilst statistically significant, does not begin to approach the level of axonal loss in 1 year old $Wld^s$ mice preparations as observed in the studies by Perry et al. (total loss of the compound action potential at 5 days post axotomy; 1992), and thus is not conclusive with regards to addressing the age-related expression of the $Wld^s$ phenotype in axons (see discussion). Similarly, the rate of axonal loss in lesioned 7 month old $Wld^s$ nerve did not approach the rate observed in wild-type preparations (Figure 4.3c). However, the effect of age on the degeneration of motor nerve terminals contrasted strongly with that of axons.

### 4.3.2 Rate of Axotomy-Induced Nerve Terminal Loss in $Wld^s$ Mice of Different Ages

Immunocytochemically labelled NMJs (NF, SV2 and α-BTX), at 3, 4, 5 and 7 days post axotomy, from 2 month (n=4329, N=19), 4 month (n=3871, N=17), 7 month (n=5319, N=14) and 12 month (n=4573, N=14) old $Wld^s$ mice FDB muscles were individually assessed as to their level of occupancy (Figure 4.4 and 4.5). The rate of decline in endplate occupancy increased in $Wld^s$ mice of 4 months compared to 2 months (Figure 4.4). For example, at 3 days post axotomy in 2 month $Wld^s$ FDB muscles there were substantially more occupied endplates than at the same time point in 4 month $Wld^s$

mice, with levels of 95.31% ±1.39 (SEM) and 33.75% ±7.96 respectively (P=0.0043, Mann-Whitney test). Similarly, at 7 days post axotomy there were significantly more occupied endplates remaining (P=0.0022) in 2 month Wld$^s$ preparations (52.29% ±4.26) compared to 4 month preparations (4.39% ±1.92). The increase in the rate of decline in endplate occupancy was even more marked in 7 month Wld$^s$ muscles than in the 4 month preparations. Thus, in the 7 month Wld$^s$ preparations at 3 days axotomy only 1.3% ±0.27 of endplates were occupied, significantly less than in both 2 month old preparations (P=0.0022; 95.31% ±1.39) and 4 month old preparations (P=0.0043; 33.75% ±7.96). There was no further significant increase in the rate of decline in endplate occupancy at both 3 (P=0.6991) and 5 (P=0.8889) days post axotomy when comparing 7 month and 12 month data.

### 4.3.3 Immunocytochemistry of Axotomised Nerve Terminals in Wld$^s$ Mice of Different Ages

Immunocytochemically labelled NMJs (NF, SV2 and α-BTX), at 3, 4, 5 and 7 days post axotomy, from 2 month (n=4329, N=19), 4 month (n=3871, N=17), 7 month (n=5319, N=14) and 12 month (n=4573, N=14) old Wld$^s$ mice FDB muscles were individually assessed as to the state of their nerve terminals. In 2 month old preparations, at 3, 5 and 7 days post axotomy and in all states of full or partial occupancy (1-100%), persistent nerve terminals appeared to be healthy, with no signs of terminal fragmentation (Figure 4.6a; also see Chapter 3). Whilst the rate of nerve terminal loss increased in 4 month

old preparations, remaining nerve terminals also retained their architecture and showed no evidence of terminal fragmentation (Figure 4.6b).

Of the few remaining nerve terminals in 7 month $Wld^s$ preparations at 3 and 5 days post axotomy, most showed no signs of terminal fragmentation (Figure 4.7a). Residual nerve branches often appeared disrupted or fragmented however, indicative of classical degenerative pathways (Figure 4.7b). Furthermore, intramuscular nerve branches identified in $Wld^s$ FDB muscles of 7 months or older were grossly fragmented, providing further evidence of classical degeneration mechanisms (Figure 4.7c).

### 4.3.4 Effect of Age on the Incidence of Partial Occupancy at Axotomised NMJs in $Wld^s$ Mice

A quantitative analysis of the immunocytochemically labelled preparations described above showed a decrease in the incidence of partial occupancy with increasing age (Figure 4.8). Thus, out of the total number of occupied endplates assessed in 2 month $Wld^s$ preparations (n=4834, N=6), 64.87% were partially occupied. This level gradually declined with increasing age, producing figures of 47.04%, 30% and 15.87% in 4 (n=523, N=17), 7 (n=120, N=14) and 12 (n=208, N=14) month preparations respectively.

It should be noted that these data (Figure 4.8 as well as Figure 4.14, see below) are presented as a percentage of the total number of *occupied* endplates, rather than simply the *total* number of endplates. This method leaves unoccupied endplates out of any analysis. The reason for using this method of analysis is that it is not possible to distinguish what mechanism was responsible for the loss of a nerve terminal from a vacated endplate. For example, in a 7 month $Wld^s$ mouse FDB muscle, 3 days post axotomy, only ~1% of nerve terminals remain. Whilst this rate of terminal loss appears to approach that of wild-types, it is not possible to say that as a result, all or some of those terminals were lost by a classical, in situ degenerative process found in wild-types, rather than a speeded up piecemeal withdrawal process. As a result, only occupied terminals were included, allowing accurate assessment of the mechanism by which they were being lost.

### 4.3.5 Ultrastructural Characteristics of Axotomised Nerve Terminal Morphology in $Wld^s$ Mice of Different Ages

Retention of nerve terminal architecture and a paucity of classical degenerative markers were features of the overwhelming majority of NMJ profiles from 2 month $Wld^s$ FDB muscle preparations at all time points following axotomy (Figure 4.9a; Chapter 3). Similar examples of fully and partially occupied endplates, with retention of nerve terminal architecture were common at NMJ profiles from 4 month $Wld^s$ FDB muscle preparations at all time points following axotomy (Figure 4.9b). Thus, at many NMJ

profiles from 4 month Wld$^s$ preparations, ultrastructural characteristics similar to those observed in 2 month old preparations were evident (e.g. NF invasion, 'giant' vesicles, retention and compression of SVs towards the presynaptic membrane; Figure 4.10). However, there was one major difference between 2 month and 4 month preparations; an increase in the incidence of a major classical degenerative marker, namely the disruption and fragmentation of nerve terminal mitochondria (Figure 4.10). An increased incidence of degenerating mitochondrial profiles (identified by swollen membranes and disrupted cristae) was observed at both fully and partially occupied endplates (Figure 4.10 and 4.11). In some instances boutons with healthy mitochondrial profiles had neighbouring boutons containing degenerative mitochondria at the same NMJ (Figure 4.11b).

The incidence of disrupted mitochondrial profiles was also high in NMJ profiles from 7 month Wld$^s$ FDB muscle preparations at all time points following axotomy (Figure 4.12). This degenerative marker was often accompanied by sparse synaptic vesicles (Figure 4.12b) and terminal membrane disruption (Figure 4.12a). In a few NMJ profiles observed, terminal Schwann cells were seen to be phagocytosing grossly fragmented nerve terminals (Figure 4.13a) in a process which bears all the hallmarks of classical degeneration. Furthermore, at the majority of vacant endplates examined in 7 month Wld$^s$ preparations (96.30% ±3.70 SEM; n=73 NMJs, N=3 muscles), terminal Schwann cell profiles were located on top of the postsynaptic folds (Figure 4.13b). This is in

contrast to 2 month preparations where only 30.04% ±7.34 (n=66, N=9) of vacant endplates had opposing terminal Schwann cell profiles.

An age-related increase in the incidence of ultrastructural markers of degeneration occurring at axotomised Wld$^s$ NMJs is shown in Figure 4.14. Thus, out of the total number of occupied endplates assessed in 2 month Wld$^s$ preparations (n=228, N=9), 3.1% showed signs of degeneration. This level gradually increased with age, whereby 39.8% (n=103, N=3) of occupied endplate profiles in 4 month Wld$^s$ preparations and 91.3% (n=23, N=4) of occupied endplate profiles in 7 month Wld$^s$ preparations contained degenerative markers. It should be noted that, as for the graph of partial occupancy (Figure 4.8), the data in Figure 4.14 is presented as a percentage of the total number of *occupied* endplates, rather than simply the *total* number of endplates (see above for explanation).

As in 2 month Wld$^s$ preparations (see Figures 3.20 and 3.21), nerve terminals from 4 and 7 month Wld$^s$ FDB muscle preparations often showed an intra-terminal accumulation of NF following axotomy (Figure 4.15). Similarly, the NF accumulation in these terminals did not appear to disrupt the polarised distribution of synaptic vesicles and mitochondria. Quantification of this phenomenon (Figure 4.16) showed that the level of NF in nerve terminals from 4 month (11.9% ±3.39SEM; n=30, N=4) Wld$^s$ axotomised FDB preparations was significantly higher than in controls (n=34, N=4; P=0.0006, Mann Whitney test). The levels of NF accumulation in 7 month

preparations (8.31% ±3.61; n=14, N=4), whilst noticeably higher, did not quite reach statistical significance compared to controls (P=0.0863).

In the majority of nerve terminal profiles from 4 month old Wld$^s$ FDB preparations, 3 days after axotomy, the numbers and distribution of synaptic vesicles appeared very similar to those seen in control and axotomised 2 month old Wld$^s$ FDB preparations (Figure 4.17a). This is in contrast to many of the terminal profiles observed from 7 month Wld$^s$ preparations, 3 days after axotomy, where synaptic vesicles were scarce (Figure 4.17b). Quantitative analysis of these nerve terminal profiles supported the qualitative observations (Figure 4.18). Thus, in 4 month old Wld$^s$ nerve terminals 3 days after axotomy (93.32SV/$\mu m^2$ ±6.32SEM; n=30, N=4), the density of synaptic vesicles was almost significantly *higher* than in control preparations (78.31SV/$\mu m^2$ ±6.04; P=0.0884, unpaired t test; n=34, N=4) and slightly higher than in 2 month Wld$^s$ (83.76SV/$\mu m^2$ ±5.70; n=26, N=3) preparations. Furthermore, in 7 month old Wld$^s$ nerve terminals 3 days after axotomy (42.56SV/$\mu m^2$ ±4.59; n=14, N=4), the density of synaptic vesicles was significantly less than in control, 2 month Wld$^s$ and 4 month Wld$^s$ preparations (P=<0.0001 for all; Figure 4.18a).

Unsurprisingly, the packing density of SVs was reduced in 7 month, but retained in 4 month, Wld$^s$ preparations, compared to controls (Figure 4.18b). 7 month Wld$^s$ nerve terminals, 3 days after axotomy, had a SV packing density of 12.31% ±1.34 (n=14, N=4). This was significantly lower (P=<0.0001, Mann Whitney test) than in control

(28.25% ±1.95; n=34, N=4) and 2 month, 3 day axotomised Wld$^s$ (40.64% ±1.71; n=26, N=3) nerve terminals. Nerve terminal profiles from 4 month Wld$^s$ FDB muscles at 3 days post axotomy (47.16% ±1.78; n=30, N=4) had a significantly higher SV packing density than control (P=<0.0001) and 2 month Wld$^s$, 3 day axotomised (P=0.0123) preparations. Quantitative analysis of the numbers of vesicles within 125nm of an active zone ('docked' vesicles) showed that there was no significant difference (P=0.8319 and P=0.2503; unpaired t test) between 4 month Wld$^s$ nerve terminals at 3 days post axotomy (5.10 ±0.22) and control (5.04 ±0.18) and 2 month, 3 day axotomised, Wld$^s$ (5.41 ±0.16) nerve terminals (Figure 4.19). This is in contrast to the numbers of docked vesicles in 7 month old Wld$^s$ preparations, 3 days after axotomy (2.52 ±0.27), which were significantly less than the numbers detected in control nerve terminals (P=<0.0001) and 3 day axotomised terminals from 2 and 4 month old Wld$^s$ mice (P=<0.0001 for both).

**Fig. 4.2 Preservation of Distal Axons Following Nerve Lesion in Young and Old Wld$^s$ Mice**

(A) Light micrograph of a transverse section through tibial nerve, 2mm proximal to the site of lesion, from a 2 month old Wld$^s$ mouse, 4 days after axotomy. The nerve appears healthy, with a good distribution of myelinated axon profiles.

(B) Light micrograph of a transverse section through tibial nerve, 2mm distal to the site of lesion, from a 2 month old Wld$^s$ mouse, 4 days after axotomy. As in the proximal stump, the distal nerve stump appears healthy, with a good distribution of myelinated axon profiles.

(C) Light micrograph of a transverse section through tibial nerve, 2mm proximal to the site of lesion, from a 7 month old Wld$^s$ mouse, 4 days after axotomy. Once again, the nerve appears healthy, with a good distribution of myelinated axon profiles.

(D) Light micrograph of a transverse section through tibial nerve, 2mm distal to the site of lesion, from a 7 month old Wld$^s$ mouse, 4 days after axotomy. Qualitatively, the nerve appears relatively healthy, with no evidence of a major reduction in axon numbers.

Scale bar = 20$\mu$m.

(A)

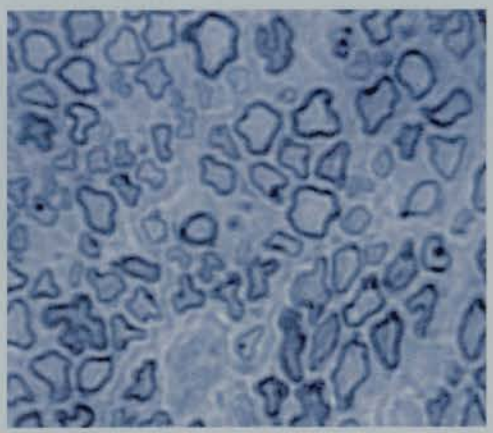

(B)

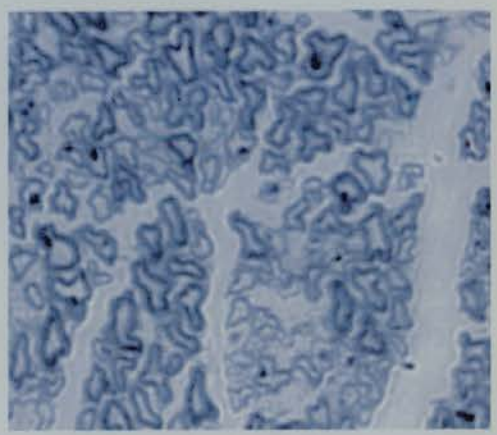

(C)

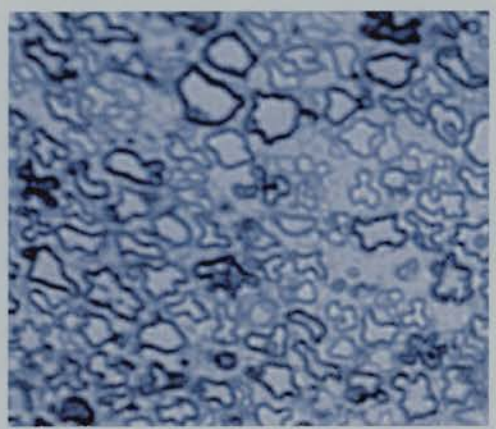

(D)

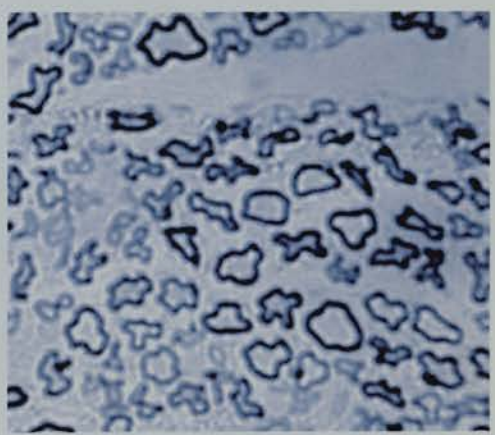

**Fig. 4.3 Quantification of the Preservation of Distal Axons Following Nerve Transection in Young and Old Wld$^s$ Mice**

(A) Bar chart representing the number of axon profiles counted in transverse sections of tibial nerve from 2mm proximal and distal to a nerve lesion in a 2 month old Wld$^s$ preparation, 4 days after axotomy. There was no significant difference between the two regions of nerve (P=0.0696, unpaired t test).

(B) Bar chart showing the number of axon profiles counted in transverse sections of tibial nerve from 2mm proximal and distal to a nerve lesion in a 7 month old Wld$^s$ preparation, 4 days after axotomy. Statistically there were significantly fewer axon profiles in the distal stump compared to the proximal nerve stump (P=<0.001, unpaired t test), but this reduction did not begin to approach the level of axon loss observed in wild-type preparations (see C).

(C) Bar chart produced from data provided in Perry et al. (1992) showing the size of the compound action potential in the distal stump of sciatic nerves from wild-type (C57Bl/6J) mice of 1 and 2 months old, 2 days post axotomy. This data shows the rapid loss of axonal function in wild-type preparations following axotomy, and is supported by earlier experiments which showed a similar loss of action potentials (Luttges et al., 1976) alongside a concomitant reduction in the levels of neurofilaments (Schlaepfer and Micko, 1978; Schlaepfer and Hasler, 1979a).

(A)

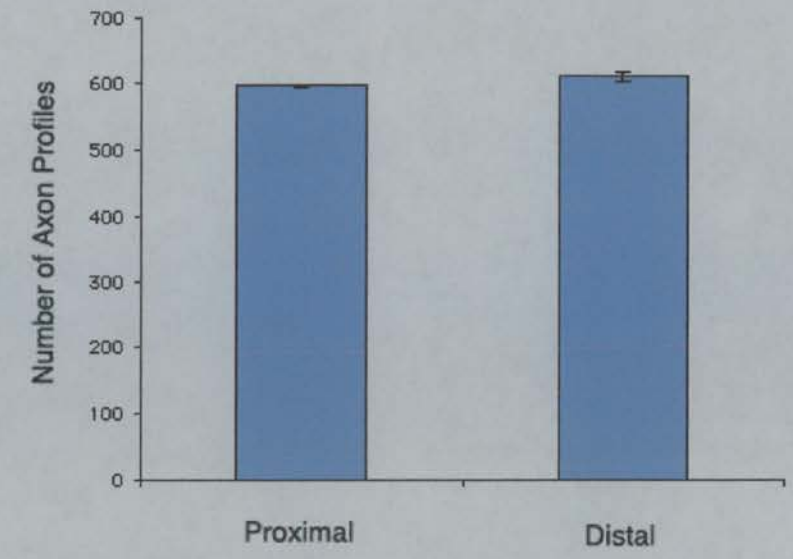
Number of Axon Profiles
700
600
500
400
300
200
100
0
Proximal
Distal

(B)

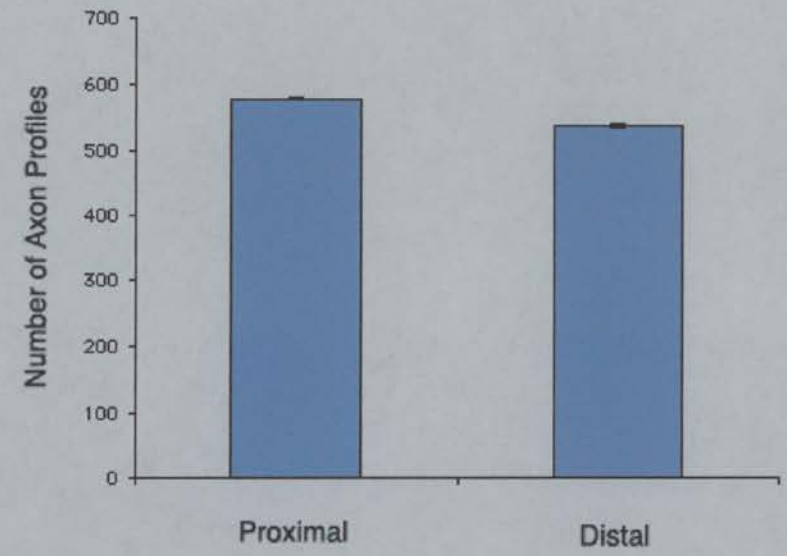
Number of Axon Profiles
700
600
500
400
300
200
100
0
Proximal
Distal

(C)

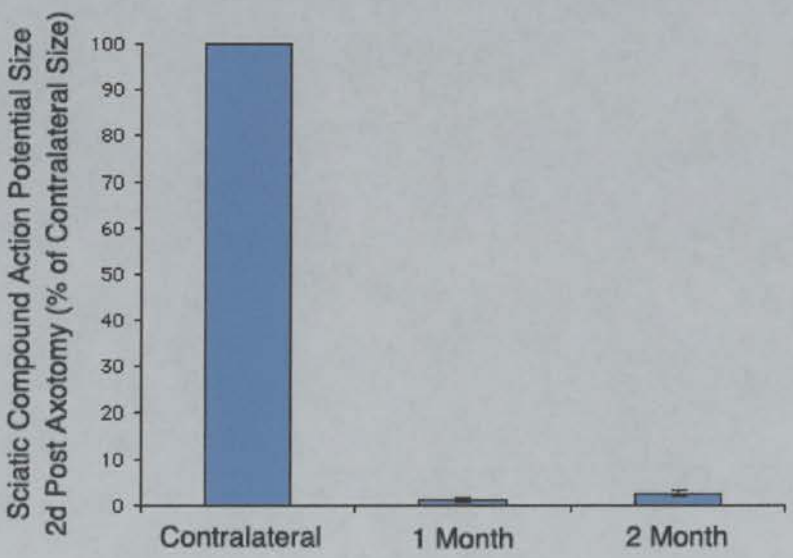
Sciatic Compound Action Potential Size
2d Post Axotomy (% of Contralateral Size)
100
90
80
70
60
50
40
30
20
10
0
Contralateral
1 Month
2 Month

**Fig. 4.4 Morphological Quantification of the Effect of Increasing Age on Endplate Occupancy (1-100%) Following Axotomy in Wld$^s$ Mice (1)**

(A) Graph of days post axotomy versus percentage of occupied endplates in 2 month old Wld$^s$ mice as calculated by counts of immunocytochemically stained (NF, SV2, α-BTX) FDB muscle preparations. Black triangles represent data from individual muscles and red triangles represent mean values.

(B) Graph of days post axotomy versus percentage of occupied endplates in 4 month old Wld$^s$ mice as calculated by counts of immunocytochemically stained (NF, SV2, α-BTX) FDB muscle preparations. Black triangles represent data from individual muscles and red triangles represent mean values.

Curves were fitted using Sigmaplot as the best sigmoidal/exponential fit to the data. Note that at this stage these curve fits should not be taken to imply any specific model or kinetic scheme underlying the degenerative processes in Wld$^s$ mice of different ages.

(A)

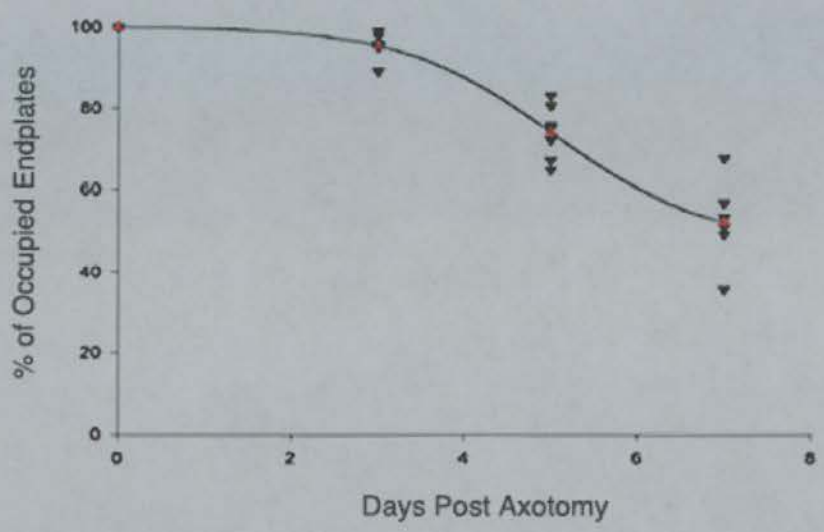
% of Occupied Endplates
100
80
60
40
20
0
0
2
4
6
8
Days Post Axotomy

(B)

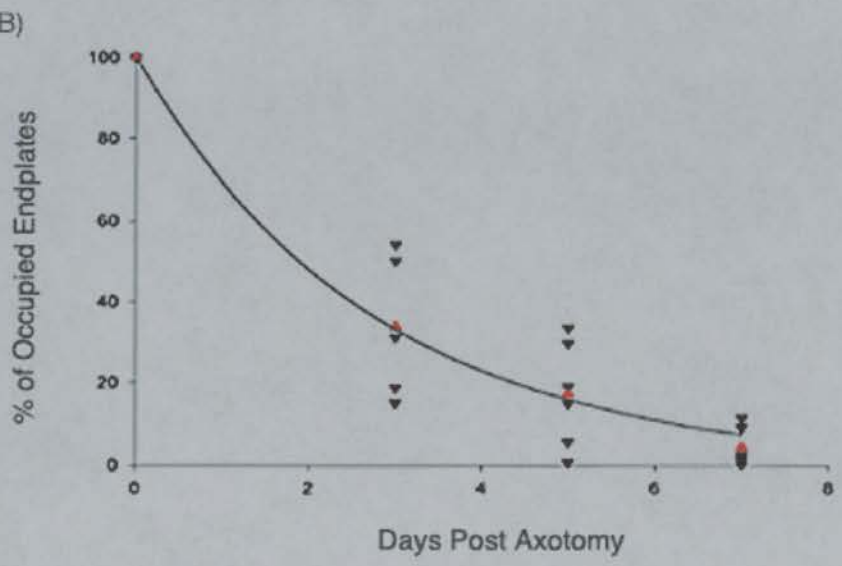
% of Occupied Endplates
100
80
60
40
20
0
0
2
4
6
8
Days Post Axotomy

**Fig. 4.5 Morphological Quantification of the Effect of Increasing Age on Endplate Occupancy (1-100%) Following Axotomy in Wld$^s$ Mice (2)**

(A) Graph of days post axotomy versus percentage of occupied endplates in 7 month old Wld$^s$ mice as calculated by counts of immunocytochemically stained (NF, SV2, α-BTX) FDB muscle preparations. Black triangles represent data from individual muscles and red triangles represent mean values.

(B) Graph of days post axotomy versus percentage of occupied endplates in 12 month old Wld$^s$ mice as calculated by counts of immunocytochemically stained (NF, SV2, α-BTX) FDB muscle preparations. Black triangles represent data from individual muscles and red triangles represent mean values.

Curves were fitted using Sigmaplot as the best sigmoidal/exponential fit to the data. Note that at this stage these curve fits should not be taken to imply any specific model or kinetic scheme underlying the degenerative processes in Wld$^s$ mice of different ages.

(A)

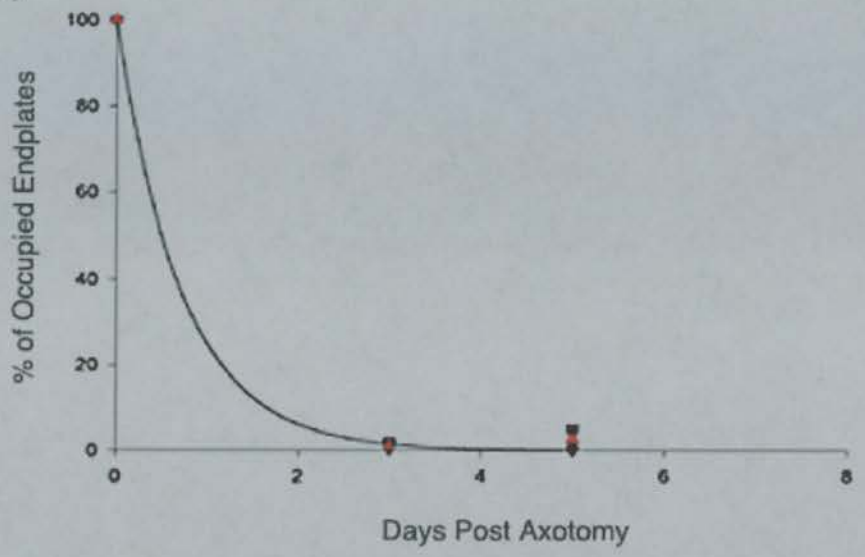
% of Occupied Endplates
100
80
60
40
20
0
0
2
4
6
8
Days Post Axotomy

(B)

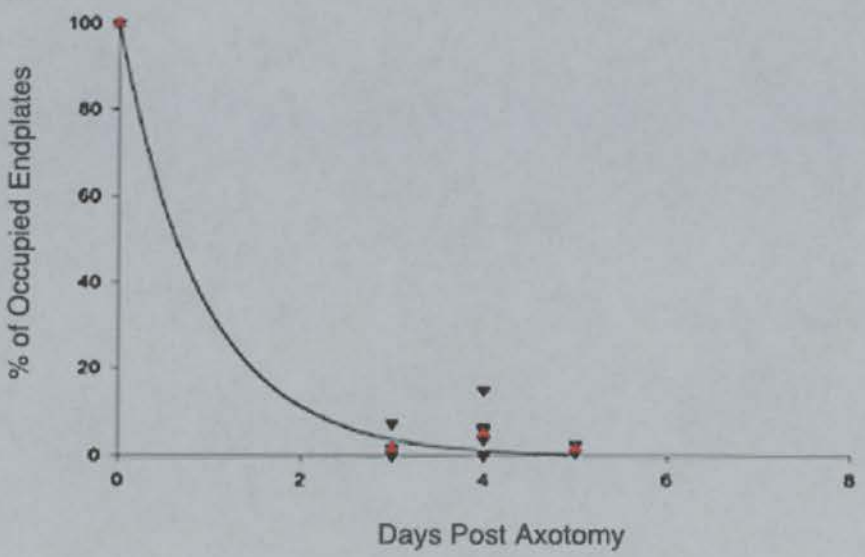
% of Occupied Endplates
100
80
60
40
20
0
0
2
4
6
8
Days Post Axotomy

**Fig. 4.6 Morphology of Axotomised NMJs from Wld$^s$ Mice of Different Ages (1).**

(A) Confocal image of three NMJs from a 2 month old Wld$^s$ mouse FDB muscle (NF, SV2 and α-BTX) 3 days post axotomy. Examples of neighbouring endplates which are fully occupied (left), partially occupied (centre) and vacant (right) are shown. The motor nerve terminals present all appear healthy. Scale bar = 20$\mu$m.

(B) Confocal image of two NMJs from a 4 month old Wld$^s$ mouse FDB muscle (NF, SV2 and α-BTX) 3 days post axotomy. This micrograph shows a vacant endplate (on the right) next to a remaining, fully occupied endplate (on the left) which appears healthy. Scale bar = 20$\mu$m.

(A)

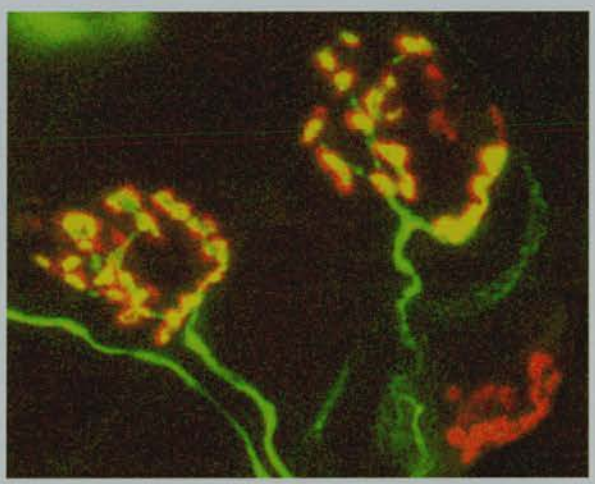

(B)

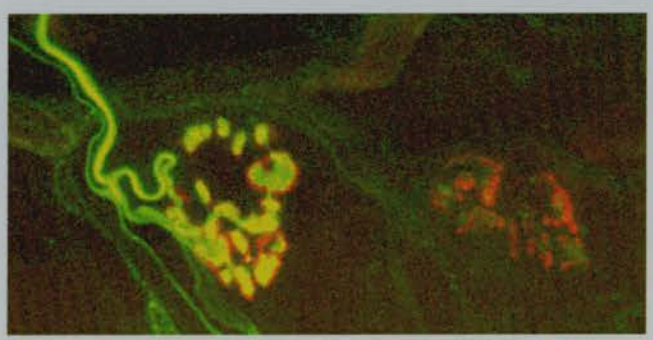

**Fig. 4.7 Morphology of Axotomised NMJs from Wld$^s$ Mice of Different Ages (2).**

(A & B) Confocal images of NMJs from a 7 month old Wld$^s$ mouse FDB muscle (NF, SV2 and α-BTX) 3 days post axotomy. Whilst the vast majority of endplates were vacant, examples of some persistent nerve terminals are shown (arrows). Scale bar = 20μm.

(C) Confocal image of NMJs from a 7 month old Wld$^s$ mouse FDB muscle (NF, SV2 and α-BTX) 3 days post axotomy. This image shows all vacant endplates alongside a fragmented, degenerating intramuscular nerve branch. Scale bar = 20μm.

(A)

(B)

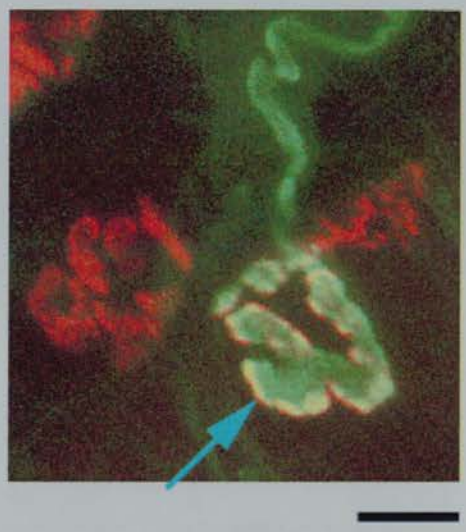

(C)

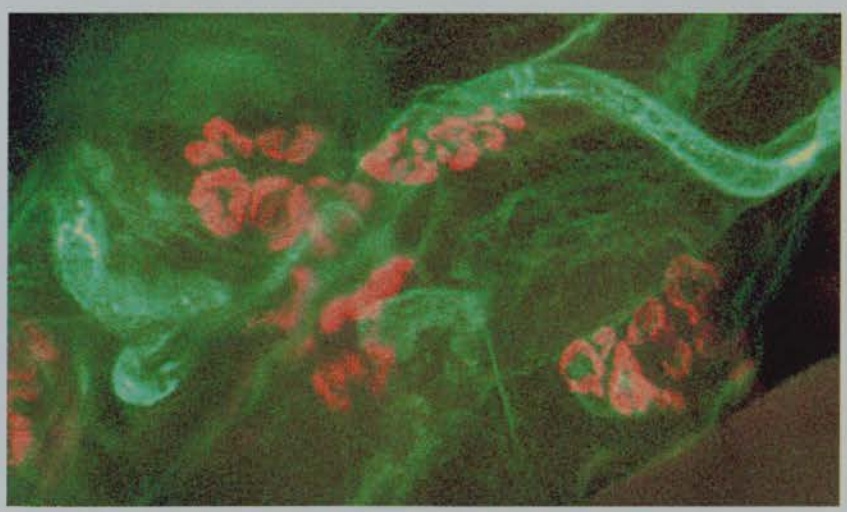

**Fig. 4.8 Morphological Quantification of the Effect of Age on the Occurrence of Partial Occupancy (1-99%) at Endplates Following Axotomy in $Wld^s$ Mice**

(A) Graph of the percentage of total occupied endplates which were partially occupied (1-99%) at all time points (3, 4, 5 and 7 days) following axotomy against the age of the animal, in immunocytochemically stained (NF, SV2, α-BTX) $Wld^s$ mice FDB muscle preparations.

(A)

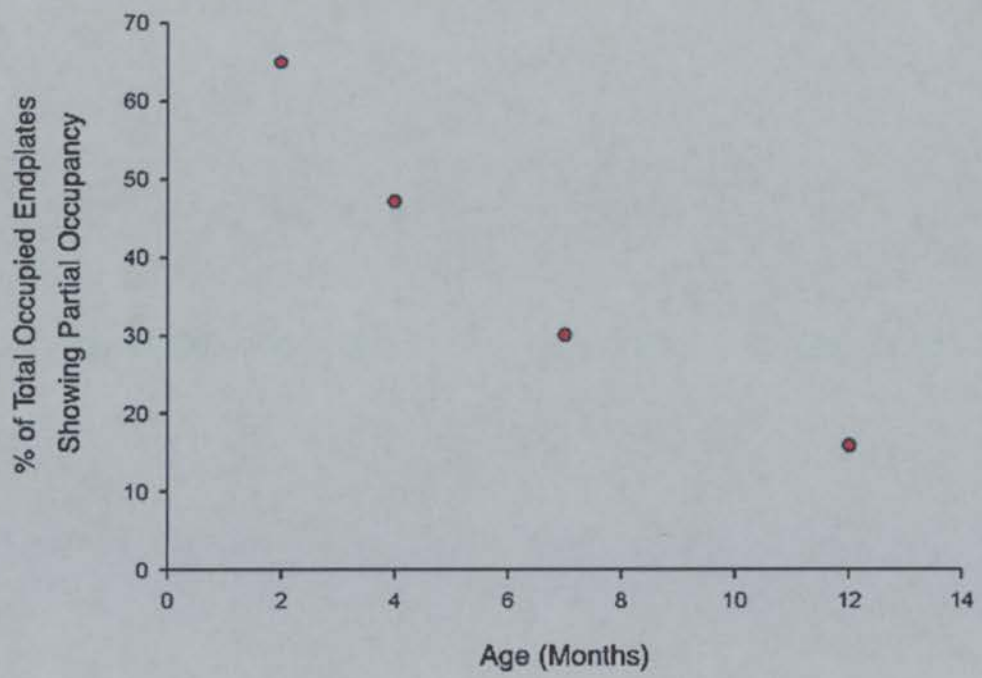
% of Total Occupied Endplates
Showing Partial Occupancy
70
60
50
40
30
20
10
0
0
2
4
6
8
10
12
14
Age (Months)

**Fig. 4.9 Qualitative Analysis of the Effect of Increasing Age on the Ultrastructure of NMJs Following Axotomy in Wld$^s$ Mice (1)**

(A) Electron micrograph of a nerve terminal bouton from a fully occupied NMJ in 2 month old Wld$^s$ mouse FDB muscle, 4 days after axotomy. Note the retention of the terminal architecture and membranes as well as a healthy distribution of SVs and mitochondria alongside an accumulation of neurofilament in the centre of the bouton. Scale bar = 2$\mu$m.

(B) Electron micrograph of two nerve terminal boutons from a fully occupied NMJ in 4 month old Wld$^s$ mouse FDB muscle, 3 days after axotomy. In this example, the terminal architecture and membranes are preserved, along with a healthy distribution of SVs and mitochondria. Scale bar = 2$\mu$m.

(A)

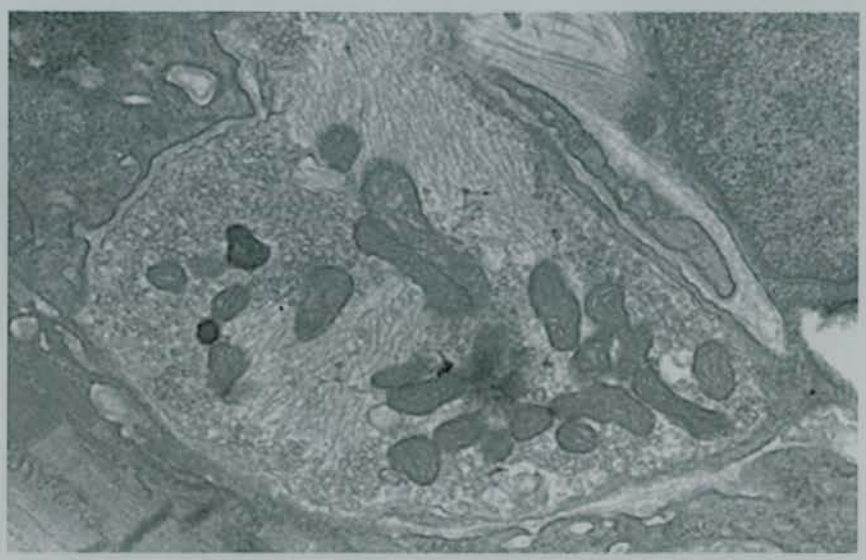

(B)

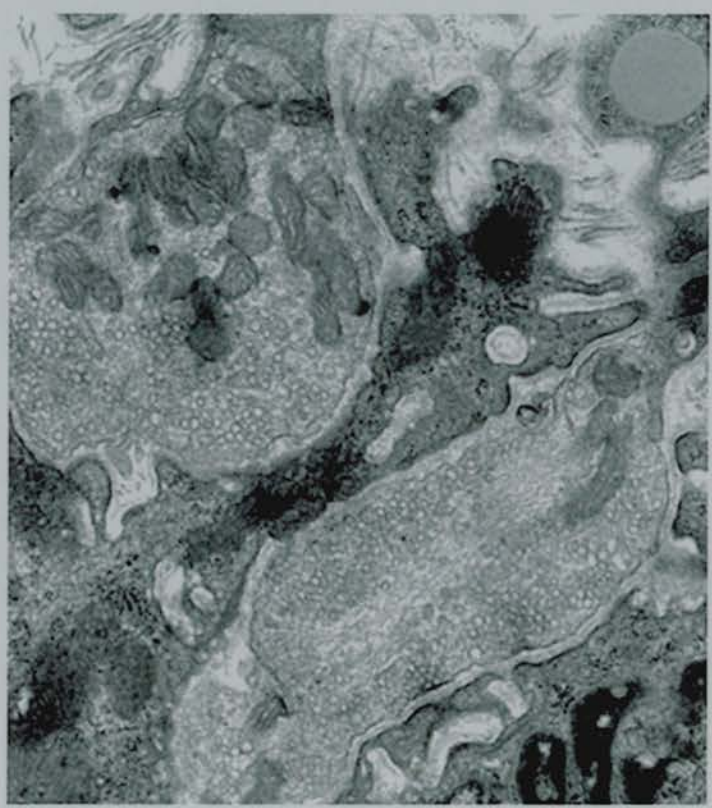

**Fig. 4.10 Qualitative Analysis of the Effect of Increasing Age on the Ultrastructure of NMJs Following Axotomy in Wld$^s$ Mice (2)**

(A) Electron micrograph of a nerve terminal bouton from a partially occupied NMJ in 4 month old Wld$^s$ mouse FDB muscle 3 days after axotomy. The bouton shown in this example shows a retention of pre- and postsynaptic architecture, NF accumulation (green star), a healthy distribution of SVs clustered towards active zones (red arrowhead) and the occasional 'giant' vesicle' (red arrow). However, the majority of mitochondria appear to be degenerating, evidenced by disrupted cristae (blue arrows). Scale bar = 1$\mu$m.

(A)

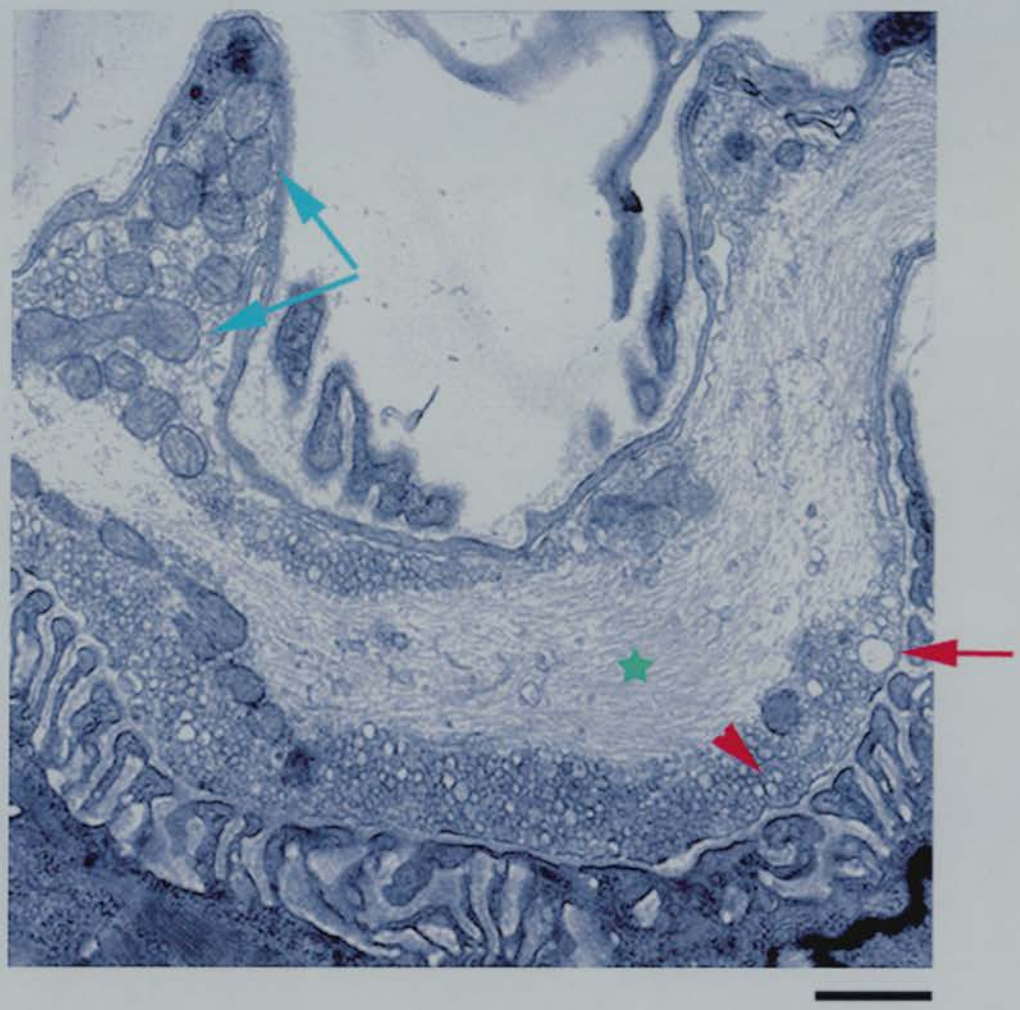

**Fig. 4.11 Qualitative Analysis of the Effect of Increasing Age on the Ultrastructure of NMJs Following Axotomy in Wld$^s$ Mice (3)**

(A) Electron micrograph of a nerve terminal bouton from a fully occupied NMJ in 4 month old Wld$^s$ mouse FDB muscle 3 days after axotomy. The mitochondria in the bouton shown are showing the classical signs of degeneration. When compared to healthy postsynaptic mitochondria (red arrow) it can be observed that they have become swollen and their cristae are disrupted and fragmented. Scale bar = 1$\mu$m.

(B) Electron micrograph of two nerve terminal boutons from a partially occupied NMJ in 4 month old Wld$^s$ mouse FDB muscle 3 days after axotomy. The bouton on the right has a normal appearance, whilst the bouton on the left contains degenerating mitochondrial profiles; although both contain intact synaptic vesicles. Scale bar = 1$\mu$m.

(A)

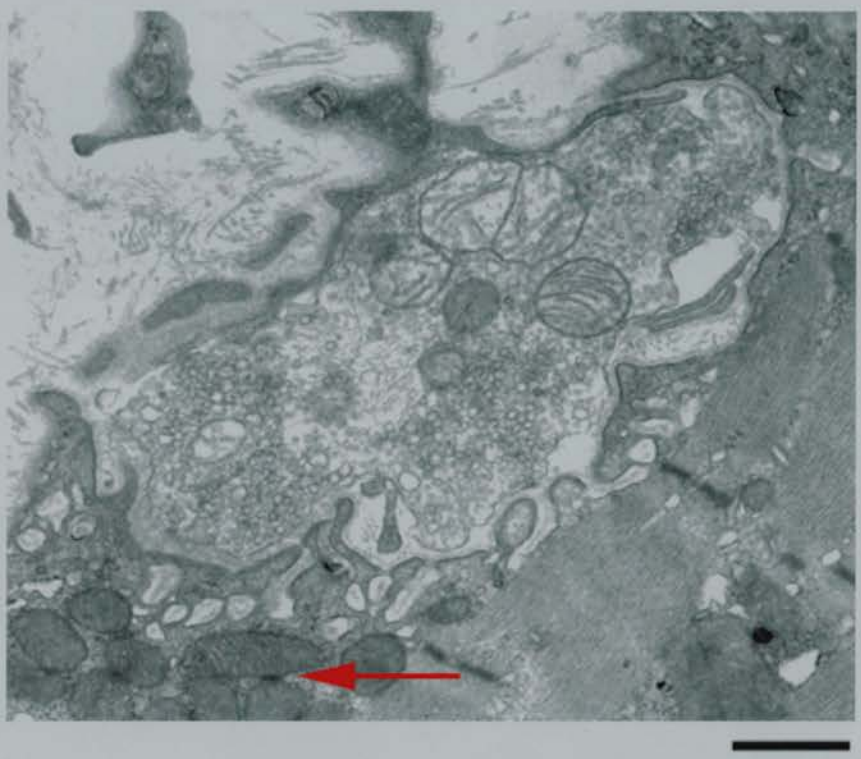

(B)

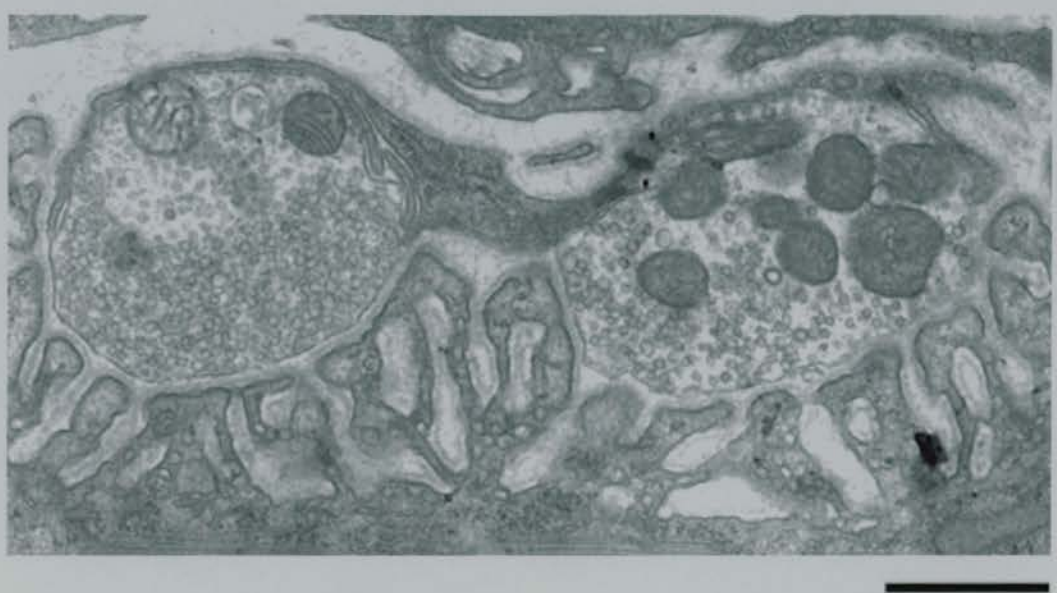

**Fig. 4.12 Qualitative Analysis of the Effect of Increasing Age on the Ultrastructure of NMJs Following Axotomy in Wld$^s$ Mice (4)**

(A) Electron micrograph of a nerve terminal bouton from a fully occupied NMJ in 7 month old Wld$^s$ mouse FDB muscle 2 days after axotomy. In this example, one of the few remaining nerve terminals is shown. Qualitative degenerative characteristics are present in all mitochondria, reduced synaptic vesicle levels and membrane disruption. Neurofilament invasion of the nerve terminal can also be observed. Scale bar = 1$\mu$m.

(B) Electron micrograph of a nerve terminal bouton from a fully occupied NMJ in 7 month old Wld$^s$ mouse FDB muscle 2 days after axotomy. Another example one of the few remaining nerve terminals is shown. Degenerative characteristics are present in the mitochondria and the bouton is severely depleted of synaptic vesicles. Scale bar = 1$\mu$m.

(A)

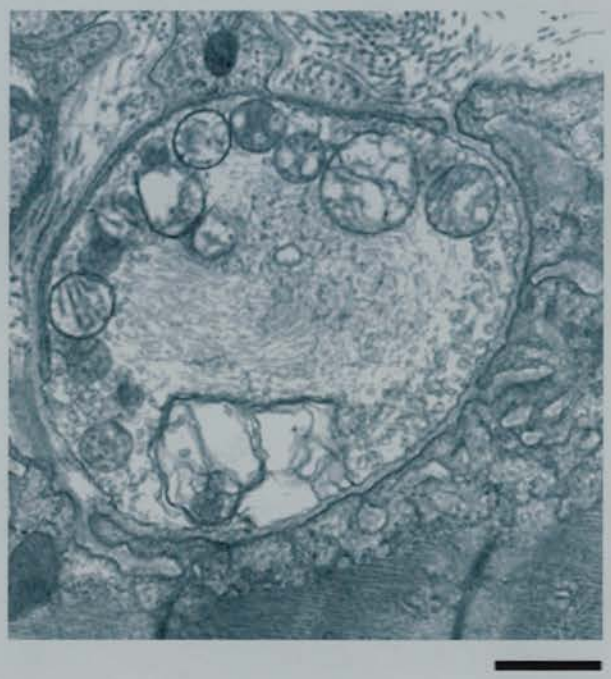

(B)

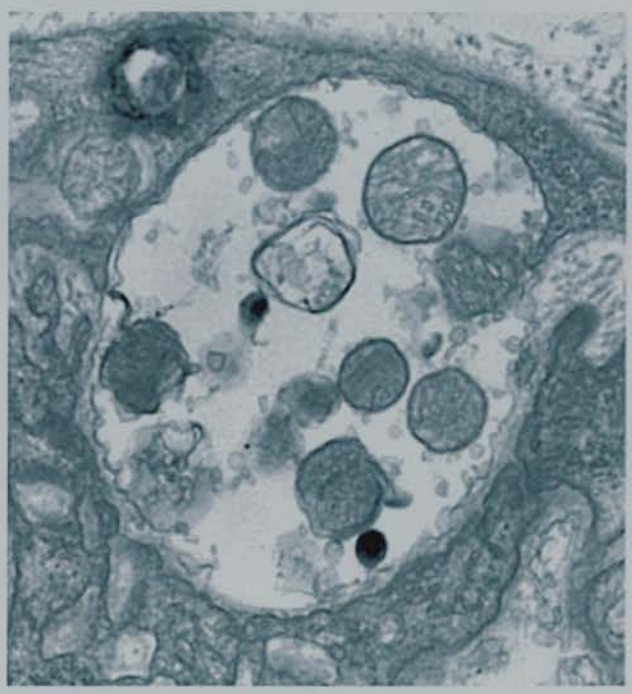

**Fig. 4.13 Qualitative Analysis of the Effect of Increasing Age on the Ultrastructure of NMJs Following Axotomy in Wld$^s$ Mice (5)**

(A) Electron micrograph of a nerve terminal bouton from a fully occupied NMJ in 7 month old Wld$^s$ mouse FDB muscle 2 days after axotomy. In this example, the fragmented remnants of a nerve terminal (red star) are being phagocytosed by a terminal Schwann cell (green star). Scale bar = 1$\mu$m.

(B) Electron micrograph of a vacant endplate from a fully occupied NMJ in 7 month old Wld$^s$ mouse FDB muscle 2 days after axotomy. A terminal Schwann cell can be seen on top of the vacated postsynaptic folds. Scale bar = 1$\mu$m.

(A)

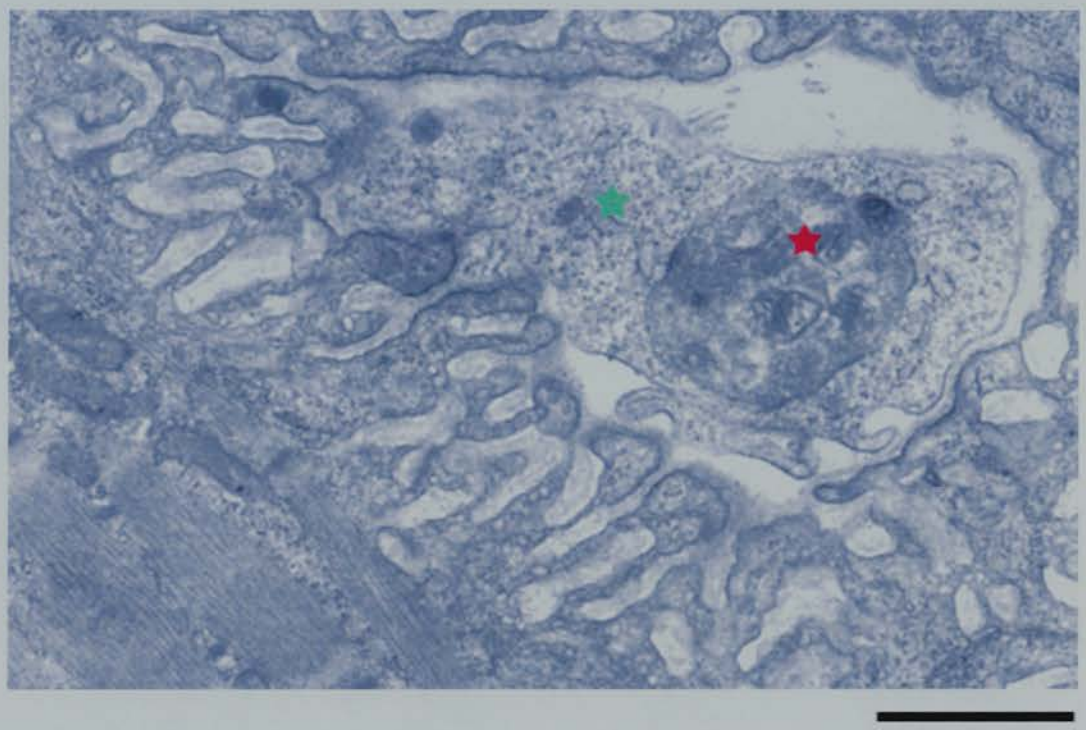

(B)

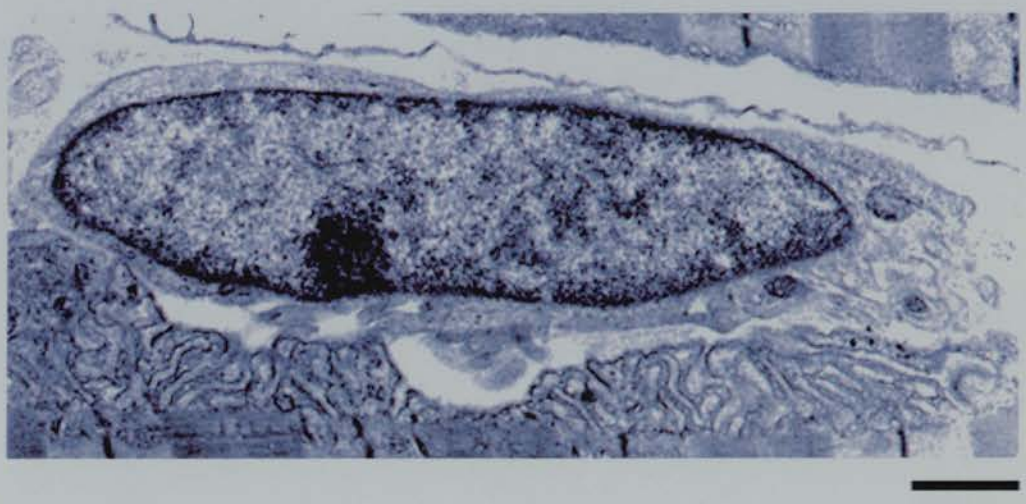

**Fig. 4.14 Ultrastructural Quantification of the Effect of Increasing Age on the Incidence of Degenerative Markers at Axotomised NMJs in Wld$^s$ Mice**

(A) Graph of the percentage of total occupied endplates which contained degenerative markers, at all time points (3, 4, 5 and 7 days) following axotomy against the age of the animal, in Wld$^s$ mice FDB muscle preparations.

(A)

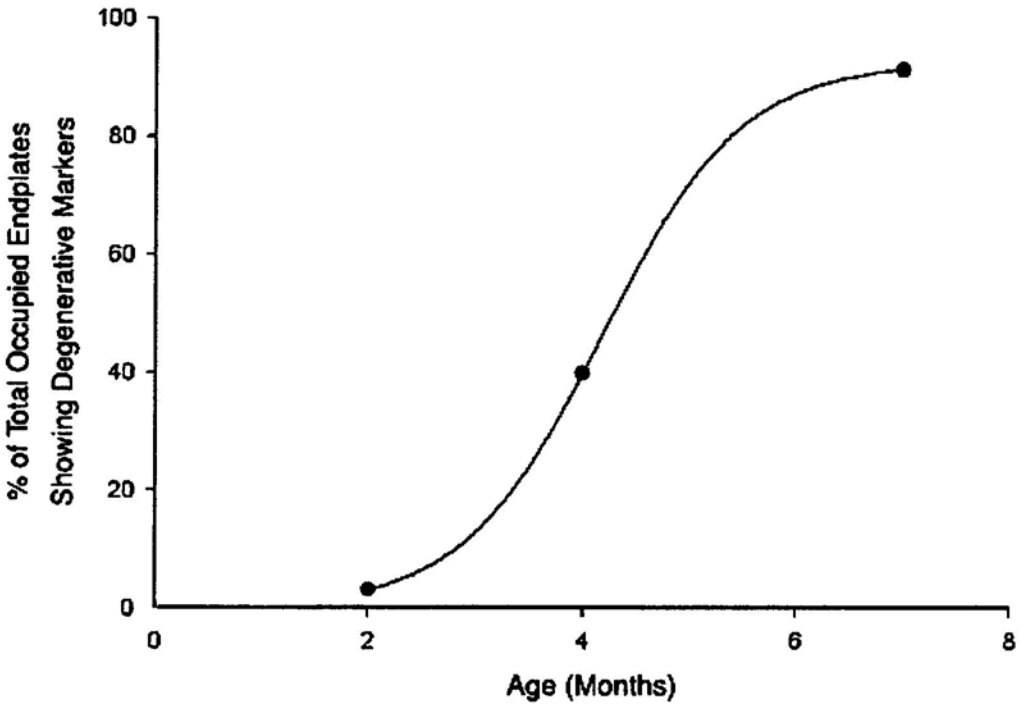
% of Total Occupied Endplates
Showing Degenerative Markers
100
80
60
40
20
0
0
2
4
6
8
Age (Months)

**Fig. 4.15 Ultrastructural Evidence for Neurofilament Accumulation at Axotomised NMJs in 4 and 7 Month Old Wld$^s$ Mice**

(A) Electron micrograph of two nerve terminal boutons from a 4 month Wld$^s$ FDB muscle, 3 days following axotomy. Both boutons have significant accumulations of NF. Scale bar = 1$\mu$m.

(B) Electron micrograph of a nerve terminal bouton from a 7 month Wld$^s$ FDB muscle, 2 days following axotomy. The bouton pictured contains a very large accumulation of NF . Scale bar = 1$\mu$m.

(A)

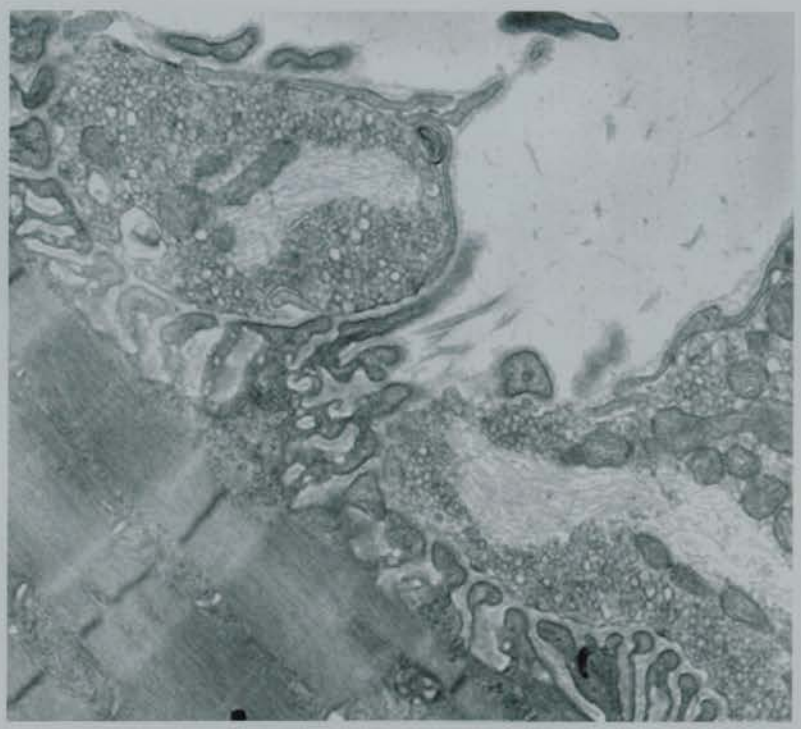

(B)

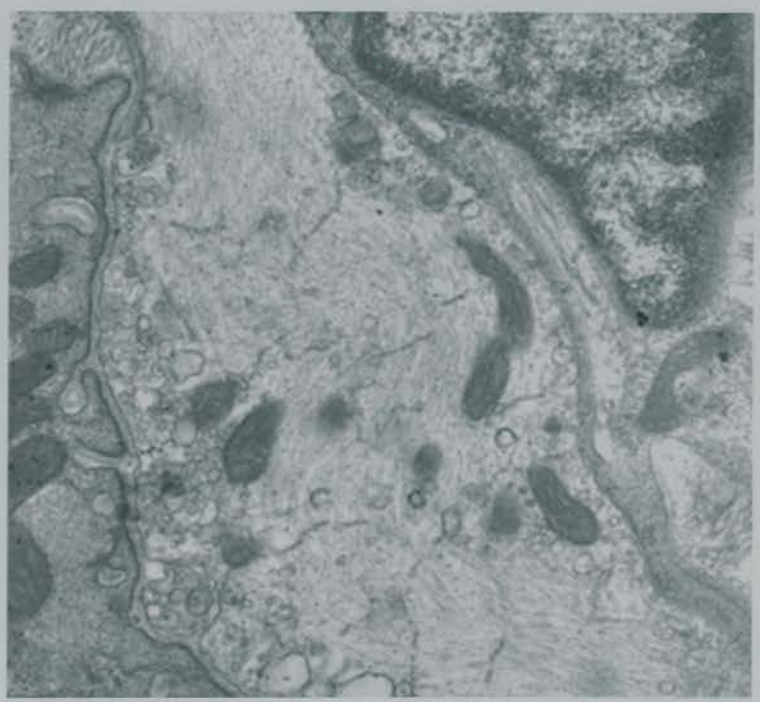

**Fig. 4.16 Ultrastructural Quantification of Neurofilament Accumulation at Axotomised NMJs in 4 and 7 Month Old Wld$^s$ Mice**

(A) Box chart showing the percentage of nerve terminal occupied by neurofilaments in Wld$^s$ mice FDB muscle preparations of different ages, 3 days post axotomy. 4 month Wld$^s$ nerve terminals have significantly increased levels of intra-terminal NF ($P=<0.001$), whilst 7 month Wld$^s$ nerve terminals have higher, but not quite reaching significance ($P=0.0863$), levels of NF, than controls. Error bars = SEM.

(A)

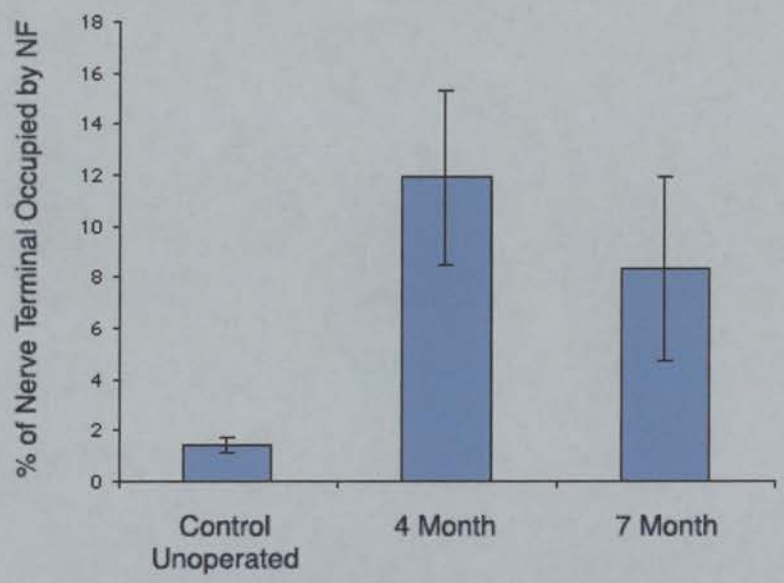
% of Nerve Terminal Occupied by NF
18
16
14
12
10
8
6
4
2
0
Control
Unoperated
4 Month
7 Month

**Fig. 4.17 Qualitative Analysis of Synaptic Vesicle Density and Localisation at Axotomised NMJs in 4 and 7 Month Old Wld$^s$ Mice**

(A) Electron micrograph of a nerve terminal bouton, 3 days post axotomy, in a 4 month old Wld$^s$ mouse FDB preparation. Note the large numbers of synaptic vesicles distributed evenly within the terminal and close to active zones on the presynaptic membrane. Scale bar = 0.5$\mu$m.

(A) Electron micrograph of a nerve terminal bouton, 2 days post axotomy, in a 7 month old Wld$^s$ mouse FDB preparation. Note the scarcity of synaptic vesicles both within the terminal and at active zones. Scale bar = 0.5$\mu$m.

(A)

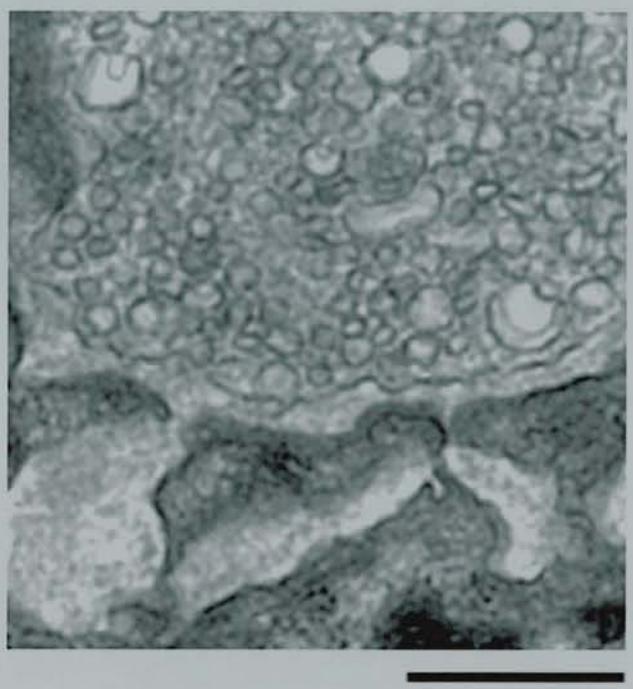

(B)

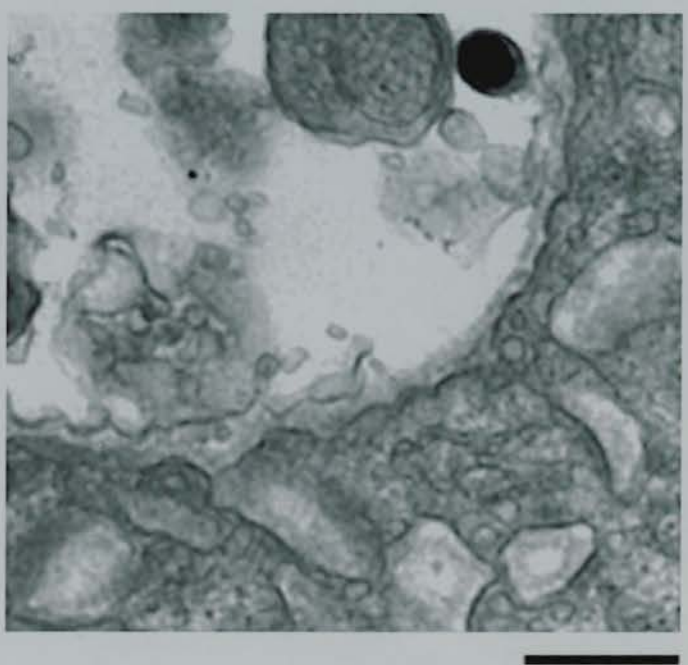

**Fig. 4.18 Ultrastructural Quantification and Comparison of Synaptic Vesicle Densities and Packing Densities at Axotomised NMJs in Control, 2, 4 and 7 Month Old Wld$^s$ Preparations**

(A) Box chart showing the density of synaptic vesicles within nerve terminals in control and 3 day axotomised FDB muscle preparations from 2, 4 and 7 month old Wld$^s$ mice. There was no significant difference between control, 2 month and 4 month preparations, whereas 7 month nerve terminals had significantly fewer SVs than the rest (P=<0.0001 for all, Mann Whitney test). Error bars = SEM.

(B) Box chart showing the packing density of synaptic vesicles within nerve terminals in control and 3 day axotomised FDB muscle preparations from 2, 4 and 7 month old Wld$^s$ mice. 4 month Wld$^s$ nerve terminals had a significantly higher packing density than both control and 2 month Wld$^s$ terminals (P=<0.0001 and P=0.0123 respectively; Mann Whitney test). 7 month Wld$^s$ nerve terminals had significantly reduced packing densities compared to all other experimental groups (P=<0.0001 for all; Mann Whitney test). Error bars = SEM.

(A)

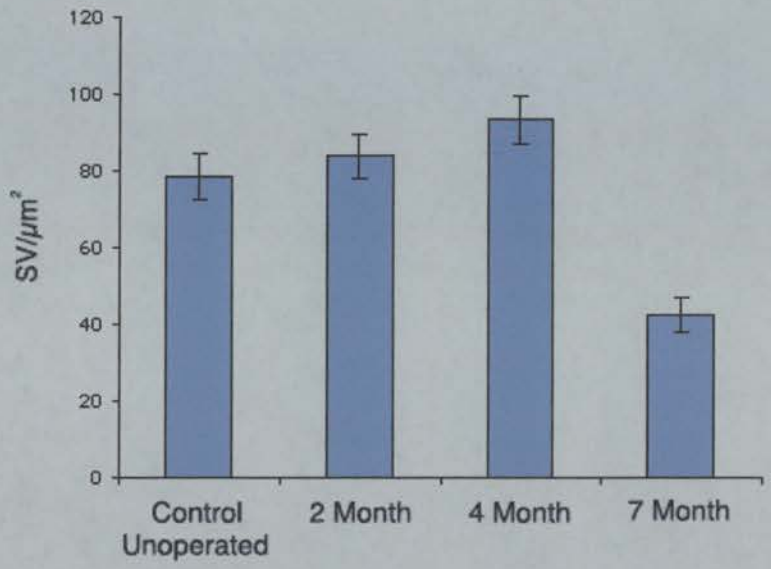
120
100
80
60
40
20
0
SV/μm²
Control
Unoperated
2 Month
4 Month
7 Month

(B)

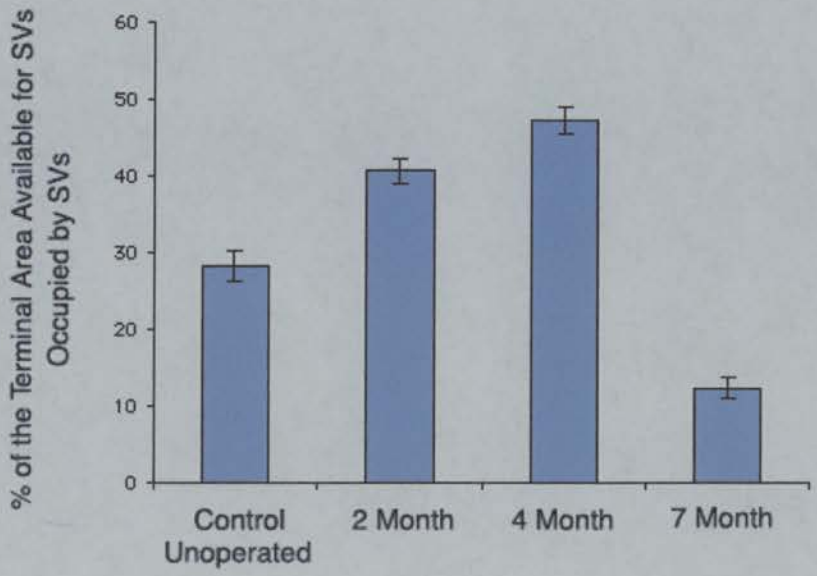
60
50
40
30
20
10
0
% of the Terminal Area Available for SVs
Occupied by SVs
Control
Unoperated
2 Month
4 Month
7 Month

**Fig. 4.19 Ultrastructural Quantification and Comparison of Synaptic Vesicle Localisation at Active Zones in Axotomised NMJs from Control, 2, 4 and 7 Month Old Wld$^s$ Preparations**

(A) Bar chart representing the number of synaptic vesicles within a 125nm radius of an active zone ('docked' vesicles) in nerve terminals from control and 3 day axotomised FDB muscle preparations from 2, 4 and 7 month old Wld$^s$ mice. There was no significant difference between control, 2 month and 4 month Wld$^s$ preparations (P=>0.253; unpaired t test), but intact nerve terminals in 7 month Wld$^s$ muscles had significantly fewer docked vesicles than in 2 and 4 month Wld$^s$ and control mice (P=<0.0001 for all; unpaired t test). Error bars = SEM.

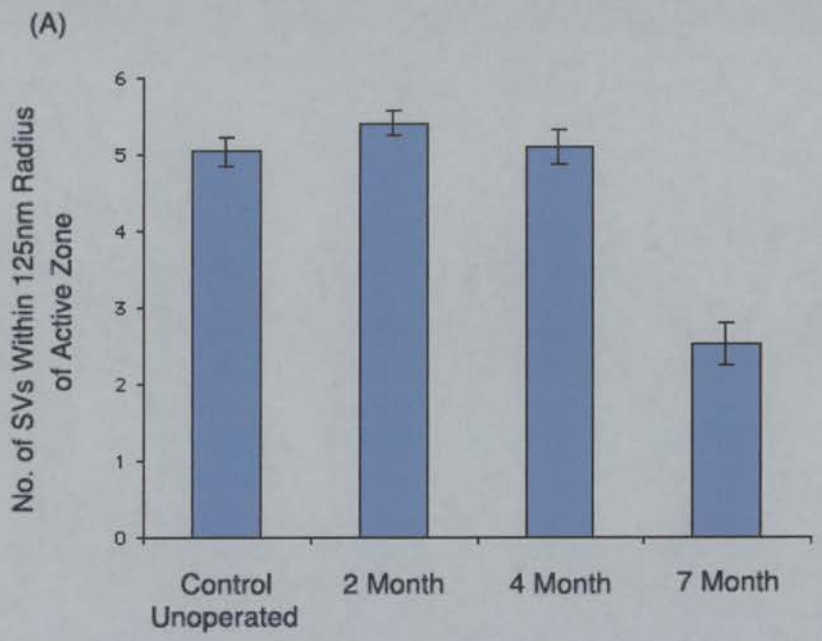
(A)
No. of SVs Within 125nm Radius of Active Zone
0
1
2
3
4
5
6
Control Unoperated
2 Month
4 Month
7 Month

## 4.4 Discussion

Whilst the morphological techniques I used tentatively suggested that the level of preservation of axons does not decline excessively with age in $Wld^s$ mice, as has previously been reported (Perry et al., 1992), I have shown, using morphological and ultrastructural analysis, that the preservation of motor nerve terminals in $Wld^s$ mice following axotomy is unequivocally reduced with age. Furthermore, the current data demonstrates that the *nature* of nerve terminal loss is also fundamentally altered with age. The interpretations of my observations alongside potential sources of error are considered in this discussion, and the hypothesis proposed in chapter 3, that presynaptic nerve terminal degeneration is distinct from axon degeneration, is advanced.

### 4.4.1 The Retention of Distal Axons Following Axotomy in $Wld^s$ Mouse Tibial Nerve Declines With Age

Changes in the rate of axonal Wallerian degeneration occurring as a result of age have been demonstrated in wild-type preparations. For example, Cook et al. (1974) showed that the rate of optic nerve degeneration was considerably slower in adult cats than in kittens. Similarly, Perry et al. (1992) showed that the rate of Wallerian degeneration in sciatic nerves from C57Bl/6J mice was significantly slower in 8 month old mice than in 1 month old mice. Previous studies (with the exception of Crawford et al., 1995) have suggested that the age related decline in the rate of axonal and nerve terminal

degeneration is reversed in Wld$^s$ mice, whereby degeneration occurs faster in older animals (Perry et al., 1992; Tsao et al., 1994; Ribchester et al.,1995). However, the morphological assessment of distal axon preservation in 2 and 7 month old axotomised Wld$^s$ tibial nerve included in the present study (Figures 4.2 and 4.3) does not support these previous findings. Whilst there was no axonal loss in 2 month preparations compared to a statistically significant axonal loss in 7 month preparations, the levels of axonal loss in the latter were small (7% at 4 days) compared to the findings of, for example, Perry et al. (100% loss at 5 days in 1 year old Wld$^s$ mice, a rate approaching that seen in wild-type preparations; Figure 4.3c). Moreover, the use of morphological methods in the current study appears to correlate more closely with the results from the study by Crawford et al. (1995), who showed that there was no age-related effect in their Wld$^s$ colony. My findings were not conclusive however, and further experiments would be required to accurately readdress the issue of the effect of age on *axon* preservation in Wld$^s$ mice. This was considered outside the scope of the present study, however. Thus, the reason for undertaking an assessment of the level of axonal loss in Wld$^s$ mice of different ages after axotomy was so that this data could be compared to the level of motor nerve terminal loss in Wld$^s$ mice of similar ages following axotomy (see below). However, now that the molecular genetics underlying the Wld$^s$ mutation have been discovered (Conforti et al., 2000; Mack et al., 2001; see Chapter 5), it should become possible to assess how differences in age-related phenotype of lesioned axons may be explained by alterations in the genotype.

### 4.4.2 The Rate of Motor Nerve Terminal Loss Following Axotomy in Wld$^s$ Mice Increases With Age

Whilst my studies of distal axon preservation following axotomy have added little weight to the argument that age reduces the phenotypic expression of the Wld$^s$ mutation, the findings from the study of the fate of motor nerve terminals in axotomised young and old Wld$^s$ FDB muscles have proved to be much more noteworthy.

My experiments show that the level of nerve terminal preservation following axotomy declines with age in Wld$^s$ mice (Figures 4.4 and 4.5). Whilst these results concur with previous findings from Ribchester et al. (1995), they are in disagreement with the findings of Crawford et al. (1995), who showed that there was no decline in the level of nerve terminal retention with age (Figure 4.1). This discrepancy may be due to differences in the techniques used by the two studies however; the current experiments were undertaken using immunocytochemical methods to label NF and SVs, whereas Crawford and colleagues employed a modified silver/cholinesterase method. The current study also suggests that loss of the Wld$^s$ phenotype occurs gradually; nerve terminals are lost more rapidly in 4 month old Wld$^s$ preparations compared to 2 month old Wld$^s$ preparations, but not as fast as nerve terminals in 7 and 12 month old Wld$^s$ mice. The lack of difference between the 7 and 12 month old Wld$^s$ data (Figure 4.5) suggests that the maximal rate of nerve terminal loss may be reached by 7 months of age.

As in the study of nerve terminal preservation in 2 month old Wld$^s$ mice described in Chapter 3, the immunocytochemical assessment of nerve terminal loss in Wld$^s$ mice of different ages was carried out in conjunction with electrophysiological experiments undertaken by Mr D Thomson. Once again, levels of nerve terminal retention were recorded in mice of 2, 4, 7 and 12 months using both methods (Figures 4.20 and 4.21) and, as in the previous comparison, electrophysiological recordings consistently gave a lower estimate of the levels of occupancy than morphological analysis (see Chapter 3 discussion for possible reasons underlying this difference). However, both methodologies revealed that the time-course of nerve terminal degeneration in 7 month and older Wld$^s$ mice approached that observed in wild-type preparations (cf. Figure 3.8).

**Fig. 4.20 Comparison of Morphological and Electrophysiological Analyses of Nerve Terminal Loss at Axotomised Wld$^s$ FDB Muscle Preparations in 2 and 4 Month old Mice.**

(A & B) Graphs of the number of occupied endplates against days post axotomy in 2 month old Wld$^s$ mouse FDB muscle preparations analysed using immunocytochemical techniques (A; NF, SV2 and α-BTX) and electrophysiological techniques (B). Black triangles represent data from individual muscles and red triangles represent the mean value (A is reproduced from Figure 3.10). Unpublished electrophysiological data courtesy of Mr D. Thomson and Dr R. Ribchester.

(C & D) Graphs of the number of occupied endplates against days post axotomy in 4 month old Wld$^s$ mouse FDB muscle preparations analysed using immunocytochemical techniques (C; NF, SV2 and α-BTX) and electrophysiological techniques (D). Black triangles represent data from individual muscles and red triangles represent the mean value (C is reproduced from Figure 4.3). Unpublished electrophysiological data courtesy of Mr D. Thomson and Dr R. Ribchester.

2 Month

(A)

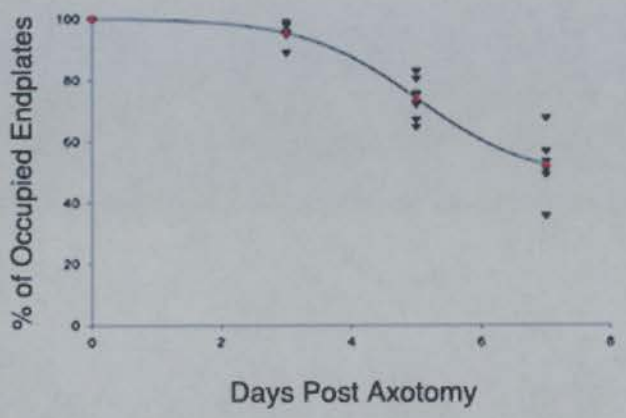


(B)

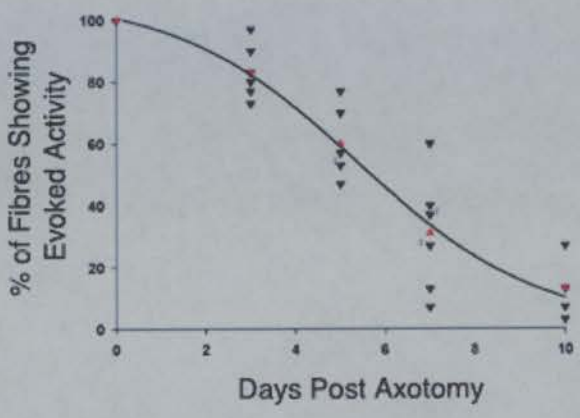


4 Month

(C)

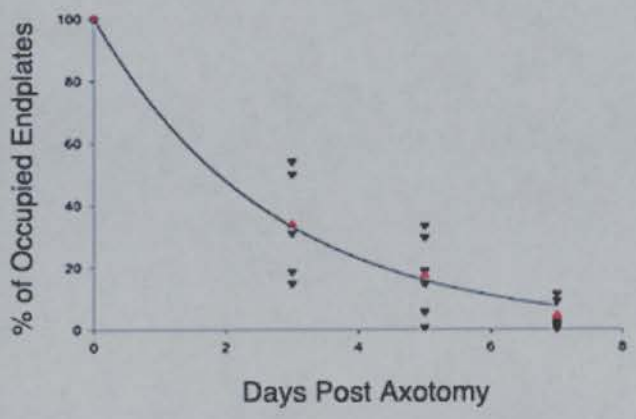


(D)

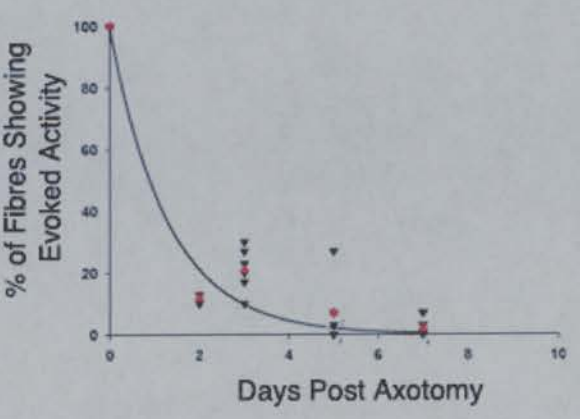

**Fig. 4.21 Comparison of Morphological and Electrophysiological Analyses of Nerve Terminal Loss at Axotomised Wld$^s$ FDB Muscle Preparations in 7 and 12 Month old Mice.**

(A & B) Graphs of the number of occupied endplates against days post axotomy in 7 month old Wld$^s$ mouse FDB muscle preparations analysed using immunocytochemical techniques (A; NF, SV2 and α-BTX) and electrophysiological techniques (B). Black triangles represent data from individual muscles and red triangles represent the mean value (A is reproduced from Figure 4.4). Unpublished electrophysiological data courtesy of Mr D. Thomson and Dr R. Ribchester.

(C & D) Graphs of the number of occupied endplates against days post axotomy in 12 month old Wld$^s$ mouse FDB muscle preparations analysed using immunocytochemical techniques (C; NF, SV2 and α-BTX) and electrophysiological techniques (D). Black triangles represent data from individual muscles and red triangles represent the mean value (C is reproduced from Figure 4.4). Unpublished electrophysiological data courtesy of Mr D. Thomson and Dr R. Ribchester.

7 Month

(A)

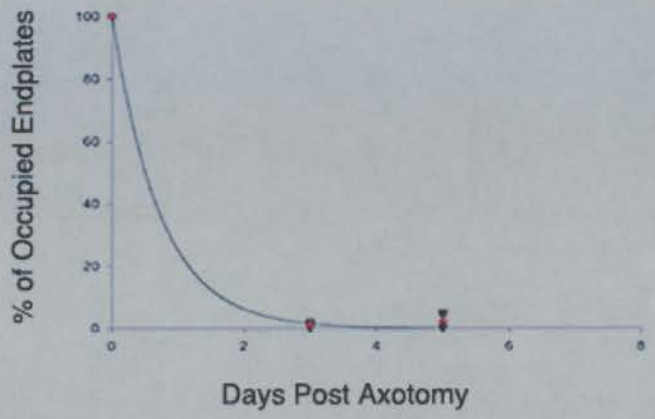


(B)

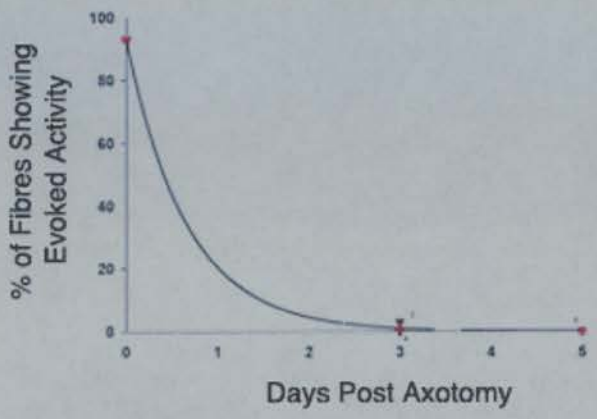


12 Month

(C)

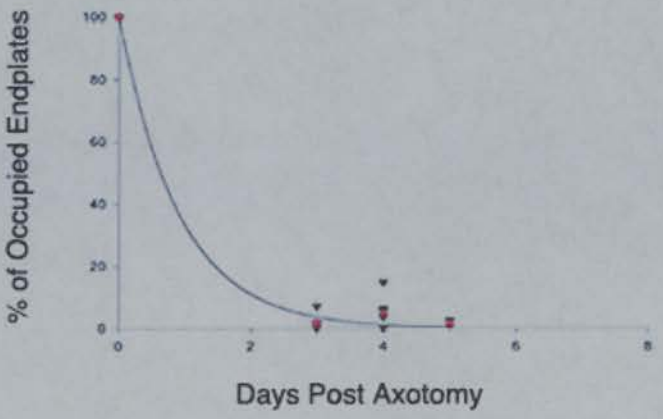


(D)

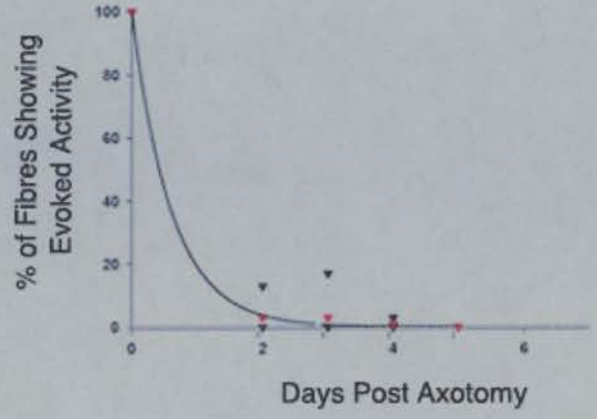

Interestingly, even though the vast majority of nerve terminals assessed at endplates in 7 and 12 month old Wld$^s$ mice were lost within 3 days of axotomy (the same as in wild-type preparations), a few NMJs had nerve terminals which persisted for up to 5 days post axotomy (Figure 4.5). One possible explanation for the preservation of a minority of nerve terminals is that they somehow retain the protection of the Wld$^s$ phenotype. This hypothesis becomes more plausible when it is noted that some of these persistent terminals showed signs of partial occupancy, associated with axotomised young Wld$^s$ nerve terminals (see below). It would therefore be of interest to ascertain whether or not all of the persistent terminals belonged to the same motor unit. If it does turn out that certain motor units are protected whilst others lose the Wld$^s$ phenotype, elucidation of any differences in the molecular characteristics of the two sub-types could provide the key to understanding what is controlling the expression of the Wld$^s$ phenotype.

When the rate of distal axonal loss was compared to the rate of nerve terminal loss in 7 month old Wld$^s$ mice following axotomy, it became apparent that motor nerve terminals are lost prior to their axons. Thus, at 4 days post axotomy, when ~98% of motor nerve terminals had been lost (Figure 4.5), ~93% of axon profile levels detected in the proximal nerve stump *remained* in the distal nerve stump. Even if the reduction in axon profiles was occurring as a result of selective motor neurone loss (motor neurones comprise 40-60% of a muscle nerve such as those supplying soleus and FDB; Boyd and Davey, 1968), this would still only equate to a 17.5-11.7% loss of axons. The notion that motor nerve terminals are lost before axons is not new however (Birks, Katz and

Miledi, 1960; Miledi and Slater, 1970). One possible explanation for the differences in the rate of loss between axons and nerve terminals is that the process of degeneration operates in a distal-proximal manner. This assumes that the process of nerve terminal degeneration is inextricably linked to the process of axonal degeneration. Hence, it would be interesting to establish whether or not the axons in these mice are degenerating in a distal-proximal manner. A second, more plausible explanation however, is that nerve terminals are being lost by a mechanism separate and distinct from that which underlies axonal degeneration, as well as the withdrawal of nerve terminals in young Wld$^s$ mice following axotomy. Moreover, these findings provide further evidence to support the hypothesis that synaptic compartments contain their own mechanisms of degeneration, separate from those present in axons and cell bodies.

### 4.4.3 Variation in the Morphological Characteristics of Motor Nerve Terminal Loss Following Axotomy in Wld$^s$ Mice of Different Ages

Morphological analysis of NMJs from Wld$^s$ mice of different ages suggested that not only was the time course of nerve terminal loss altered in older animals, but also the *nature* of nerve terminal loss was transformed. The initial evidence for this suggestion came from immunocytochemical analyses of the incidence of partial occupancy in Wld$^s$ mice of different ages (Figure 4.8). These data showed a progressive decrease in the incidence of partial occupancy with increasing age in Wld$^s$ mice. This suggests that

nerve terminals in older Wld$^s$ mice are reverting to an in situ process of degeneration, more reminiscent of classical Wallerian degeneration than the apparent withdrawal from the endplate of nerve terminals associated with young Wld$^s$ mice after axotomy. Interestingly, of the few remaining nerve terminals in both 7 and 12 month old Wld$^s$ preparations after nerve lesion ~15-30% still showed signs of partial occupancy. These findings support the hypothesis that some of the 'persistent' nerve terminals in older Wld$^s$ preparations are retained due to a continued local action of the Wld$^s$ phenotype. One other possible explanation for these findings however, is that the evidence of partial occupancy indicates that these nerve terminals are undergoing remodelling, or were undergoing remodelling when the nerve lesion occurred. This may suggest that nerve terminals which are undergoing remodelling could also gain some sort of protection against rapid degeneration.

Electron microscopic investigation of nerve terminal profiles in Wld$^s$ mice of different ages added significant weight to the hypothesis that nerve terminals are lost by a different mechanism in old (7 months plus) Wld$^s$ mice compared to young (2 month and under) Wld$^s$ mice. These experiments have unequivocally demonstrated that the nature of nerve terminal loss reverts from a piecemeal withdrawal of terminal boutons, with a retention of subcellular organelles and terminal architecture, to a classical in situ degenerative process involving a gross destruction of nerve terminal architecture and organelles (Figure 4.9a and Figure 4.12). The 8.7% of terminals which persisted in 7 month Wld$^s$ preparations, without any signs of degeneration, provide further evidence

that some nerve terminals, or motor units, retain the protection of the Wld$^s$ phenotype, even when the majority of others show no signs of resistance to degeneration.

Quantification of qualitative degenerative markers in Wld$^s$ mice revealed a progressive increase in their incidence with increasing age (Figure 4.14). When the graph in Figure 4.14 is compared with the partial occupancy graph in Figure 4.8, it is clear that as the incidence of partial occupancy falls, the incidence of degeneration increases. Interestingly, both graphs show that the loss/gain of each process is progressive, whereby animals of 4 months of age appear to be in a transitional period, with reduced levels of partial occupancy occurring alongside increased levels of degenerative markers. Specific ultrastructural analysis of NMJs from 4 month old Wld$^s$ preparations confirmed that markers of both piecemeal withdrawal (partial occupancy with retained membranes and organelles) and classical degeneration (swollen and disrupted mitochondria) could be detected, sometimes at the same NMJ (Figure 4.9b, 4.10 and 4.11a). Occasionally, a nerve terminal bouton with retained ultrastructure was observed only a couple of micrometres away from a bouton with degenerative characteristics (Figure 4.11b). This situation could arise for a number of reasons. It is possible that the degenerating mitochondrial profiles simply represent normal levels of mitochondrial turnover (~20% in control preparations; Winlow and Usherwood, 1975). This explanation would be acceptable in boutons containing low numbers of mitochondria (such as in Figure 4.11b), where out of one or two mitochondria profiles either, or both, were degenerating (thereby giving a value of 50-100% of degenerating mitochondria,

classifying the bouton as 'degenerating'). The large numbers of degenerating mitochondria in most terminals however (such as in Figures 4.10 and 4.11a), suggests that this explanation could not apply to the majority of NMJs examined. A more feasible explanation for differing levels of mitochondrial degeneration at the same NMJ could be that the regulation of degenerative mechanisms is controlled on a local (i.e. $\mu$ms) level. This could be conceivably be achieved by a selective trafficking of 'synaptic maintenance' factor(s) into nerve terminal boutons (see below). Furthermore, the findings that mitochondria appear to be the only degenerative marker occurring in axotomised 4 month old Wld$^s$ nerve terminals may suggest that mitochondria are the most susceptible of terminal organelles to degeneration, supported by findings in previous studies that mitochondrial swelling and lysis is one of the earliest signs of wild-type terminal degeneration (Manolov, 1974; Winlow and Usherwood, 1975). Moreover, it seems apparent that the progression of wild-type degeneration at nerve terminals occurs independently of mitochondrial damage; nerve terminals with degenerating mitochondrial profiles (i.e. 4 month Wld$^s$ axotomised preparations) do not inevitably proceed to a complete degenerative processes, indicated by the lack of any of the other classical markers of Wallerian degeneration (reduced synaptic vesicle densities, terminal membrane fragmentation and phagocytosis by the terminal Schwann cell).

Ultrastructural quantification of NMJs in Wld$^s$ mice revealed further significant differences in the degenerative processes occurring at different ages. There was a clear

accumulation of neurofilament in nerve terminal boutons from 4 and 7 month old Wld$^s$ mice, 3 days after axotomy, compared to controls (Figure 4.15 and 4.16). This distinctive accumulation in 4 and 7 month Wld$^s$ nerve terminals was very similar in distribution to that seen in 2 month old Wld$^s$ mice at 3 days post axotomy (cf. Figure 3.20), and the levels of NF were not significantly higher (P=0.0619 and P=0.6287 respectively; Mann Whitney test). These findings suggest that NF accumulation is not a characteristic specific to withdrawing nerve terminals. Indeed, it is to be expected that nerve terminals that have persisted for a couple of days following axotomy should contain NF accumulation, as slow axonal transport has been shown to persist in severed distal nerve stumps, leading to an accumulation of NF at the proximal and distal extremities (see Chapter 3 discussion; Watson et al., 1993). Furthermore, intra-terminal NF accumulations have been previously described by Manolov (1974) in the few nerve terminals remaining at twenty hours or more following axotomy in wild-type rats.

Whilst NF accumulation has been shown to occur in Wld$^s$ mice of all ages following axotomy, variations in synaptic vesicle populations, packing densities and localisation were detected in mice of different ages. For example, synaptic vesicle levels observed in 2 and 4 month Wld$^s$ nerve terminals, at 3 days post axotomy, show no reduction compared to control levels (Figure 4.17a and 4.18a). Indeed, the packing density of SVs was significantly higher in both 2 and 4 month preparations than in controls. The most likely cause for this increase in packing densities is the invasion of neurofilament. Because NF accumulation reduces the area available for SVs within a nerve terminal,

added to the fact that there is no reduction in the overall density of SVs, this results in a compression of the vesicles into a smaller area. Subsequent analysis of the number of 'docked' synaptic vesicles (Figure 4.19) in 2 and 4 month old $Wld^s$ FDB muscle preparations showed that there was no increase in these levels. This supports the hypothesis, raised in Chapter 3, that the maximal level of vesicle docking is achieved in control preparations. These results are dissimilar to those gained from 7 month $Wld^s$ preparations at 3 days after axotomy. Synaptic vesicles were scarce in these preparations (Figure 4.17 and 4.18a). This data closely resembles the findings of Manolov (1974) and Winlow and Usherwood (1975), who showed a similar reduction of SVs in wild-type preparations within 3-24 hours of axotomy, providing further evidence that the loss of nerve terminals in 7 month $Wld^s$ mice occurs by a process more akin to classical 'Wallerian-like' degeneration than piecemeal withdrawal. Furthermore, significant reductions in the packing density and number of 'docked' vesicles were detected in 3 day axotomised 7 month $Wld^s$ preparations compared to controls (Figure 4.8b and 4.9). Interestingly, the mean levels of synaptic vesicles at 3 days post axotomy were still almost half of that seen in controls, whereas Manolov (1974) and Winlow and Usherwood (1975) describe an almost total loss of SVs in wild-type terminals within a couple of days of axotomy. It is possible that the majority of nerve terminals in 7 month $Wld^s$ axotomised NMJ preparations do undergo a similar level of synaptic vesicle loss as observed in wild-type preparations, but that this is masked to a certain extent by the way that the current data was collected. This can be explained by the presence of a few persistent nerve terminals, which have retained

ultrastructure and organelles in 7 month Wld$^s$ preparations at 3 days after axotomy, possibly protected by a retention of the Wld$^s$ phenotype (see above). That these terminals remain, and their retained synaptic vesicles are included in the analysis, somewhat biases the data. Alternatively, it is possible that the degenerative process observed at axotomised NMJs from 7 month old Wld$^s$ mice occurs by a less severe process as than that of Wallerian degeneration in wild-type preparations, and as a result, the effect on the synaptic vesicle population is not so striking.

Finally, evidence for a transition in the nature of terminal loss is provided by analysing vacant endplates with no overlying nerve terminal. At the majority of vacant endplates observed in 7 month Wld$^s$ preparations (96.30%), cellular profiles, presumably of terminal Schwann cells (cf. Miledi and Slater, 1968), were in close contact with the postsynaptic folds (Figure 4.13b). This is in contrast to 2 month Wld$^s$ preparations where only 30.04% of vacant endplates were contacted by a cellular profile. Retention of terminal Schwann cell processes at vacant NMJs has been shown to occur following wild-type nerve terminal degeneration in frog and rat muscle (Birks, Katz and Miledi, 1959; Birks, Katz and Miledi, 1960; Miledi and Slater, 1968; Miledi and Slater, 1970). By contrast, studies of processes which involve withdrawal of nerve terminals, such as synapse elimination in reinnervated sternomastoid muscle, suggest that Schwann cells are removed from the endplate alongside motor nerve terminals (Culican et al., 1998). This provides further evidence to support the hypothesis that 7 month Wld$^s$ terminals are lost by a 'Wallerian-type" process whereas 2 month Wld$^s$ terminals are lost by a

separate and distinct withdrawal mechanism, thereby suggesting that synaptic compartments contain more than one mechanism capable of producing synaptic degeneration.

### 4.4.4 Possible Mechanisms Underlying an Age Related Decline in the Wld$^s$ Phenotype

One of the most logical explanations for a reduction in the effectiveness of the Wld$^s$ phenotype with age would be a concurrent reduction in the expression of the Wld$^s$ gene. Molecular studies from the lab of Dr M.P. Coleman in Cologne have demonstrated that this is not the case however. A western blot showing the continued expression of the Wld protein as well as the Ube4b protein in Wld$^s$ mice of up to a year old is shown in Figure 4.22. This suggests that the increased rate of loss of motor nerve terminals in older Wld$^s$ mice may be controlled by other mechanisms. More specifically, it may be due to the action of a 'synaptic maintenance factor', the levels of which decline with age. It is possible that such a factor may be responsible for initiating the withdrawal, rather than degeneration, of nerve terminals under conditions such as disuse or axotomy. Furthermore, it could be envisaged that a 'synaptic maintenance factor' may be responsible for initiating many of the withdrawal processes which occur in vivo, such as synapse elimination. Synapse elimination occurs normally in Wld$^s$ mice (Parson et al., 1997), thus I am not suggesting that the mechanisms of synapse withdrawal are in any way abnormal in these mice. In this model, selective trafficking

**Fig. 4.22 Wld$^s$ Protein Expression in Brain.**

(A) Western blot showing the continued expression of the Wld protein and Ube4b protein in brains of Wld$^s$ mice of 3 months and 1 year of age. Unpublished data courtesy of Dr M.P. Coleman.

(A)

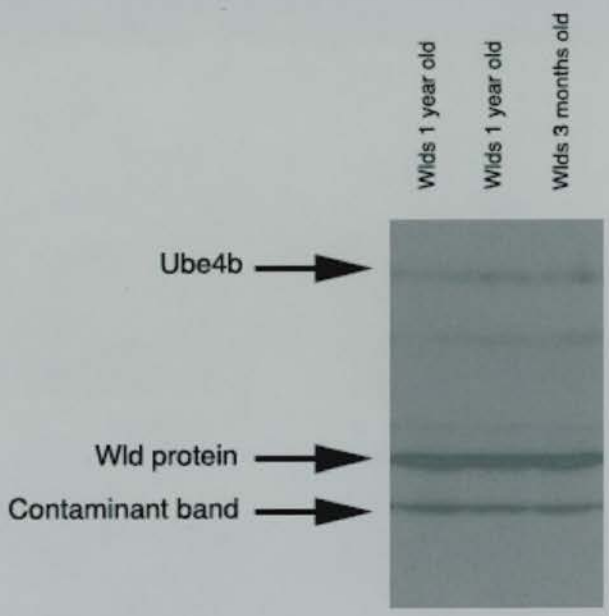
Wlds 1 year old
Wlds 1 year old
Wlds 3 months old
Ube4b
Wld protein
Contaminant band

of such a factor into 'winning' nerve terminals at competing polyinnervated endplates would lead to a subsequent loss of the 'maintenance' factor in 'losing' terminals, leading to their elimination via a process of withdrawal. Similarly, in my young $Wld^S$ preparations, it is possible that, in the absence of Wallerian degeneration (which normally masks synapse specific events), axotomy leads to a reduction in the production of, and places a physical barrier to stop the trafficking of, such a factor from the cell body. Thus, when the residual amount of factor left in the distal stump is consumed, terminals withdraw from the endplate. If the levels of expression of such a 'synaptic maintenance' factor decline with age then it is possible that in older $Wld^s$ mice, insufficient levels are present to neither retain synaptic terminals nor cause their withdrawal from the endplate following axotomy, therefore allowing separate, Wallerian-like degenerative mechanisms to remove nerve terminals. This hypothesis seems plausible when the fact that age has significant effects on both the physical and functional properties of neurones is considered, whereby in older animals both myelinated and unmyelinated nerve fibres are lost, many remaining fibres have deteriorating myelin sheaths and axons often appear atrophied (for review see Verdu et al., 2000).

This 'synaptic maintenance' factor hypothesis also provides a possible explanation for the preservation of a small sub-set of motor nerve terminals following axotomy in 7 month old $Wld^s$ preparations as well as the appearance of intermediate characteristics of withdrawal and degeneration in 4 month old $Wld^s$ preparations. If the switching off of

such a factor occurs asynchronously in different motor neurones, then it is possible that some will still retain the Wld$^s$ phenotype, even at 7 months of age. However, there is one other possible explanation for the retention of some nerve terminals in older mice in light of the 'synaptic maintenance' factor hypothesis. It is possible that a few motor axons have been subjected to some form of injury whilst in vivo. It has been shown that piecemeal nerve terminal withdrawal occurs from polyinnervated endplates established as a result of nerve injury in adult mice (Taxt, 1983; Rich and Lichtman, 1989a; Barry and Ribchester, 1995; Culican et al., 1998), which may suggest that the 'withdrawal' phenotype, controlled by such a factor, may be upregulated in neurones following injury.

The existence of both withdrawal and degeneration characteristics at the same NMJs in 4 month old Wld$^s$ mice (partial occupancy and terminal retention alongside mitochondrial degeneration; Figure 4.9, 4.10 and 4.11) can also be explained by the presence of a 'synaptic maintenance' factor. If the levels of such a factor are only just enough to produce the retention and withdrawal of nerve terminals, it remains possible that individual boutons which are not getting quite enough of the factor start to show signs of classical degeneration (mitochondrial swelling and lysis). These could happily coexist with other boutons of the same nerve terminal which, either due to slightly better trafficking or retention, show no signs of degeneration. Therefore, the sudden increase in Wallerian-like characteristics between 4 and 7 months of age may represent a critical point in the life of a neurone, when the levels of such a factor are no longer

high enough to have a protective effect, and as a result, Wallerian-type characteristics prevail at axotomised motor nerve terminals. It would be very interesting to study differences in the molecular characteristics of individual boutons at a nerve terminal, to examine their dependence or independence on other boutons under normal and destabilising conditions such as axotomy or synapse elimination.

The findings of an age related phenotypic expression in the $Wld^s$ mouse suggest that one way to identify a molecule which could be responsible for maintaining synapses could be to search for neuronal proteins whose expression declines with age. For example, by using a combination of micro-array (gene chip) and 2D gel electrophoresis techniques on neuronal tissue, it would be possible to search through thousands of candidate mRNA or protein molecules. This could be undertaken in a way in which those molecules which are expressed in an age-dependent manner, or even have undergone age-related post-translational modifications, could be detected. Furthermore, an expansion of this 'synaptic maintenance factor' hypothesis could be attained by introducing computational modelling of the mechanisms of action of such a factor, in a similar fashion to that which has been previously undertaken with regard to the competition for neurotrophic factor in the development of nerve connections (van Ooyen and Willshaw, 1999).

### 4.4.5 Summary

The data presented in this chapter unequivocally demonstrate that, at least in the stock supplied by Harlan-olac and maintained or bred in Edinburgh, both the rate and nature of nerve terminal loss following axotomy in $Wld^s$ mice changes with age. The decline in the phenotypic expression of the $Wld^s$ mutation results in a transition from piecemeal withdrawal of nerve terminals following axotomy in young (2 month old) $Wld^s$ mice, to classical 'Wallerian-like' degeneration of terminals in animals of 7 months and older, with characteristics of both present in 4 month old $Wld^s$ NMJs. The probable difference in the effect of age on axons and motor nerve terminals provides further evidence to support the hypothesis that nerve terminals are lost by mechanisms distinct from that of axons and soma. Moreover, my data suggest that even in old $Wld^s$ mice, the mechanism of nerve terminal degeneration, whilst not being the same responsible for nerve terminal loss in young $Wld^s$ mice, is still separate and independent of axon degeneration. Furthermore, the current data provides evidence indicating the existence of a 'synaptic maintenance factor', responsible for initiating the withdrawal of nerve terminals under conditions such as axotomy or disuse, the levels of which decline with age. It still remains unclear however, as to what molecular component in the $Wld^s$ genotype is responsible for its axotomy-induced phenotype. This question will be addressed in the final experimental chapter.

# Results Chapter 5

# 5. Responses of Ube4b/Nmnat (Wld$^s$) Transgenic Mice Motor Nerve Terminals to Axotomy

## 5.1 Background

The molecular genetics underlying the Wld$^s$ mutation remained a mystery until fairly recently. Initial studies showed that the Wld$^s$ mutation is controlled by a single autosomal dominant gene, which maps on to the distal end of mouse chromosome 4, the region homologous with human chromosomal region 1p34-1p36 (Perry et al., 1990b; Lyon et al., 1993). Subsequent analysis showed that the Wld$^s$ locus consists of an 85-kb tandem triplication within the candidate region (Coleman et al., 1998), containing the exons of three genes within the repeat sequence (Conforti et al., 2000). Two of these genes, Ube4b, a ubiquitination factor, and Nmnat, a key enzyme in the synthetic pathway of $NAD^+$ (Magni et al., 1999), have been shown to span the proximal and distal boundaries of the repeat unit, forming a chimeric Ube4b/Nmnat gene which expresses a 43kDa fusion protein (see Figure 1.3; Conforti et al., 2000). The third gene, a retinol binding protein, Rbp7, is not expressed in the nervous system and is now considered not to exert any influence on the Wld$^s$ phenotype (Conforti et al., 2000).

Whilst the Ube4b/Nmnat chimeric gene (hereafter referred to, tentatively as 'wallerin') is a strong candidate for producing the Wld$^s$ phenotype, in order to test the hypothesis that the chimeric gene is both necessary and sufficient to explain the Wld$^s$ phenotype,

transgenic mice expressing the chimeric gene have been generated and the effect of axotomy on motor nerve terminals has been assessed. The characterisation of the wallerin gene is part of an ongoing team effort, and the results in this chapter represent my contribution to this enterprise. Evidence is presented that expression of the wallerin gene, under the action of the β-actin promoter, results in a manifestation of the $Wld^s$ phenotype, thereby preserving disconnected axons and motor nerve terminals following axotomy. Furthermore, the data show that a similar kind of axotomy-induced piecemeal retraction of motor nerve terminals seems to occur following axotomy, appearing much the same as described previously at young $Wld^s$ mutant mice NMJs (Chapter 3; Mattison et al., 1996; Ribchester et al., 1999). This provides strong evidence to suggest that slow synapse withdrawal is not unique to the $Wld^s$ mouse, but rather that it reflects a secondary degeneration process inherent in the synaptic compartment that is revealed only when Wallerian degeneration of axons is blocked.

Immunocytochemical and electron microscopic data are presented regarding the morphological and ultrastructural characteristics of NMJs in 1 month old transgenic mice at 2, 3 and 5 days post axotomy. Qualitative and quantitative examination of such preparations provided an overview of the temporal and morphological aspects of motor nerve terminal loss in these mice. Comparison with data from control and 2 month $Wld^s$ preparations, generated in previous chapters, allowed for an accurate assessment of the level of expression of the $Wld^s$ phenotype in Ube4b/Nmnat transgenic mice. Parallel biochemical studies (T. Mack and M.P. Coleman) and electrophysiological

studies (D. Thomson and R.R. Ribchester) support the findings presented here (see Appendix 1).

## 5.2 Methods

The majority of experiments contained within the current chapter were undertaken using methods previously described in Chapter 2. The following section contains details of methods which are specific to this chapter.

### 5.2.1 Generation of Ube4b/Nmnat Transgenic Mice

The production of Ube4b/Nmnat transgenic mice was undertaken by Dr M.P. Coleman's laboratory in Cologne (Figure 5.1). Appendix 1 contains the description of how these mice were generated by Dr Coleman and colleagues.

**Fig. 5.1 Transgene Construct for Ube4b/Nmnat Transgenic Mice**

(A) The transgene construct. The chimeric cDNA was expressed with non-coding exon 1 of β-actin under the control of a human β-actin promoter and terminated with the SV40 polyadenylation signal.

(B) Southern blot showing the incorporation of the Ube4b/Nmnat transgene in the 4839, 4830 and 4836 lines of transgenic mice and a non-transgenic control mouse. The 4836 line shows the strongest incorporation of the transgene and is the line used for all experiments in the current study.

Figure adapted from Mack et al. (2001).

A

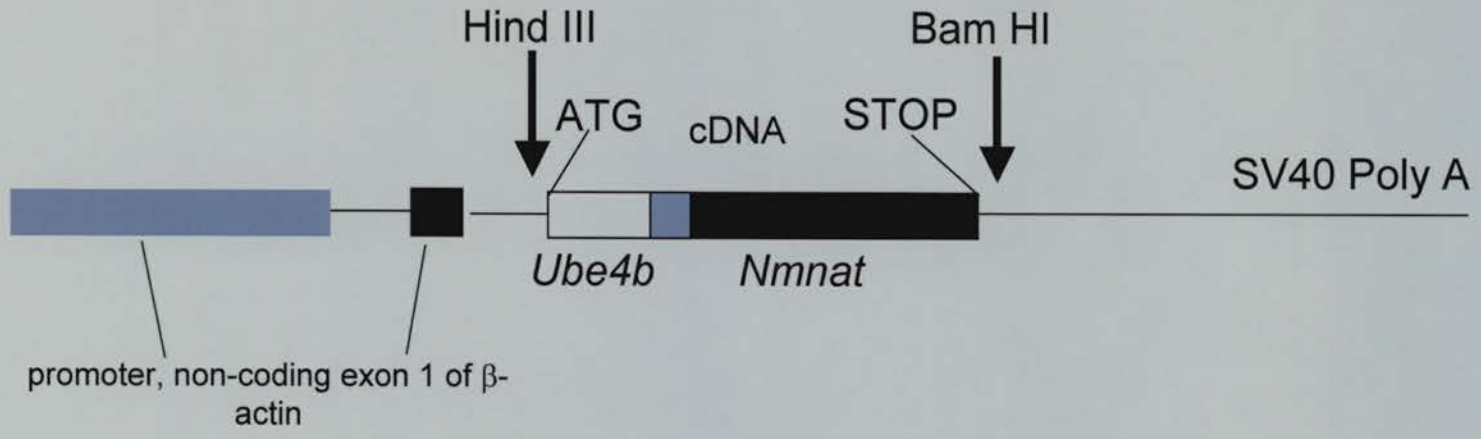
Hind III
Bam HI
ATG
cDNA
STOP
SV40 Poly A
Ube4b
Nmnat
promoter, non-coding exon 1 of β-actin

B


4830
4836
4839
Non Tg
Endogenous sequences
4.5 kb
3.0 kb
1.1 kb (transgene)

### 5.2.2 Processing of Ube4b/Nmnat Transgenic Mouse Tissue for Immunocytochemistry and Electron Microscopy

All experiments utilising Ufd2/Nmnat transgenic mice were carried out on isolated FDB or 4$^{th}$ deep lumbrical muscle preparations obtained from young (2 months or under) mice from the breeding colony maintained in Dr M.P.Coleman's lab in Cologne. Muscle preparations were dissected in Cologne, and fixed immediately for either immunocytochemistry (4% paraformaldehyde) or electron microscopy (4% paraformaldehyde/2.5% glutaraldehyde). Tissue for immunocytochemical analysis was taken by courier to Edinburgh (along with living preparations for physiological experiments) in phosphate buffer or HEPES buffered physiological saline. I carried out the remainder of the immunocytochemical protocol and fluorescence/confocal microscopic analysis in Edinburgh (see Chapter 2). Tissue for electron microscopic analysis was washed in 0.1M phosphate buffer and post-fixed in 1% osmium in Cologne before being mailed to Edinburgh, where I carried out standard EM processing, observation and analysis (see Chapter 2).

## 5.3 Results

### 5.3.1 Morphological Preservation and Partial Occupancy at NMJs in Ube4b/Nmnat Transgenic Mice following Axotomy

Immunocytochemically labelled NMJs (NF, SV2 and α-BTX) from 2 day (n=86, N=1), 3 day (n=81, N=1) and 5 day (n=318, N=2) axotomised 1 month old wallerin transgenic mice 4$^{th}$ deep lumbrical muscles were individually assessed as to their level of occupancy. All of the nerve terminals observed at all time points post axotomy showed retained pre- and postsynaptic architecture (Figure 5.2). At 2 days post axotomy, in remarkable contrast to wild-types (see Chapter 3), all Wallerin transgenic endplates were still occupied. This prevalence decreased to 97.53% at 3 days and 90.03% ±2.83 SEM at 5 days after axotomy (Figure 5.3). These muscles reportedly twitched in response to cutting the nerve when they were dissected, and synaptic potentials were recorded from the impaled FDB muscle fibres (D. Thomson and R.R. Ribchester, personal communication).

Evidence for partial occupancy of endplates following axotomy was found in all wallerin transgenic preparations, ranging from only one or two terminal boutons missing through to retraction bulb formation (Figure 5.4 and 5.5). Quantification of this

phenomenon showed that the occurrence of partially occupied endplates did not increase much above the level observed in controls (see Chapter 3) until 5 days post axotomy, when 22.25% ±12.51SEM of endplates were partially occupied (Figure 5.6).

### 5.3.2 Ultrastructural Evidence for Preservation of NMJs in Wallerin Transgenic Mice following Axotomy

Qualitative ultrastructural analysis of NMJ profiles from 5 day axotomised wallerin transgenic FDB muscle preparations confirmed that nerve terminals were retained without any degenerative changes (i.e. intact mitochondria, synaptic vesicles and terminal membranes; Figure 5.7). Occasionally, examples of nerve terminals with neurofilament invasion and/or a paucity of synaptic vesicles were observed (Figure 5.8). Quantification of NF levels (Figure 5.9) revealed that there was a significant increase (P=0.0015; Mann Whitney test) in 5 day axotomised wallerin transgenic mice nerve terminals (6.32% ±1.68SEM; n=20, N=2) compared to controls (1.42% ±0.33; n=34, N=4). However, the levels of NF accumulation were significantly less than those observed in 2 month old $Wld^s$ mice preparations at 5 days post axotomy (17.32% ±2.63; P=0.0047; n=26, N=4).

Qualitative analysis, suggesting that some terminals from 5 day axotomised wallerin transgenic mice preparations had a paucity of synaptic vesicles, was supported by quantitative analysis (Figure 5.10). Synaptic vesicle densities were significantly

reduced in 1 month transgenic preparations at 5 days post axotomy (39.51 SV/$\mu m^2$ ±4.81SEM), by almost 50% compared to control (78.31 SV/$\mu m^2$ ±6.04; P=<0.0001, unpaired t test) and 2 month old, 5 day axotomised $Wld^s$ (78.75 SV/$\mu m^2$ ±5.72; P=<0.0001) preparations. Furthermore, even though many wallerin transgenic nerve terminals contained accumulations of NF (see above), the packing density of synaptic vesicles (21.21% ±3.35) were significantly reduced compared to both control (28.25% ±1.95; P=0.0168, Mann Whitney test) and 2 month, 5 day axotomised $Wld^s$ (41.40% ±2.18; P=<0.0001) preparations.

Qualitative analysis of electron micrographs of NMJs from 5 day axotomised wallerin transgenic mice FDB muscles suggested that the subcellular localisation of synaptic vesicles was altered (Figure 5.11a). Quantitative analysis of the numbers of 'docked' vesicles (classified as vesicles within 125nm of an active zone; see Chapter 2 for explanation) showed a significant reduction in wallerin transgenic mice FDB muscle nerve terminals, with levels of 3.17 ±0.24SEM (n=48, N=2), compared to both control (5.04 ±0.18; P=<0.0001, unpaired t test; n=75, N=4) and 2 month, 5 day axotomised $Wld^s$ (5.25 ±0.17; P=<0.0001; n=55, N=4) muscles.

**Fig. 5.2 Morphology of Axotomised NMJs in Ube4b/Nmnat Transgenic Mice.**

(A) Stereo pair of confocal micrographs of five NMJs from a 1 month old Ube4b/Nmnat homozygote transgenic mouse 4$^{th}$ deep lumbrical muscle (NF, SV2 and α-BTX) 5 days post axotomy. All NMJs have intact axons and motor nerve terminals, showing no signs of fragmentation. Scale bar = 20$\mu$m.

(A)

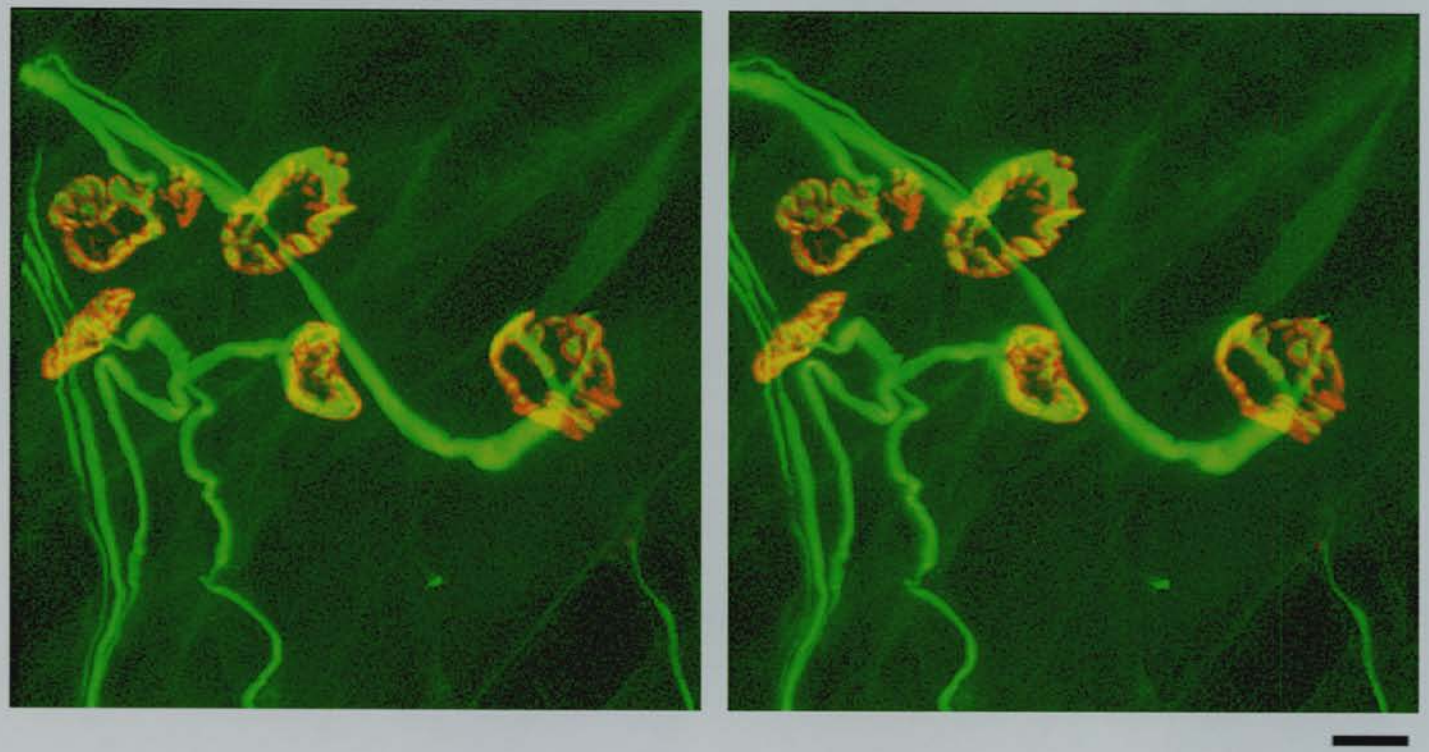

**Fig. 5.3 Morphological Quantification of Motor Nerve Terminal Preservation in Ube4b/Nmnat Transgenic Mice Following Axotomy.**

(A) Graph of the percentage of occupied endplates (both fully and partially occupied) against days post axotomy in Ube4b/Nmnat homozygote transgenic mice 4$^{th}$ deep lumbrical muscle preparations, as assessed by immunocytochemistry (NF, SV2 and α-BTX).

(A)

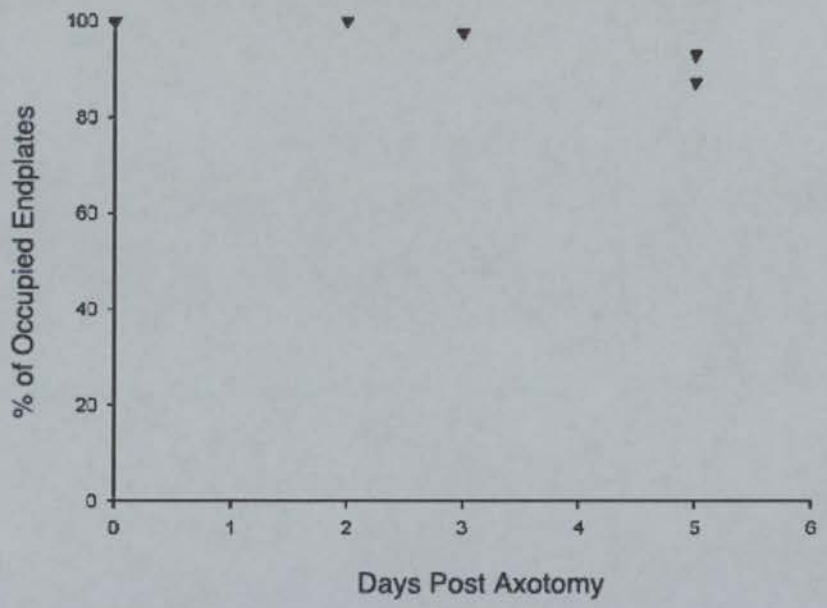
% of Occupied Endplates
100
80
60
40
20
0
0
1
2
3
4
5
6
Days Post Axotomy

**Fig. 5.4 Morphological Evidence for Partial Occupancy at Endplates of Ube4b/Nmnat Transgenic Mice Following Axotomy (1).**

(A) Confocal micrograph of four NMJs from a 1 month old wallerin homozygote transgenic mouse 4$^{th}$ deep lumbrical muscle (NF, SV2 and α-BTX) 5 days post axotomy. Two endplates are partially occupied, with areas of endplate not contacted by overlying nerve terminal boutons (arrows). Note the intensity of neurofilament staining in the axon branches. Scale bar = 20$\mu$m.

(A)

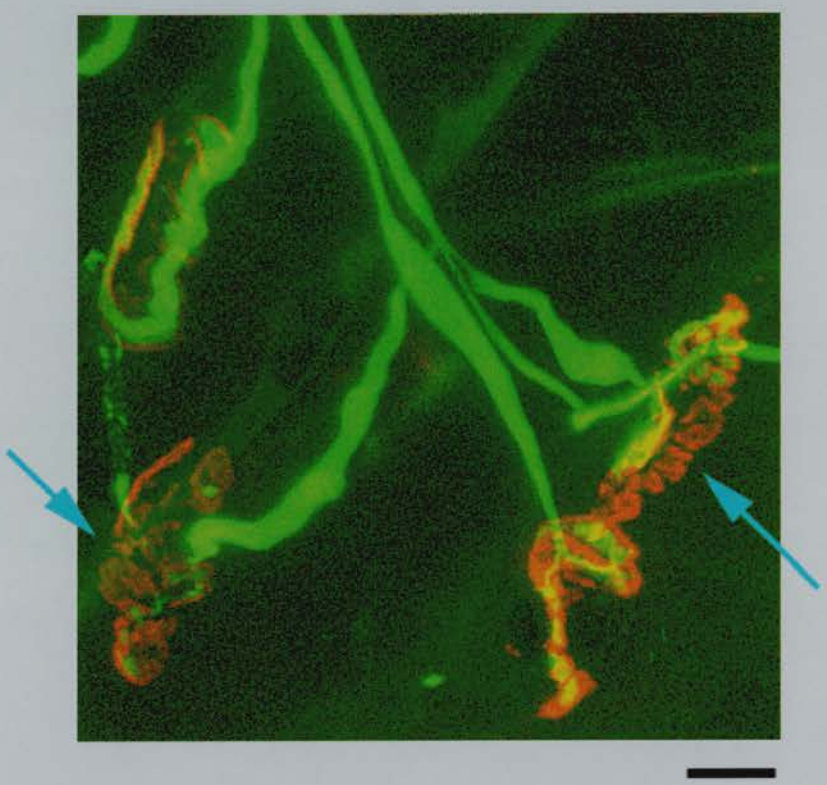

**Fig. 5.5 Morphological Evidence for Partial Occupancy at Endplates of Ube4b/Nmnat Transgenic Mice Following Axotomy (2).**

(A) 'Stereo pair' confocal image of four NMJs from a 1 month old Ube4b/Nmnat homozygote transgenic mouse 4$^{th}$ deep lumbrical muscle (NF, SV2 and $\alpha$-BTX) 5 days post axotomy. The endplate second from the left is only contacted by a retraction bulb (characterised by a thin axonal process terminating in a bulbous swelling). The other three NMJs have intact axons and motor nerve terminals, showing no signs of fragmentation or degeneration. Scale bar = 20$\mu$m.

(A)

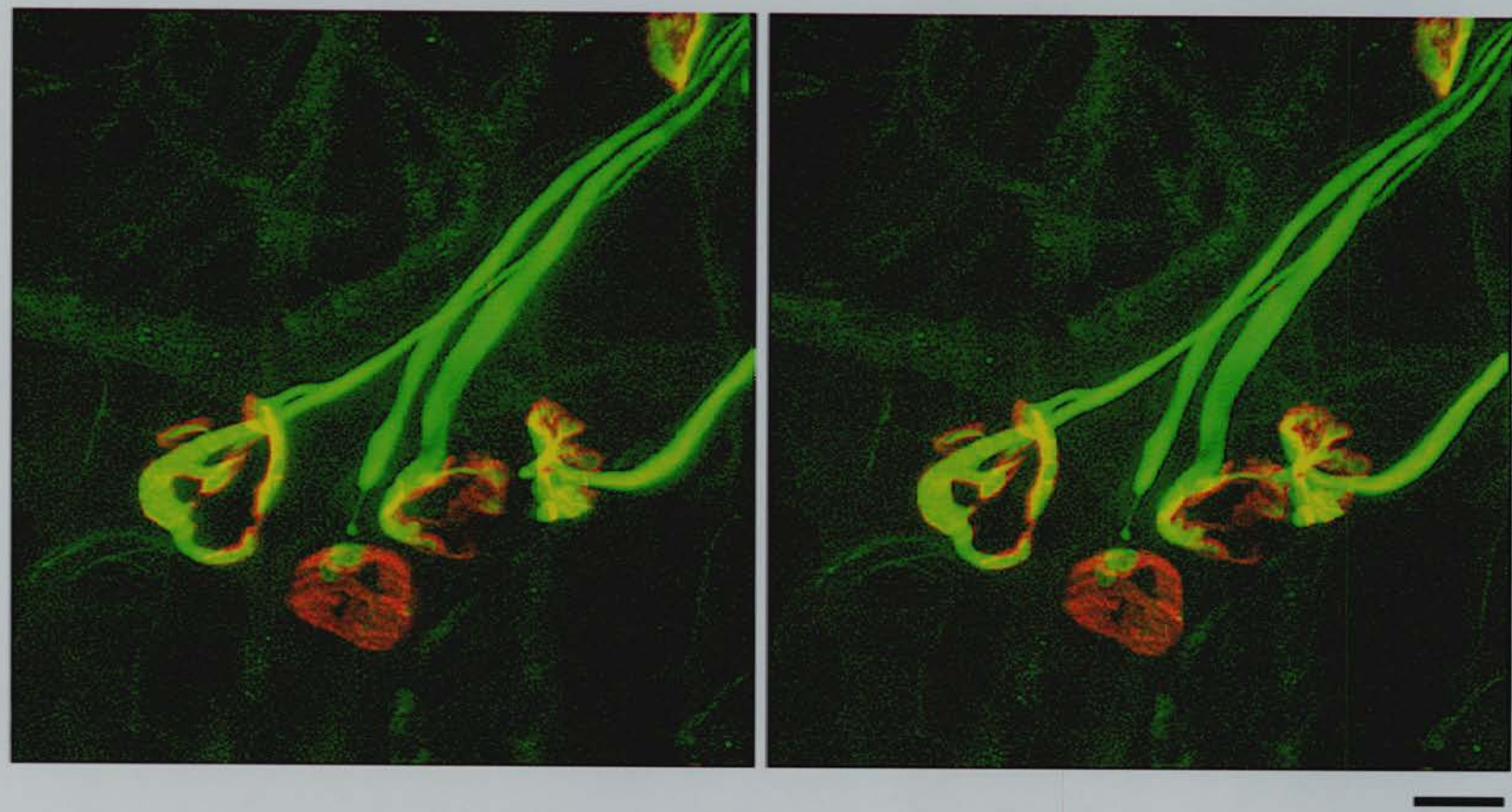

**Fig. 5.6 Morphological Quantification of Partial Occupancy at Endplates of Ube4b/Nmnat Transgenic Mice Following Axotomy.**

(A) Graph of the percentage of partially occupied endplates against days post axotomy in Ube4b/Nmnat homozygote transgenic mice 4$^{th}$ deep lumbrical muscle preparations, as assessed by immunocytochemistry (NF, SV2 and α-BTX).

(A)

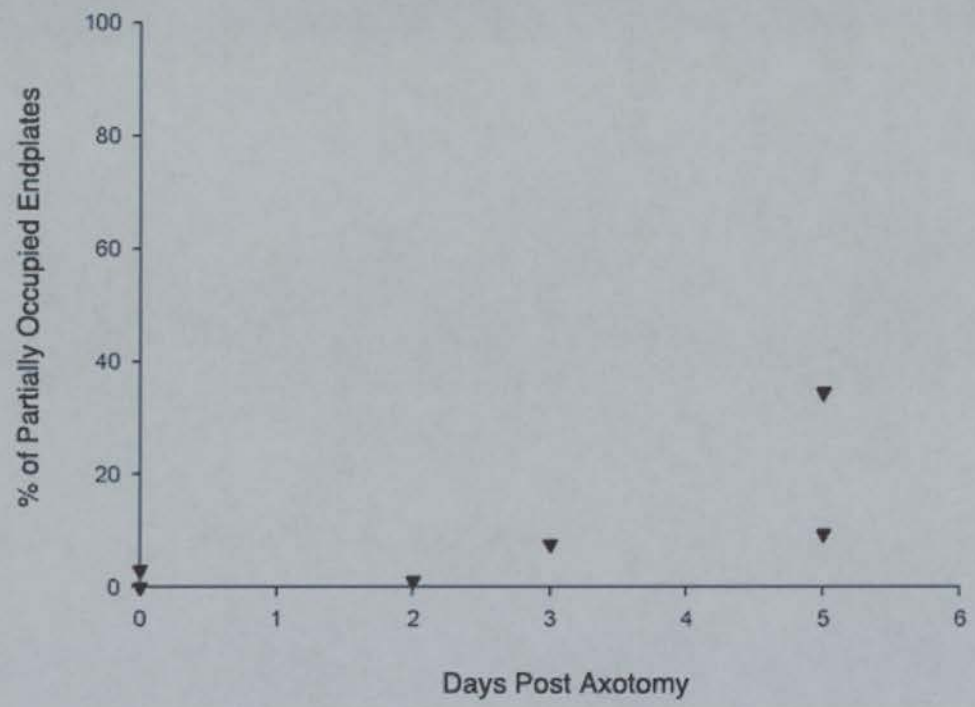
% of Partially Occupied Endplates
100
80
60
40
20
0
0
1
2
3
4
5
6
Days Post Axotomy

**Fig. 5.7 Ultrastructural Preservation of Motor Nerve Terminals at Axotomised NMJs in Ube4b/Nmnat Transgenic Mice.**

(A) Electron micrograph of a NMJ from a 1 month old Ube4b/Nmnat homozygote transgenic mouse FDB muscle 5 days post axotomy. The nerve terminal appears to have normal levels and distribution of synaptic vesicles and mitochondria alongside well preserved membranes. Scale bar = 1$\mu$m.

(A)

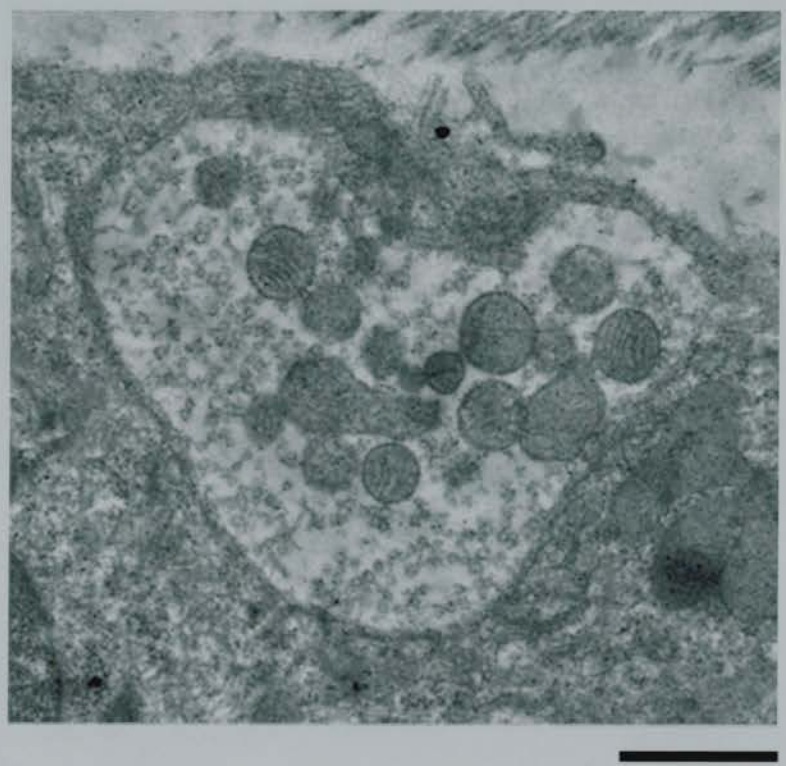

**Fig. 5.8 Ultrastructural Alterations in Subcellular Organelles in Ube4b/Nmnat Transgenic Mice Axotomised NMJs.**

(A) Electron micrograph of a NMJ from a 1 month old Ube4b/Nmnat homozygote transgenic mouse FDB muscle 5 days post axotomy. The nerve terminal appears to have a small NF accumulation in the centre of the terminal and a paucity of synaptic vesicles. Scale bar = 1$\mu$m.

(B) Electron micrograph of a NMJ from a 1 month old Ube4b/Nmnat homozygote transgenic mouse FDB muscle 5 days post axotomy. Whilst no mitochondria or discernable NF are present, a paucity of synaptic vesicles is apparent. Scale bar = 1$\mu$m.

(A)

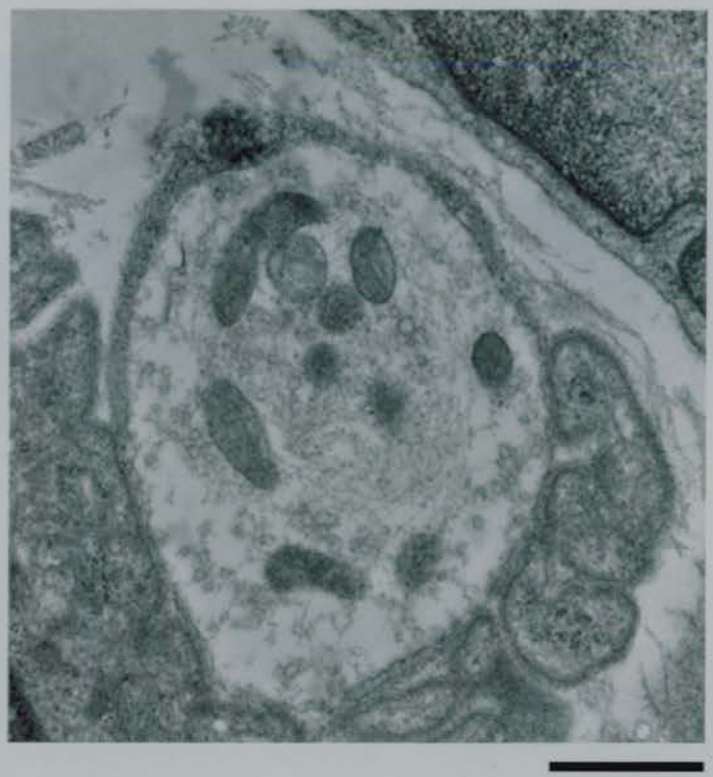

(B)

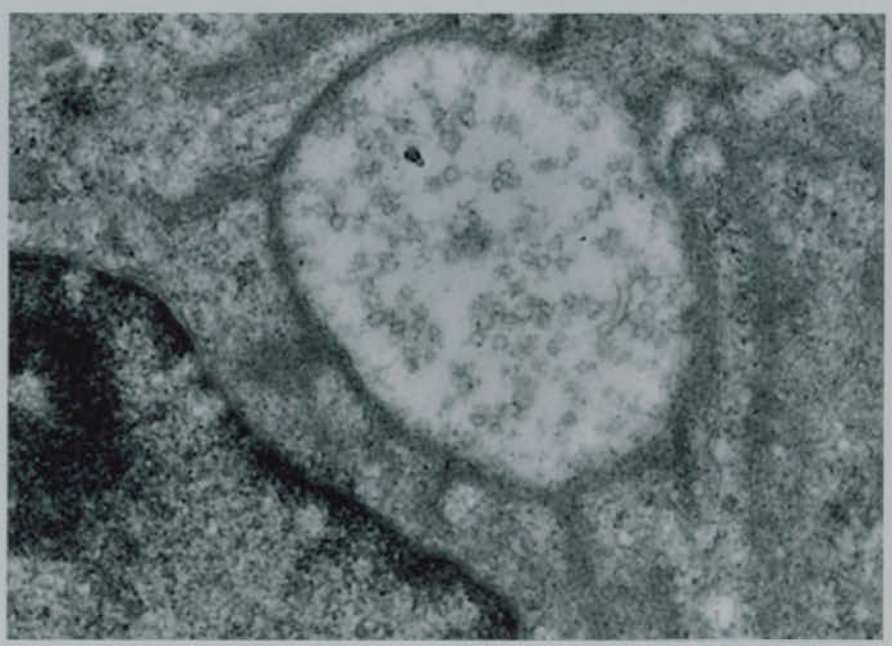

**Fig. 5.9 Ultrastructural Quantification of Neurofilament Levels in Axotomised Motor Nerve Terminals from Ube4b/Nmnat Transgenic Mice.**

(A) Bar chart showing the percentage of nerve terminal occupied by neurofilament in control FDB muscle, 2 month $Wld^s$ FDB muscle 5 days post axotomy and Ube4b/Nmnat homozygote transgenic FDB muscle 5 days post axotomy. Significant accumulations of NF were detected in transgenic nerve terminals compared to control preparations ($P=0.0015$; Mann Whitney test). The levels of NF were significantly less than in the 2 month $Wld^s$ preparations however ($P=0.0047$). Error bars = SEM.

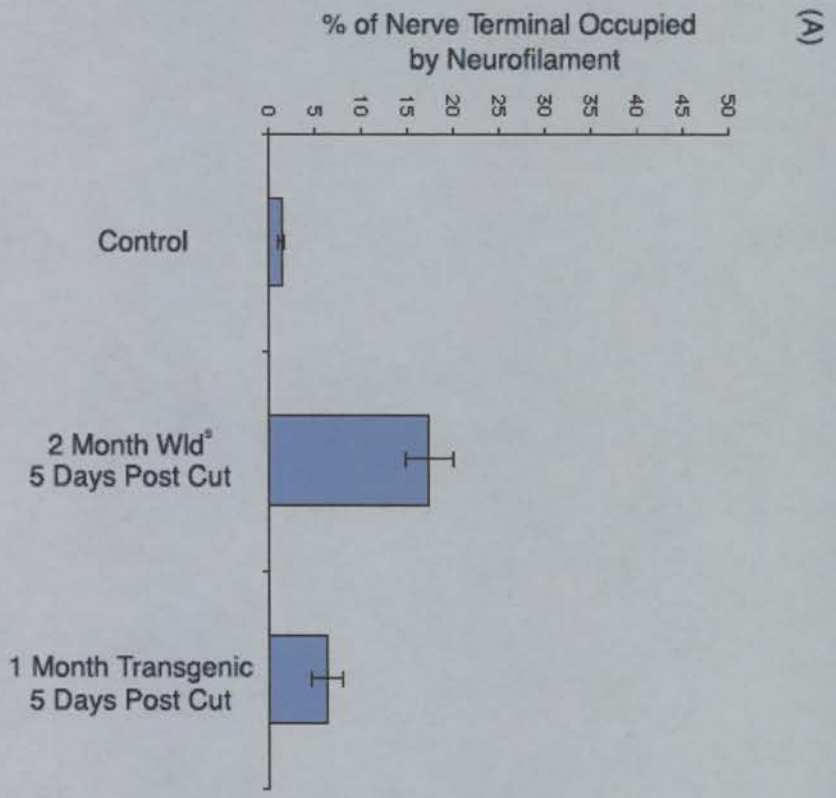
% of Nerve Terminal Occupied
by Neurofilament
0
5
10
15
20
25
30
35
40
45
50
Control
2 Month Wld^s
5 Days Post Cut
1 Month Transgenic
5 Days Post Cut

(A)

**Fig. 5.10 Ultrastructural Quantification of Synaptic Vesicle Densities and Packing Densities in Axotomised Motor Nerve Terminals from Ube4b/Nmnat Transgenic Mice.**

(A) Bar chart showing the density of synaptic vesicles in nerve terminals from control FDB muscle, 2 month $Wld^s$ FDB muscle 5 days post axotomy and Ube4b/Nmnat homozygote transgenic FDB muscle 5 days post axotomy. Transgenic motor nerve terminals contained significantly reduced SV densities compared to both control and 2 month $Wld^s$ preparations ($P=<0.0001$ for both; unpaired t test). Error bars = SEM.

(B) Bar chart showing the packing density of synaptic vesicles in nerve terminals (see chapter 2 for explanation) from control FDB muscle, 2 month $Wld^s$ FDB muscle 5 days post axotomy and Ube4b/Nmnat homozygote transgenic FDB muscle 5 days post axotomy. Transgenic motor nerve terminals contained significantly reduced SV packing densities compared to both control and 2 month $Wld^s$ preparations ($P=0.0168$ and $P=<0.0001$ respectively; Mann Whitney test). Error bars = SEM.

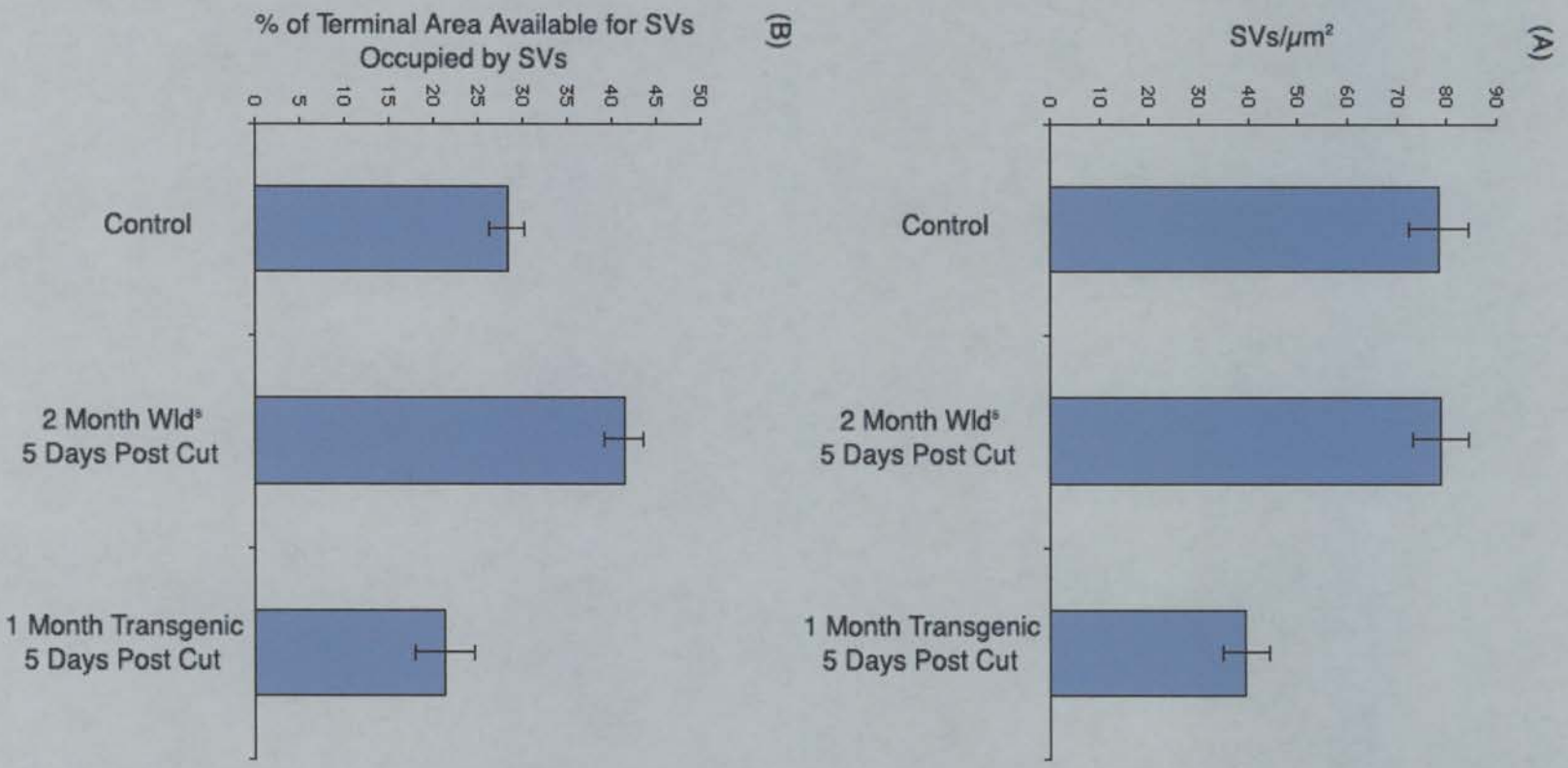
% of Terminal Area Available for SVs Occupied by SVs
(B)
0
5
10
15
20
25
30
35
40
45
50
Control
2 Month Wld$^s$ 5 Days Post Cut
1 Month Transgenic 5 Days Post Cut
SVs/$\mu m^2$
(A)
0
10
20
30
40
50
60
70
80
90
Control
2 Month Wld$^s$ 5 Days Post Cut
1 Month Transgenic 5 Days Post Cut

**Fig. 5.11 Qualitative and Quantitative Assessment of Synaptic Vesicle Localisation in Axotomised Motor Nerve Terminals from Ube4b/Nmnat Transgenic Mice.**

(A) Electron micrograph of a NMJ from a Ube4b/Nmnat homozygote transgenic FDB muscle 5 days post axotomy. Whilst the pre- and postsynaptic architecture appear intact, the numbers of vesicles clustered around active zones are reduced. Scale bar = 0.5$\mu$m.

(B) Bar chart showing the number of synaptic vesicles within 125nm of active zones ('docked' vesicles) in nerve terminals from control FDB muscle, 2 month Wld$^s$ FDB muscle 5 days post axotomy and Ube4b/Nmnat homozygote transgenic FDB muscle 5 days post axotomy. Transgenic motor nerve terminals contained significantly reduced numbers of 'docked' synaptic vesicles compared to both control and 2 month Wld$^s$ preparations (P=<0.0001 for both; unpaired t test). Error bars = SEM.

(A)

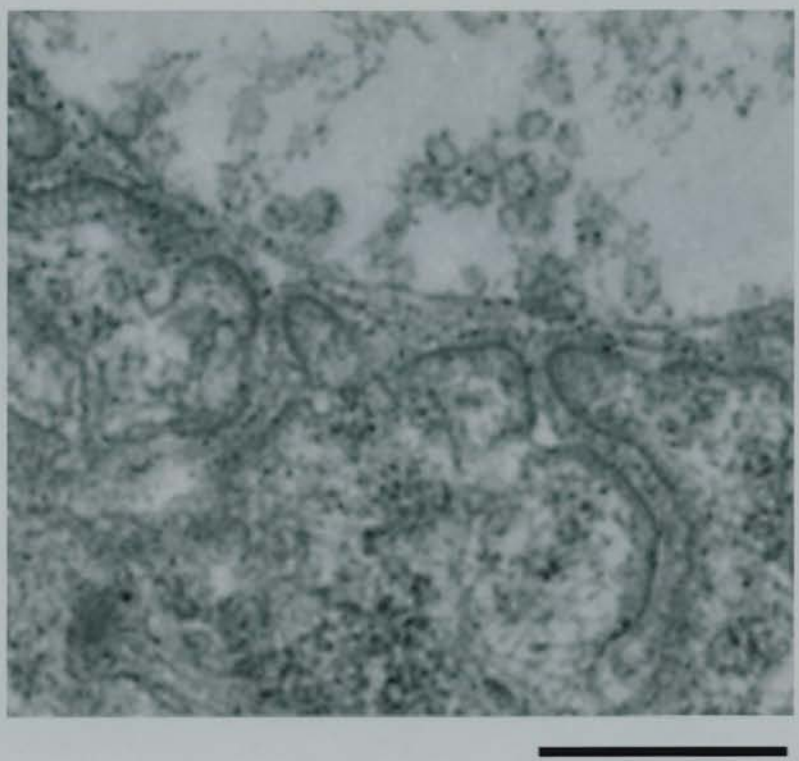

(B)

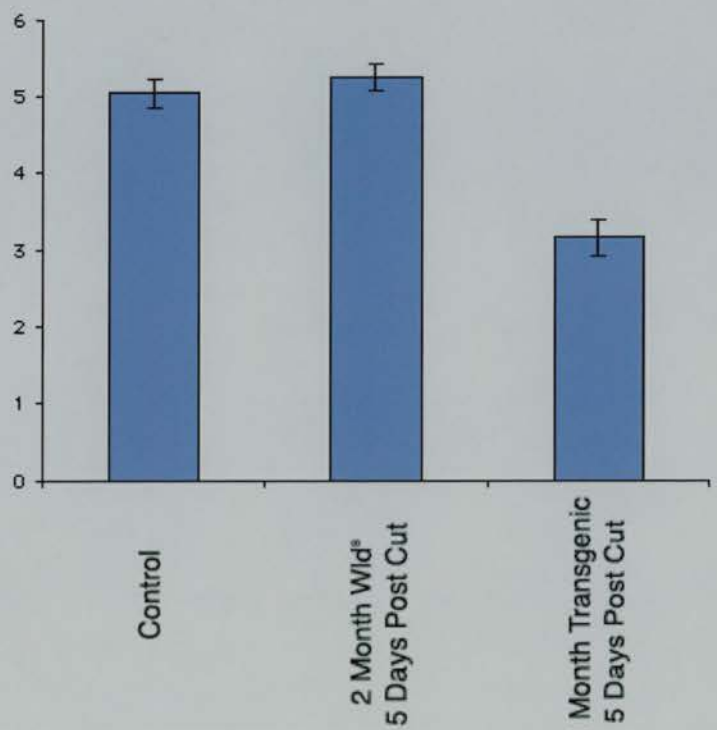
6
5
4
3
2
1
0
Control
2 Month Wld^s
5 Days Post Cut
1 Month Transgenic
5 Days Post Cut

## 5.4 Discussion

In this chapter, the role of the wallerin chimeric gene in producing the axotomy-induced phenotype observed in Wld$^s$ mice was assessed. Both immunocytochemical and electron microscopic studies on axotomised neuromuscular preparations from transgenic mice expressing the wallerin gene demonstrate that this chimeric gene confers a phenotype that strongly resembles the Wld$^s$ phenotype. Not only were motor nerve terminals preserved in these mice after axotomy, but examples of partially occupied endplates supplied by thin axon collaterals with occasional accumulations of NF were identified, very similar in appearance to those observed in young Wld$^s$ mice muscle preparations following axotomy. Furthermore, these findings strongly suggest that the unmasking of synapse-specific events, such as axotomy-induced synapse withdrawal, is not unique to the Wld$^s$ mouse. However, my EM data suggest that the response of motor nerve terminals in Wld$^s$ and wallerin transgenic mice were not quite the same. The possible reasons for the discrepancies are discussed, but they do not detract from the conclusion that transgenic expression of the chimeric wallerin gene profoundly inhibits both axonal and synaptic degeneration.

### 5.4.1 Comparison of Synaptic Events Following Axotomy at NMJs in Wallerin Transgenic and Wld$^s$ Mutant Mice

The preservation of motor nerve terminals for up to 5 days post axotomy in wallerin transgenic preparations showed that the axotomy-induced Wld$^s$ phenotype was present in these mice (Figure 5.2 and 5.3). A comparison with the levels of nerve terminal retention observed in young Wld$^s$ mice (Figure 3.10) at similar time points following axotomy suggested that transgenic mice motor nerve terminals were *more* protected against degeneration than Wld$^s$ nerve terminals (with levels of 97.53% occupancy versus 90.03% at 3 days post axotomy and 95.31% versus 74.05% at 5 days post axotomy). Whilst the numbers of transgenic preparations assessed (4 muscles in total) were lower than those from 2 month old Wld$^s$ mice (19 muscles in total) due to a limited availability of transgenic tissue, these findings suggested that the expression, or effectiveness, of the Wld$^s$ phenotype may be enhanced in the former. To be certain of such a conclusion however, it would be necessary to extend the current transgenic study in the parameters of both the numbers of muscle preparations assessed and the number of time points following axotomy (i.e. extend to 7 and 10 days post axotomy). These experiments will hopefully become feasible when the transgenic breeding colony in Cologne is more strongly established and/or a sub-colony is founded in Edinburgh. Another possibility is that the differences between nerve terminal preservation in wallerin transgenic mice and Wld$^s$ mutant mice following axotomy may occur as a

result of the genetic background on which the transgenic was bred (the transgenics were produced from a 75% C57Bl/6J and 25% CBA line rather than a pure C57Bl/6 line) to the Wld$^s$ phenotype. Strain-specific differences have previously been shown to contribute to alterations in the sensitivity of peripheral nerves to spontaneous age-related changes (including degeneration; Tabata et al., 2000). Thus, axons and motor nerve terminals from different mice strains might also differ in their sensitivity to degenerative signals.

Whilst the morphological characteristics associated with partial occupancy (areas of unoccupied postsynaptic receptors next to occupied regions with intact nerve terminal; see Chapter 3) were present in both wallerin transgenic and Wld$^s$ mice following axotomy, differences in the incidence of partial occupancy of endplates were observed (compare Figures 5.4, 5.5 and 5.6 with Figures 3.12, 3.13 and 3.14). The lower incidence of partial occupancy at 5 days post axotomy in transgenic mice compared to 2 month old Wld$^s$ mice (22.25% and 54.58% respectively) suggested that the onset of nerve terminal withdrawal was delayed in transgenic mice. This conclusion was supported by the findings that the overall preservation of nerve terminals was higher in transgenic mice compared to Wld$^s$ mice at the same time point following axotomy (see above). Additional evidence to support this hypothesis comes from the experimental data which showed that the levels of partial occupancy at wallerin transgenic mice endplates did not increase much above the basal levels, attributed to remodelling processes (see Chapter 3), seen in non-axotomised preparations, until 5 days post

axotomy. To test this hypothesis fully however, further experiments would need to be undertaken, extending the time points in the wallerin transgenic mice study to 7 and 10 days post axotomy, in order to assess whether or not the time course of nerve terminal loss progresses in a similar fashion to that observed in $Wld^s$ mice, albeit delayed in its onset. Unfortunately, this will not be possible until the transgenic mice become more readily available. Finally, my findings could also be explained by the 'synaptic maintenance factor' hypothesis proposed in Chapter 4. It is possible that differences in the expression or effectiveness of such a factor between various species of mice may account for the increased retention and delayed withdrawal of nerve terminals observed in the transgenic compared to $Wld^s$ mutant mice.

Taken together, the findings that nerve terminal preservation and partial occupancy of endplates occur in wallerin transgenic mice after axotomy provides further evidence to support the hypothesis that the withdrawal of motor nerve terminals occurs via a synapse specific form of degeneration, independently of axonal degeneration. The data also suggest that both nerve terminal retention and piecemeal withdrawal following axotomy are not features unique to axotomy in the $Wld^s$ mouse, but implies that they can be elicited in other strains of mouse when axonal degeneration is delayed. The further implications of these findings are considered in the final discussion.

Ultrastructural analysis of NMJs in wallerin transgenic mice showed that nerve terminal preservation following axotomy was conferred by the wallerin chimeric gene, thereby

confirming its ability to regulate expression the Wld$^s$ phenotype. Nerve terminal profiles from wallerin transgenic preparations, 5 days after axotomy (Figure 5.7 and 5.8), often appeared very similar to those from 2 month old Wld$^s$ preparation at the same time following axotomy (Figure 3.11, 3.18, 3.20 and 3.22), showing no signs of classical degeneration: with retention of terminal membranes, intact mitochondria and no invasion of terminal Schwann cell processes into the synaptic cleft. Quantification of NF levels showed a significant accumulation in wallerin transgenic mice nerve terminals at 5 days post axotomy compared to control preparations (Figure 5.9). Interestingly, the levels of NF accumulation were significantly less than observed in 2 month old Wld$^s$ nerve terminals at 5 days post axotomy. This could have occurred as a result of a reduced rate of slow axoplasmic flow in the severed transgenic mice distal nerve stumps. It would be interesting therefore, to measure the rate of transport of NFs within severed axons from wallerin transgenic mice, as well as to compare the spatio-temporal aspects of NF accumulation in the synaptic compartments of wallerin transgenic and Wld$^s$ mutant mice.

Qualitative and quantitative differences in the numbers of synaptic vesicles were also apparent between wallerin transgenic mice nerve terminal profiles, and similar profiles from control and 2 month old Wld$^s$ preparations. Thus, mean synaptic vesicle densities, mean packing densities and the mean number of 'docked' SVs were all significantly reduced in transgenic mice 5 days after axotomy (Figure 5.10 and 5.11). Interestingly, a few nerve terminal profiles had a density and distribution of SVs that was above the

mean value observed in control and 2 month $Wld^s$ preparations at 5 days post axotomy. This led to the conclusion that the reduction in SVs was not an artefact of tissue processing, and was supported by electrophysiological findings (from Mr D. Thomson and Dr R.R. Ribchester, personal communication). Whilst the morphological data showed a clear retention of motor nerve terminals in wallerin transgenic mice following axotomy, intracellular recordings detected a much lower level of functional nerve terminal preservation. This could be accounted for by the reduction in the overall numbers of, and numbers of 'docked', SVs in the majority of transgenic nerve terminals.

Whilst the reasons for the reduction in synaptic vesicle numbers remain unclear, it is possible that motor nerve terminals in the transgenic strain of mice have synaptic vesicle recycling machinery which is more susceptible to axotomy induced changes (reduction of synaptic vesicles occurs in wild-type preparations following axotomy; Miledi and Slater, 1970; Manolov, 1974; Winlow and Usherwood, 1975) than in $Wld^s$ mutant mice. It is possible that the mechanisms responsible for producing synaptic vesicle recycling, such as clathrin-mediated endocytosis (Maycox et al., 1992; De Camilli and Takei, 1996) and/or 'kiss and run' endocytosis (Klingauf et al., 1998), are impaired following axotomy. For example, alterations in the activity of proteins such as the clathrin adaptor AP180 and α-adaptin have previously been shown to alter the number of synaptic vesicles in *drosophila* synapses (Zhang et al., 1998; Gonzalez-Gaitan and Jackle, 1997). Thus, it is possible that such proteins may be more

vulnerable to a loss of function following axotomy in the transgenic than in the Wld$^s$ mice. Whatever the reasons for this decline in SV numbers however, these findings show that a reduction in the numbers of SVs, as in the case of degenerating mitochondria (see Chapter 4), does not inevitably lead to degeneration of the nerve terminal.

### 5.4.2 Possible Mechanisms Underlying the Wld$^s$ Phenotype

Whilst the current study has provided a qualitative and quantitative description of the synaptic events which occur at axotomised wallerin transgenic and Wld$^s$ mouse NMJs, little is still known as to the underlying mechanisms responsible for producing delayed axonal degeneration as a result of the Wld$^s$ phenotype. Previous studies of the Wld$^s$ mutant mouse phenotype have resulted in a proposed hypothesis that the cell body of a neurone may provide a maintenance factor which is transported to the extremities of the cell via axoplasmic transport and inhibits the initiation of Wallerian degeneration (Glass et al., 1993; Buckmaster et al., 1995). The Wld$^s$ mutation may cause either a stabilisation of such a factor, or may impair the axonal machinery responsible for its transport or breakdown, thereby prolonging the initiation of Wallerian degeneration following separation from the cell body.

The hypothesis that the $Wld^s$ phenotype may be due to the impairment or failure of axonal transport was examined by Glass and colleagues (Glass and Griffin, 1991; Watson, Glass and Griffin, 1993; Glass and Griffin, 1994), but refuted with the demonstration that bi-directional transport of neurofilaments continues at a normal rate for up to 14 days post axotomy. Tsao et al (1994) also found no abnormalities in neurofilament phosphorylation and stability. A number of studies have addressed the possibility that an altered regulation of $Ca^{2+}$ ions within the nerve causes the $Wld^s$ phenotype. For instance, both Glass et al (1994) and Buckmaster et al (1995) demonstrated that degeneration in $Wld^s$ axons, as in wild type axons, is calcium dependent. Their data also suggest that calcium dependent Wallerian degeneration associated proteases are present in $Wld^s$ axons, but that these may require higher levels of calcium for their activation than in normal axons. However, Tsao et al (1994) found that the levels of calcium-activated proteases in $Wld^s$ axons were normal and Glass et al (1998) found no evidence for a defect in the m-calpain 80kD subunit. The calpain system of neurofilament degradation therefore appears to be functioning normally, but the possibility that calpain activation by calcium is impaired in the $Wld^s$ mouse has not been ruled out.

Recent evidence in support of the hypothesis that calcium ions may play a pivotal role in the regulation of the $Wld^s$ phenotype was provided by experiments examining the role of NAD on intracellular $Ca^{2+}$ regulation. Both cyclic ADP-ribose (cADPR) and nicotinic acid adenine dinucleotide phosphate (NAADP), derivatives of NAD and

NADP respectively, initiate release of $Ca^{2+}$ from intracellular stores (Lee, 1999; Ziegler, 2000; Podesta et al., 2000). This has led to the suggestion that NAD derivatives are endogenous modulators of intracellular $Ca^{2+}$ (White et al., 2000) and may also have a role in the modulation of neurotransmitter release from pre-synaptic nerve terminals (Mothet et al., 1998). This hypothesis is noteworthy given the identification of Nmnat in the $Wld^s$ genotype (Conforti et al., 2000).

Intriguingly, a recent study by Benavides et al (2000) suggests that the elevation of intracellular $Ca^{2+}$ in $Wld^s$ hippocampal neurones following depolarisation is significantly less than in control preparations. They suggest that this is evidence for abnormal calcium ion entry into $Wld^s$ neurones. However, if the mutation produces abnormal calcium buffering, perhaps via its effects on NAD levels, this could perhaps explain their findings.

Finally, proteins targeted by ubiquitin (Laney and Hochstrasser, 1999) may play a critical role in the $Wld^s$ phenotype. It is possible that the fragment of Ube4b expressed in the chimeric $Wld^s$ protein may act to competitively inhibit the action of native Ube4b (a "dominant-negative" effect), or alternatively increase the overall levels of active ubiquitin within a neurone. Furthermore, alterations in the level of ubiquitin have been shown to change the growth and function of synapses; whereby antagonisation of the ubiquitination pathway produces synaptic outgrowth and dysfunction (DiAntonio et al.,2001). Thus, it will be interesting to discover therefore whether the mutation in the

Wld$^s$ mouse affects the degradation of all, some or none of the constituent proteins of the axon and motor nerve terminal. This could perhaps be examined by creating transgenic animals in which the Ube4b fragment or Nmnat are independently expressed.

### 5.4.3 Summary

The data presented in the current chapter strongly suggest that the wallerin chimeric gene is responsible for producing the Wld$^s$ phenotype. Furthermore, current findings demonstrate that a delay in axonal degeneration unmasks an independent mechanism of synapse specific degeneration, separate and distinct from axonal and somatic degeneration. Moreover, the data presented show that the synapse specific degeneration (withdrawal) process can be unmasked wherever and whenever axonal degeneration is delayed, and is not unique to the Wld$^s$ mouse. However, I concede that further experiments are required to make more assured conclusions with regard to the temporal characteristics of nerve terminal withdrawal at axotomised wallerin transgenic mice NMJs, and these should be undertaken as soon as more of the transgenic mice become available.

Taken together with data from previous chapters, the current findings strongly support the hypothesis that nerve terminals are lost by a compartmentalised mechanism of degeneration, separate from those which underlie the degeneration of axons and cell bodies. This hypothesis is addressed fully in the final discussion, and a compartmentalised model of neurodegeneration is proposed.

# General Discussion

# 6. General Discussion

Nerve section in wild-type rodents normally results in the rapid removal of distal axons and motor nerve terminals, via Wallerian degeneration. This thesis supports and builds upon previous studies which have shown that this process is delayed in the Wld$^s$ mutant mouse, whereby disconnected axons and motor nerve terminals are preserved for days or weeks, rather than hours (Lunn et al., 1989; Ribchester et al., 1995). Furthermore, previous studies have suggested that, whilst axons retain their structural and functional properties, motor nerve terminals appear to be lost from the endplate via a process of synapse withdrawal (Mattison et al., 1996; Ribchester et al., 1999; Mattison, 1999, PhD Thesis, University of Edinburgh). The current study supports these hypotheses by providing novel morphological data to demonstrate that axotomised nerve terminals in Wld$^s$ mice of 2 months and younger undergo a withdrawal from the endplate, as evidenced by the increased incidence of partially occupied NMJs. Moreover, this study unequivocally demonstrates that axotomised Wld$^s$ nerve terminals are capable of being removed from the endplate by more than one mechanism. The regulation of these mechanisms is dependent upon the age of the animal, but both processes appear to be distinct from that of classical Wallerian degeneration. Experiments utilising transgenic mice expressing the Ube4b/Nmnat ('wallerin') chimeric gene (the candidate Wld$^s$ gene; Conforti et al., 2000), as well as demonstrating that the wallerin gene confers the Wld$^s$ phenotype, showed that these synapse specific forms of degeneration are not unique to the Wld$^s$ mouse, and that they can be observed in NMJ preparations from other strains

of mouse where axonal degeneration is similarly delayed. Taken together, the results from the current study suggest that synapses have their own, compartmentalised mechanisms of degeneration following disconnection from their cell body, separate and distinct from that of axonal degeneration. Thus, this discussion attempts to place the current findings in the context of previous notions with regard to a physical and functional compartmentalisation of the neurone, and culminates in a proposed model of the neurone pertaining to neurodegeneration.

## 6.1 Compartmentalisation of Neurodegeneration – Morphology and Function

It is now widely accepted that a neurone is a highly polarised cell, containing many separate sub-cellular domains or compartments (the cell body and dendrites, the axon and the synaptic terminals), each dedicated to performing specific functions within the cell. From a purely morphological point of view, the cell body is clearly defined as it contains the nucleus and major cytoplasmic organelles such as the endoplasmic reticulum (Peters et al., 1991). In contrast, the dendritic tree emanating from the cell body is distinct from the latter due to the scarcity of major cytoplasmic organelles, replaced by a complex array of cytoskeletal proteins such as microtubules and neurofilaments (Zigmond et al., 1999). Similarly, the axon has a paucity of major organelles, instead containing very high levels of cytoskeletal proteins such as neurofilaments and microtubules, extending into the axon from bundles in the cell body

(Peters and Jones, 1984; Peters et al., 1991). Interestingly, in many instances the synaptic compartment of the neurone is not acknowledged as being separate from the somatic and axonal domains (for example, see Zigmond et al., 1999), even though it is morphologically distinctive. The large numbers of synaptic vesicles, nerve terminal mitochondria and specialised combinations of membranous and cytoskeletal networks (for example the 'active zone material' localised to active zones on the presynaptic membrane, Palay, 1956; Harlow et al., 2001) not found extra-synaptically, alongside a reduction in the levels of regular axonal cytoskeletal proteins (Palade and Palay, 1954; Yee et al., 1988), strongly suggest that synaptic terminals should be considered as a distinct morphological unit, separate from the axon and cell body.

The distinctive functional properties of synaptic terminals provide further, compelling evidence that they should be regarded as a distinct domain with respect to a compartmentalisation of the neurone. The ability to release neurotransmitter in both an activity dependent and independent fashion is a property largely exclusive to the nerve terminal. Thus, the molecular machinery for producing the synaptic vesicle cycle is uniquely concentrated within the nerve terminal (Betz and Angleson, 1998): whereby proteins such as synaptophysin and synaptobrevins (Elferink and Scheller, 1993), Synapsins I and II (Sudhof and Jahn, 1991) and the Vesicular Ach transporter (Erickson et al., 1994) are all present. Similarly, the distribution of ion channels within nerve terminals is unique, to provide the necessary regulation required for sensitive yet controlled synaptic vesicle release; P-type calcium channels, voltage-gated potassium

and voltage-gated calcium channels are all heavily localised within nerve terminal membranes (Uchitel et al., 1992; Robitaille et al., 1993; Day et al., 1997).

Similar compartmentalisation of function can be found in the axonal domain, specialised to propagate action potentials along its length, allowing the transmission of electrical impulses over long distances. Once again, the precise distribution of ion channels within the membrane of the compartment confers these specialised properties (Hille, 1992), but interactions with other cell types such as Schwann cells also play a key role in axonal function. For example, in myelinated neurones sodium channels are tightly clustered around the nodes of Ranvier (interspersed ~200$\mu$m-2mm throughout the length of the axon; Nicholls et al, 1992) whilst potassium channels are sequestered in the paranodal region (England et al., 1996; Rasband et al., 1998), an arrangement brought about due to the pattern of myelination by Schwann cells (England et al., 1996). This arrangement of insulating myelin and highly specific distribution of ion channels leads to a large increase in the conduction velocity of the axon (via the process of 'saltatory conduction'; Huxley and Stampfli, 1949; Bostock and Sears, 1978), thereby enhancing its function. The cell body too, is clearly compartmentalised with regard to function. Whereas the axon and synaptic terminals are specialised for the conduction and transmission of nerve impulses, the cell body is adapted for protein synthesis. The nuclei of most neuronal cells are large compared to other cell types, consistent with their function of creating and maintaining a large cellular volume (Peters et al., 1991). Furthermore, the molecular machinery for protein synthesis and distribution is highly

concentrated in neuronal cell bodies (Nissl substance, Sanford et al., 1955), facilitating transcription of the many different genes required for neuronal function and subsequent high levels of protein production.

## 6.2 Compartmentalisation of Neurodegeneration – Pathophysiology

Whereas the structural and functional compartments of the neurone are relatively well defined and are readily exposed via experimental investigation, there has been little debate of a possible compartmentalisation of the neurone with regard to pathophysiology. Thus, it is only in the last few years that evidence has been provided to suggest that the mechanisms of axonal (Wallerian) degeneration are separate and distinct from those which underlie somatic degeneration.

There are numerous cellular and molecular degenerative mechanisms by which cells, including neurones, can be destroyed. The two best understood processes are 'classical' necrosis and 'classical' apoptosis. Necrosis is a term used to describe the major form of pathological degeneration, usually occurring following injury (Ankarcrona et al., 1995; Martin, 2001). Whilst necrosis of cells involves a gross destruction of the cellular ultrastructure, resulting in an inflammatory response (Zigmond et al., 1999), apoptosis (a form of programmed cell death common during CNS development, Oppenheim, 2001) occurs by a more discreet pathway, whereby degenerating cells are packaged into membrane bound apoptotic bodies (Kerr et al., 1972). The phagocytosis of cells

undergoing apoptosis by in situ macrophages or adjacent cells acting as temporary macrophages (such as glial cells) results in the removal of the degenerating cell without an inflammatory response (Zigmond et al., 1999). At an ultrastructural level, the process of apoptosis occurs with a retention of sub-cellular organelles (although mitochondrial alterations such as membrane depolarisation, oxyradical accumulation and calcium overload occur, Mattson et al., 1998a) and a shrinkage of the cell, whilst necrotic cell death involves a swelling of the cell, rupture of cell membranes and disruption of organelles (Roy and Sapolsky, 1999; Zigmond et al., 1999; Martin, 2001). Historically the two processes of necrosis and apoptosis have been deemed to be distinct (Kerr et al., 1972; Kerr et al., 1995). Recent evidence suggests that the two may be the extremes of an apoptosis-necrosis cell death continuum however, whereby mitochondrial function and calcium-dependent enzymes alongside growth factor expression and gene expression (e.g. Bcl-2 and Bax) are critical factors in regulating the pathway of degeneration (Martin, 2001; Ankarcrona et al., 1995; Choi, 1996; Bennett and Huxlin, 1996; Roy and Sapolsky, 1999; Yuan and Yanker, 2000). Analysis of neuronal cell body degeneration reveals many of these markers of 'classical' apoptosis. For example, in the majority of instances somatic degeneration is accompanied by DNA degradation (Kerr et al., 1972; Kerr et al., 1995), is inhibited by neuronal growth factors and by over-expression of genes such as Bcl-2 (Dubois-Dauphon et al., 1994; Deckwerth and Johnson, 1994; Sagot et al., 1995; Burne et al., 1996), and is dependent on the presence of caspases (particularly caspase-3, Janicke et al., 1998; Woo et al., 1998; Keramaris et al., 2000). It has been shown that apoptosis is not the only

mechanism of cell death present in cell bodies however. Oppenheim et al. (2001) have shown that when apoptosis is prevented during development by the genetic deletion of caspases, normal levels of cell death occur, but via a non-apoptotic pathway of degeneration (see below).

Evidence for the existence of different degenerative mechanisms in separate domains of the neurone becomes apparent when comparing the process of apoptotic somatic degeneration with that of axonal Wallerian degeneration. The theory that apoptosis and necrosis form the extremes of a cell death continuum (Martin, 2001) appears to be supported by such a comparison, whereby Wallerian degeneration occurs by mechanisms which display markers of both necrosis and apoptosis. For example, the production of ovoid bodies during Wallerian degeneration of the axon (see Chapter 1) appear very similar to apoptotic bodies formed during apoptosis. Furthermore, both apoptosis and Wallerian degeneration are calcium dependent phenomena, reliant on the action of calpains and calcium-dependent proteases (Schlaepfer and Hasler, 1979b; Croall and DeMartino, 1991; Glass et al., 1994; Squier et al., 1994; Chan and Mattson, 1999). Wallerian degeneration can not include all aspects of apoptosis (e.g. DNA degradation, Kerr et al., 1972; Kerr et al., 1995) because axotomised distal stumps do not include motoneurone cell bodies. This does not rule out the possibility that apoptotic-like processes are occurring however, as it has previously been shown that apoptosis can occur in the absence of RNA or protein synthesis (Martin, 1993) and in cells lacking nuclei (Ellerby et al., 1997; Jacobson et al., 1994). Thus, the suggestion

by a number of authors that axonal degeneration might be viewed as a form of 'cytoplastic apoptosis' (Ribchester et al., 1995; Buckmaster et al., 1995; Alvarez et al., 2000), appears plausible. The possibility that Wallerian degeneration occurs *primarily* by apoptotic-like mechanisms is not as plausible however. The swelling and lysis of sub-cellular organelles such as mitochondria and cytoskeletal proteins (Vial, 1958; Honjin et al., 1959; Ballin and Thomas, 1969; Donat and Wisniewski, 1973; Schlaepfer and Hasler, 1979a), alongside the invasion of foreign macrophages in an inflammatory response (Lunn et al., 1989; Perry et al., 1990c), suggest that necrotic pathways are also a major mechanistic presence during Wallerian degeneration.

Molecular studies of axon degeneration have also demonstrated that non-apoptotic pathways are responsible, at least in part, for producing Wallerian pathways. For example; firstly, over-expression of the anti-apoptotic gene Bcl-2 has been shown to protect cell bodies, but not axons, from degeneration in models of injury and motor neurone disease (Burne et al., 1996; Sagot et al., 1995); and secondly, application of the apoptotic insult amyloid β-peptide has been shown to activate caspases in cell bodies, but not in axons (Mattson et al., 1998b; but see Ivins et al., 1998). Similarly Finn et al. (2000) demonstrated that caspase-3 is not activated during Wallerian degeneration, prompting the authors to suggest that a neurone contains more than one mechanism for self-destruction. However, the initial evidence for an independent mechanism of degeneration in axons was provided in an elegant study by Deckwerth and Johnson (1994). In their study of sympathetic neurones from the superior cervical

ganglion of Wld$^s$ mice in culture, these authors demonstrated that when NGF was removed from the culture solution, axons survived whilst cell bodies underwent apoptosis, thereby showing that Wallerian degeneration can occur independently of growth factor regulation. Wallerian degeneration has also been shown to utilise molecular mechanisms distinct from those present during apoptosis, for example; Tumour Necrosis Factor-alpha (TNF-α) has been shown to play a major role in the recruitment of foreign macrophages (Liefner et al., 2000) during Wallerian degeneration. Finally, the demonstration that the wallerin chimeric gene is sufficient and necessary to produce the Wld$^S$ phenotype (current study; Conforti et al., 2000; Mack et al., 2001), demonstrates that Wallerian degeneration is under the control of genetic influences, separate from those which control somatic apoptosis.

The demonstration by current experiments, supported by data from previous studies (Mattison et al., 1996; Ribchester et al., 1999; Mattison, 1999, PhD Thesis, University of Edinburgh), that axotomised nerve terminals are removed from the endplate by more than one mechanism, *both* distinct from the process of axonal Wallerian degeneration, suggests that synaptic terminals also have separate compartmentalised mechanisms of neurodegeneration. The retraction of nerve terminal boutons in young Wld$^s$ preparations bears many hallmarks of classical apoptosis; firstly, sub-cellular organelles such as mitochondria and synaptic vesicles are preserved throughout the process; secondly, there is a general preservation of nerve terminal architecture and terminal membranes; and thirdly, there is no leakage of degenerating cytological

elements from the nerve terminal into the extra-cellular space, and hence no inflammatory response. It would therefore be of interest to ascertain whether other markers of apoptosis are present during this process. For example, it would be possible, using serial EM reconstruction techniques, to undertake measurements of nerve terminal volume during the retraction process, to examine if there is any shrinkage or swelling of the compartment. However, the withdrawal of nerve terminals does not, and can not, involve all the mechanisms which underlie classical apoptosis because of the lack of a nucleus. As a result I tentatively suggest the term 'synaptosis' to describe this series of events.

Similar 'synaptotic' processes can be observed throughout the nervous system under varying conditions, thereby suggesting that 'synaptosis' is not simply a secondary process only associated with delayed axonal degeneration. For example, blocking fast axonal transport with batrachotoxin, causes nerve terminals to retract from endplates within 18 hours; but they then grow back (Hudson et al., 1984). Nerve terminals also retract in a reversible, "non-Wallerian" fashion following a single subcutaneous injection of the organophosphate sarin (Kawabuchi et al., 1991). Furthermore, Rich and Lichtman (1989) observed comparable, reversible nerve terminal withdrawal from degenerating muscle fibres and nerve terminals have also been shown to retract in piecemeal fashion in a mouse model of myasthenia gravis, suggesting a role for the postsynaptic cell in the withdrawal process (Rich et al., 1994).

The best understood example of the retraction of nerve terminals occurs during the process of synapse elimination however, an essential step in the formation or reformation of normal neuromuscular innervation patterns that takes place in postnatal development or following reinnervation (see Chapter 1). Thus, nerve terminals undergoing withdrawal during synapse elimination are removed from the endplate bouton-by-bouton, ending with the formation of a characteristic 'retraction bulb' (Brown et al., 1976; Riley, 1977; Riley, 1981; Balice-Gordon et al., 1993; Gan and Lichtman, 1998). A direct comparison of immunocytochemical data from the current and previous studies utilising the $Wld^s$ mouse (Mattison et al., 1996; Parson et al., 1998; Ribchester et al., 1999) with similar immunocytochemical data from neonatal mice NMJs undergoing synapse elimination (Balice-Gordon et al., 1993; Balice-Gordon and Lichtman, 1993; Gan and Lichtman, 1998; Sanes and Lichtman, 1999) suggested that these two events have very similar morphological and temporal characteristics. Moreover, when the ultrastructural characteristics of nerve terminal withdrawal during synapse elimination and following axotomy in young $Wld^s$ mutant and wallerin transgenic mice are compared, many similarities prevail. Both processes occur with no apparent degeneration of nerve terminals, whereby the incidence of markers such as mitochondrial disruption and lysis, terminal membrane fragmentation and terminal Schwann cell phagocytosis are rare (current study; Korneliussen and Jansen, 1976; Riley, 1977; Riley, 1981; Bixby, 1981). This suggests that the withdrawal of nerve terminals during synapse elimination may also be occurring via a process of 'synaptosis'. Moreover, it would be of great interest to study the

ultrastructural characteristics of synapse withdrawal phenomena in preparations such as those described above (following the blockade of fast axonal transport, Hudson et al., 1984; following the application of sarin, Kawabuchi et al., 1991; following the degeneration of the postsynaptic cell, Rich and Lichtman, 1989; and in a mouse model of myasthenia gravis, Rich et al., 1994) to assess if degenerative characteristics are similarly absent.

The findings from the current study, that axotomised nerve terminals from older $Wld^s$ mouse preparations are removed by a process more akin to classical Wallerian degeneration than 'synaptosis', yet still distinct from axonal degeneration, confirms that the synaptic compartment contains more than one mechanism of degeneration. Nerve terminal loss in the older $Wld^s$ mice displays many more signs of necrosis than apoptosis. For example; sub-cellular organelles such as mitochondria undergo swelling and lysis, synaptic vesicle densities are reduced and terminal membranes become fragmented. It has previously been shown that degenerating nerve terminals in wild-type preparations are phagocytosed by the terminal Schwann cell (Miledi and Slater, 1970; Manolov, 1974; Winlow and Usherwood, 1975), and a similar process appears to be occurring in preparations from old $Wld^s$ mice. It would be of interest to establish whether or not foreign macrophages are involved in this synaptic degeneration process, as they are during axonal degeneration (Lunn et al., 1989; Perry et al., 1990c), or whether the phagocytotic process occurs by adjacent cells and without an inflammatory response, more characteristic of apoptosis.

The occurrence of nerve terminal 'synaptosis' at young Wld$^s$ mice NMJs, and Wallerian-like degeneration at old Wld$^s$ mice NMJs following axotomy are not isolated examples of one degenerative process being unmasked by the disruption of another. Thus, after genetic deletion of caspase-3 and caspase-9 in developing mouse postmitotic neurones, normal neuronal cell loss occurs, but by a mechanism separate and distinct from the classical apoptotic pathways observed in wild-type preparations (Oppenheim et al., 2001). This suggests that all neuronal compartments may have more than one mechanism of degeneration capable of bringing about removal of that segment of the neurone, although a secondary mechanism of degeneration has yet to be described in axons. It should be noted however that the current study provides novel evidence for independent mechanisms of synaptic degeneration in the *peripheral* nervous system but offers no insights concerning such events in the *central* nervous system. Thus, whilst axon preservation has been demonstrated in the CNS of Wld$^s$ mice (Perry et al., 1990a; Ludwin and Bisby, 1992), it has not been established whether or not synaptic connections are also preserved following nerve lesion. It would therefore be of great interest to establish whether or not synaptic terminals in the CNS of young Wld$^s$ mice are not only retained, but are also retracted from postsynaptic cells following axotomy. And furthermore, to assess whether age has a similar effect on the regulation of which mechanism(s) is/are to be responsible for synaptic terminal degeneration. It is possible to speculate that synaptic withdrawal processes may occur following nerve lesion in the CNS of young Wld$^s$ mice, as synaptic withdrawal mechanisms have previously been

shown to occur at young CNS synapses. For example, during developmental reorganisation (synapse elimination) in mammalian autonomic ganglia, the withdrawal of supernumerary inputs have been demonstrated using both morphological and electrophysiological techniques (Johnson and Purves, 1981; Lichtman, 1977; Lichtman and Purves, 1980).

Taken together, the findings discussed above suggest that, alongside morphological and functional characteristics, the neurone is compartmentalised with regard to neurodegeneration. This hypothesis is demonstrated in the model of neurodegeneration shown in Figure 6.1, which proposes that the cell body, axon and synaptic terminal domains of the neurone each have at least one independent mechanism of degeneration, regulated by the action of different genes. Whilst these mechanisms are illustrated as being independent in the proposed model, the notion that apoptosis and necrosis are extremes on a cell death continuum (Martin, 2001) suggests that all the proposed pathways of neurodegeneration may also be part of the same continuum. Furthermore, the demonstration that multiple methods of degeneration are present in some neuronal compartments, and that the detection of their presence depends upon the level of masking by another mechanism, suggests that it is the *expression* of each mechanism which is regulated independently in different domains of the neurone rather than different mechanistic machinery being present per se.

**Fig. 6.1 Model of the Compartmental Organisation of Degeneration Mechanisms in the Neurone.**

(A) Genes regulating cell body degeneration by apoptosis (blue) and axon degeneration (magenta) are given in parentheses. The genes controlling synaptic degeneration (yellow) have not yet been defined. Figure previously published in Gillingwater and Ribchester (2001).

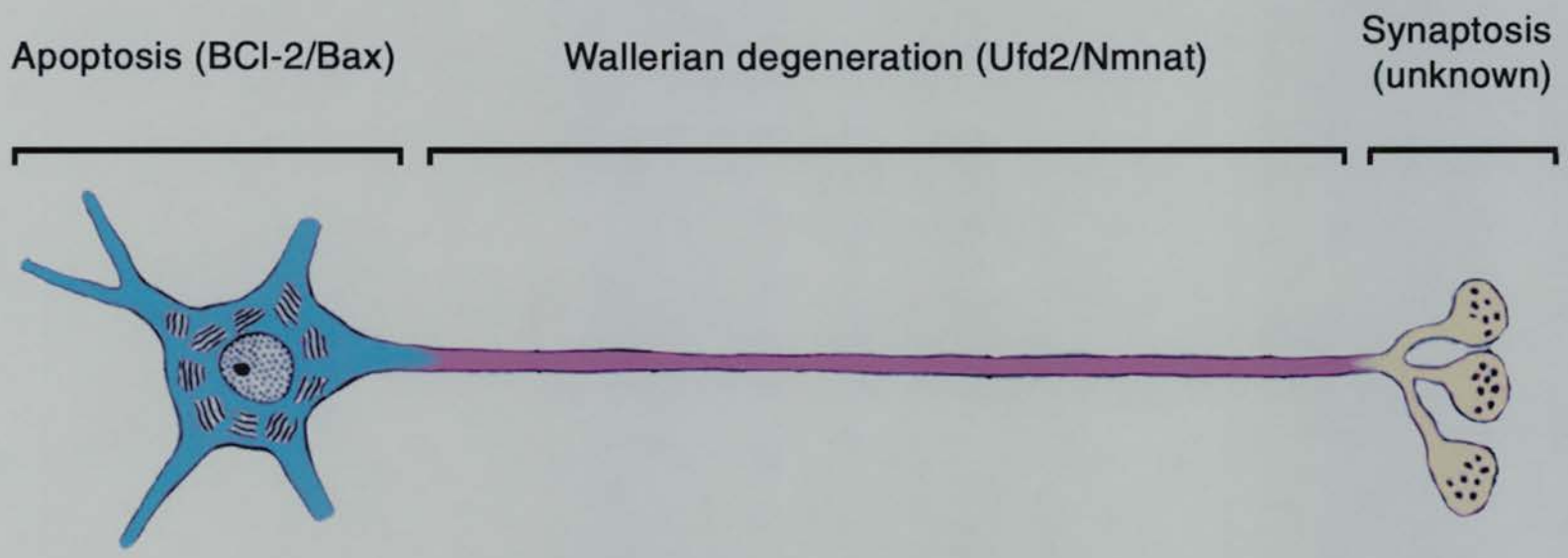
Apoptosis (BCl-2/Bax)
Wallerian degeneration (Ufd2/Nmnat)
Synaptosis
(unknown)

## 6.3 Compartmentalisation of Neurodegeneration – Molecular Mechanisms

The molecular mechanisms which regulate synapse specific degeneration, in any of the circumstances described above, remain unknown. However, recent molecular studies have provided evidence to support the hypothesis that synaptic degeneration can be regulated independently of axonal and somatic degeneration. Experiments utilising CNS neurones have shown that activation of apoptotic pathways by exposure to amyloid β-peptide does not produce caspase activation in axons, but does produce caspase activation in cortical synaptosomes (Mattson et al., 1998b). Similar evidence for 'synaptic apoptosis' was provided by experiments which showed that apoptotic biochemical cascades are selectively triggered at synaptic sites (Mattson et al., 1998a, b; Mattson, 2000; Guo and Mattson, 2000). For example, exposure of cortical synaptosomes to levels of the apoptotic stimuli $Fe^{2+}$ and staurosporine which induce apoptosis in primary cultured hippocampal and cortical neurones resulted in mitochondrial alterations (membrane depolarisation, oxyradical accumulation and calcium overload), a loss of membrane phospholipid asymmetry and caspase activation (Mattson et al., 1998a). Further evidence that the synaptosomes were undergoing apoptotic-like degeneration was produced by demonstrating that these apoptotic processes could be prevented by the administration of the caspase inhibitor zVAD-fmk (Mattson et al., 1998a).

Following the demonstration that synapses contain their own molecular machinery to instigate compartmental degenerative processes, it is possible to speculate that such apoptotic-like molecular mechanisms are also activated during 'synaptosis'. It should be possible to address this question by repeating the $Wld^s$ axotomy experiments detailed in the present study, but this time in conjunction with the sub-cutaneous administration of apoptosis-blocking agents such as zVAD-fmk. If these experiments reveal any effect on the morphological or temporal aspects of nerve terminal retraction in axotomised young $Wld^s$ preparations, it would provide strong evidence that 'synaptosis' occurs by mechanisms similar to classical apoptosis. Furthermore, it would be interesting to examine possible differences in the molecular machinery active in synaptic compartments of young and old $Wld^s$ neurones following axotomy, to assess to what extent apoptotic and necrotic processes are being expressed, independently or in conjunction with one another. Moreover, it is plausible to suggest that the intermediate characteristics of axotomised nerve terminals in $Wld^s$ mice of ~4 months of age, whereby markers of both apoptotic and necrotic cell death are apparent, is evidence for a transition on the apoptosis-necrosis cell death continuum. A molecular investigation of the degenerative processes occurring in $Wld^s$ mice of a transitional age may therefore shed light on the mechanisms which regulate the expression of apoptotic versus necrotic cell death.

The discovery of the molecular genetics underlying the $Wld^s$ phenotype, advanced by data from the current study, provide some indicators as to possible underlying molecular

mechanisms. It was originally thought that the identification of Nmnat in the $Wld^s$ genotype (Conforti et al., 2000) would provide insights into the molecular mechanisms which underlie the axotomy-induced phenotype. Nmnat has been identified as the enzyme responsible for the synthesis of NAD within neurones (Emanuelli et al., 2001), and evidence that NAD can regulate intracellular calcium levels via the release of intracellular calcium stores has recently been provided (Lee, 1999; Ziegler, 2000; Podesta et al., 2000). It was therefore suggested that expression of the wallerin chimeric gene may up-regulate the production of NAD, which would in turn act as a maintenance factor, possibly even the 'synaptic maintenance factor' discussed previously. This hypothesis has been somewhat refuted however by recent experiments from Dr M.P. Coleman's laboratory which have shown that NAD levels are normal in $Wld^s$ neurones (personal communication).

The identification of an N-terminal fragment of Ubiquitination factor E4B (Ube4b) in the $Wld^s$ genotype (Conforti et al., 2000) suggests that the ubiquitin system may be altered in these mice. The ubiquitin system of intracellular proteolysis is crucial for the control of protein activity, localisation and selection for degradation, thereby regulating processes such as apoptosis (Hochstrasser, 1996; Hershko and Ciechanover, 1998; Laney and Hochstrasser, 1999). It has been demonstrated that the yeast homologue of Ube4b, whilst not being essential for cell viability (Johnson et al., 1995), is a conjugation factor involved in the multi-ubiquitination of proteins, whereby in the absence of Ubiquitination factor E4, ubiquitination is initiated but does not proceed to

proteosomal degradation in vivo (Koegl et al., 1999). Furthermore, E4 Ubiquitination factors have been linked to cell survival under stress conditions (Koegl et al., 1999). As the $Wld^s$ protein only contains 70 of the 1173 amino acids of Ube4b, it is unlikely that this confers full multi-ubiquitination or cell survival properties on the $Wld^s$ protein, but it may have a related role which could feasibly alter the function of the ubiquitin system (Mack et al., 2001).

Altered function of the ubiquitin system of intracellular proteolysis has previously been implicated in the pathogenesis of diseases such as Alzheimer's and Parkinson's. For example, it has been shown that impairment in substrate recognition or the supply of free ubiquitin leads to accumulation of unwanted proteins in neurones (for review see Layfield et al., 2001). Alterations in the selection of axonal proteins for degradation could therefore lead to the preservation of specific cytoskeletal proteins such as NF in the distal nerve stump following lesion in $Wld^s$ mice. Moreover, ubiquitin-dependent mechanisms have been shown to regulate *synaptic* growth and function at the Drosophila NMJ. For example, expression of the yeast de-ubiquitinating protease UBP2, producing antagonisation of the ubiquitination pathway in neurones, leads to an elaboration of the synaptic branching pattern (including a significant increase in the numbers of synaptic boutons) and a severe reduction in presynaptic transmitter release (DiAntonio et al., 2001). The authors of this study concluded that "a balance between positive and negative regulators of ubiquitination controls the structure and function of a synapse". These findings suggest that the control of synapse specific morphology and

degeneration, including the withdrawal of motor nerve terminals at axotomised young $Wld^s$ and wallerin transgenic mice NMJs, may be regulated, in part, by the ubiquitin system.

The findings that age has an effect on the expression of the $Wld^s$ phenotype at axotomised nerve terminals suggests that whatever the underlying molecular machinery is, it is altered with age. The hypothesis that a, as yet unidentified, 'synaptic maintenance factor' may be responsible for controlling the preservation and degeneration of nerve terminals appears feasible however, and as a result it will be interesting to discover whether certain proteins in the neurone are differently regulated with increasing age. Whilst the expression of the $Wld^s$ protein does not decline with age, it is possible that such a maintenance factor has an altered susceptibility to ubiquitination or other cell regulation mechanisms in older animals. However, it is also important that the actions of retrograde factors on neuronal structure and function are not overlooked. For example, a recent study by Snider and colleagues showed that sustained postnatal subcutaneous administration of the retrograde factor glial cell line derived neurotrophic factor (GDNF) is capable of producing a "state of continuous synaptic remodelling" (Keller-Peck et al., 2001). These findings suggest that GDNF is capable of regulating both the sprouting and withdrawal of nerve terminal boutons in vivo, and therefore may exert some effects on the fate of axotomised $Wld^s$ motor nerve terminals. However, evidence that the expression of GDNF and its receptors in the peripheral nervous system do not decline with age (Golden et al., 1999), and in some

cases *increase* with age (Ming et al., 1999), suggests that whilst GDNF may exert some influence over the retention and plasticity of synaptic terminals, it does not fulfil the criteria for an age-dependent regulatory mechanism as is present in the $Wld^s$ mouse.

## 6.4 Conclusion

The current study provides evidence that mechanisms of degeneration within neurones are highly compartmentalised (Figure 6.1), whereby cell bodies (apoptosis), axons (Wallerian degeneration) and synaptic terminals (synaptosis) all have their own, independently regulated degenerative pathways. These findings offer a re-assessment of the current accepted model of neurodegeneration. The implications for understanding neurodegenerative diseases such as Parkinson's and Alzheimer's could be significant. For example, synapse-specific forms of degeneration could play an important, hitherto unappreciated role in these distressing and debilitating conditions.

# Bibliography

Abercrombie, M. & Johnson, M.L. (1946) Quantitative histology of Wallerian degeneration. I. Nuclear population in rabbit sciatic nerve. *Journal of Anatomy* **80:** 37-50

Albright, T.D., Jessell, T.M., Kandel, E.R. & Posner, M.I. (2000) Neural science: A century of progress and the mysteries that remain. *Cell* **100:** S1-S55

Allt, G. (1976) Pathology of the peripheral nerve. In *The Peripheral Nerve,* ed. Landon, D.N. Chapman & Hall, London. 666-739

Alvarez, J., Giuditta, A. & Koenig, E. (2000) Protein synthesis in axons and terminals: Significance for maintenance, plasticity and regulation of phenotype with a critique of slow transport theory. *Progress in Neurobiology* **62:** 1-62

Alvarez de Toledo, G., Fernandez-Chacon, R. & Fernandez, J.M. (1993) Release of secretory products during transient vesicle fusion. *Nature* **363**: 554-558

Ankarcrona, M., Dypbukt, J.M., Bonfoco, E., Zhivotovsky, B., Orrenius, S., Lipton, S.A. & Nicotera, P. (1995) Glutamate-induced neuronal death: a succession of necrosis or apoptosis depending on mitochiondrial function. *Neuron* **15:** 961-973

Apel, E.D., Lewis, R.M., Grady, R.M. & Sanes, J.R. (2000) Syne-1, a dystrophin- and klarsicht-related protein associated with synaptic nuclei at the neuromuscular junction. *Journal of Biological Chemistry* **275:** 31986-31995

Araque, A., Li, N., Doyle, R.T. & Haydon, P.G. (2000) SNARE protein-dependent glutamate release from astrocytes. *Journal of Neuroscience* **20:** 666-673

Arce, V., Pollock, R.A., Philippe, J.M., Pennica, D., Henderson, C.E. & De Apeyrie're, O. (1998) Synergistic effects of Schwann- and muscle-derived factors on motoneuron survival include GDNF and cardiotrophin-1 (CT-1). *Journal of Neuroscience*
**18:** 1440-1448

Bagust, J., Lewis, D.M. & Westerman, R.A. (1973) Polyneuronal innervation of kitten skeletal muscles. *Journal of Physiology* **229:** 241-255

Balice-Gordon, R.J., Chua, C.K., Nelson, C.C. & Lichtman, J.W. (1993) Gradual loss of synaptic cartels precedes axon withdrawal at developing neuromuscular junctions. *Neuron* **11:** 801-815

Balice-Gordon, R.J. & Lichtman, J.W. (1993) In vivo observations of pre- and postsynaptic changes during the transition from multiple to single innervation at developing neuromuscular junctions. *Journal of Neuroscience* **13:** 834-855

Balice-Gordon, R.J. & Lichtman, J.W. (1994) Long-term synapse loss induced by focal blockade of postsynaptic receptors. *Nature* **372:** 519-524

Ballin, R.H.M. & Thomas, P.K. (1969) Changes at the nodes of Ranvier during Wallerian degeneration: an electron microscope study. *Acta Neuropathologica (Berlin)* **14:** 237-249

Barry, J.A., Mattison, R.J., Nelson, C., Lichtman, J.W. & Ribchester, R.R. (1997) Schwann cell sprouting in a mutant mouse with slowed Wallerian degeneration. *Society for Neuroscience Abstracts* **23**: P244.10

Barry, J.A. & Ribchester, R.R. (1995) Persistent polyneuronal innervation in partially denervated rat muscle after reinnervation and recovery from prolonged nerve conduction block. *Journal of Neuroscience* **15:** 6327-6339

Benavides, E., Miranda, M. & Alvarez, J. (2000) Cytosolic calcium pulses in $Wld^s$ mouse neurones. *Journal of Physiology* **523:** 28P

Bennett, M.K. & Pettigrew, A.G. (1974) The formation of synapses in striated muscle during development. *Journal of Physiology* **241:** 515-545

Bennett, M.R. & Huxlin, K.R. (1996) Neuronal cell death in the mammalian nervous system: the calmortin hypothesis. *General Pharmacology* **27:** 407-419

Bennett, M.V.L. (2000) Seeing is relieving: electrical synapses between visualised neurons. *Nature Neuroscience* **3:** 7-9

Betz, W.J. & Angleson, J.K. (1998) The synaptic vesicle cycle. *Annual Review of Physiology* **60**: 347-363

Betz, W.J. & Bewick, G.S. (1992) Optical analysis of synaptic vesicle recycling at the frog neuromuscular junction. *Science* **255**: 200-203

Betz, W.J., Caldwell, J.H. & Ribchester, R.R. (1979) The size of motor units during post-natal development of rat lumbrical muscle. *Journal of Physiology* **297:** 463-478

Betz, W.J., Caldwell, J.H. & Ribchester, R.R. (1980) The effects of partial denervation at birth on the development of muscle fibres and motor units in rat lumbrical muscle. *Journal of Physiology* **303:** 265-279

Betz, W.J., Mao, F. & Bewick, G.S. (1992) Activity-dependent fluorescent staining and destaining of living vertebrate motor nerve terminals. *Journal of Neuroscience* **12:** 363-375

Beuche, W. & Friede, R.L. (1984) The role of non-resident cells in Wallerian degeneration. *Journal of Neurocytology* **13:** 767-796

Bezzi, P., Carmignoto, G., Pasti, L., Vesce, S., Rossi, D., Rizzini, B.L., Pozzan, T. & Volterra, A. (1998) Prostoglandins stimulate calcium-dependent glutamate release in astrocytes. *Nature* **391:** 281-285

Birks, R., Huxley, H.E. & Katz, B. (1960) The fine structure of the neuromuscular junction. *Journal of Physiology* **150:** 134-144

Birks, R., Katz, B. & Miledi, R. (1959) Electron microscopic observations on degenerating nerve-muscle junctions of the frog. *Journal of Physiology* **146:** 45-46P

Birks, R., Katz, B. & Miledi, R. (1960) Physiological and structural changes at the amphibian myoneural junction, in the course of nerve degeneration. *Journal of Physiology* **150:** 145-168

Bisby, M.A. & Chen, S. (1990) Delayed Wallerian degeneration in sciatic nerves of C57Bl/Ola mice is associated with impaired regeneration of sensory axons. *Brain Research* **530:** 117-120

Bittner, G.D. (1988) Long-term survival of severed distal axonal stumps in vertebrates and invertebrates. *American Zoologist* **28:** 1165-1179

Bixby, J.L. (1981) Ultrastructural observations on synapse elimination in neonatal rabbit skeletal muscle. *Journal of Neurocytology* **10:** 81-100

Boeke, J. (1921) The innervation of striped muscle fibres and Langley's receptive substance. *Brain* **44:** 1-22

Bostock, H. & Sears, T.A. (1978) The internodal axon membrane: Electrical excitability and continous conduction in segmental demyelination. *Journal of Physiology* **280:** 273-301

Bowe, M.A. & Fallon, J.R. (1995) The role of agrin in synapse formation. *Annual Review of Neuroscience* **18:** 443-462

Boyd, I.A. & Davey, M.R. (1968) Composition of peripheral nerves. E & S Livingstone Ltd. Edinburgh and London.

Brecknell, J.E. & Fawcett, J.W. (1996) Axonal regeneration. *Biological Reviews of the Cambridge Philosophical Society* **71:** 227-255

Brosamle, C. & Kuffler, D.P. (1996) Rapid dispersal of clustered postsynaptic nuclei following dissociation of skeletal muscle fibers. *Journal of Experimental Biology* **199:** 2359-2367

Brown, M.C., Jansen, J.K.S. & Van Essen, D.C. (1976) Polyneuronal innervation of skeletal muscle in new-born rats and it's elimination during maturation. *Journal of Physiology* **261:** 387-422

Brown, M.C., Booth, C.M., Lunn, E.R. & Perry, V.H. (1991) Delayed response to denervation in muscles of C57Bl/Ola mice. *Neuroscience* **43:** 279-283

Brown, M.C., Lunn, E.R. & Perry, V.H. (1991a) Poor growth of mammalian motor and sensory axons into intact proximal nerve stumps. *European Journal of Neuroscience* **3:** 1366-1369

Brown, M.C., Lunn, E.R. & Perry, V.H. (1992) Consequences of slow Wallerian degeneration for regenerating motor and sensory axons. *Journal of Neurobiology* **23:** 521-536

Brown, M.C., Perry, V.H., Hunt, S.P. & Lapper, S.R. (1993) Further studies on motor and sensory nerve regeneration in mice with delayed Wallerian degeneration. *European Journal of Neuroscience* **6:** 420-428

Buckmaster, E.A., Perry, V.H. & Brown, M.C. (1995) The rate of Wallerian degeneration in cultured neurons from wild type and C57Bl/Wld$^s$ mice depends on time in culture and may be extended in the presence of elevated $K^+$ levels. *European Journal of Neuroscience* **7:** 1596-1602

Büngner, O.V. (1891) Uber die degenerations und regenerationsvorgange am nerven nach verletzungen. In: Ide, C. (1996) Peripheral nerve regeneration. *Neuroscience Research* **25:** 101-121

Burne, J.F., Staple, J.K. & Raff, M.C. (1996). Glial cells are increased proportionally in transgenic optic nerves with increased numbers of axons. *Journal of Neuroscience* **16:** 2064-2073

Bussetto, G., Buffelli, M., Tognana, E., Bellico, F. & Cangiano, A. (2000) Hebbian mechanisms revealed by electrical stimulation at developing rat neuromuscular junctions. *Journal of Neuroscience* **20:** 685-695

Callaway, E.M., Soha, J.M. & Van Essen, D.C. (1987) Competition favouring inactive over active motor neurons during synapse elimination. *Nature* **328:** 422-426

Cardasis, C.A. & Padykula, H.A. (1981) Ultrastructural evidence indicating reorganization at the neuromuscular junction in the normal rat soleus muscle. *Anatomical Record* **200:** 41-59

Carroll, S.L. & Frohnert, P.W. (1998) Expression of JE (monocyte chemoattractant protein-1) is induced by sciatic axotomy in wild type rodents but not in C57Bl/Wld$^s$ mice. *Journal of Neuropathology and Experimental Neurology* **57:** 915-930

Cavalieri, M., Durso, D., Lassa, A., Pierdominici, E., Robello, M. & Grasso, A. (1987) Characterization and some properties of the venom gland extract of a theridiid spider (Steatoda-paykulliana) frequently mistaken for black-widow spider (Latrodectus-tredecimguttatus). *Toxicon* **25:** 965-974

Chan, S.L. & Mattson, M.P. (1999) Caspase and calpain substrates: roles in synaptic plasticity and cell death. *Journal of Neuroscience Research* **58:** 167-190

Chaudry, V., Glass, J.D. & Griffin J.W. (1992) Wallerian degeneration in peripheral nerve disease. *Neurologic Clinics* **10:** 613-627

Chen, B.M. & Grinnell, A.D. (1995) Integrins and modulation of transmitter release from motor nerve terminals by stretch. *Science* **269:** 1578-1580

Choi, D.W. (1996) Ischemia-induced neuronal apoptosis. *Current Opinion in Neurobiology* **6:** 667-692

Chow, R.H., von Ruden, L. & Neher, E. (1992) Delay in vesicle fusion revealed by electrochemical monitoring of single secretory events in adrenal chromaffin cells. *Nature* **356**: 60-63

Cohen, I., Rimer, M., Lomo, T. & McMahan, U.J. (1997) Agrin-induced postsynaptic-like apparatus in skeletal muscle fibres in vivo. *Molecular and Cellular Neuroscience* **9:** 237-253

Cohen, M.W. & Godfrey, E.W. (1992) Early appearance of and neuronal contribution to agrin-like molecules at embryonic frog nerve-muscle synapses formed in culture. *Journal of Neuroscience* **12:** 2982-2992

Cohen, M.W., Hoffstrom, B.G. & DeSimone, D.W. (2000) Active zones on motor nerve terminals contain $\alpha 3\beta 1$ integrin. *Journal of Neuroscience* **20**: 4912-4921

Coleman, M.P., Conforti, L., Buckmaster, E.A., Tarlton, A., Ewing, R.M., Brown, M.C., Lyon, M.F. & Perry, V.H. (1998) An 85-kb tandem triplication in the slow Wallerian degeneration (Wld$^s$) mouse. *Proceedings of the National Academy of Sciences of the USA* **95:** 9985-9990

Conforti, L., Tarlton, A., Mack, T.G.A., Mi, W., Buckmaster, E.A., Wagner, D., Perry, V.H. & Coleman, M.P. (2000) A *Ufd2/D4Cole1e* chimeric protein and overexpression of *Rbp7* in the slow Wallerian degeneration ($Wld^S$) mouse. *Proceedings of the National Academy of Sciences of the USA* **97:** 11377-11382

Connor, E.A., McMahan, U.J. & Marshall, R.M. (1987) Cell accumulation in the junctional region of denervated muscle. *Journal of Cell Biology* **104:** 109-120

Cook, R.D., Ghetti, B. & Wisniewski, H.M. (1974) The pattern of Wallerian degeneration in the optic nerve of newborn kittens: an ultrastructural study. *Brain Research* **75:** 261-275

Costanzo, E.M., Barry, J.A. & Ribchester, R.R. (1999) Co-regulation of synaptic efficacy at stable polyneuronally innervated neuromuscular junctions in reinnervated rat muscle. *Journal of Physiology* **521:** 365-374

Costanzo, E.M., Barry, J.A. & Ribchester, R.R. (2000) Competition at silent synapses in reinnervated skeletal muscle. *Nature Neuroscience* **3:** 694-700

Court, F.A., Brophy, P.J. & Ribchester, R.R. (2001) Effects of peripheral demyelination on neuromuscular transmission and glial cell organisation in periaxin gene-deficient mice. *Journal of Physiology* Presented at the September meeting of the Physiological Society. In press.

Couteaux, R. (1973) In: Structure and function of muscle. [Ed. Bourne, G.H] **2:** 483-530. Academic Press, New York

Crawford, T.O., Hsieh, S-T., Schryer, B.L. & Glass, J.D. (1995) Prolonged axonal survival in transected nerves of C57Bl/Ola mice is independent of age. *Journal of Neurocytology* **24:** 333-340

Croall, D.E. & DeMartino, G.N. (1991) Calcium-activated neutral protease (calpain) system: structure, function, and regulation. *Physiological Reviews* **71:** 813-847

Culican, S.M., Nelson, C.C. & Lichtman, J.W. (1998) Axon withdrawal during synapse elimination at the neuromuscular junction is accompanied by disassembly of the postsynaptic specialization and withdrawal of Schwann cell processes. *Journal of Neuroscience* **18:** 4953-4965

Dal Canto, M.C. & Gurney, M.E. (1995) Neuropathological changes in 2 lines of mice carrying a transgene for mutant human cu,zn sod, and in mice overexpressing wild-type human sod - a model of familial amyotrophic-lateral-sclerosis (fals). *Brain Research* **676:** 25-40

Dale, H.H., Feldberg, W. & Vogt, M. (1936) Release of acetylcholine at voluntary motor nerve endings. *Journal of Physiology* **86**: 353-380

Day, N.C., Wood, S.J., Ince, P.G., Volsen, S.G., Smith, W., Slater, C.R. & Shaw, P.J. (1997) Differential localization of voltage-dependent calcium channel α1 subunits at the human and rat neuromuscular junction. *Journal of Neuroscience* **17**: 6226-6235

De Aguilar, J-L. G., Gordon, J.W., Rene, F., Lutz-Bucher, B., Kienlen-Campard, P. & Loeffler, J-P. (1999) A mouse model of familial amyotrophic lateral sclerosis expressing a mutant superoxide dismutase 1 shows evidence of disordered transport in the vasopressin hypothalamo-neurohypophysial axis. *European Journal of Neuroscience* **11:** 4179-4187

De Camilli, P. & Takei, K. (1996) Molecular mechanisms in synaptic vesicle endocytosis and recycling. *Neuron* **16:** 481-486

Deckwerth, T.L. & Johnson, E.M. (1994) Neurites can remain viable after the destruction of the neuronal soma by programmed cell death. *Developmental Biology* **165:** 63-72

Dekkers, J. & Navarrete, R. (1998) Persistence of somatic and dendritic growth associated processes and induction of dendritic sprouting in motoneurones after neonatal axotomy in the rat. *Neuroreport* **9:** 1523-1527

Delgado, R., Maureira, C., Oliva, C., Kidokoro, Y. & Labarca, P. (2000) Size of vesicle pools, rates of mobilization, and recycling at neuromuscular synapses of a drosophila mutant, shibre. *Neuron* **28:** 941-953

Dell Castillo, J. & Katz, B. (1954) Quantal components of the endplate potential. *Journal of Physiology* **124:** 560-573

DiAntonio, A., Haghighi, A.P., Portman, S.L., Lee, J.D., Amaranto, A.M. & Goodman, C.S. (2001) Ubiquitin-dependent mechanisms regulate synaptic growth and function. *Nature* **412:** 449-452

Donat, J.R. & Wisniewski, H.M. (1973) The spatio-temporal pattern of Wallerian degeneration in mammalian peripheral nerves. *Brain Research* **53:** 41-53

Dubois-Dauphin, M., Frankowski, H., Tsujimoto, Y., Huarte, J. & Martinou, J-C. (1994) Neonatal motoneurons overexpressing the Bcl-2 protooncogene in transgenic mice are protected from axotomy-induced cell death. *Proceedings of the National Academy of Sciences of the USA* **91:** 3309-3313

Edwards, S.N. & Tolkovsky, A.M. (1994) Characterization of apoptosis in cultured rat sympathetic neurons after nerve growth factor withdrawal. *Journal of Cell Biology* **124:** 537-546

El Hachimi, K.H., Chaunu, M.P., Brown, P. & Foncin, J.F. (1998) Modifications of oligodendroglial cells in spongiform encephalopathies. *Experimental Neurology* **154:** 23-30

Elferink, L.A. & Scheller, R.H. (1993) Synaptic vesicle proteins and regulated exocytosis. *Journal of Cell Science [suppl]* **17**: 75-79

Ellerby, H.M., Martin, S.J., Ellerby, L.M., Naiem, S.S., Rabizadeh, S., Salvesen, G.S., Casiano, C.A., Cahsman, N.R., Green, D.R. & Bredesen, D.E. (1997) Establishment of a cell-free system of neuronal apoptosis: comparison of premitochondrial, mitochondrial and postmitochondrial phases. *Journal of Neuroscience* **17:** 6165-6178

Emanuelli, M., Carnevali, F., Saccucci, F., Peirella, F., Amici, A., Raffaelli, N. & Magni, G. (2001) Molecular cloning, chromosomal localization, tissue mRNA levels, bacterial expression, and enzymatic properties of human NMN adenylyltransferase. *Journal of Biological Chemistry* **276:** 406-412

England, J.D., Levinson, S.R. & Shrager, P. (1996) Immunocytochemical investigations of sodium channels along nodal and internodal portions of demyelinating axons. *Microscopy Research and Technique* **34:** 445-451

Erickson, J.D., Varoqui, H., Schafer, M.K-H., Modi, W., Diebler, M.F., Weihe, E., Rand, J., Eiden, L.E., Bonner,T.I. & Usdin, T.B. (1994) Functional identification of a vesicular acetylcholine transporter and its expression from a cholinergic gene locus. *Journal of Biological Chemistry* **269**: 21929-21932

Fatt, P. & Katz, B. (1951) An analysis of the end-plate potential recorded with an intracellular electrode. *Journal of Physiology* **115:** 320-370

Fatt, P. & Katz, B. (1952) Spontaneous subthreshold activity at motor nerve endings. *Journal of Physiology* **117:** 109-128

Finn, J.T., Weil, M., Archer, F., Siman, R., Srinivasan, A. & Raff, M.C. (2000) Evidence that Wallerian degeneration and localized axon degeneration induced by local neurotrophin deprivation do not involve caspases. *Journal of Neuroscience* **20:** 1333-1341

Fladby, T. & Jansen, J.K.S. (1987) Postnatal loss of synaptic terminals in the partially denervated mouse soleus muscle. *Acta Physiologica Scandinavica* **129:** 239-246

Flucher, B.E. & Daniels, M.P. (1989) Distribution of $Na^+$ channels and ankyrin in neuromuscular junctions is complementary to that of acetylcholine receptors and the 43kD protein. *Neuron* **3**: 163-175

Friede, R.L. & Martinez, A.J. (1970) Analysis of axon-sheath relations during early Wallerian degeneration. *Brain Research* **19:** 199-212

Fruttiger, M., Schachner, M. & Martini, R. (1995) Tenascin-C expression during Wallerian degeneration in C57Bl/Wld$^s$ mice: possible implications for axonal regeneration. *Journal of Neurocytology* **24:** 1-14

Fu, S.Y. & Gordon, T. (1997) The cellular and molecular basis of peripheral nerve regeneration. *Molecular Neurobiology* **14:** 67-116

Fujimura, H., Lacroix, C. & Said, G. (1991) Vulnerability of nerve-fibers to ischemia - A quantitative light and electron-microscope study. *Brain* **114:** 1929-1942

Gan, W-B. & Lichtman, J.W. (1998) Synaptic segregation at the developing neuromuscular junction. *Science* **282:** 1508-1511

Gautam, M., Noakes, P.G., Moscoso, L., Rupp, F., Scheller, R.H., Merlie, J.P. & Sanes, J.R. (1996) Defective neuromuscular synaptogenesis in agrin-deficient mutant mice. *Cell* **85:** 525-535

George, E.R., Glass, J.D. & Griffin, J.W. (1995) Axotomy-induced axonal degeneration is mediated by calcium influx through ion-specific channels. *Journal of Neuroscience.* **15:** 6445-6452

Georgiou, J., Robitaille, R., Trimble, W.S. & Charlton, M.P. (1994) Synaptic regulation of glial protein expression in-vivo. *Neuron* **12:** 443-455

Gesemann, M., Denzer, A.J. & Ruegg, M.A. (1995) Acetylcholine receptor-aggregating activity of agrin isoforms and mapping of the active site. *Journal of Cell Biology* **128:** 625-636

Gillingwater, T.H., Kalikulov, D., Ushkaryov, Y. & Ribchester, R.R. (1999) Comparison of effects of α-latrotoxin with a partially purified toxin from another theridiid spider, Steatoda paykulliana, on exocytosis at mouse neuromuscular junctions. *Journal of Physiology* **520:** 40P

Gillingwater, T.H. & Ribchester, R.R. (2001) Compartmental neurodegeneration and synaptic plasticity in the Wld$^s$ mutant mouse. *Journal of Physiology* **534:** 627-639

Glass, J.D., Brushart, T.M., George, E.B. & Griffin, J.W. (1993) Prolonged survival of transected nerve fibres in C57Bl/Ola Mice is an intrinsic characteristic of the axon. *Journal of Neurocytology* **22:** 311-321

Glass, J.D. & Griffin, J.W. (1991) Neurofilament redistribution in transected nerves: Evidence for bidirectional transport of neurofilaments. *Journal of Neuroscience.* **11:** 3146-3154

Glass, J.D. & Griffin, J.W. (1994) Retrograde transport of radiolabeled cytoskeletal proteins in transected nerves. *Journal of Neuroscience* **14:** 3915-3921

Glass, J.D., Nash, N., Dry, I., Culver, D., Levey, A.I. & Wesselingh, S. (1998) Cloning of M-Calpain 80kD subunit from the axonal degeneration-resistant $Wld^s$ mouse mutant. *Journal of Neuroscience Research* **52:** 653-660

Glass, J.D., Schryer, B.L. & Griffin, J.W. (1994) Calcium-mediated degeneration of the axonal cytoskeleton in the Ola mouse. *Journal of Neurochemistry* **62:** 2472-2475

Golden, J.P., DeMaro, J.A., Osborne, P.A., Milbrandt, J. & Johnson, E.M. (1999) Expression of neurturin, GDNF, and GDNF family-receptor mRNA in the developing and mature mouse. *Experimental Neurology* **158:** 504-528

Gonzalez-Gaitan, M. & Jackle, H. (1997) Role of drosophila α-adaptin in presynaptic vesicle recycling. *Cell* **88:** 767-776

Goodearl, A.D., Yee, A.G., Sandrock, A.W., Corfas, G. & Fischbach, G.D. (1995) ARIA is concentrated in the synaptic basal lamina of the developing chick neuromuscular junction. *Journal of Cell Biology* **130:** 1423-1434

Gramolini, A.O., Wu, J. & Jasmin, B.J. (2000) Regulation and functional significance of utrophin expression at the mammalian neuromuscular synapse. *Microscopy Research and Technique* **49**: 90-100

Grinnell, A.D. (1995) Dynamics of nerve-muscle interaction in developing and mature neuromuscular junctions. *Physiological Reviews* **75**: 789-824

Grinnell, A.D., Letinsky, M.S. & Rheuben, M.R. (1979) Competitive interaction between foreign nerves innervating frog skeletal muscle. *Journal of Physiology* **289:** 241-262

Guo, Z.H. & Mattson, M.P. (2000) In vivo 2-deoxyglucose administration preserves glucose and glutamate transport and mitochondrial function in cortical synaptic terminals after exposure to amyloid β-peptide and iron: Evidence for a stress response. *Experimental Neurology* **166:** 173-179

Hall, S.M. (1993) Observations on the progress of Wallerian degeneration in transected peripheral nerves of C57Bl/Wld Mice in the presence of recruited macrophages. *Journal of Neurocytology* **22:** 480-490

Hallpike, J.F. (1976) Histochemistry of peripheral nerve and nerve terminals. In *The Peripheral Nerve,* ed. Landon, D.N., Chapman & Hall, London. 605-665

Harlow, M.L., Ress, D., Stoschek, A., Marshall, R.M. & McMahan, U.J. (2001) The architecture of active zone material at the frog's neuromuscular junction. *Nature* **409:** 479-484

Henkel, A.W., Lubke, J. & Betz, W.J. (1996) FM1-43 dye ultrastructural localization in and release from frog motor nerve terminals. *Proceedings of the National Academy of Sciences of the USA* **93:** 1918-1923

Herdegen, T. & Leah, J.D. (1998) Inducible and constitutive transcription factors in the mammalian nervous system: Control of gene expression by jun, fos and krox, and creb/atf proteins. *Brain Research Reviews* **28:** 370-490

Herdegen, T. & Zimmermann, M. (1994) Expression of c-jun and jund transcription factors represent specific changes in neuronal gene expression following axotomy. *Progress in Brain Research* **103:** 153-169

Herrera, A.A., Banner, L.R. & Nagaya, N. (1990) Repeated, in vivo observation of frog neuromuscular junctions: remodelling involves concurrent growth and retraction. *Journal of Neurocytology* **19:** 85-99

Hershko, A. & Ciechanover, A. (1998) The ubiquitin system. *Annual Review of Biochemistry* **67:** 425-479

Heumann, R., Korsching, S., Bandtlow, C. & Thoenen, H. (1987) Changes of nerve growth factor synthesis in non-neuronal cells in response to sciatic nerve transection. *Journal of Cell Biology* **104:** 1623-1631

Heuser, J.E., Reese, T.S., Dennis, M.J., Jan, Y., Jan, L. & Evans, L. (1979) Synaptic vesicle exocytosis captured by quick freezing and correlated with quantal transmitter release. *Journal of Cell Biology* **81:** 275-300

Hill, R.R., Robbins, N. & Fang, Z.P. (1991) Plasticity of presynaptic and postsynaptic elements of neuromuscular junctions repeatedly observed in living adult mice. *Journal of Neurocytology* **20:** 165-182

Hille, B. (1992) Ion channels in excitable membranes. 2nd Ed. Sinauer, USA. 291-314.

Hirano, A., Donnenfeld, H., Sasaki, S. & Nakano, I. (1984) Fine structural observations of neurofilamentous changes in amyotrophic lateral sclerosis. *Journal of Neuropathology and Experimental Neurology* **43:** 461-470

Hirji, R., Coulthard, R. & Govind, C.K. (2000) Regenerated synaptic terminals on a crayfish slow muscle identify with transplanted phasic or tonic axons. *Journal of Neurobiology* **45:** 185-193

Hirokawa, N., Sobue, K., Kanda, K., Harada, A. & Yorifuji, H. (1989) The cytoskeletal architecture of the presynaptic terminal and molecular structure or synapsin I. *Journal of Cell Biology* **108**: 111-126

Hochstrasser, M. (1996) Ubiquitin-dependent protein degradation. *Annual Review of Genetics* **30:** 405-439

Hodgkin, A.L., Huxley, A.F. & Katz, B. (1952) Measurement of current voltage relations in the membrane of the giant axon of *Loligo*. *Journal of Physiology* **116:** 424-448

Honjin, R., Nakamura, T. & Imura, M. (1959) Electron microscopy of peripheral nerve fibres. iii) On the axoplasmic changes during Wallerian degeneration. *Okajimas Folia Anatomica Japonica* **33:** 131-156

Hubel, D.H., Wiesel, T.N. & LeVay, S. (1977) Plasticity of ocular dominance columns in the monkey striate cortex. *Philosophical Transactions of the Royal Society, London B* **278:** 377-409

Hudson, C.S., Deshpande, S.S. & Albuquerque, E.X. (1984) Consequences of axonal transport blockade by batrachotoxin on mammalian neuromuscular junction. III. An ultrastructural study. *Brain Research* **296:** 319-332

Huttenlocher, P.R., Decourten, C., Garey, L.J. & Vanderloos, H. (1982) Synaptogenesis in human visual-cortex - evidence for synapse elimination during normal development. *Neuroscience Letters* **33:** 247-252

Huxley, A.F. & Stampfli, R. (1949) Evidence for saltatory conduction in peripheral myelinated nerve fibers. *Journal of Physiology* **108:** 315-339

Ijkema-Paassen, J. & Gramsbergen, A. (1998) Polyneural innervation in the psoas muscle of the developing rat. *Muscle and Nerve* **21:** 1058-1063

Ivins, K.J., Bui, E.T.N. & Cotman, C.W. (1998) β-amyloid induces local neurite degeneration in cultured hippocampal neurons: Evidence for neuritic apoptosis. *Neurobiology of Disease.* **5:** 365-378

Jacobson, M.D., Burne, J.F. & Raff, M.C. (1994) Programmed cell death and bcl-2 protection in the absence of a nucleus. *EMBO Journal* **13:** 1899-1910

Jahromi, B.S., Robitaille, R. & Charlton, M.P. (1992) Transmitter release increases intracellular calcium in perisynaptic Schwann cells *in situ*. *Neuron* **8:** 1069-1077

Janicke, R.U., Sprengart, M.L., Wati, M.R. & Porter, A.G. (1998) Caspase-3 is required for DNA fragmentation and morphological changes associated with apoptosis. *Journal of Biological Chemistry* **273:** 9357-9360

Jenkins, R & Hunt, S.P. (1991) Long term increase in the levels of c-jun mRNA and jun protein-like immunoreactivity in motor and sensory neurons following axon damage. *Neuroscience Letters* **129:** 107-110

Jennings, C. (1994) Death of a synapse. *Nature* **372:** 498-499

Johnson, D.A. & Purves, D. (1981) Post-natal reduction of neural unit size in the rabbit cilliary ganlion. *Journal of Physiology* **318:** 143-159

Johnson, E.S., Ma, P.C.M., Ota, I. & Varshavsky, A. (1995) A proteolytic pathway that recognises ubiquitin as a degradation signal. *Journal of Biological Chemistry* **270:** 17442-17456

Johnson, I.P. & Duberley, R.M. (1998) Motoneuron survival and expression of neuropeptides and neurotrophic factor receptors following axotomy in adult and ageing rats. *Neuroscience* **84:** 141-150

Jones, G., Meier, T., Lichtsteiner, M., Witzemann, V., Sakmann, B. & Brenner, H.R. (1997) Induction by agrin of ectopic and functional postsynaptic-like membrane in innervated muscle. *Proceedings of the National Academy of Sciences of the USA* **94:** 2654-2659

Jordan, C.L., Letinsky, M.S. & Arnold, A.P. (1988) Synapse elimination occurs late in the hormone-sensitive levator ani muscle of the rat. *Journal of Neurobiology* **19:** 335-356

Kandel, E.R., Schwartz, J.H. & Jessell, T.M. (1991) *Principles of Neural Science* 3rd Ed. Elsevier Science Publishing, USA.

Katz, B. (1969) The release of neural transmitter substances. In The Xth Sherrington Lecture (Springfield, IL: Thomas)

Katz, B. & Miledi, R. (1969) Tetrodotoxin-resistant electric activity in presynaptic terminals. *Journal of Physiology* **203:** 459-487

Kawabuchi, M., Cintra, W.M., Deshpande, S.S. & Albuquerque, E.X. (1991). Morphological and electrophysiological study of distal motor nerve fiber degeneration and sprouting after irreversible cholinesterase inhibition. *Synapse* **8:** 218-228

Keller-Peck, C.R., Feng, G., Sanes, J.R., Yan, Q., Lichtman, J.W. & Snider, W.D. (2001) Glial cell line-derived neurotrphic factor administration in postnatal life results in motor unit enlargement and continous synaptic remodelling at the neuromuscular junction. *Journal of Neuroscience* **21:** 6136-6146

Kelly, R.B. (1993) Storage and release of neurotransmitters. *Neuron [suppl]* **10**: 43-53

Keramaris, E., Stefanis, L., MacLaurin, J., Harada, N., Kazuaki, T., Ishikawa, T., Taketo, M.M., Robertson, G.S., Nicholson, D.W., Slack, R.S. & Park, D.S. (2000) Involvement of caspase 3 in apoptotic death of cortical neurons evoked by DNA damage. *Molecular and Cellular Neuroscience* **15:** 368-379

Kerr, J.F., Goble, G.C., Winterford, C.M. & Harmon, B.V. (1995) Anatomical methods in cell death. *Methods in Cell Biology* **46:** 1-28

Kerr, J.F., Wyllie, A.H. & Currie, A.R. (1972) Apoptosis: A basic biological phenomenon with wide-ranging implications in tissue kinetics. *British Journal of Cancer* **26:** 239-257

Klingauf, J., Kavalali, E.T. & Tsien, R.W. (1998) Kinetics and regulation of fast endocytosis at hippocampal synapses. *Nature* **394:** 581-585

Knudson, C.M., Tung, K.S., Tourtellotte, W.G., Brown, G.A. & Korsmeyer, S.J. (1995) Bax-deficient mice with lymphoid hyperplasia and male germ cell death. *Science* **270:** 96-99

Koegl, M., Hoppe, T., Schlenker, S., Ulrich, H.D., Mayer, T.U. & Jentsch, S. (1999) A novel ubiquitination factor, E4, is involved in multiubiquitin chain assembly. *Cell* **96:** 635-644

Korneliussen, H & Jansen, J.K.S. (1976) Morphological aspects of the elimination of polyneuronal innervation of skeletal muscle fibres in newborn rats. *Journal of Neurocytology* **5:** 591-604

Krejci, E., Thomine, S., Boschetti, N., Legay, C., Sketelj, J. & Massoulie, J. (1997) The mammalian gene of acetylcholinesterase-associated collagen. *Journal of Biological Chemistry* **272:** 22840-22847

Kuffler, S.W. & Yoshikami, D. (1975) The number of transmitter molecules in a quantum: An estimate from iontophoretic application of acetylcholine at the neuromuscular synapse. *Journal of Physiology* **251:** 465-482

Kugelberg, E. (1976) Adaptive transformation of rat soleus muscle units during growth. *Journal of the Neurological Sciences* **27:** 269-289

Kuromi, H. & Kidokoro, Y. (1998) Two distinct pools of synaptic vesicles in single presynaptic boutons in a temperature-sensitive Drosophila mutant, shibire. *Neuron* **20:** 917-925

Laney, J.D. & Hochstrasser, M. (1999) Substrate targeting in the ubiquitin system. *Cell* **97:** 427-430

Lapper, S.R., Brown, M.C. & Perry, V.H. (1994) Motor neuron death induced by axotomy in neonatal mice occurs more slowly in a mutant strain in which Wallerian degeneration is very slow. *European Journal of Neuroscience* **6:** 473-477

Layfield, R., Alban, A., Mayer, R.J. & Lowe, J. (2001) The ubiquitin protein catabolic disorders. *Neuropathology and Applied Neurobiology* **27:** 171-179

Leah, J.D., Herdegen, T. & Bravo, R. (1991) Selective expression of jun proteins following axotomy and axonal transport block in peripheral nerves in the rat: evidence for a role in the regeneration process. *Brain Research* **566:** 198-207

Lee, H.C. (1999) A unified mechanism of enzymatic synthesis of two calcium messengers: cyclic ADP-ribose and NAADP. *Biological Chemistry* **380:** 785-793

LeVay, S., Wiesel, T.N. & Hubel, D.H. (1980) The development of occular dominance columns in normal and visually deprived monkeys. *Journal of Comparative Neurology* **191:** 1-51

Levenson, D. & Rosenbluth, J. (1990) Electrophysiologic changes accompanying Wallerian degeneration on frog sciatic nerve fibres. *Brain Research* **523:** 230-236

Levy, D., Kubes, P. & Zochodne, D.W. (2001) Delayed peripheral nerve degeneration, regeneration and pain in mice lacking inducible nitric oxide synthase. *Journal of Neuropathology and Experimental Neurology* **60:** 411-421

Lichtman, J.W. (1977) The reorganization of synaptic connexions in the rat submandibular ganglion during post-natal development. *Journal of Physiology* **273:** 155-177

Lichtman, J.W. & Colman, H. (2000) Synapse elimination and indelible memory. *Neuron* **25:** 269-278

Lichtman, J.W., Magrassi, L. & Purves, D. (1987) Visualisation of neuromuscular junctions over periods of several months in living mice. *Journal of Neuroscience* **7:** 1215-1222

Lichtman, J.W. & Purves, D. (1980) The elimination of redundant preganglionic innervation to hamster sympathetic ganglion cells in early post-natal life. *Journal of Physiology* **301:** 213-228

Lichtman, J.W. & Wilkinson, R.S. (1987) Properties of motor units in the transverses abdominis muscle of the garter snake. *Journal of Physiology* **393:** 355-374

Liefner, M., Siebert, H., Sachse, T., Michel, U., Kollias, G. & Bruck, W. (2000) The role of TNF-α during Wallerian degeneration. *Journal of Neuroimmunology* **108:** 147-152

Lim, S.M., Guiloff, R.J & Navarrete, R. (2000) Interneuronal survival and calbindin-D28k expression following motoneuron degeneration. *Journal of the Neurological Sciences* **180:** 46-51

Lohof, A.M., Delhaye-Bouchaud, N. & Mariani, J. (1996) Synapse elimination in the central nervous system: functional significance and cellular mechanisms. *Reviews in Neuroscience* **7:** 85-101

Lømo, T. & Waerhaug, O. (1985) Motor endplates in fast and slow muscles of the rat: What determines their differences? *Journal of Physiology* **80:** 290-297

LoPachin, R.M. & Lehning, E.J. (1997) Mechanism of calcium entry during axon injury and degeneration. *Toxicology and Applied Pharmacology* **143:** 233-244

Love, F.M. & Thompson, W.J. (1998) Schwann cells proliferate at rat neuromuscular junctions during development and regeneration. *Journal of Neuroscience* **18:** 9376-9385

Lubinska, L. (1977) Early course of Wallerian degeneration in myelinated fibres of the rat phrenic nerve. *Brain Research* **130:** 47-63

Luco, J.V. & Eyzaguirre, C. (1955) Fibrilation and hypersensitivity to Ach in denervated muscle. *Journal of Neurophysiology* **18:** 65-73

Ludwin, S.K. & Bisby, M.A. (1992) Delayed Wallerian degeneration in the central nervous system of Ola mice: an ultrastructural study. *Journal of the Neurological Sciences* **109:** 140-147

Lunn, E.R., Perry, V.H., Brown, M.C., Rosen, H. & Gordon, S. (1989) Absence of Wallerian degeneration does hinder regeneration in peripheral nerve. *European Journal of Neuroscience* **1:** 27-33

Luttges, M.W., Kelly, P.T. & Gerren, R.A. (1976) Degenerative changes in mouse sciatic nerves: Electrophoretic and electrophysiologic characterisations. *Experimental Neurology* **50:** 706-733

Lyon, M.F., Ogunkolade, B.W., Brown, M.C., Atherton, D.J. & Perry, V.H. (1993) A gene affecting Wallerian nerve degeneration maps distally on mouse chromosome 4. *Proceedings of the National Academy of Sciences of the USA* **90:** 9717-9720

Mack. T.G.A., Reiner, M., Beirowski, B., Mi, W., Emanuelli, M., Wagner, D., Thomson, D., Gillingwater, T.H., Conforti, L., Shama Fernando, F., Tarlton, A., Addicks, K., Magni, G., Ribchester, R.R., Perry, V.H. & Coleman, M.P. (2001) Injured axons and their synapses are protected from Wallerian degeneration by a Ube4b/Nmnat chimeric gene. *Under review by Nature Neuroscience.*

Magni, G., Amici, A., Emanuelli, M., Raffaelli, N. & Ruggieri, S. (1999) Enzymology of $NAD^+$ synthesis. *Advances in Enzymology and Related Areas of Molecular Biology* **73:** 135-182

Manolov, S. (1974) Initial changes in the neuromuscular synapses of denervated rat diaphragm. *Brain Research* **65:** 303-316

Martin, A.R. (1979) The effect of membrane capacitance on non-linear summation of synaptic potentials. *Journal of Theoretical Biology* **59:** 179-187

Martin, L.J. (2001) Neuronal cell death in nervous system development, disease, and injury. *International Journal of Molecular Medicine* **7:** 455-478

Martin, S.J. (1993) Protein or RNA synthesis inhibition induces apoptosis of mature human $CD4^+$ T cell blasts. *Immunology Letters* **35:** 125-134

Martin, S.J., Grimwood, P.D. & Morris, R.G.M. (2000) Synaptic plasticity and memory: an evaluation of the hypothesis. *Annual Review of Neuroscience* **23:** 649-711

Martinou, J.C., Dubois-Dauphin, M., Staple, J.K., Rodriguez, I., Frankowsky, H., Missotten, M., Albertini, P., Talabot, D., Catsicas, S., Pietra, C. & Huarte, J. (1994) Overexpression of bcl-2 in transgenic mice protects neurons from naturally occurring cell death and experimental ischaemia. *Neuron* **13:** 1017-1030

Mastalgia, F.L., McDonald, W.I. & Yogendran, K. (1976) Nodal changes during the early stages of Wallerian degeneration of central nerve fibres. *Journal of the Neurological Sciences* **30:** 259-67

Mattison, R.J. (1999) Synapse withdrawal at the neuromuscular junction in a mouse with slow Wallerian degeneration ($Wld^s$). PhD Thesis, University of Edinburgh, UK.

Mattison, R.J., Thomson, D., Barry, J.A. & Ribchester, R.R. (1996) Sudden death of axotomized motor nerve terminals at neuromuscular junctions in Wld(s) mice. *Journal of Physiology* **495:** 152P-153P

Mattson, M.P. (2000) Apoptosis in neurodegenerative disorders. *Nature Reviews Molecular Cellular Biology* **1:** 120-129

Mattson, M.P., Keller, J.N. & Begley J.G. (1998a) Evidence for synaptic apoptosis. *Experimental Neurology* **153:** 35-48

Mattson, M.P., Partin, J. & Begley, J.G. (1998b) Amyloid β-peptide induces apoptosis-related events in synapses and dendrites. *Brain Research* **807:** 167-176

Maycox, P.R., Link, E., Reetz, A., Morris, S.A. & Jahn, R. (1992) Clathrin-coated vesicles in nervous tissue are involved primarily in synaptic vesicle recycling. *Journal of Cell Biology* **118:** 1379-1388

McArdle, J.J. (1975) Complex end-plate potentials at the regenerating neuromuscular junction of the rat. *Experimental Neurology* **49:** 629-638

McDonald, W.I. (1972) The time course of conduction failure during degeneration of a central tract. *Experimental Brain Research* **14:** 550-556

McMahan, U.J. (1990) The agrin hypothesis. *Cold Spring Harbor Symposia on Quantitative Biology* **55:** 407-418

Meier, T. & Wallace, B.G. (1998) Formation of the neuromuscular junction: molecules and mechanisms. *Bioessays* **20:** 819-829

Mikucki, S.A. & Oblinger, M.M. (1991) Corticospinal neurons exhibit a novel pattern of cytoskeletal gene expression after injury. *Journal of Neuroscience Research* **30:** 213-225

Miledi, R. & Slater, C.R. (1968) Electrophysiology and electron-Microscopy of rat neuromuscular junctions after nerve degeneration. *Proceedings of the Royal Society, London, B.* **169:** 289-306

Miledi, R. & Slater, C.R. (1970) On the degeneration of rat neuromuscular junctions after nerve section. *Journal of Physiology* **207:** 507-528

Ming, Y., Bergman, E., Edstrom, E. & Ulfhake, B. (1999) Evidence for increased GDNF signalling in aged sensory and motor neurons. *Neuroreport* **10:** 1529-1535

Mirsky, R. & Jessen, K.R. (1996) Schwann cell development, differentiation and myelination. *Current Opinion in Neurobiology* **6:** 89-96

Morgan, J.I. & Curran, T. (1991) Stimulus-transcription coupling in the nervous system: Involvement of the inducible proto-oncogenes fos and jun. *Annual Review of Neuroscience* **14:** 421-451

Morrison, B.M., Shu, I-W., Wilcox, A.L., Gordon, J.W. & Morrison, J.H. (2000) Early and selective pathology of light chain neurofilament in the spinal cord and sciatic nerve of G86R mutant superoxide dismutase transgenic mice. *Experimental Neurology* **165:** 207-220

Mothet, J-P., Fossier, P., Meunier, F-M., Stinnakre, J., Tauc, L. & Baux, G. (1998) Cyclic ADP-ribose and calcium-induced calcium release regulate neurotransmitter release at a cholinergic synapse of Aplysia. *Journal of Physiology* **507:** 405-414

Nagler, K., Mauch, D.H. & Pfrieger, F.W. (2001) Glia-derived signals induce synapse formation in neurones of the rat central nervous system. *Journal of Physiology* **533:** 665-679

Narayanan, S., Fu, L., Pioro, E., DeStefano, N., Collins, D.L., Francis, G.S., Antel, J.P., Matthews, P.M. & Arnold, D.L. (1997) Imaging of axonal damage in multiple sclerosis: Spatial distribution of magnetic resonance imaging lesions. *Annals of Neurology* **41:** 385-391

Nicholls, J.G., Martin, A.R. & Wallace, B.G. (1992) *From Neuron to Brain* 3rd Ed. Sinauer Associates Massachusetts, USA.

Nieke, J. & Schachner, M. (1985) Expression of the neural cell adhesion molecules L1 and N-CAM and their common carbohydrate epitope L2/HNK-1 during development and after transection of the mouse sciatic nerve. *Differentiation* **30:** 141-151

Nijhawan, D., Honapour, N. & Wang, X. (2000) Apoptosis in neural development and disease. *Annual Review in Neuroscience* **23:** 73-87

O'Brien, R.A.D., Ostberg, A.J.C. & Vrbova, G. (1978) Observations on the elimination of polyneuronal innervation in developing mammalian skeletal muscle. *Journal of Physiology* **282:** 571-582

O'Hanlon, G.M., Plomp, J.J., Chakrabarti, M., Morrison, I., Wagner, E.R., Goodyear, C.S., Yin, X.Y., Trapp, B.D.T., Conner, J., Molenaar, P.C., Stewart, S., Rowan, E.G. & Willison, H.J. (2001) Anti-GQ1b ganglioside antibodies mediate complement-dependent destruction of the motor nerve terminal. *Brain* **124:** 893-906

Oorschot, D.E. & McLennan, I.S. (1998) The trophic requirements of mature motoneurons. *Brain Research* **789:** 315-321

Oppenheim, R.W., Flavell, R.A., Vinsant, S., Prevette, D., Kuan, C-Y. & Rakic, P. (2001) Programmed cell death of developing mammalian neurons after genetic deletion of caspases. *Journal of Neuroscience* **21:** 4752-4760

Palade, G.E. & Palay, S.L. (1954) Electron microscope observations of interneuronal and neuromuscular synapses. *Anatomical Record* **118:** 335

Palay, S.L. (1956) Synapses in the central nervous system. *Journal of Biophysical and Biochemical Cytology* **2:** 193-202

Parson, S.H., Davie, N. & Ribchester, R.R. (1998) Synapse elimination in organ culture of $Wld^s$ mouse skeletal muscle. *Journal of Physiology* **507:** 30P

Parson, S.H., Dilley, J., Gandhi, N., Gillingwater, T.H. & Ribchester, R.R. (1998a) Schwann cell responses at disconnected nerve terminals in organ cultures of $Wld^s$ mouse neuromuscular junctions. *Society for Neuroscience Abstracts* **24:** 413.17P

Parson, S.H., Mackintosh, C.L. & Ribchester, R.R. (1997) Elimination of motor nerve terminals in neonatal mice expressing a gene for slow wallerian degeneration (C57Bl/Wlds). *European Journal of Neuroscience* **9:** 1586-1592

Patton, B.L., Cunningham, J.M., Thyboll, J., Kortesmaa, J., Westerblad, H., Edstrom, L., Tryggvason, K. & Sanes, J.R. (2001) Properly formed but improperly localized synaptic specialisations in the absence of laminin alpha 4. *Nature Neuroscience* **4:** 597-604

Perry, V.H. & Anthony, D.C. (1999) Axon damage and repair in multiple sclerosis. *Philosophical Transactions of the Royal Society of London, B* **354:** 1641-1647

Perry, V.H., Brown, M.C. & Lunn, E.R. (1990a) Very slow retrograde and Wallerian degeneration in the CNS of C57Bl/Ola mice. *European Journal of Neuroscience* **3:** 102-105

Perry, V.H., Brown, M.C. & Tsao, J.W. (1992) The effectiveness of the gene which slows the rate of Wallerian degeneration in C57Bl/Ola mice declines with age. *European Journal of Neuroscience* **4:** 1000-1002

Perry, V.H., Lunn, E.R., Brown, M.C., Cahusac, S. & Gordon, S. (1990b) Evidence that the rate of Wallerian degeneration is controlled by a single autosomal dominant gene. *European Journal of Neuroscience* **2:** 408-413

Perry, V.H., Brown, M.C., Lunn, E.R., Tree, P. & Gordon, S. (1990c) Evidence that very slow Wallerian degeneration in C57Bl/Ola mice is an intrinsic property of the peripheral nerve. *European Journal of Neuroscience* **2:** 802-808

Peters, A. & Jones, E.G. (1984) Cellular components of the cerebral cortex, Vol. 1. Plenum, New York

Peters, A., Palay, S.L. & Webster, H.D. (1991) The fine structure of the nervous system: Neurons and their supporting cells. 3rd Ed. Oxford University Press, New York

Peters, M.F., Sadoulet-Puccio, H.M., Grady, R.M., Kramarcy, N.R., Kunkel, L.M., Sanes, J.R., Sealock, R. & Froehner, S.C. (1998) Differential membrane localization and intermolecular associations of alpha-dystrobrevin isoforms in skeletal muscle. *Journal of Cell Biology* **142**: 1269-1278

Pettmann, B. & Henderson, C.E. (1998) Neuronal cell death. *Neuron* **20:** 633-647

Pevsner, J., Hsu, S.C., Braun, J.E., Calakos, N., Ting, A.E., Bennett, M.K. & Scheller, R.H. (1994) Specificity and regulation of a synaptic vesicle docking complex. *Neuron* **13**: 353-361

Podesta, M., Zocchi, E., Pitto, A., Usai, C., Franco, L., Bruzzone, S., Guida, L., Bacigalupo, A., Scadden, D.T., Walseth, T.F., De Flora, A. & Daga, A. (2000) Extracellular cyclic ADP-ribose increases intracellular free calcium concentration and stimulates proliferation of human hemopoietic progenitors. *Faseb Journal* **14:** 680-690

Purves, D. (1988) Body and brain: A trophic theory of nerve connections. Harvard, Boston.

Purves, D. & Lichtman, J.W. (1985) Principles of neural development. Sunderland, MA. Harvard University Press.

Raabe, T.D., Nguyen, T., Archer, C. & Bittner, G.D. (1996) Mechanisms of the maintenance and eventual degradation of neurofilament proteins in the distal segments of severed goldfish Mauthner axons. *Journal of Neuroscience* **16:** 1605-1613

Ramon Y Cajal, S. (1928) Degeneration and regeneration of the nervous system (trans. May, R.M.) Oxford University Press, London.

Ranvier, L.A. (1878) Lecons sur l'histologie du systeme nerveux. *Vol 1.* Savy, Paris.

Rasband, M.N., Trimmer, J.S., Schwartz, T.L., Levinson, S.R., Ellisman, M.H., Schachner, M. & Shrager, P. (1998) Pottasium channel distribution, clustering, and function in remyelinating rat axons. *Journal of Neuroscience* **18:** 36-47

Redfern, P.A. (1970) Neuromuscular transmission in new-born rats. *Journal of Physiology* **209:** 701-709

Reger, J.F. (1954) Electron microscopy of the motor end-plate in intercostals muscle of the rat. *Anatomical Record* **118:** 344

Reger, J.F. (1955) Electron microscopy of the motor end-plate in rat intercostal muscle. *Anatomical Record* **122:** 1-16

Reger, J.F. (1958) The fine structure of neuromuscular synapses of gastrocnemii from mouse and frog. *Anatomical Record* **130:** 7-23

Reger, J.F. (1959) Studies on the fine structure of normal and denervated neuromuscular junctions from mouse gastrocnemius. *Journal of Ultrastructural Research* **2:** 269-282

Reier, P.J. & Hughes, A. (1972) Evidence for spontaneous axon degeneration during peripheral nerve maturation. *American Journal of Anatomy* **135:** 147-152

Reist, N.E., Werle, M.J. & McMahan, U.J. (1992) Agrin released by motor neurons induces the aggregation of acetylcholine receptors at neuromuscular junctions. *Neuron* **8:** 865-868

Reynolds, M.L. & Woolf, C.J. (1992) Terminal Schwann cells elaborate extensive processes following denervation of the motor endplate. *Journal of Neurocytology* **21:** 50-66

Ribchester, R.R. (1988) Activity-dependent and -independent synaptic interactions during reinnervation of partially denervated rat muscle. *Journal of Physiology* **401:** 53-75

Ribchester, R.R. (2001) Development and plasticity of neuromuscular connections. In, Brain and Behaviour in Human Neural Development. Ed. A.F. Kalverboer & A. Gramsbergen. Kluwer Academic Press. In Press.

Ribchester, R.R. & Barry, J.A. (1994) Spatial versus consumptive competition at polyneuronally innervated neuromuscular junctions. *Experimental Physiology* **79:** 465-494

Ribchester, R.R., Mao, F. & Betz, W.J. (1994) Optical measurements of activity-dependent membrane recycling in motor nerve terminals of mammalian skeletal muscle. *Proceedings of the Royal Society, London, B.* **255:** 61-66

Ribchester, R.R., Pakiam, J.G., O'Carroll, C.M., Thomson, D., Mattison, R.J., Costanzo, E.M., Gillingwater, T.H. & Barry, J.A. (1999) Impaired neuromuscular transmission preceding synapse withdrawal in axotomized adult $Wld^s$ mutant mouse skeletal muscle. *Journal of Physiology* **520:** 76P

Ribchester, R.R., Tsao, J.W., Barry, J.A., Asgari_Jirandeh, N., Perry, V.H. & Brown, M.C. (1995) Persistence of neuromuscular junctions after axotomy in mice with slow Wallerian degeneration (C57Bl/$Wld^s$). *European Journal of Neuroscience* **7:** 1641-1650

Ribchester, R.R., Thomson, D., Haddow, L.J. & Ushkaryov, Y.A. (1998) Enhancement of spontaneous transmitter release at neonatal mouse neuromuscular junctions by the glial cell line-derived neurotrophic factor (GDNF). *Journal of Physiology* **512:** 635-641

Rich, M.M., Coleman, H. & Lichtman, J.W. (1994) In vivo imaging shows loss of synaptic sites from neuromuscular junctions in a model of myasthenia gravis. *Neurology* **44:** 2138-2144

Rich, M.M. & Lichtman, J.W. (1989) Motor nerve terminal loss from degenerating muscle fibres. *Neuron* **3:** 677-688

Rich, M.M. & Lichtman, J.W. (1989a) In vivo visualization of presynaptic and postsynaptic changes during synapse elimination in reinnervated mouse muscle. *Journal of Neuroscience* **9:** 1781-1805

Richards, D.A., Guatimosim, C. & Betz, W.J. (2000) Two endocytic recycling routes selectively fill two vesicle pools in frog motor nerve terminals. *Neuron* **27:** 551-559

Riley, D.A. (1977) Spontaneous elimination of nerve terminals from the endplates of developing skeletal myofibers. *Brain Research* **134:** 279-285

Riley, D.A. (1981) Ultrastructural evidence for axon retraction during the spontaneous elimination of polyneuronal innervation of the rat soleus muscle. *Journal of Neurocytology* **10:** 425-440

Robertson, J.D. (1956) The ultrastructure of a reptilian myoneural junction. *Journal of Biophysical and Biochemical Cytology* **2:** 381-394

Robitaille, R. (1995) Purinergic receptors and their activation by endogenous purines at perisynaptic glial cells of the frog neuromuscular junction. *Journal of Neuroscience* **15:** 7121-7131

Robitaille, R., Garcia, M.L., Kaczorowski, G.J. & Charlton, M.P. (1993) Functional colocalization of calcium and calcium-gated potassium channels in control of neurotransmitter release. *Neuron* **11**: 645-655

Robitaille, R., Jahromi, B.S. & Charlton, M.P. (1997) Muscarinic calcium responses resistant to muscarinic antagonists at perisynaptic Schwann cells of the frog neuromuscualr junction. *Journal of Physiology* **504:** 337-347

Rochon, D., Rousse, I. & Robitaille, R. (2001) Synapse-glia interactions at the mammalian neuromuscular junction. *Journal of Neuroscience* **21:** 3819-3829

Roden, R.L., Donahue, S.P., Schwartz, G.A., Wood, J.G. & English, A.W. (1991) 200kD neurofilament protein and synapse elimination in the rat soleus. *Synapse* **9:** 239-243

Romanes, G.J. (1941) The development and significance of the cell columns in the ventral horn of the cervical and upper thoracic spinal cord of the rabbit. *Journal of Anatomy* **76:** 112-130

Rosenthal, J.L. & Taraskevich, P.S. (1977) Reduction of multiaxonal innervation at the neuromuscular junction of the rat during development. *Journal of Physiology* **270:** 299-310

Roy, M. & Sapolsky, R. (1999) Neuronal apoptosis in acute necrotic insults: why is this subject such a mess? *Trends in Neurosciences* **22:** 419-422

Rutkowski, J.L., Tuite, G.F., Lincoln, P.M., Boyer, P.J., Tennekoon, G.I. & Kunkel, S.L. (1999) Signals for proinflammatory cytokine secretion by human Schwann cells. *Journal of Neuroimmunology* **101:** 47-60

Sagot, Y., Dubois-Dauphin, M., Tan, S.A., De Bilbao, F., Aebischer, P., Martinou, J.C. & Kato, AC. (1995) Bcl-2 overexpression prevents motoneuron cell body loss but not axonal degeneration in a mouse model of a neurodegenerative disease. *Journal of Neuroscience* **15:** 7727-7733

Salpeter, M.M. & Loring, R.H. (1985) Nicotinic acetylcholine receptors in vertebrate muscle: properties, distribution and neural control. *Progress in Neurobiology* **25**: 297-325

Sanes, J.R. & Lichtman, J.W. (1999) Development of the vertebrate neuromuscular junction. *Annual Review of Neuroscience* **22**: 389-442

Sanford, L., Palay, M.D. & Palade, G.E. (1955) The fine structure of neurons. *Journal of Biophysical and Biochemical Cytology* **1:** 69-88

Santafe, M.M., Garcia, N., Lanuza, M.A., Uchitel, O.D. & Tomas, J. (2001) Calcium channels coupled to neurotransmitter release at dually innervated neuromuscular junctions in the newborn rat. *Neuroscience* **102:** 697-708

Schikorski, T. & Stevens, C.F. (2001) Morphological correlates of functionally defined synaptic vesicle populations. *Nature Neuroscience* **4:** 391-395

Schaeffer, L., de Kerchove d'Exaerde, A. & Changeux, J-P. (2001) Targeting transcription to the neuromuscular synapse. *Neuron* **31:** 15-22

Schafer, M., Fruttiger, M., Montag, D., Schachner, M. & Martini, R. (1996) Disruption of the gene for the myelin-associated glycoprotein improves axonal regrowth along myelin in C57Bl/Wld$^s$ mice. *Neuron* **16:** 1107-1113

Schlaepfer, W.W. & Hasler, M.B. (1979a) The persistence and possible externalisation of axonal debris during Wallerian degeneration. *Journal of Neuropathology and Experimental Neurology* **38:** 242-252

Schlaepfer, W.W. & Hasler, M.B. (1979b) Characterization of the calcium-induced disruption of neurofilaments in rat peripheral nerve. *Brain Research* **168:** 299-309

Schlaepfer, W.W. & Micko, S. (1978) Chemical and structural changes of neurofilaments in transacted rat sciatic nerve. *Journal of Cell Biology* **78:** 369-378

Sea, T., Ballinger, M.L. & Bittner, G.D. (1995) Cooling of peripheral myelinated axons retards Wallerian degeneration. *Experimental Neurology* **133:** 85-95

Sheller, R.A. & Bittner, G.D. (1992) Maintenance and synthesis of proteins for an anucleate axon. *Brain Research* **580:** 68-80

Sherrington, C.S. (1897) The central nervous system, Vol.III. In A textbook of physiology, 7th edition, M.Foster ed. (London: MacMillan)

Sherrington, C.S. (1906) The integrative action of the nervous system. Yale University Press, New Haven, USA.

Shi, B. & Stanfield, B.B. (1996) Differential sprouting responses in axonal fiber systems in the dentate gyrus following lesions of the perforant path in $Wld^s$ mutant mice. *Brain Research* **740:** 89-101

Smallheiser, N.R. & Crain, S.M. (1984) The possible role of "sibling neurite bias" in the coordination of neurite extension, branching and survival. *Journal of Neurobiology* **15:** 517-529

Smit, A.B., Syed, N.I., van Minnen, J., Klumperman, J., Kits, K.S., Lodder, H., van der Schors, R.C., van Elk, R., Sorgedrager, B., Brejc, K., Sixma, T.K. & Geraerts, W.P.M. (2001) A glia-derived acetylcholine-binding protein that modulates synaptic transmission. *Nature* **411:** 261-268

Sommer, C. & Schafers, M. (1998) Painful mononeuropathy in C57Bl/Wld mice with delayed Wallerian degeneration: differential effects of cytokine production and nerve regeneration on thermal and mechanical hypersensitivity. *Brain Research* **784:** 154-162

Son, Y-J. & Thompson, W.J. (1995a) Schwann cell processes guide regeneration of peripheral axons. *Neuron* **14:** 125-132

Son, Y-J. & Thompson, W.J. (1995b) Nerve sprouting in muscle is induced and guided by processes extended by Schwann cells. *Neuron* **14:** 133-141

Squier, M.K.T., Miller, A.C.K., Malkinson, A.M. & Cohen, J.J. (1994) Calpain activation in apoptosis. *Journal of Cellular Physiology* **159:** 229-237

Subang, M.C., Bisby, M.A. & Richardson, P.M. (1997) Delay of CNTF decrease following peripheral nerve injury in C57Bl/Wld mice. *Journal of Neuroscience Research* **49:** 563-568

Sudhof, T.C. (2000) The synaptic vesicle cycle revisited. *Neuron* **28:** 317-320

Sudhof, T.C. & Jahn, R. (1991) Proteins of synaptic vesicles involved in exocytosis and membrane recycling. *Neuron* **6**: 665-677

Tabata, H., Ikegami, H. & Kariya, K. (2000) A parallel comparison of age-related peripheral nerve changes in three different strains of mice. *Experimental Animals* **49:** 295-299

Tanner, S.L., Storm, E.E. & Bittner, G.D. (1995) Maintenance and degradation of proteins in intact and severed axons: implications for the mechanisms of long-term survival of anucleate crayfish axons. *Journal of Neuroscience* **15:** 540-548

Taxt, T. (1983) Local and systemic effects of tetrodotoxin on the formation and elimination of synapses in reinnervated adult rat muscle. *Journal of Physiology* **340:** 175-194

Tello, J.F. (1917) Genesis de las terminaciones nerviosas motrices y sensitivas. *Travaux du Laboratorire de Recherches Biologiques de l'Universite de Madrid* **15:** 101-199

Tetzlaff, W., Alexander, S.W., Miller, F.D. & Bisby, M.A. (1991) Response of facial and rubrospinal neurons to axotomy:Changes in mRNA expression for cytoskeletal proteins and GAP-43. *Journal of Neuroscience* **11:** 2528-2544

Thompson, W. & Jansen, J.K.S. (1977) The extent of sprouting of remaining motor units in partly denervated immature and adult rat soleus muscle. *Neuroscience* **2:** 523-535

Torigoe, K., Hashimoto, K. & Lundborg, G. (1999) A role of migratory Schwann cells in a conditioning effect of peripheral nerve regeneration. *Experimental Neurology* **160:** 99-108

Trachtenberg, J.T. & Thompson, W.J. (1997) Nerve terminal withdrawal from rat neuromuscular junctions induced by neureglin and Schwann cells. *Journal of Neuroscience* **17:** 6243-6255

Trojaborg, W. (1998) Acute and chronic neuropathies: new aspects of Guillain-Barre syndrome and chronic inflammatory demyelinating polyneuropathy, an overview and an update. *Electroencephalography and Clinical Neurophysiology* **107:** 303-316

Tsao, J.W., Brown, M.C., Carden, M.J., McLean, W.G. & Perry, V.H. (1994) Loss of the compound action potential: an electrophysiological, biochemical and morphological study of early events in axonal degeneration in the C57Bl/Ola Mouse. *European Journal of Neuroscience* **6:** 516-524

Tsao, J.W., George, E.B. & Griffin, J.W. (1999) Temperature modulation reveals three distinct stages of Wallerian degeneration. *Journal of Neuroscience* **19:** 4718-4726

Tsao, J.W., Paramananthan, N., Parkes, H.G. & Dunn, J.F. (1999a) Altered brain metabolism in the C57Bl/Wld mouse strain detected by magnetic resonance spectroscopy: Association with delayed Wallerian degeneration? *Journal of the Neurological Sciences* **168:** 1-12

Uchitel, O.D., Protti, D.A., Sanchez, V., Cherskey, B.D., Sugimori, M. & Llinas, R. (1992) P-type voltage-dependent calcium channel mediates presynaptic calcium influx and transmitter release in mammalian synapses. *Proceedings of the National Academy of Science, USA* **89**: 3330-3333

Usherwood, P.N.R., Cochrane, D.G. & Rees, D. (1968) Changes in structural, physiological, and pharmacological properties of insect excitatory nerve-muscle synapses after motor nerve section. *Nature* **318:** 589-591

Usherwood, P.N.R. & Rees, D. (1973) Quantitative studies of the spatial distribution of synaptic vesicles within normal and degenerating motor axons of the locust. *Comparative Biochemistry and Physiology* **43A:** 103-118

Usmanov, P.B., Kazakov, I., Kalikulov, D., Atakuziev, B.U., Yukelson, L.Y. & Tashmukhamedov, B.A. (1985) The channel-forming component of the teridiidae spider venom neurotoxins. *General Physiology and Biophysics* **4:** 185-193

Vallee, R.B. & Bloom, G.S. (1991) Mechanisms of fast and slow axonal transport. *Annual Review of Neuroscience* **14:** 59-92

Van Ooyen, A. & Willshaw, D.J. (1999) Competition for neurotrophic factor in the development of nerve connections. *Proceedings of the Royal Society, London, B.* **266:** 883-892

Verdu, E., Ceballos, D., Vilches, J.J. & Navarro, X. (2000) Influence of aging on peripheral nerve function and regeneration. *Journal of the Peripheral Nervous System* **5:** 191-208

Vial, J.D. (1958) The early changes in the axoplasm during Wallerian degeneration. *Journal of Biophysical and Biochemical Cytology* **4:** 551-555

Villa, P.G., Henzel, W.J., Sensenbrenner, M., Henderson, C.E. & Pettmann, B. (1998) Calpain inhibitors, but not caspase inhibitors, prevent actin proteolysis and DNA fragmentation during apoptosis. *Journal of Cell Science* **111:** 713-722

Waller, A. (1850) Experiments on the section of the glossopharyngeal and hypoglossal nerves of the frog, and observations of the alterations produced thereby in the structure of their primitive fibres. *Philosophical Transactions of the Royal Society, London B.* **140:** 423-429

Wang, G.K. (1985) The long-term excitability of myelinated nerve fibres in the transected frog sciatic nerve. *Journal of Physiology* **368:** 309-321

Wang, M-S., Wu, Y., Culver, D.G. & Glass, J.D. (2001) The gene for slow wallerian degeneration ($Wld^s$) is also protective against vincristine neuropathy. *Neurobiology of Disease* **8:** 155-161

Wang, Z.Z., Mathias, A., Gautam, M. & Hall, Z.W. (1999) Metabolic stabilization of muscle nicotinic acetylcholine receptors by rapsyn. *Journal of Neuroscience* **19**: 1998-2007

Watson, D.F., Glass, J.D. & Griffin, J.W. (1993) Redistribution of cytoskeletal proteins in mammalian axons disconnected from their cell bodies. *Journal of Neuroscience* **13:** 4354-4360

Waxman, S.G. (1997) Axon-glia interactions: Building a smart nerve fibre. *Current Biology* **7:** 406-410

Weddel, G. & Glees, P. (1941) The early stages in the degeneration of cutaneous nerve fibres. *Journal of Anatomy* **76:** 65-93

Werle, M.J. & Herrera, A.A. (1987) Synaptic competition and the persistence of polyneuronal innervation at frog neuromuscular junctions. *Journal of Neurobiology* **18:** 375-389

Werle, M.J. & Herrera, A.A. (1991) Elevated levels of polyneuronal innervation persist for as long as two years in reinnervated frog neuromuscular junctions. *Journal of Neurobiology* **22:** 97-103

White, T.A., Johnson, S., Walseth, T.F., Lee, H.C., Graeff, R.M., Munshi, C.B., Prakesh, Y.S., Sieck, G.C. & Kannan, M.S. (2000) Subcellular localization of cyclic ADP-ribosyl cyclase and cyclic ADP-ribose hydrolase activities in porcine airway smooth muscle. *Biochimica Et Biophysica Acta-Molecular Cell Research.* **1498:** 64-71

Whittaker, V.P., Michaelson, I.A. & Kirkland, R.J.A. (1964) The separation of synaptic vesicles from nerve-ending particles ("synaptosomes"). *Biochemical Journal* **90**: 293-303

Wiesel, T.N. (1982) Postnatal development of the visual cortex and the influence of environment. *Nature* **299:** 583-591

Wigston, D.J. (1989) Remodeling of neuromuscular junctions in adult mouse soleus. *Journal of Neuroscience* **9:** 639-647

Winlow, W. & Usherwood, P.N.R. (1975) Ultrastructural studies of normal and degenerating mouse neuromuscular junctions. *Journal of Neurocytology* **4:** 377-394

Woo, M., Hakem, R., Soengas, M.S., Duncan, G.S., Shahinian, A., Kagi, D., Hakem, A., McCurrach, M., Khoo, W., Kaufman, S.A., Senaldi, G., Howard, T., Lowe, S.W. & Mak, T.W. (1998) Essential contribution of caspase 3/CPP32 to apoptosis and its associated nuclear changes. *Genes and Development* **12:** 806-819

Wood, S.J. & Slater, C.R. (1997) The contribution of postsynaptic folds to the safety factor for neuromuscular transmission in rat fast- and slow-twitch muscles. *Journal of Physiology* **500**: 165-176

Wood, S.J. & Slater, C.R. (1998) Beta-spectrin is colocalized with both voltage-gated sodium channles and ankyrin (G) at the adult rat neuromuscular junction. *Journal of Cell Biology* **140**: 675-684

Yee, W.C., Pestronk, A., Alderson, K. & Yuan, C.M. (1988) Regional heterogeneity in the distal motor axon - 3 zones with distinctive intrinsic components. *Journal of Neurocytology* **17:** 649-656

Yuan, J. & Yanker, B.A. (2000) Apoptosis in the nervous system. *Nature* **407:** 802-809

Zhang, B., Koh, Y.H., Beckstead, R.B., Budnik, V., Ganetzky, B. & Bellen, H.J. (1998) Synaptic vesicle size and number are regulated by a clathrin adaptor protein required for endocytosis. *Neuron* **21:** 1465-1475

Zhang, Z., Fujiki, M., Guth, L. & Steward, O. (1996) Genetic influences on cellular reactions to spinal cord injury: a wound-healing response present in normal mice is impaired in mice carrying a mutation ($Wld^s$) that causes delayed Wallerian degeneration. *Journal of Comparative Neurology* **371:** 485-495

Zhou, D.X., Lambert, S., Malen, P.L., Carpenter, S., Boland, L.M. & Bennett, V. (1998) Ankyrin (G) is required for clustering of voltage-gated Na channels at axon initial segments and for normal action potential firing. *Journal of Cell Biology* **143**: 1295-1304

Ziegler, M. (2000) New functions of a long-known molecule - Emerging roles of NAD in cellular signalling. *European Journal of Biochemistry* **267:** 1550-1564

Zigmond, M.J., Bloom, F.E., Landis, S.C., Roberts, J.L. & Squire, L.R. (1999) Fundamental neuroscience. Academic Press, San Diego

# Appendix

# Appendix 1

The following appendix contains methodological and experimental data produced by others to support the findings of the current study concerning the generation and characterisation of the Ube4b/Nmnat (Wallerin) transgenic mice.

## A.1 Generation of the Ube4b/Nmnat Transgenic Mouse

The production of Ube4b/Nmnat transgenic mice was undertaken by Dr M.P. Coleman's laboratory in Cologne (see Figure 5.1 for transgene construct). The following description of how these mice were generated is taken from a collaborative paper by Drs. Coleman and Ribchester, of which I am a co-author (Mack et al., 2001).

"Chimeric *Ube4b/Nmnat* cDNA was amplified by RT-PCR from $Wld^S$ brain using Platinum Pfx polymerase (Gibco-BRL) and *Bam*HI and *Hind*III-tagged primers, before cloning into plasmid pHβAPr-1 (kindly supplied by Tom Vogt, University of Princeton). The human β-actin promoter drove expression of chimeric cDNA with the first (non-coding) exon of β-actin, thus mimicking the ubiquitous expression in $Wld^S$ mice. DNA sequencing confirmed the absence of errors and a 6 kb fragment containing the promoter, cDNA and polyadenylation signal was released by *Nde*I/*Eco*RI double digestion and gel-purified in the absence of ethidium bromide using QIAquick extraction (Qiagen). The transgene was injected into pronuclei of CBA X C57 F1

single-cell embryos by the service of Dr. George Kollias, Pasteur Institute, Athens. Nine founders were identified from 62 pups and eight were analysed.

DNA was prepared from a 5 mm tail biopsy or from spleen taken post mortem using the Nucleon HT kit (Amersham Pharmacia). Presence or absence of the 1.1 kb transgene coding region was determined using alkaline Southern blotting of a *Bam*HI/*Hind*III double digest onto Hybond N+ filters (Amersham Pharmacia) followed by hybridisation with a $^{32}$P-labelled probe of the full length chimeric gene coding sequence."

## A.2 Electrophysiological Studies on Ube4b/Nmnat Transgenic Mice

The preservation of functional axons and motor nerve terminals following axotomy in Ube4b/Nmnat transgenic mice was shown using intracellular recording techniques from FDB muscle preparations, undertaken by Mr D. Thomson and Dr R.R. Ribchester in our laboratory. Some results from this study are shown in Figure A.1.

## A.3 Molecular Studies on Ube4b/Nmnat Transgenic Mice

The preservation of distal axons following axotomy in Ube4b/Nmnat transgenic mice was also demonstrated by producing western blots of NF levels in axotomised sciatic

nerve, undertaken in Dr M. Coleman's laboratory in Cologne. The results of these experiments are shown in Figure A.2.

**Fig. A.1 Functional Preservation of Motor Axons and Motor Nerve Terminals in Ube4b/Nmnat Transgenic Mice Following Axotomy**

(A) An electrophysiological trace taken from a sample of muscle fibres in a homozygous 4836 Ube4b/Nmnat mouse FDB muscle preparation 3 days after sciatic nerve section. This figure shows the occurrence of both endplate potentials (EPPs) in response to nerve stimulation and spontaneous activity (random, uniquantal MEPPs) in these muscle fibres, demonstrating the persistence of neuromuscular transmission in these preparations.

(B) Graph of the percentage of fibres showing activity against days post axotomy. Each triangle represents data from an individual FDB muscle preparation.

(A)

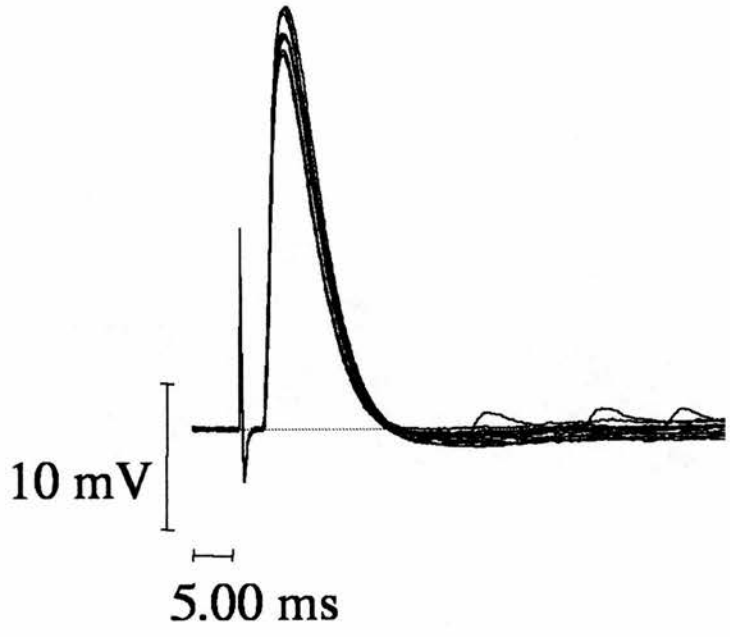
10 mV
5.00 ms

(B)

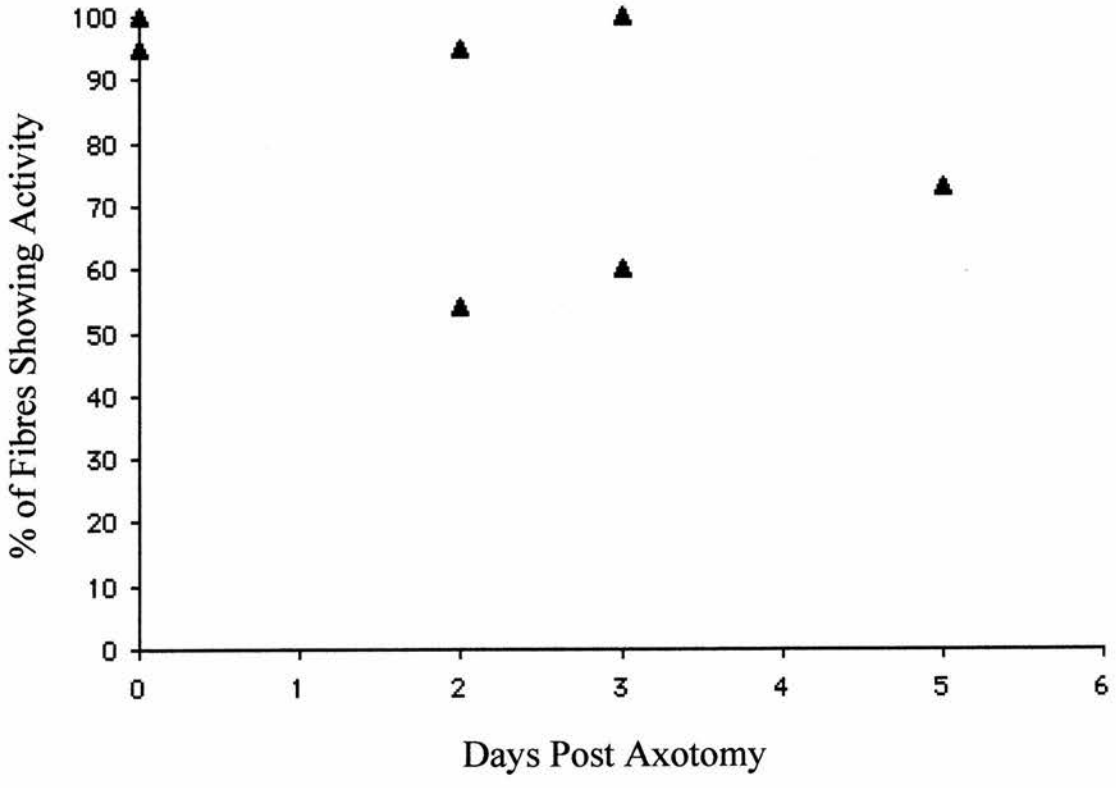
% of Fibres Showing Activity
100
90
80
70
60
50
40
30
20
10
0
0
1
2
3
4
5
6
Days Post Axotomy

**Fig. A.2 Preservation of Neurofilaments in Ube4b/Nmnat Transgenic Mice Sciatic Nerves Following Axotomy**

(A) A western blot showing the retention of NF proteins in axotomised $Wld^s$ and Ube4b/Nmnat transgenic mouse distal sciatic nerve stumps at 3 and 5 days after axotomy.

(A)

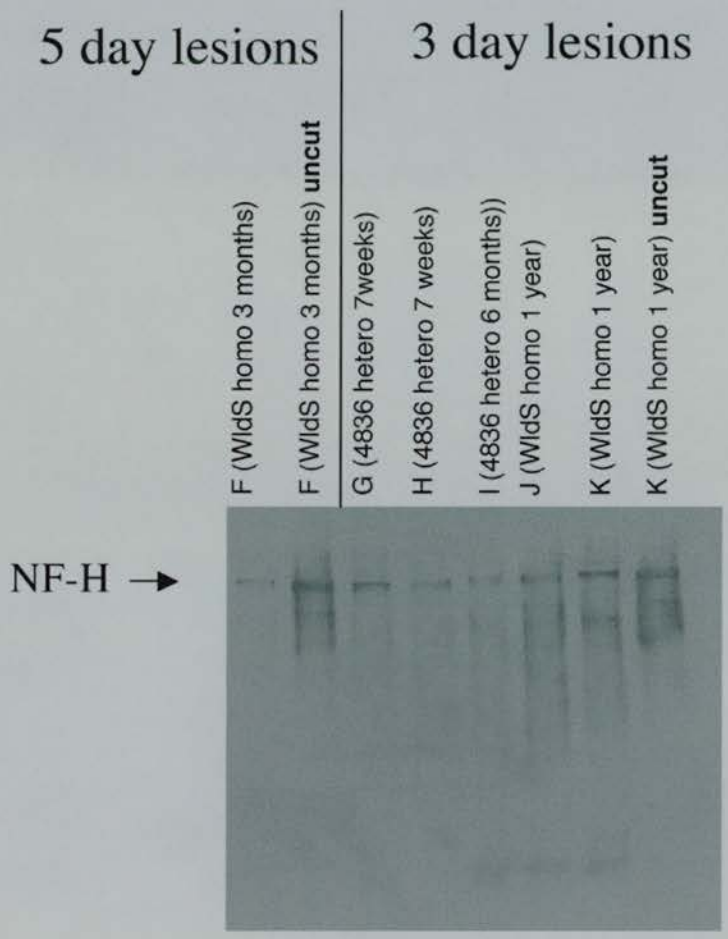
5 day lesions
3 day lesions
F (WldS homo 3 months)
F (WldS homo 3 months) uncut
G (4836 hetero 7weeks)
H (4836 hetero 7 weeks)
I (4836 hetero 6 months))
J (WldS homo 1 year)
K (WldS homo 1 year)
K (WldS homo 1 year) uncut
NF-H